OPTIMAL DESIGN UNDER UNCERTAINTY VIA CVAR (CONDITIONAL VALUE AT RISK)

by

Sıla Kumbasar

B.S., Chemical Engineering, Boğaziçi University, 2009

Submitted to the Institute for Graduate Studies in
Science and Engineering in partial fulfillment of
requirements for the degree of
Master of Science

Graduate Program in Chemical Engineering
Boğaziçi University
2012

to my mother & father

ACKNOWLEDGEMENTS

I would like to express my truthfull gratitude to my supervisor Professor Uğur Akman for his valuable contributions, support and guidance during the preparation of this thesis.

I wish to thank my family for their continuous support in all steps of my life.

ABSTRACT

OPTIMAL DESIGN UNDER UNCERTAINTY VIA CVaR (CONDITIONAL VALUE AT RISK)

The aim of this thesis work is to investigate the possibility of controlling and (re)shaping the statistical probability distribution of optimal objective function values in optimization problems related to process synthesis, design, and operation under uncertainty via imposing CVaR (Conditional Value at Risk) constraints. Probability distributions of the process model outputs are obtained by Monte Carlo Sampling/Simulation (MCS). Both the sequential and simultaneous computations of CVaR are studied. In the sequential approach, distribution of the optimal process output is generated first via MCS and then CVaR of this distribution is assessed. In the simultaneous approach, CVaR of the process output's distribution is obtained in a single stage by augmenting the process/optimization model equations for each and every realization of the input uncertainties and by solving these augmented equations together with the equations of the CVaR. These sequential and simultaneous approaches are applied to simple yet illustrious benzoic acid plant and alkylation plant examples. For the profit and cost distributions of these process models, expected value, skewness/kurtosis, $CVaR^{+}$, $CVaR^{-}$, difference between $CVaR^{+}$ and $CVaR^{-}$, Rachev Ratio (RR), linearized RR, and some linear combinations of them are considered. $CVaR^{-}$ and $CVaR^{+}$ are defined for the risk (left) and reward (right) sides of a probability distribution disjointedly. The results show that under the simultaneous scheme, where minimization of the difference between $CVaR^{+}$ and $CVaR^{-}$ or minimization of the RR is used as the objective, or when they are linearly adjoined to a main objective such as the expected profit it is possible to (re)shape the probability distribution of optimal objective function values. Contrary to applications in economics and finance where CVaR and the RR are exclusively used to make the loss distribution less skewed to the left, in this work, the difference between $CVaR^{+}$ and $CVaR^{-}$ or the RR are both successfully utilized to compress the distribution of the optimal profit around its mean in order to increase certainty on the mean optimal profit, despite uncertainties in process inputs.

ÖZET

RKaD (RİSKE KOŞULLU AÇIK DEĞER) YAKLAŞIMIYLA BELİRSİZLİK ALTINDA OPTİMAL TASARIM

Bu tez çalışmasının amacı; RKaD (Riske Koşullu açık Değer) kısıtlarını uygulayarak belirsizlik altında süreç sentezi, tasarımı ve işletimi ile ilgili optimizasyon problemlerinde optimal amaç fonksiyonu değerlerinin istatistiksel olasılık dağılımını kontrol etme / (yeniden) şekillendirme olasılığını incelemektir. Süreç modeli çıktılarının olasılık dağılımları, Monte Carlo Örneklemesi (MCÖ) yoluyla elde edilmiştir. RKaD'ın hem sıralı hem de eşzamanlı hesaplamaları çalışılmıştır. Sıralı yaklaşımda, ilk olarak MCS ile optimal süreç çıktısının dağılımı elde edilmiş ve sonrasında bu dağılımın RKaD'si belirlenmiştir. Eşzamanlı yaklaşımda, süreç çıktısının dağılımının RKaD'si, girdi belirsizliklerinin her bir gerçekleşmesi için büyütülen süreç/optimizasyon model denklemlerinin RKaD denklemleriyle birlikte tek bir aşamada çözülmesinden elde edilmiştir. Bu sıralı ve eşzamanlı yaklaşımlar benzoik asit ünitesi modeli ve alkilasyon ünitesi modeli gibi basit fakat açıklayıcı süreç modellerine uyarlanmıştır. Bu süreç modellerinin kâr ve zarar dağılımları için, beklenen değer, çarpıklık/basıklık, $RKaD^{+}$, $RKaD^{-}$, $RKaD^{+}$ ile $RKaD^{-}$ arasındaki fark, Rachev Rasyosu (RR), doğrusallaştırılmış RR ve bunların bazı doğrusal birleşimleri göz önüne alınmıştır. $RKaD^{-}$ ve $RKaD^{+}$, bir olasılık dağılımının risk (sol) ve kazanç (sağ) yönlerini belirtmek için birbirlerinden ayrı olarak tanımlanmıştır. Sonuçlar göstermiştir ki, $KRaD^{+}$ ile $KRaD^{-}$ arasındaki farkın yahut RR'nin minimizasyonlarının amaç olarak kullanıldığı ya da bunların ortalama kâr gibi asıl amaca doğrusal olarak bitiştirildiği eşzamanlı şema altında, optimal amaç fonksiyonu değerlerinin olasılık dağılımını (yeniden) şekillendirmek mümkün olabilmektedir. RKaD ve RR'nin yalnızca kayıp dağılımlarını daha az sola çarpık yapmak için kullanıldığı ekonomi ve finanstaki uygulamaların aksine, bu çalışmada girdi belirsizliklerine rağmen ortalama optimal kâr üzerindeki kesinliği artırmak amacıyla hem $KRaD^{+}$ ile $KRaD^{-}$ arasındaki fark hem de RR ortalamanın çevresindeki optimal kâr dağılımını sıkıştırmakta başarıyla kullanılmıştır.

TABLE OF CONTENTS

LIST OF FIGURES

LIST OF TABLES

LIST OF SYMBOLS

a	Subscript of Benzoic Acid for BAP model
$\boldsymbol{A}$	Coefficient vector of inequality constraints
$\boldsymbol{A_{eq}}$	Coefficient vector of equality constraints
A_c	Condensor area for BAP model
A_{cool}	Cooler area for BAP model
A_e	Evaporator area for BAP model
A_{pc}	Partial condensor area for BAP model
b	Subscript of Benzene for BAP model
$\boldsymbol{B}$	Right hand side vector of inequality constraints
$\boldsymbol{B_{eq}}$	Right hand side vector of equality constraints
$B(\alpha, \beta)$	Beta function
$\boldsymbol{c}$	Coefficient of CVaR in Equation 2.5
cl	Confidence interval
C_p	Average heat capacity for BAP model
d	Distribution coefficient for BAP model
$\boldsymbol{d}$	Vector of design variables
$E(\boldsymbol{X})$	Expected value of $\boldsymbol{X}$
exc_1	Evaporator cost for BAP model
exc_2	Condensor cost for BAP model
exc_3	Cooler cost for BAP model
exc_4	Partial condensor cost for BAP model
F	Feed rate for BAP model
F_α	Continuous form of CVaR^+ of a frequency distribution
$\bar{F}_\alpha$	Discrete form of CVaR^+ of a frequency distribution
F_α^*	CVaR^+ of the distribution
$F_{(1-\alpha)}$	Continuous form of CVaR^- of a frequency distribution
$\bar{F}_{(1-\alpha)}$	Discrete form of CVaR^- of a frequency distribution
$F_{(1-\alpha)}^*$	CVaR^- of the distribution

$f(\boldsymbol{x},\boldsymbol{y})$	Loss function associated with the decision vector **x** in R^n and random vector **y** in R^m
$f(x;\alpha,\beta)$	Probability density function for the Beta distribution
$\boldsymbol{g}$	Vector of inequality constraints
$\boldsymbol{h}$	Vector of equality constraints
H_{vap}	Enthalpy of vaporization of benzene for BAP model
H_{steam}	Enthalpy of superheated steam for BAP model
H_{vap}^{sat}	Enthalpy of saturated steam-vapor for BAP model
H_{liq}^{sat}	Enthalpy of saturated steam-liquid for BAP model
i	Scenario index
I	Inverse error function for VaR and CVaR, I_{VaR} and I_{CVaR}
J	Performance function (cost, profit, etc.)
lb	Lower bound
$\boldsymbol{m}$	$t \times \boldsymbol{z}$
$M_{[k:N]}$	k^{th} percentile of N ordered values
n	Number of stages for settler for BAP model
N	Number of scenarios
$n(x;\mu,\sigma)$	Probability density function for the Normal/Gaussian distribution
$\boldsymbol{p}$	Vector of uncertain variables
P	Cumulative distribution functional in Section 3.1
$p(\boldsymbol{y})$	Probability density function
P_t	Price at time t
P_{t-1}	Price at previous time period
R_t	Return at time t
t	Auxiliary variable, $(1/\mathrm{CVaR}^{-})$
T_{apr}	Approach temperature
T^{sat}	Temperature of saturated steam for BAP model
T_{steam}	Temperature of superheated steam for BAP model
$\boldsymbol{u}$	Vector of manipulated variables
$u(x;\alpha,\beta)$	Probability density function for the Uniform/Rectangular distribution

U_{con}	Overall heat-transfer coefficient for benzene-water condenser
U_{exc}	Overall heat-transfer coefficient for benzene-water exchanger
U_{ev}	Overall heat-transfer coefficient for benzene-water evaporator
ub	Upper bound
$\boldsymbol{v_m}$	Vector of VaR^- multiplied with t
$\boldsymbol{v_p}$	Vector of VaR^+ multiplied with t
w	Flow rate of Benzene, Benzoic Acid or Water for BAP model
$\boldsymbol{x}$	Vector of decision variables
x_b	Mass fraction of benzoic acid to water in feed for BAP model
$\boldsymbol{X}$	Set of random variables
$\boldsymbol{y}$	Vector of random variables
$\boldsymbol{z}$	Vector of auxiliary variables
Z_i	Outcome of the objective for the current scenario
α	Confidence interval (0,1)
β	1− Confidence interval
γ	Auxiliary variable for the right side of the distribution
γ^*	VaR^+ of the distribution at the optimal solution
Γ	Gamma function
η	Auxiliary variable for the left side of the distribution
η^*	VaR^- of the distribution at the optimal solution
λ	Weighting coefficient of the objective function, $0 \leq \lambda \leq 1$
μ	Mean value
ρ	Density
σ	Standard deviation
Φ	Profit function for the AP
$\psi(\boldsymbol{x}, \gamma)$	Cumulative distribution function
Ω	Profit target

LIST OF ACCRONYMS/ABBREVIATIONS

AP	Alkylation Plant
BAP	Benzoic Acid Plant
ben	Benzene make up cost for BAP model
$benz$	Benzene flow rate for BAP model
$cash$	Annual Cash Flow for BAP model
CVaR	Conditional Value at Risk
$CVaR^{+/-}$	CVaR for the right and left side of the distribution
DIFM	Difference between mean value and $CVaR^{-}$
DIFP	Difference between $CVaR^{+}$ and mean value
$elect$	Electricity cost for BAP model
$equip$	Equipment cost for BAP model
FCI	Fixed capital investment for BAP model
frp	Discount (or time value conversion) factor for BAP model
$labor$	Labor cost for BAP model
$lang$	Lang factor for BAP model
LP	Linear Programming
$main$	Maintenance cost for BAP model
MCS	Monte Carlo Simulation
MILP	Mixed Integer Linear Programming
MINLP	Mixed Integer Non-Linear Programming
MRR	Modified Rachev Ratio
msd, msb	Marshall & Swift Cost Index for BAP model
NLP	Non-Linear Programming
nMCS	Number of Monte Carlo Simulations
NPW	Net Present Worth
$ocost$	Operating cost for BAP model
$overh$	Overhead for BAP model
$PVaR$	Parametric VaR for the right side and left side, $PVaR_{\alpha}$ and $PVaR_{(1-\alpha)}$

$PCVaR$	Parametric CVaR for the right side and left side, $PCVaR_{\alpha}$ and $PCVaR_{(1-\alpha)}$
$pump$	Pump cost for BAP model
RR	Rachev Ratio
$sales$	Sales cost for BAP model
set	Settler cost for BAP model
set_1	Total settler cost for BAP model
$steam$	Steam cost for BAP model
sup	Supervision cost for BAP model
$taxins$	Tax and insurance for BAP model
TCI	Total capital investment for BAP model
$time$	Production time per year for BAP model
VaR	Value at Risk
$VaR^{+/-}$	VaR for the right and left side of the distribution
vol	Settler volume for BAP model
$water$	Water cost BAP model
WC	Working capital for BAP model

1. INTRODUCTION

Economics has always been integrated with engineering disciplines. However, the use of advanced financial (engineering) tools, especially those that are related to risk and uncertainty, have not been widespread in engineering research and have not been integrated into engineering curricula. For example, Chemical Engineering education involves the problem of economically designing a plant with a specified production capacity to produce a chemical product with specified properties. Net present worth and a rate of return on investment values are obtained deterministically using a cash flow profile which is computed on the basis of fixed costs and specified availabilities of raw materials and utilities such as energy.

Today's engineer, in a world full of changing conditions, is expected to determine the right design capacity and economical level of flexibility under market uncertainty. Therefore maximizing expected profit with novel planning aspects is a necessary condition. However, this is not sufficient; the risks associated with the expected profit must also be assessed and taken into account during process engineering calculations. (Barbaro and Bagajewicz, 2004; Bagajewicz, 2005)

In mid 1980s, the concept of flexibility was introduced to consider the possible changes in raw materials' quality and availability, and expected variations in product specifications. However, this early flexibility concept did not involve a well-defined risk definition and was in short of statistical methodology; it was solely based on a predefined region of operability where a process was considered to be flexible if it could operate under input or output variations defined over a hyperrectangular region the size of which was related to uncertainty. Halemane and Grossmann (1983) showed that, given a polyhedral region of uncertain parameters, the critical point(s) that limit flexibility lie at the vertices of this region if the constraints are convex. Considering non-linearity (or, non-convexity), Grossmann and Floudas (1987) showed that the "critical vertex point" conclusion of Halemane and Grossmann may not hold for non-convex feasible regions, and presented a two-stage iterative Mixed Integer Non-Linear Programming (MINLP) method, which they called as the active constraint strategy, for finding non-vertex critical

points that limit flexibility. In order to assess the flexibility of a given design, Swaney and Grossmann (1985) proposed the concept of “flexibility index” which basically measures the size of the region of feasible operation, i.e., the maximum possible deviation of uncertain parameters from their nominal values such that the plant remains feasible.

After mid 1990s the shares of uncertainty and risk in process systems engineering increased mostly due to globalization, reflected by the increased traffic of energy and raw materials imports (Barbaro and Bagajewicz, 2004; Bagajewicz, 2005; Pongsakdi *et al.*, 2006; Whitnack *et al.*, 2009). In reality, for most of the Chemical Engineering problems as well, the decisions are made under uncertainty. In some such cases, the presence of discrete decisions results in stochastic MINLP problems complicates the model and its solution further (Halemane and Grossmann, 1983; Acevedo and Pistikopoulos, 1998; Pistikopoulos, 1995). To solve such problems, two-stage stochastic programming has been widely used (Paules and Floudas, 1992; Acevedo and Pistikopoulos, 1998; Pintaric and Kravanja, 2000). In this approach, the first-stage decisions are taken before the uncertainty is revealed. The other decisions made after the uncertain data become known (the decisions made after the uncertainty is revealed) are called the second-stage or recourse decisions. The expected value of the cost (or profit) is referred to as the recourse function. In general, stochastic programming problems involve the evaluation of multi-dimensional integrals which is difficult to solve. In order to solve these systems numerical integration methods such as the Gaussian Quadratures/Cubatures have been used in the literature (Stroud, 1971; Miller and Rice, 1983; Pistikopoulos and Ierapetritou, 1995; DeVuyst and Preckel, 2007).

Alternatively, utilization of sampling techniques such as the Monte Carlo Sampling/Simulation (MCS) that involves deterministic optimization using the samples generated, have drawn large interest in literature (Acevedo and Pistikopoulos, 1996; Kalagnanam and Diwekar, 1997, Mak *et al.*, 1999; Goyal and Ierapetritou, 2007). Among the sampling methods, the Hammersley Sequence Sampling (HSS) technique which shows uniform properties in multidimension, and is 3 to 100 times faster than Latin Hypercube Sampling (LHS) and pure MCS, is succesfully used in process engineering computations (Diwekar and Rubin, 1991; Diwekar and Kalagnanam, 1997; Kim and Diwekar, 2002; Diwekar, 2003; Diwekar 2008). Acevedo and Pistikopoulos (1996) compared Gaussian numerical integration methods and MCS methods and concluded that cubature methods are

more favorable for lower dimensional problems and sampling-based methods are better for the larger problems. In these techniques, assigned probability distributions of the uncertain input parameters are sampled from the multi-variable uncertain parameter domain and the corresponding probability distributions of the output parameters are obtained. All these different sampling techniques aim to generate independent and uniformly distributed pseudo-random numbers efficiently such that the statistical properties of the outputs converge to true (large-sample) values with less number of scenario simulations.

Although advanced financial tools are not widely used in engineering, as stated at the beginning, economic considerations should also include risk management while setting up the stochastic problems in engineering. The measures of risk management created first for the finance sector may be used for engineering purposes as well. Some of the risk measures cited by Bagajewicz (2005) are: the variability, cumulative probability for a given aspiration level, downside risk, upper partial mean, value at risk (VaR), downside expected profit, regret analysis by Riggs, (1968), chance constraints by Charnes and Cooper (1959), the Sharpe ratio by Sharpe, (1966), risk-adjusted return on capital, certainty equivalent approach by Keown *et al.*, (2002), risk premium, risk adjusted net present worth (NPW) by Keown *et al.*, (2002), and real option valuation. Also, some of the new measures are opportunity value (or upside potential), and the risk area ratio (Aseeri and Bagajewicz, 2004).

Considering profit, the risk is defined as the probability of the actual profit of the design (x) being less than or equal to the profit target (Ω), i.e., $Risk(x, \Omega) = P\{Profit(x) \leq \Omega\}$. This definition of risk is used for many years in the petroleum industry (McCray, 1975) and in the process engineering literature (Rodera and Bagajewicz, 2000; Barbaro and Bagajewicz, 2003, 2004; Gupta and Maranas, 2003). Nowadays, the disciplines converge and influence each other; as a result VaR is used in many areas including engineering risk analysis and assessment (www.gloriamundi.org). The concept of Value at Risk (VaR), as a measure of risk, stems from the sector needs in financial risk management and risk control. VaR is defined as “the maximum loss you are likely to incur on your portfolio with a specified probability”. It is a probabilistic measure of potential losses which was introduced by J.P. Morgan (Guldimann, 2000). The relationship between the VaR and the risk definition indicated above is given by Barbaro

and Bagajewicz (2004). According to the authors, VaR under a desired confidence level related to profit is the difference between the inverse probability density function of risk and the expected value of profit of design, i.e., $VaR(x, p_\Omega) = E[Profit(x)] - Risk^{-1}(x, \Omega)$ where $p_\Omega = Risk(x, \Omega)$.

Another, but computationally more convenient, measure of risk for the banking and finance industry, the Conditional Value at Risk (CVaR), or the Expected Tail Loss (ETL), is defined as the expected value (mean) of the losses beyond VaR (Uryasev, 2000). Rockafellar and Uryasev (2000) further developed the CVaR for its more convenient use in portfolio optimizations. The major contribution of Rockafellar and Uryasev (2000) is their reformulation of the CVaR as a Linear Programming (LP) problem. The inclusion of CVaR measure in classical portfolio optimization problems requires only the addition of CVaR-related linear constraints to the original constraints of the portfolio optimization problem. A simple description of the approach for minimizing CVaR and optimization problems with CVaR constraints can be found in the literature (Uryasev, 2000; Rockafellar and Uryasev, 2000; Krokhmal *et al.*, 2001; Rockafellar and Uryasev, 2001). CVaR and VaR are the risk measures that are represented with single numbers; ideal in presenting to boards as disclosure in annual reports. CVaR, like VaR is used in various areas including process engineering risk analysis as can be seen in some recent works of Verderame and Floudas (2010, 2011).

Lately, both VaR and CVaR find use as alternative methods of tackling uncertainty issues in various (non-financial) engineering problems. In economics and finance, VaR and CVaR are almost exclusively used for the loss (negative return) side of the probability distribution, as the last word “risk” implies. However, many engineering problems under uncertainty require the assessment of probability distribution characteristics of the opposite (gain/profit) side, or even, the assessment of both the positive (reward) and negative (risk) sides, simultaneously. Therefore, in this thesis work, CVaR formulations are developed for the risk ($CVaR^-$) and reward ($CVaR^+$) sides for their mutually exclusive use as well as their simultaneous consideration.

In this thesis, various prototypes of the “optimal synthesis and/or design under uncertainty” problems are (re)formulated as “optimal CVaR-based synthesis and/or design

under uncertainty" problems. The optimization models are solved using GAMS and/or MATLAB. It is demonstrated that the statistical probability distribution of synthesis / design / operation costs or profits may be (re)shaped as favorably as possible (positively skewed for profit objectives, negatively skewed for cost objectives) via imposing suitable CVaR constraints by augmenting the synthesis / design / operation constraints with the CVaR-related linear constraints.

In the second chapter of the thesis, the VaR and CVaR are theoretically explained. Optimization formulations of CVaR via Uryasev's approach are developed for both the risk (left) and reward (right) sides of a probability distribution. Linear optimization of Rachev Ratio and its variants are discussed in the second chapter as well. In the third chapter, the development of the mathematical formulation for the optimal design under uncertainty via CVaR and utilization of the MCS method are explained together with the estimation of CVaR via sequential and simultaneous methods. Applications of CVaR for the optimization of variety of process models, namely, the benzoic acid plant and the alkylation plant, are demonstrated in the fourth chapter. The results and conclusions are summarized in the fifth chapter together with suggestions for the future work. Mass and energy balances and related tables for the benzoic acid plant model are present in Appendix A. Some selected MATLAB and GAMS codes are given in Appendix B and C, respectively.

2. VALUE AT RISK AND CONDITIONAL VALUE AT RISK

In this chapter, theoretical derivations of the Value at Risk (VaR) and Conditional Value at Risk (CVaR) are presented together with some of their mathematical properties. Formulations for the optimization of CVaR via Uryasev's approach are developed both for the risk (left) and reward (right) sides of a probability distribution. Additionally, linear optimization of Rachev Ratio are presented at the end of the chapter.

2.1. Value at Risk (VaR)

In the finance sector, institutions need to measure risks and compare across different trading positions for portfolio management. For this purpose, it is necessary to quantify return volatility, which is one of the oldest measures of risk. Modern portfolio theory and common practice define this volatility as the standard deviation (which is interpreted as risk) of the price percentage change or, more formally, the standard deviation of the continuously compounded percentage price change (Ballesca-Loyo, 1999):

$$Volatility = Risk = Standard\ deviation\ of\ R_t = \ln(P_t/(P_{t-1}))$$

where

R_t = Return at time t (day, week, month, ...)

P_t = Price at time t

P_{t-1} = Previous period price

The above simple measure of risk (standart deviation) has some limitations such as the assumption of the normal distribution of returns. To combine risks into a single risk measure which is simple enough that anyone can understand, J.P. Morgan developed a widely used risk measure of the risk of loss on a specific portfolio of financial assets, namely, the VaR. They published the methodology and gave free access to estimates of the necessary underlying parameters in 1994 (Kolman, 1998). Since then, it is heavily used for financial risk assessment and management.

VaR is a method that quantizes risk during a standardized period in terms of probable loss. Barbaro and Bagajewicz (2004) clarify the relation between VaR and risk. They define that VaR is the difference between the inverse probability density function of risk and the expected value of outcome of design at a desired confidence level. VaR can be interpreted as the maximum expected loss (or the minimum profit), at a given level of confidence. Although developed for and well respected in the finance sector, VaR is also finding application areas increasingly in engineering; especially in quantifying and interpreting the risk associated with an investment, design, operation, etc.

In order to obtain VaR, first a confidence level (*cl*) should be set. For instance, for a given a value of 95% *cl*, the VaR becomes the point on the x-axis that separates 95% of the area of observations from 5% of tail observations. For a standard-normal distribution (i.e., N ~ (0, 1): distribution with mean = 0 and standard deviation = 1), the VAR for 95% *cl* is –1.645.

The two computational methods of VaR are “parametric” and “historical” methods. Parametric VaR uses a fitted normal distribution curve to calculate the VaR. Historical VaR (historical simulation VaR) puts all observations in order and selects the observation located to the left of the defined probability density area set by the confidence level. For n observations and for a given confidence level (*cl*), the resulting VaR becomes $[(1-cl)n+1]^{st}$ observation. Monte Carlo Simulation (MCS) method and the Central Limit Theorem are generally used for obtaining random samples for historical simulation of VaR.

2.2. Conditional Value at Risk (CVaR)

Conditional Value at Risk (CVaR), also called Mean Excess Loss, Mean (Expected) Shortfall, Expected Tail Loss, or Tail VaR, is considered to be a more consistent measure of risk than VaR. For continuous distributions, CVaR is the expected loss exceeding the VaR. For discrete distributions, CVaR is the weighted average of the VaR and losses exceeding that VaR. CVaR is an upper bound for VaR, therefore, minimization of CVaR also minimizes VaR (Larsen *et al.*, 2002). VaR and CVaR are both illustrated with Figure 2.1, where the *cl* is shown as α.

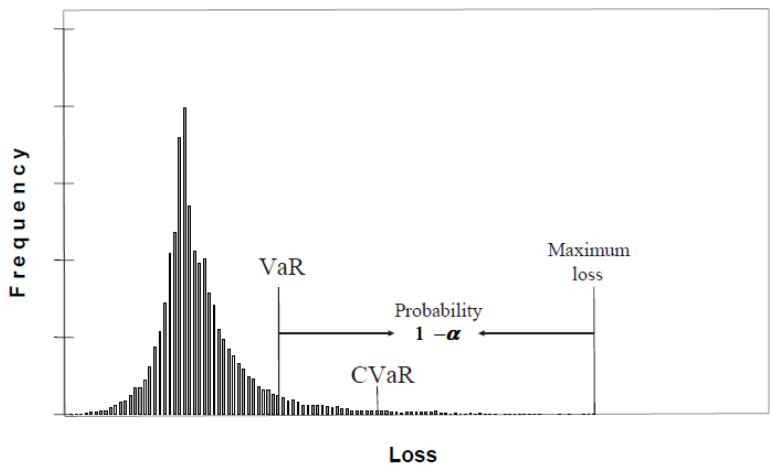

Figure 2.1. Illustration of VaR and CVaR (Uryasev, 2000).

2.3. Comparison of VaR and CVaR

Although VaR is a very popular measure of risk, it has undesirable mathematical characteristics such as a lack of subadditivity and convexity (Arztner *et al.*, 1997; Arztner *et al.*, 1999; Dowd, 2005; Uryasev, 2010). VaR is coherent only when it is based on the standard deviation of normal distributions (for a normal distribution VaR is proportional to the standard deviation when $\mu = 0$ and $\sigma = 1$) (Powell and Allen, 2009). Furthermore, VaR can ill-behave as a function of portfolio positions and can exhibit multiple local extrema (Uryasev, 2010). However, CVaR quantifies risks beyond VaR and is a consistent and coherent risk measure (Arztner *et al.*, 1999); it is transition-equivariant, positively homogeneous, convex, applicable to non-symmetric distributions like beta distribution and has a nice convex function with a global optimum (Rockafellar and Uryasev, 2001; Pflug, 2001). As it is seen from Figure 2.2, where the x-axis defines the portfolio position (portfolio weight as decision variable in a portfolio optimization with two assets), CVaR is convex, but VaR may be non-convex (Uryasev, 2010).

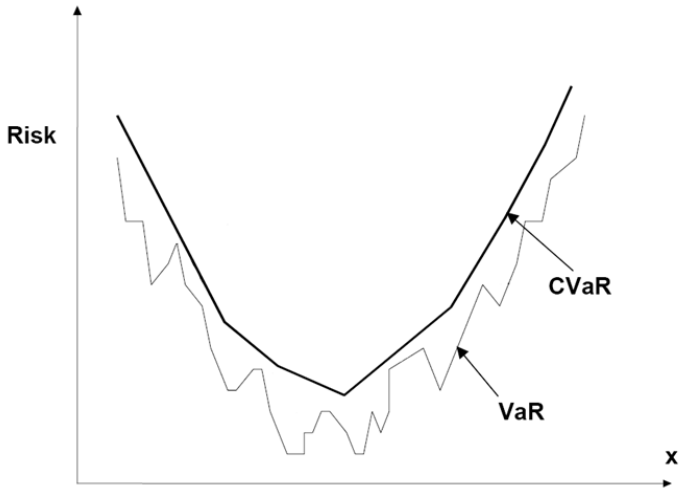

Figure 2.2. CVaR is convex and VaR ≤ CVaR (Uryasev, 2010).

2.4. Some VaR and CVaR Properties and Relationships

In this section some properties of VaR, CVaR, and their relationships are given (Pflug, 2001). Some mathematical definitions of VaR and CVaR (Rockafellar and Uryasev, 2000) can be stated as follows: $\boldsymbol{X} = f(\boldsymbol{x}, \boldsymbol{y})$ is positive outcome (profit as positive quantity, cost as positive quantity, negative of loss as negative quantity, ...) associated with (depending on) the deterministic decision vector $\boldsymbol{x} \in \mathbf{X} \subset \mathbb{R}^n$ and the random vector $\boldsymbol{y} \in \mathbb{R}^m$, $p(\boldsymbol{y})$ is probability density function of the random vector $\boldsymbol{y}$, $\Psi(\boldsymbol{x}, \gamma)$ is cumulative probability distribution function less than γ for fixed $\mathbf{x}$ i.e., $\Psi(\boldsymbol{x}, \gamma) = \mathbb{P}(\boldsymbol{X} \leq \gamma) = \int_{f(\boldsymbol{x},\boldsymbol{y}) \leq \gamma} p(\boldsymbol{y}) d\boldsymbol{y}$, $VaR_\alpha(\boldsymbol{X})$ is value-at-risk as the α-quantile, i.e. $VaR_\alpha(\boldsymbol{X}) = \Psi^{-1}(\boldsymbol{x}, \gamma)$, where Ψ^{-1} is the right continuous inverse of Ψ, $CVaR_\alpha(\boldsymbol{X})$ is conditional expectation of $\boldsymbol{X}$, given that $\boldsymbol{X} \geq VaR_\alpha$, i.e., $CVaR_\alpha(\boldsymbol{X}) = \mathbb{E}(\boldsymbol{X} | \boldsymbol{X} \geq VaR_\alpha(\boldsymbol{X}))$.

Some basic properties of VaR_α (Pflug, 2001) are as follows:

(i) VaR_α is translation-equivariant, i.e.

$$VaR_\alpha(\boldsymbol{X} + c) = VaR_\alpha(\boldsymbol{X}) + c \tag{2.1}$$

where $c \in \mathbb{R}$ is constant.

(ii) VaR_α is positively homogeneous, i.e.

$$VaR_\alpha(c\boldsymbol{X}) = c\, VaR_\alpha(\boldsymbol{X}) \tag{2.2}$$

if $c \in \mathbb{R}^+$ is a positive constant.

(iii) VaR_α is equal to the reflection of $VaR_{1-\alpha}$ with respect to the origin, i.e.

$$VaR_\alpha(\boldsymbol{X}) = -\, VaR_{(1-\alpha)}(-\boldsymbol{X}) \tag{2.3}$$

Some important properties of $CVaR_\alpha$ (Pflug, 2001) are as follows:

(i) $CVaR_\alpha$ is translation-equivariant, i.e.

$$CVaR_\alpha(\boldsymbol{X} + c) = CVaR_\alpha(\boldsymbol{X}) + c \tag{2.4}$$

where $c \in \mathbb{R}$ is constant.

(ii) $CVaR_\alpha$ is positively homogeneous, i.e.

$$CVaR_\alpha(c\boldsymbol{X}) = c\, CVaR_\alpha(\boldsymbol{X}) \tag{2.5}$$

if $c \in \mathbb{R}^+$ is a positive constant.

(iii) If X has a density, then

$$E(\boldsymbol{X}) = (1-\alpha)CVaR_\alpha(\boldsymbol{X}) - \alpha\, CVaR_{(1-\alpha)}(-\boldsymbol{X}) \tag{2.6}$$

(iv) $CVaR_\alpha$ is convex in the following sense: For arbitrary (not necessarily independent) random variables X_1 and X_2 and $0 < \lambda < 1$,

$$CVaR_\alpha(\lambda X_1 + (1-\lambda)X_2) \leq \lambda\, CVaR_\alpha(X_1) + (1-\lambda)\, CVaR_\alpha(X_2) \tag{2.7}$$

In portfolio optimization, the objectives of the optimization problems of VaR and CVaR are expressed as min $VaR_\alpha(\boldsymbol{X})$ and min $CVaR_\alpha(\boldsymbol{X})$, respectively. Equivalently, one can replace these two objectives with max $VaR_{(1-\alpha)}(-\boldsymbol{X})$ and max $CVaR_{(1-\alpha)}(-\boldsymbol{X})$ using the third properties (Equation 2.3 and Equation 2.6) of VaR_α and $CVaR_\alpha$.

In order to give the relationship between VaR and CVaR Pflug (2001) firstly defines the percentile (M):

$M_{[k:N]}(X_1, \dots, X_N)$ denotes the kth percentile of N ordered values, i.e. the kth largest value among the elements of the **X** vector after being ranked in increasing order. For consistency, one can state that $M_{[1:N]} = \min(X_1, \dots, X_N)$ and $M_{[N:N]} = \max(X_1, \dots, X_N)$. Then, VaR and CVaR for discrete distributions may be written as follows (Pflug, 2001):

VaR_α is the kth percentile of **X** where k is the floor of αN, i.e.

$$VaR_\alpha(\boldsymbol{X}) = M_{[\lfloor \alpha N \rfloor:N]}(\boldsymbol{X}) \tag{2.8}$$

$CVaR_\alpha$ is the expected value of $\boldsymbol{X} = f(\boldsymbol{x}, y)$ given that $f(\boldsymbol{x}, y) \geq VaR_\alpha$, i.e.

$$CVaR_\alpha(\boldsymbol{X}) = \frac{1}{N} \sum_{\{f(\boldsymbol{x}, y_i) \geq VaR_\alpha\}} f(\boldsymbol{x}, y_i) \tag{2.9}$$

Incorporating these definitions of VaR and CVaR for discrete distributions with the objectives of the optimization problems of VaR and CVaR, Pflug (2001) states that it is a nonlinear, nonconvex problem.

2.5. Derivation of VaR^+, VaR^-, $CVaR^+$, and $CVaR^-$

Rockafellar and Uryasev (2000) discovered a novel way for the optimization of/with CVaR. Their formulation, which will be called as the "Uryasev's formulation" allows the computation of CVaR (and VaR as byproduct) via Linear Programming (LP). This practical and extremely effective approach, as will be demonstrated later in this thesis,

allows the simultaneous consideration of the optimal design and risk (uncertainty) objectives, via LP formulation, if the plant model is also linear.

Below, is the summary of the derivation of Rockafellar and Uryasev (2000); modified in such a way that the variables refer not only to portfolio optimization but the design under uncertainty in general. Rockafellar and Uryasev derive their formulation by considering portfolio losses. In order to comply with standards in statistics, they multiply the portfolio loss term with minus one in order to reflect (and thus map) the portfolio losses (that lie naturally on the left side) to the right side of the probability distribution, after which they use standard statistical considerations. However, here in this thesis, since both the losses (left-side of distribution) and gains (right-side of distribution) are considered, the derivation of Rockafellar and Uryasev is modifed to account for such two-sided considerations without reflecting or any other mapping tricks. In other words, the modifications to the original derivation of Rockafellar and Uryasev enable the use of losses (negative numbers) and gains (positive numbers) as they naturally lie on the left and right sides of the probablity distribution, respectively.

Using the outcomes, $f(\boldsymbol{x},\boldsymbol{y})$, and probability density function, $p(\boldsymbol{y})$, the cumulative probability distribution function $\Psi(\boldsymbol{x},\gamma)$ for fixed (deterministic) $\boldsymbol{x}$ is written in the following equation (Rockafellar and Uryasev, 2000) as defined in Section 2.3.

$$\Psi(\boldsymbol{x},\gamma) = \int_{f(\boldsymbol{x},\boldsymbol{y})\leq\gamma} p(\boldsymbol{y})d\boldsymbol{y} \tag{2.10}$$

Ψ is defined as the probability of $f(\boldsymbol{x},\boldsymbol{y})$ not exceeding γ. Since Ψ is assumed to be continuous everywhere and non-decreasing with respect to γ, VaR_α is the left endpoint of the nonempty interval consisting of the values γ such that $\Psi(\boldsymbol{x},\gamma) = \alpha$ where α is the confidence level, i.e. $\Psi(\boldsymbol{x}, VaR_\alpha) = \alpha$ or the optimal value of γ is VaR_α (Rockafellar and Uryasev, 2000). In general, confidence level, α is taken as 95%, i.e. $\alpha = 0.95$ and $\beta = (1-\alpha) = 0.05$. The cumulative distribution function determines the behavior of this random variable and it is fundamental in defining VaR and CVaR (Rockafellar and Uryasev, 2000).

The following equations (Equation 2.11 and Equation 2.12), actually determine / locate VaR$^+$ and CVaR$^+$ for the right side of the probability distribution of $f(\boldsymbol{x},\boldsymbol{y})$. For the right side where naturally positive outcomes of $f(\boldsymbol{x},\boldsymbol{y})$ lie,

$$VaR^+ = VaR_\alpha = min\,\{\gamma:\ \Psi(\boldsymbol{x},\gamma) \geq \alpha\} \tag{2.11}$$

where $\Psi(\boldsymbol{x},\gamma)$ is defined in Equation 2.10.

For illustrative reasons, the random variable is taken as a one dimensional vector **y** in Figure 2.3 and 2.4. VaR$^+$ for the right side of probability distribution of $f(\boldsymbol{x},\boldsymbol{y})$ is shown in Figure 2.3.

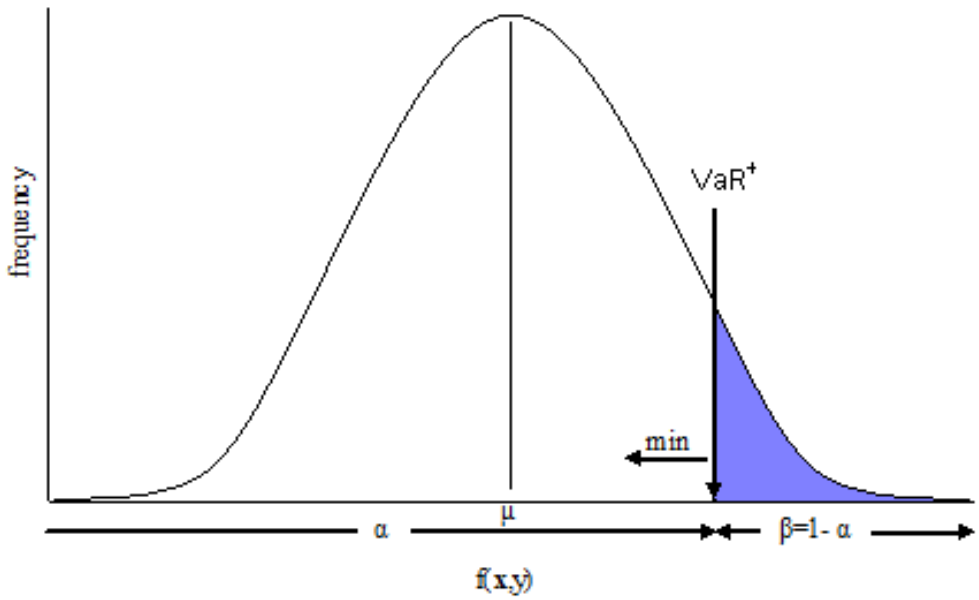

Figure 2.3. Illustration of VaR$^+$ for the right side of probability distribution of $f(\boldsymbol{x},\boldsymbol{y})$.

In this figure one can see that for the right side, so called the upside tail, VaR$^+$ gives the minimum possible value that can be obtained for $f(\boldsymbol{x},\boldsymbol{y})$ at, for example, 95% confidence level. This means that, one is now aware that with 95% probability $f(\boldsymbol{x},\boldsymbol{y})$ will not take a value more than the obtained VaR$^+$, or with 5% probability it will take a value more than the obtained VaR$^+$.

Since $CVaR_\alpha$ is the conditional expectation (mean) of the outcome associated with $\boldsymbol{x}$ relative to that outcome being greater than or equal to VaR_α, $CVaR^+$ (or $CVaR_\alpha$) for the right side of the probability distribution of $f(\boldsymbol{x},\boldsymbol{y})$ is determined by the following equation (Rockafellar and Uryasev, 2000):

$$CVaR^+ = CVaR_\alpha = (1-\alpha)^{-1} \int_{f(\boldsymbol{x},\boldsymbol{y}) \geq VaR_\alpha} f(\boldsymbol{x},\boldsymbol{y})\, p(\boldsymbol{y}) d\boldsymbol{y} \tag{2.12}$$

Equation 2.12 shows the mathematical expression of $CVaR_\alpha$ which is the conditional expectation of the outcome associated with $\boldsymbol{x}$ relative to that outcome being greater than or equal to VaR_α. As mentioned before, $\Psi(\boldsymbol{x}, VaR_\alpha) = \alpha$. The probability that $f(\boldsymbol{x},\boldsymbol{y}) \geq VaR_\alpha$ is then equal to $1-\alpha$. Therefore $CVaR_\alpha$ is obtained by dividing the integral by $(1-\alpha)$.

Figure 2.4 illustrates both VaR^+ and $CVaR^+$ for the right side of probability distribution of $f(\boldsymbol{x},\boldsymbol{y})$. The probability distribution includes a one dimensional random vector **y** since the figure is one dimensional.

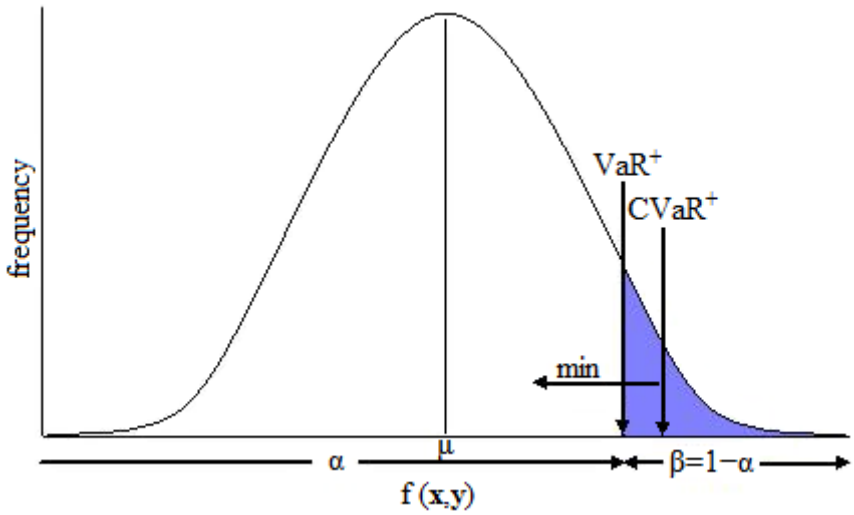

Figure 2.4. Illustration of VaR^+ and $CVaR^+$ for the right side of probability distribution of $f(\boldsymbol{x},\boldsymbol{y})$.

Combining Equation 2.11 and 2.12 Rockafellar and Uryasev (2000) define F_α function from which $CVaR^+$ can be derived:

$$F_\alpha(\boldsymbol{x},\gamma) = \gamma + (1-\alpha)^{-1} \int_y [f(\boldsymbol{x},\boldsymbol{y}) - \gamma]^+ \, p(\boldsymbol{y}) d\boldsymbol{y} \tag{2.13}$$

where $[t]^+ = t$ when $t > 0$ but $[t]^+ = 0$ when $t \leq 0$.

By definition, $F_\alpha(\boldsymbol{x},\gamma)$ is convex and continuously differentiable and it is assumed that $\Psi(\boldsymbol{x},\gamma)$ is continuous with respect to γ. Then the γ values minimizing F_α are obtained by equating derivative of F_α (with respect to γ) to zero, which can easily be found to satisfy $\Psi(\boldsymbol{x},\gamma) - \alpha = 0$. Furthermore, the value of γ minimizing F_α is exactly the VaR_α value. This result is summarized by the following equation,

$$\min_\gamma F_\alpha(\boldsymbol{x},\gamma) = F_\alpha(\boldsymbol{x}, VaR_\alpha) \tag{2.14}$$

Incorporating F_α (Equation 2.13), with the definitions of $CVaR_\alpha$ (Equation 2.12) and Ψ (Equation 2.10), into Equation 2.14, Rockafellar and Uryasev (2000) obtain a novel definition for $CVaR_\alpha$ given by Equation 2.15.

$$CVaR_\alpha = \min_\gamma F_\alpha(\boldsymbol{x},\gamma) \tag{2.15}$$

Rockafellar and Uryasev (2000) also show that, minimizing the $CVaR_\alpha$ of the outcomes associated with $\boldsymbol{x}$ is equivalent to minimizing $F_\alpha(\boldsymbol{x},\gamma)$ with respect to $(\boldsymbol{x},\gamma)$ as in the following equation,

$$\min_{\boldsymbol{x}} CVaR_\alpha = \min_{(\boldsymbol{x},\gamma)} F_\alpha(\boldsymbol{x},\gamma) \tag{2.16}$$

Also, the discrete form of performance function F_α, namely $\bar{F}_\alpha$, which can be approximated by sampling the probability distribution of $f(\boldsymbol{x},\boldsymbol{y})$, can be written as,

$$\bar{F}_\alpha(\boldsymbol{x},\gamma) = \gamma + \frac{1}{N(1-\alpha)} \sum_{k=1}^{N} [f(\boldsymbol{x}, y_k) - \gamma]^+ \tag{2.17}$$

where $[t]^+ = t$ when $t > 0$ but $[t]^+ = 0$ when $t \leq 0$.

For the left side of probability distribution of $f(\boldsymbol{x},\boldsymbol{y})$ where naturally negative outcomes of $f(\boldsymbol{x},\boldsymbol{y})$ lie, the cumulative probability distribution function $\Psi(\boldsymbol{x},\eta)$ for fixed (deterministic) $\boldsymbol{x}$ is given in the following equality similar to Equation 2.10.

$$\Psi(\boldsymbol{x},\eta) = \int_{f(\boldsymbol{x},\boldsymbol{y})\leq\eta} p(\boldsymbol{y})d\boldsymbol{y} \tag{2.18}$$

Using $f(\boldsymbol{x},\boldsymbol{y})$ instead of $\boldsymbol{X}$, Equation 2.3 takes the form,

$$VaR_{\alpha}\big(f(\boldsymbol{x},\boldsymbol{y})\big) = -\,VaR_{(1-\alpha)}\big(-f(\boldsymbol{x},\boldsymbol{y})\big) \tag{2.19}$$

which means that calculating VaR^{+} of $f(\boldsymbol{x},\boldsymbol{y})$ is same as calculating the negative of VaR^{-} of reflected $f(\boldsymbol{x},\boldsymbol{y})$.

The optimal η in Equation 2.18 is $\mathrm{VaR}_{(1-\alpha)}$. Then, and VaR^{-} (or $\mathrm{VaR}_{(1-\alpha)}$) for the right side of the probability distribution of $f(\boldsymbol{x},\boldsymbol{y})$ is determined by the following equation:

$$VaR^{-} = VaR_{(1-\alpha)} = max\,\{\eta \in \mathbb{R}\colon\ \Psi(\boldsymbol{x},\eta) \leq 1-\alpha\} \tag{2.20}$$

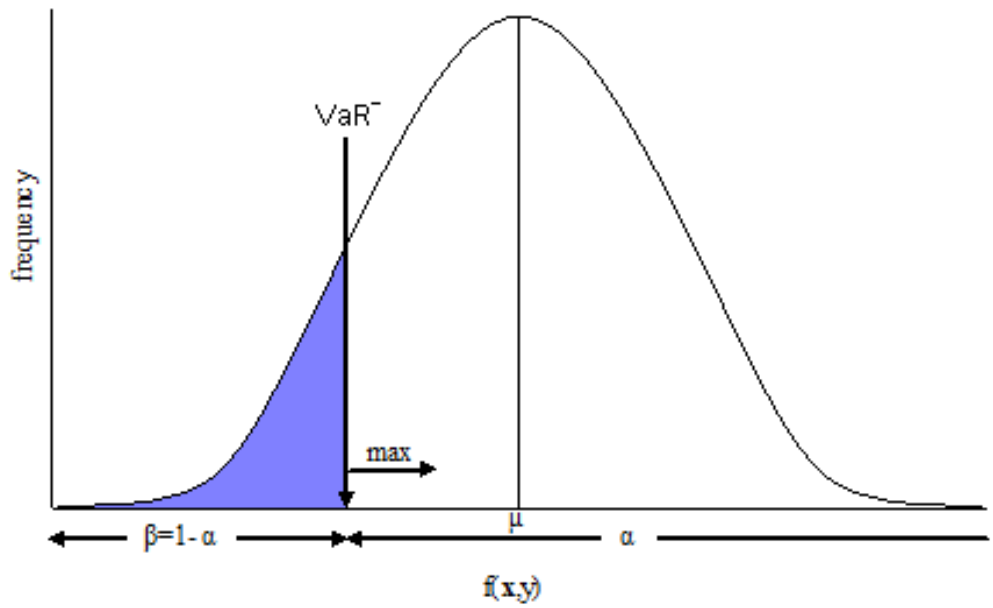

Figure 2.5. Illustration of VaR^{-} for the left side of probability distribution of $f(\boldsymbol{x},\boldsymbol{y})$.

Figure 2.5 illustrates VaR^{-} for the left side of probability distribution of $f(\boldsymbol{x},\boldsymbol{y})$. In this figure one can see that for the left side, so called the downside tail, VaR^{-} gives the maximum possible value that can be obtained for $f(\boldsymbol{x},\boldsymbol{y})$ at, for example, 95% confidence level. This means that, one is now aware that with 95% probability $f(\boldsymbol{x},\boldsymbol{y})$ will not take a value less than the obtained VaR^{-}, or with 5% probability it will take a value less than the obtained VaR^{-}.

Similarly, CVaR$_{(1-\alpha)}$ can also be written as,

$$CVaR_{(1-\alpha)} = (1-\alpha)^{-1} \int_{f(\boldsymbol{x},\boldsymbol{y}) \leq VaR_{(1-\alpha)}} f(\boldsymbol{x},\boldsymbol{y}) p(\boldsymbol{y}) d\boldsymbol{y} \tag{2.21}$$

Then, $F_{(1-\alpha)}$ is written as,

$$F_{(1-\alpha)}(\boldsymbol{x},\eta) = \eta - (1-\alpha)^{-1} \int_{y} [f(\boldsymbol{x},\boldsymbol{y}) - \eta]^{-}\, p(\boldsymbol{y}) d\boldsymbol{y} \tag{2.22}$$

Discrete form of Equation 2.22, $\bar{F}_{(1-\alpha)}$, can be written as,

$$\bar{F}_{(1-\alpha)}(\boldsymbol{x},\eta) = \eta - \frac{1}{N(1-\alpha)} \sum_{i=1}^{N} [f(\boldsymbol{x}, y_i) - \eta]^{-} \tag{2.23}$$

where $[t]^{-} = t$ when $t < 0$ but $[t]^{-} = 0$ when $t \geq 0$.

Figure 2.6 illustrates both VaR^{-} and CVaR^{-} for the left side of probability distribution of $f(\boldsymbol{x},\boldsymbol{y})$. The probability distribution includes a one dimensional random vector **y** since the figure is one dimensional.

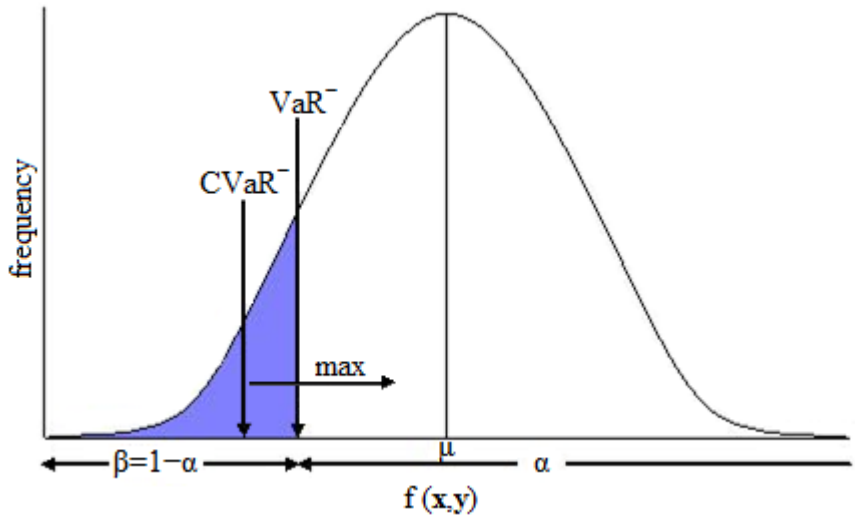

Figure 2.6. Illustration of VaR⁻ and CVaR⁻ for the left side of probability distribution of $f(\boldsymbol{x},\boldsymbol{y})$.

2.6. Parametric VaR and CVaR

Assuming that the random variable (e.g., J_{NPW}) is normally distributed, with arbitrary mean μ and arbitrary standard deviation σ, the parametric VaR (PVaR) and parametric CVaR (PCVaR) can be computed analytically based on the two parameters of a normal distribution, μ and σ as follows (Rockafellar and Uryasev, 2000):

$$\begin{aligned} I_{VaR} &= \sqrt{2}\, erf^{-1}(2\alpha - 1) \\ PVaR^{+} &= PVaR_{\alpha} = \mu + I_{VaR}\, \sigma \\ PVaR^{-} &= PVaR_{(1-\alpha)} = \mu - I_{VaR}\, \sigma \end{aligned} \tag{2.24}$$

$$\begin{aligned} I_{CVaR} &= \left[\sqrt{2\pi}\, e^{(1-\alpha)\left(erf^{-1}(2\alpha-1)\right)^{2}}\right]^{-1} \\ PCVaR^{+} &= PCVaR_{\alpha} = \mu + I_{CVaR}\, \sigma \\ PCVaR^{-} &= PCVaR_{(1-\alpha)} = \mu - I_{CVaR}\, \sigma \end{aligned} \tag{2.25}$$

where, $PVaR$ is parametric VaR for the right side and left side, $PVaR_{\alpha}$ and $PVaR_{(1-\alpha)}$, $PCVaR$ is parametric CVaR for the right side and left side, $PCVaR_{\alpha}$ and $PCVaR_{(1-\alpha)}$, I is

inverse error function for VaR and CVaR, I_{VaR} and I_{CVaR}, μ is mean value of J_{NPW}, σ is standard deviation of J_{NPW}.

2.7. Optimization Formulations of CVaR$^+$ and CVaR$^-$

$\bar{F}_\alpha$ and $\bar{F}_{(1-\alpha)}$ for discrete distributions are restated in the following equations

$$\bar{F}_\alpha(\boldsymbol{x},\gamma) = \gamma + \frac{1}{N(1-\alpha)}\sum_{i=1}^{N}[f(\boldsymbol{x},y_i) - \gamma]^+ \tag{2.26}$$

where, $[t]^+ = t$ when $t > 0$, otherwise $[t]^+ = 0$.

$$\bar{F}_{(1-\alpha)}(\boldsymbol{x},\eta) = \eta - \frac{1}{N(1-\alpha)}\sum_{i=1}^{N}[f(\boldsymbol{x},y_i) - \eta]^- \tag{2.27}$$

where $[t]^- = t$ when $t < 0$, otherwise $[t]^- = 0$.

The computation of CVaR$^+$ and CVaR$^-$ via solution of the optimization problem defined by Equation 2.24 and Equation 2.25 is difficult due to discontinuity arising from the terms $[t]^+$ and $[t]^-$. However, Rockafellar and Uryasev (2000) showed that the computation of CVaR can be posed as an LP problem via exact linearization of the discontinuous term. The solution of the LP problem also yields the corresponding VaR$^+$ or VaR$^-$.

In order to convert Equation 2.24 or Equation 2.25 to exactly equivalent LP form Rockafellar and Uryasev (2000) define an auxiliary variable vector, $\boldsymbol{z}$, with lower bound of zero and of dimension N (number of samples) to get rid of the discontinuity and add an additional linear constraint vector of dimension N.

For CVaR$^+$:

$$\min_{\gamma, z_i^+} \quad F_\alpha = \gamma + \frac{1}{N(1-\alpha)} \sum_{i=1}^{N} z_i^+$$

$$\begin{aligned} s.t. \quad & z_i^+ \geq f(\boldsymbol{x}, \boldsymbol{y}) - \gamma \qquad i = 1, \dots, N \\ & z_i^+ \geq 0 \qquad i = 1, \dots, N \end{aligned} \tag{2.28}$$

For CVaR$^-$:

$$\max_{\eta, z_i^-} \quad F_{(1-\alpha)} = \eta - \frac{1}{N(1-\alpha)} \sum_{i=1}^{N} z_i^-$$

$$\begin{aligned} s.t. \quad & z_i^- \geq \eta - f(\boldsymbol{x}, \boldsymbol{y}) \qquad i = 1, \dots, N \\ & z_i^- \geq 0 \qquad i = 1, \dots, N \end{aligned} \tag{2.29}$$

where, γ^* is VaR$^+$ of the distribution at the optimal solution, ($\gamma^* = VaR^+$), η^* is VaR$^-$ of the distribution at the optimal solution, ($\eta^* = VaR^-$), F_α^* is CVaR$^+$ of the distribution at the optimal solution, ($F_\alpha^* = CVaR^+$), $F_{(1-\alpha)}^*$ is CVaR$^-$ of the distribution at the optimal solution, ($F_{(1-\alpha)}^* = CVaR^-$), α is confidence percentile (cl) (usually taken as 0.95), N is number of scenarios (nMCS samples, N = nMCS), $\boldsymbol{z}$ is auxiliary variable, i is scenario index, $\boldsymbol{x}$ is deterministic fixed variables (portfolio weights, design variables, ...), $\boldsymbol{y}$ is probabilistic uncertain variables (stock returns, raw material cost scenarios, ...), f is random variable determined by $\boldsymbol{x}$ and $\boldsymbol{y}$ values.

Once the random variable $f(\boldsymbol{x}, \boldsymbol{y})$ vector is determined, for example via MCS, the solutions of these LPs give VaR$^+$, CVaR$^+$, VaR$^-$ and CVaR$^-$ of the probability distribution of $f(\boldsymbol{x}, \boldsymbol{y})$, respectively.

2.8. Rachev Ratio and its Linear Optimization

In financial engineering applications, particularly in portfolio optimizations, the use of CVaR as the objective function aims at the diversification of the assets such that the porfolio risk charaterized by CVaR (actually, CVaR$^-$) is minimized subject to satisfaction

of the desired portfolio return constraint. In other words, in bulk of the applications, the concern is at the risk of losses, i.e., the left side of the return distribution where naturally negative return values lie (assuming that the mean value of the returns is zero). However, it is also desirable for investors to invest in a portfolio, the return distribution of which has a high probability of reward (i.e., the right side of the return distribution is of concern). Actually, the statistical measure "skewness" correctly describes the main wish of common investors who prefer portfolios with positively-skewed return distributions (skewed to the right). Unfortunately, in real markets, it is almost impossible to find set of several stocks that will form a portfolio with significant positive skewness and, at the same time, that will have very low risk of loss, and yet, at the same time, that will satisfy minimum desired mean portfolio return criterion. In reality, what is observed is that the stocks that show high probability of large gains also show high probability of large losses (as extreme values or not).

In order to consider both the risk and reward sides of the distribution of portfolio returns simultaneously and thus to obtain a portfolio distribution with positive skewness (more probability of positive returns) a new risk performance measure, called Rachev Ratio (RR), was proposed by Biglova *et al.* (2004). The RR, which can be put in words as "the ratio of expected surplus and expected shortfall" (Konno *et al.*, 2011), is defined as follows (Biglova *et al.*, 2004):

$$RR = \frac{CVaR^{+}}{CVaR^{-}} \tag{2.30}$$

When the RR is used in portfolio optimization as the objective function to be maximized, the NLP problem becomes nonconvex. If the CVaRs in the numerator and denominator of RR are calculated using percentiles (see Equation 2.8), as done in Biglova and Rachev (2004), the RR, in theory, can be maximized (i.e., RR can be used as the objective function in portfolio optimization) using a global NLP solver to avoid getting trapped in local extrema. However, if the Uryasev's linear formulation (Rockafellar and Uryasev, 2000) is substituted for the CVaR terms of the numerator and denominator of the RR in Equation 2.30, the NLP problem becomes nonconvex since the ratio of two linear (convex) functions is nonconvex. Yet, this is not the major problem; the impossibility of maximizing the RR with Uryasev's linear formulation is due to the fact that $CVaR^{+}$ in the

numerator, when maximized, is unbounded. Similarly, $CVaR^{-}$ in the denominator, when expressed via Uryasev's linear form, cannot be minimized (in order to maximize the RR) since $CVaR^{-}$ in the minimization direction is also unbounded. These unboundednesses are due to unbounded z's in Equation 2.28 and Equation 2.29. The unboundedness due to unbounded z's stems from the fact that the cumulative distribution functions in the definitions of VaR_{α} and $CVaR_{\alpha}$ are nondecreasing and right-continuous (Rockafellar and Uryasev, 2001), therefore maximizing one of these functions results in unbounded solution. Actually, Figures 2.4 and 2.6 pictorially depict the bounded directions for minimization of $CVaR^{+}$ and maximization of $CVaR^{-}$ via small arrows on the probability distributions, respectively.

In the literature, there are two attempts to solve the RR maximization problem without calculating the percentiles directly as represented by Equation 2.8 (i.e., as ordered set of numbers).

The first one is due to Stoyanov *et al.* (2007) where the unboundedness in the numerator ($CVaR^{+}$ related) is avoided using an optimization representation of the percentile computation of $CVaR^{+}$, where the percentile is considered as the largest α^{th} number in an ordered sequence (α is the confidence level), and the CVaR is taken as the mean of the remaining numbers greater than the percentile. The denominator ($CVaR^{-}$) is calculated through Uryasev's linear optimization form. However, optimization representation of the percentile calculation leads to a large MILP itself, where the cardinality of the set of binary variables is equal to the number of scenarios (e.g., number of daily returns). Therefore, as commented by Stoyanov *et al.* (2007), this method of maximizing RR is not practical for large problems.

The second one is due to Konno *et al.* (2011) where the maximization RR is first converted to minimization of 1/RR (i.e., min $CVaR^{-}$ / $CVaR^{+}$). Starting thus with minimization of the ratio of two linear functions, the authors then resort to Charnes and Cooper transformation (Charnes and Cooper, 1962) which converts the nonlinear ratio minimization problem to a standard LP with the use of auxiliary variables and augmented set of constraints. Unfortunately, Charnes and Cooper transformation works if the nominator and denominator are either both positive or both negative. In order to solve this

problem the authors propose a novel method; they subtract/add the mean of the distribution to the original scenario numbers from/to the numerator/denomintor of the original RR, respectively, and thus make sure that all data are positive. The ratio of this shifted data is no more identical to the known RR so they call it Modified Rachev Ratio (MRR) and solve the problem by minimizing 1/MRR as minimization of ($CVaR^{-}$ + mean) / ($CVaR^{+}$ − mean). However, more importantly, the Charnes and Cooper transformation introduces a nonconvex equality constraint which turns out to be related to the sum of M largest numbers of a sequence, and the authors represent this constraint by a system of linear equalities and inequalities by introducing 0-1 integer variables. Therefore, this time, the optimization representation of the sum of M largest numbers of a sequence leads to a large MILP itself, where the cardinality of the set of binary variables is, again, equal to the number of scenarios (e.g., number of daily returns). Therefore, as commented by Konno *et al.* (2011) as well, this method of minimizing 1/RR is not practical for large problems.

As mentioned at the onset of this section, in finance applications, the RR, as the ratio of expected surplus (reward/gain) to expected shortfall (risk/loss), is maximized to obtain a portfolio return distribution with positive skewness. The minimization of RR does not have a significant meaning for the finance sector and thus, has never been considered in portfolio optimizations. However, in engineering applications under uncertainty, the minimization of the RR may have a meaning as important as its maximization. For instance, it may be of interest to compress the probability distribution of scenarios due to uncertainties (e.g., distribution of ROI, NPW, profit, cost, etc. under uncertain raw materials / energy cost, market demand, etc.) around the mean which makes the mean more certain, or, in other words, less risky. Therefore the minimization of the RR is also considered in this thesis work. What is further considered in this thesis work, similar to minimizing RR, is the minimization of the difference between the positive (e.g., Equation 2.28) and negative (e.g., Equation 2.29) risk measures, i.e., minimization of [$CVaR^{+}$ − $CVaR^{-}$]. This approach does basically the same job of compressing the probability distribution around the mean to make the mean more certain (less risky) and is much simpler; requiring no further modification to Uryasev's linear form for CVaR.

The derivation for the linearization of RR minimization is parallel to what was done by Konno *et al.* (2011) for the minimization of 1/RR. However, the minimization of RR

does not involve the unboundedness problem, and thus, is simpler; yielding only LP. The starting point is the Charnes and Cooper transformation for the ratio of the sums of linear functions, i.e., the following optimization problem is considered:

$$\begin{aligned} \min_{\boldsymbol{x}} \quad & \left(\sum_{j\in J} c_j x_j + \alpha\right) / \left(\sum_{j\in J} d_j x_j + \beta\right) \\ \text{s.t.} \quad & \sum_{j\in J} a_{ij} x_j \geq b_i \qquad \forall\, i \in I \\ & x_j \geq 0 \qquad \forall\, j \in J \end{aligned} \tag{2.31}$$

Assuming the value of the denominator of the objective function is positive, a new scalar variable, t, is introduced via the following equation:

$$t = \frac{1}{\sum_{j\in J} d_j x_j + \beta} \tag{2.32}$$

The objective function is written in terms of t in Equation 2.33. An additional constraint for the modified version of Equation 2.31 is added. Also, due to the positive values assumption for the denominator of the objective function, $t > 0$ is added as a constraint.

$$\begin{aligned} \min_{\boldsymbol{x}, t} \quad & \sum_{j\in J} c_j x_j\, t + \alpha t \\ \text{s.t.} \quad & \sum_{j\in J} a_{ij} x_j \geq b_i \quad \forall\, i \in I \\ & \sum_{j\in J} d_j x_j t + \beta t = 1 \\ & t > 0 \\ & x_j \geq 0 \quad \forall\, j \in J \end{aligned} \tag{2.33}$$

Then, both sides of the original constraints are multiplied by t and new variables y_j are inserted instead of "x_j multiplied by t".

$$y_j = x_j t \qquad \forall\, j \in J \tag{2.34}$$

$$\begin{aligned} \min_{\boldsymbol{y},t} \quad & \textstyle\sum_{j\in J} c_j y_j + \alpha t \\ \text{s.t.} \quad & \textstyle\sum_{j\in J} a_{ij} y_j \geq b_i t \quad \forall\, i \in I \\ & \textstyle\sum_{j\in J} d_j y_j + \beta t = 1 \\ & t > 0 \\ & y_j \geq 0 \quad \forall\, j \in J \end{aligned} \tag{2.35}$$

Since the ratio of the sums of linear functions are optimized in the original problem addressed by the Charnes and Cooper transformation, the values α and β in Equation 2.31 are two constants. The transformation is applied to minimization of RR, in other words, minimization of [CVaR$^+$ / CVaR$^-$] as follows. The two constants α and β in Equation 2.31 are considered as zero in this case and x_j in Equation 2.31 contains γ (optimum value of which corresponds to VaR$^+$) and η (optimum value of which corresponds to VaR$^-$) as two of its last three elements, and the last element refers to the scalar variable t. Letting $k = 1/N(1-\alpha)$ minimization of [CVaR$^+$ / CVaR$^-$] (i.e., Equation 2.28 divided by Equation 2.29) can be written as,

$$\min \quad \frac{\left(\gamma + k\sum_{i=1}^{N} z_i^+\right)}{\left(\eta - k\sum_{i=1}^{N} z_i^-\right)} \tag{2.36}$$

where, z_i^+ and z_i^- coming from the constraints in Equation 2.28 and 2.29 are given in Equation 2.37. The outcomes of $f(\boldsymbol{x},\boldsymbol{y})$ are expressed with J_i.

$$\begin{aligned} z_i^+ &\geq J_i - \gamma & i &= 1,\dots,N \\ z_i^- &\geq \eta - J_i & i &= 1,\dots,N \\ z_i^+ &\geq 0 & i &= 1,\dots,N \\ z_i^- &\geq 0 & i &= 1,\dots,N \end{aligned} \tag{2.37}$$

Combining the two inequalities in Equation 2.38 and adding one into the last row for the scalar variable t, the augmented vector of variables, $\mathbf{x}$, is formed. This vector $\mathbf{x}$ packs all the variables in CVaR$^+$ and CVaR$^-$ optimization formulations into the form suitable for the Charnes and Cooper transformation given above.

$$\mathbf{x}_{(2N+3)\times 1} = [z_1^+ \quad z_2^+ \quad \dots \quad z_N^+ \quad z_1^- \quad z_2^- \quad \dots \quad z_N^- \quad \gamma \quad \eta \quad 1]' \tag{2.38}$$

Following the Charnes and Cooper transformation steps, after introducing t, the new augmented vector of auxiliary variables **y** is obtained as follows.

$$\mathbf{y}_{(2N+3)\times 1} = [z_1^+ t \quad z_2^+ t \quad \dots \quad z_N^+ t \quad z_1^- t \quad z_2^- t \quad \dots \quad z_N^- t \quad \gamma t \quad \eta t \quad t]' \tag{2.39}$$

The coefficient vector for the numerator in Equation 2.36 is named as **c** and the coefficient vector for the denominator is called **d**. When written for CVaR$^+$ and CVaR$^-$ forms, they take the following forms.

$$\mathbf{c}_{1\times(2N+3)} = [(k \quad k \quad \dots \quad k)_{1\times N} \quad (0 \quad 0 \quad \dots \quad 0)_{1\times N} \quad 1 \quad 0 \quad 0] \tag{2.40}$$

$$\mathbf{d}_{1\times(2N+3)} = [(0 \quad 0 \quad \dots \quad 0)_{1\times N} \quad (-k \quad -k \quad \dots \quad -k)_{1\times N} \quad 0 \quad 1 \quad 0] \tag{2.41}$$

Rearranging the inequality constraints in Equation 2.37 and multiplying by t,

$$-z_i^+ t - \gamma t + J_i t \leq 0 \quad \text{and} \quad -z_i^- t + \eta t - J_i t \leq 0 \tag{2.42}$$

Then, the coefficient matrix and the right-hand-side vector for the inequality constraints are given below in matrices **A** and **B**, respectively.

$$\mathbf{A} = \begin{bmatrix} (-\mathbf{I})_{2N\times 2N} & \begin{pmatrix} -\mathbf{1} \\ \mathbf{0} \end{pmatrix}_{2N\times 1} & \begin{pmatrix} \mathbf{0} \\ \mathbf{1} \end{pmatrix}_{2N\times 1} & \begin{pmatrix} \mathbf{J} \\ -\mathbf{J} \end{pmatrix}_{2N\times 1} \\ 0 \dots & 0 & 0 & -1 \end{bmatrix}_{(2N+1)\times(2N+3)} \tag{2.43}$$

$$\mathbf{B} = [\mathbf{0}]_{(2N+1)\times 1} \tag{2.44}$$

Finally, via the reformulation of Equation 2.36 in terms of the above definitions of **x**, **y**, **c**, **d**, **A**, and **B**, an equivalent matrix form of Equation 2.35 for the linearized RR minimization is obtained as the following LP formulation.

$$\begin{aligned} \min_{\mathbf{y}} \quad & \mathbf{c}\,\mathbf{y} \\ \text{s.t.} \quad & \mathbf{A}\,\mathbf{y} \leq \mathbf{B} \\ & \mathbf{d}\,\mathbf{y} = 1 \\ & \mathbf{y} \geq 0 \end{aligned} \tag{2.45}$$

The solution of the above large LP gives the optimal values of the auxiliary decision variables, $\mathbf{y}^*$. Assuming that the last element of this vector, t, is nonzero, the optimal original augmented vector, $\mathbf{x}^*$, is obtained by dividing $\mathbf{y}^*$ via t^*. Counting from the last element backwards, the second and third elements of $\mathbf{x}^*$ give η^* and γ^* which are true VaR^- and VaR^+ values of the probability distribution of J_i. $\mathrm{CVaR}^\pm$ values can then be obtained by evaluating the denominator.

As a final remark, it should be noted here that the maximization or minimization of skewness, which is the third moment of a probability distribution, though possible in theory, belongs to nonconvex NLP class, and requires global solution of highly nonlinear 3rd moment equations, and thus, is not practiced in real life large portfolio optimization problems; although higher moment optimizations in portfolio optimization receives some interest from academia lately.

3. PROCESS OPTIMIZATION UNDER UNCERTAINTY VIA CVaR

In this chapter, first optimization problems under uncertainty are categorized and some Monte Carlo Simulation (MCS) methods are briefly mentioned. Then, mathematical formulations for "the optimal design under uncertainty via CVaR" problem are developed, and the suggested sequential and simultaneous solution methods via the MCS are discussed. Different objective functions are considered and their expected outcomes are discussed and presented with illustrations.

3.1. Optimization under Uncertainty

In general, the "optimal synthesis, design, and operation under uncertainty" type problems are posed as stochastic optimization problems. The objective is to maximize the expected value of the performance function over all possible realizations of uncertain parameters under design / operation constraints (in view of engineering purposes, mass and energy balances as equality constraints, equipment limitations as inequality constraints, etc). Typically, the objective (performance) function is the maximization of profit, e.g., in terms of the Net Present Worth (NPW), or minimization of the cost. The uncertain parameters may be the market demand, production volume, raw-material availability, raw-material price, product price, and process inputs (temperature, pressure, flowrate, compositions, ...).

In literature, optimization under uncertainty is generally categorized as "here and now", "wait and see", and "chance constrained optimization" (Vajda, 1972; Nemhauser *et al*., 1989; Diwekar, 2008).

In the "here and now" class of problems, probabilistic optimization problems are solved, where the objective function and constraints should be represented probabilistically. The probabilistic/stochastic measures may be the expected value, mode, variance, percentile, etc. which yield optimal solutions at a given level of confidence. The generalized representation of this type of problem may be given as follows:

$$\begin{aligned} \underset{\boldsymbol{x}}{opt} \quad & J = P_1(\boldsymbol{j}(\boldsymbol{x},\boldsymbol{u})) \\ s.t \quad & P_2\big(\boldsymbol{h}(\boldsymbol{x},\boldsymbol{u})\big) = 0 \\ & P_3(\boldsymbol{g}(\boldsymbol{x},\boldsymbol{u}) \geq \boldsymbol{0}) \geq \alpha \end{aligned} \tag{3.1}$$

where $\boldsymbol{x}$ stands for decision variables and $\boldsymbol{u}$ symbolize uncertain variables, $\boldsymbol{j}$ is the objective function associated with $\boldsymbol{x}$ and each realization of $\boldsymbol{u}$, $\boldsymbol{P}$ represents the cumulative distribution functional (e.g., an operator such as the expected value), J is the value of the objective (e.g., the expected value of the objective), α is the confidence level, $\boldsymbol{h}$ and $\boldsymbol{g}$ specify equality and inequality constraints, respectively.

The following figure (Diwekar, 2008) shows that for the "here and now" problems, the stochastic model lies inside the optimization loop.

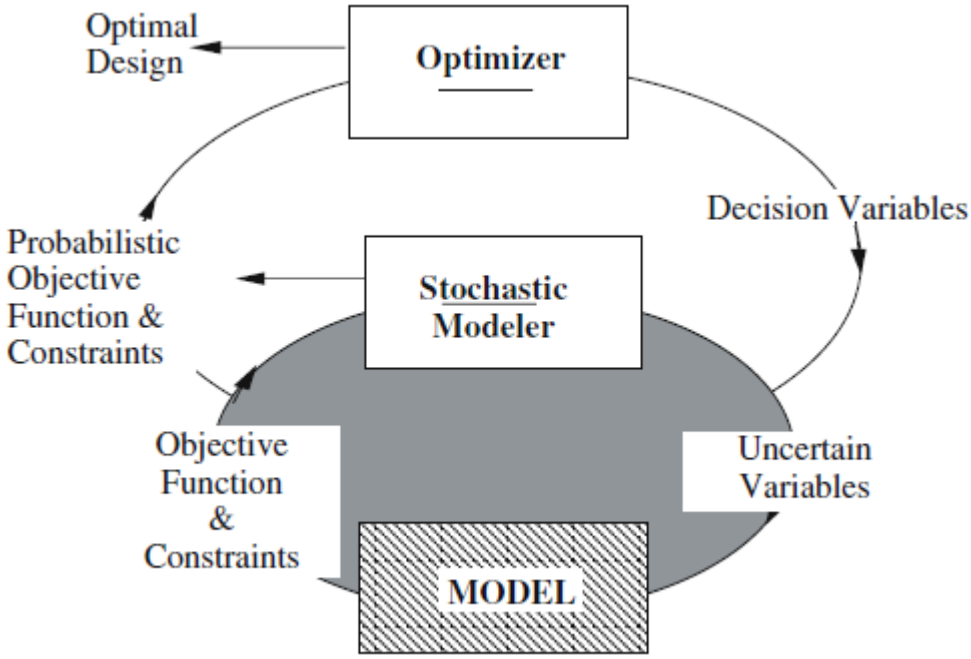

Figure 3.1. Model for Here and Now type of problems (Diwekar, 2008).

In the "wait and see" class of problems, random values are assigned to the uncertain parameters at each MCS trial. Therefore, for each random sample, the uncertainty problem becomes deterministic type of problem. Then, the deterministic optimization problems are solved, where deterministic optimal decisions are taken at each random scenario. The mathematical formulation for these problems may be given as:

$$\begin{aligned} \underset{\boldsymbol{x}}{opt} \quad & Z_i = \boldsymbol{z}(\boldsymbol{x}, \boldsymbol{u}_i^*) \\ s.t \quad & \boldsymbol{h}(\boldsymbol{x}, \boldsymbol{u}_i^*) = \boldsymbol{0} \\ & \boldsymbol{g}(\boldsymbol{x}, \boldsymbol{u}_i^*) \leq \boldsymbol{0} \end{aligned} \tag{3.2}$$

where $\boldsymbol{x}$ is the vector of decision variables, $\boldsymbol{u}^*$ is the vector of values of uncertain variables corresponding to each scenario or sample, $\boldsymbol{z}$ is the output (objective) function associated with $\boldsymbol{x}$ and each realization of $\boldsymbol{u}^*$, Z_i is the outcome of the objective (e.g., the expected value) for each realization of $\boldsymbol{u}^*$, i represents the current scenario, $\boldsymbol{h}$ and $\boldsymbol{g}$ respectively, represent the equality and inequality constraints associated with $\boldsymbol{x}$ and $\boldsymbol{u}^*$.

The visual representation of this category is given by Figure 3.2 (Diwekar, 2008) which shows that the deterministic model forms the inner loop and stochastic model forms the outer loop.

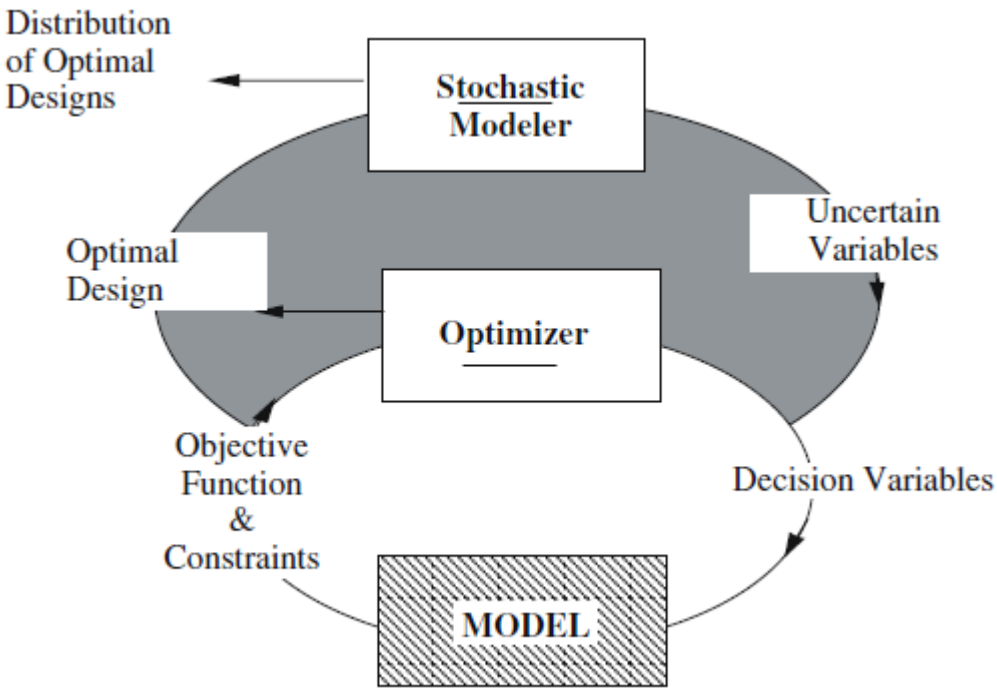

Figure 3.2. Model for Wait and See type of problems (Diwekar, 2008).

Chance-constrained optimization may also be considered as the “here and now” type problem. However, it involves constraints that are not expected to be satisfied always. For this kind of problems, the distribution of the uncertain variables, $\boldsymbol{u}$, is assumed to be a

stable distribution, and such constraints are converted into deterministic ones. If the shape of a distribution is preserved under linear combination of independent copies of itself, it has a stable distribution (Nolan, 2011). As examples of stable distributions we can state normal, cauchy, uniform, and chi-square distributions among others. In chance-constrained optimization, uncertainty distributions are stable distribution functions, and if the uncertain variables appear linearly in the chance constraint, then the model satisfies the convexity conditions. A general formulation for chance-constrained optimization may be given as:

$$\begin{aligned} \underset{\boldsymbol{x}}{opt} \quad & J = P_1\big(\boldsymbol{j}(\boldsymbol{x},\boldsymbol{u})\big) = E(\boldsymbol{j}(\boldsymbol{x},\boldsymbol{u})) \\ s.t \quad & P(\boldsymbol{g}(\boldsymbol{x}) \leq \boldsymbol{u}) \leq \alpha \end{aligned} \tag{3.3}$$

where P_1 shows the cumulative distribution functional which may be equal to the expectation operator, $E(\boldsymbol{j})$. For chance constrained optimization, $\boldsymbol{j}$ is the outcome function associated with $\boldsymbol{x}$ and $\boldsymbol{u}$, the inequality constraint which involves P as the probability of $\boldsymbol{g}(\boldsymbol{x})$ being less than $\boldsymbol{u}$, represents the chance constraint, α is the level of confidence, and $\boldsymbol{g}$ represents the inequality constraint associated with $\boldsymbol{x}$ and $\boldsymbol{u}$.

Among the widely used distribution functions used in the chance-constrained optimization, the uniform, normal and beta distributions (the normal distribution is used for the distribution of the uncertain variables in this thesis) are reviewed below for the ease of referencing.

Probability density function for the *Uniform/Rectangular* distribution is

$$u(x;\alpha,\beta) = \begin{cases} \frac{1}{\beta-\alpha} & for\ \alpha < x < \beta \\ 0 & elsewhere \end{cases} \tag{3.4}$$

$$-\infty < \alpha < \beta < \infty$$

Mean and variance:

$$\mu = \frac{\alpha+\beta}{2} \quad and \quad \sigma^2 = \frac{1}{12}(\beta-\alpha)^2 \tag{3.5}$$

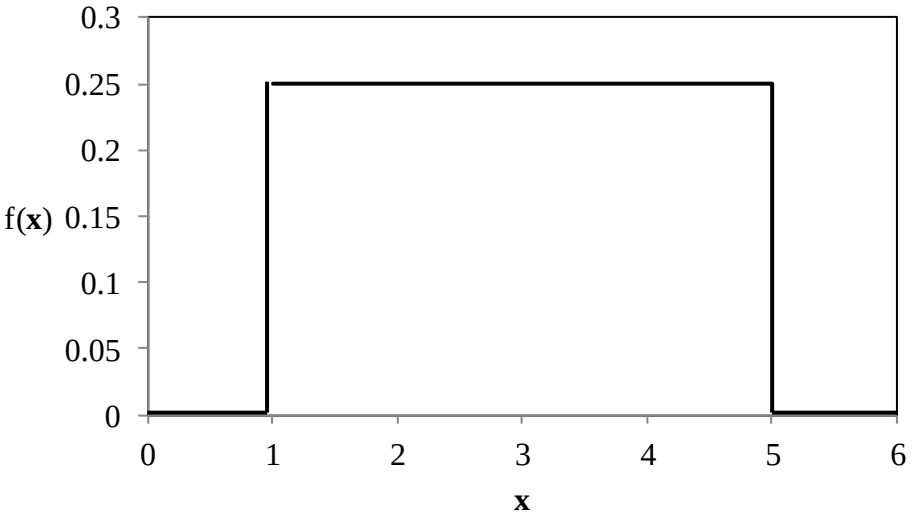

Figure 3.3. A uniform distribution.

Probability density function for the *Normal/Gaussian* distribution is

$$n(x;\mu,\sigma) = \frac{1}{\sigma\sqrt{2\pi}} e^{-\frac{1}{2}\left(\frac{x-\mu}{\sigma}\right)^2} \qquad for\ -\infty < x < \infty$$
$$\mu > 0\ and\ \sigma > 0 \tag{3.6}$$

If a random variable, $\boldsymbol{x}$, has a normal distribution, it is called as the normal random variable. Mean and variance are the parameters of this distribution. When $\mu = 0$ and $\sigma = 1$ the distribution is called as the standard-normal distribution.

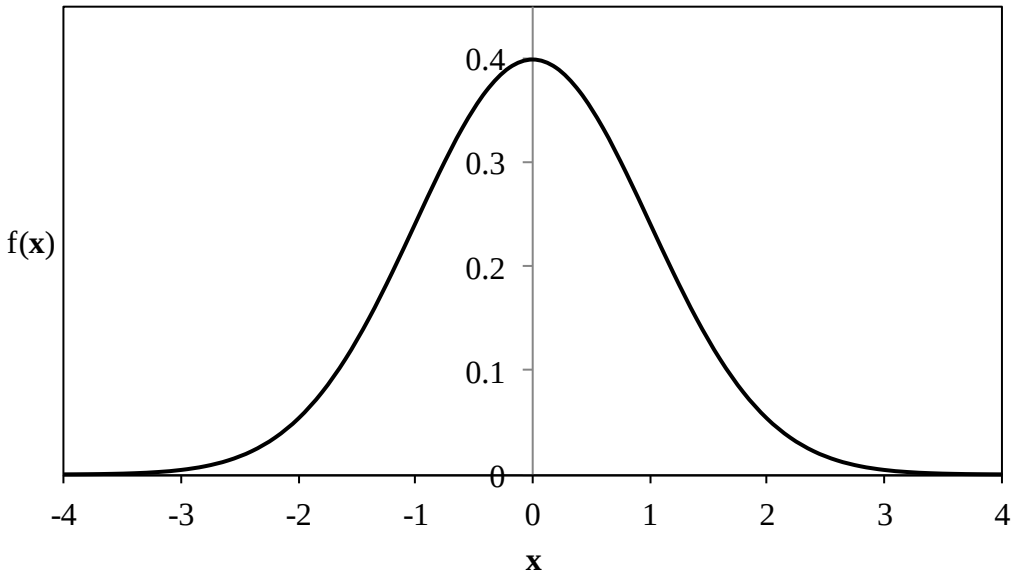

Figure 3.4. The standard normal distribution.

Probability density function for the *Beta* distribution is

$$f(x;\alpha,\beta) = \begin{cases} \frac{1}{B(\alpha,\beta)} x^{\alpha-1}(1-x)^{\beta-1} & for\ 0 < x < 1 \\ 0 & elsewhere \end{cases} \tag{3.7}$$

$$\alpha > 0\ and\ \beta > 0$$

$B(\alpha,\beta)$ is the Beta function which is defined in terms of Gamma function.

$$B(\alpha,\beta) = \frac{\Gamma(\alpha)\Gamma(\beta)}{\Gamma(\alpha+\beta)} \tag{3.8}$$

Mean and variance:

$$\mu = \frac{\alpha}{\alpha+\beta} \quad and \quad \sigma^2 = \frac{\alpha\beta}{(\alpha+\beta)^2(\alpha+\beta+1)} \tag{3.9}$$

For $\alpha = \beta = 1$ the Beta distribution becomes a uniform distribution between zero and one. If α and β are both greater than one the distribution is zero at the end points. If α and/or β is less than one f(0)→∞ and/or f(1)→∞. (Walck, 1996)

The Beta distribution for $\alpha = 6$, $\beta = 3$ and $\alpha = 3$, $\beta = 6$ are shown as examples in the following figure.

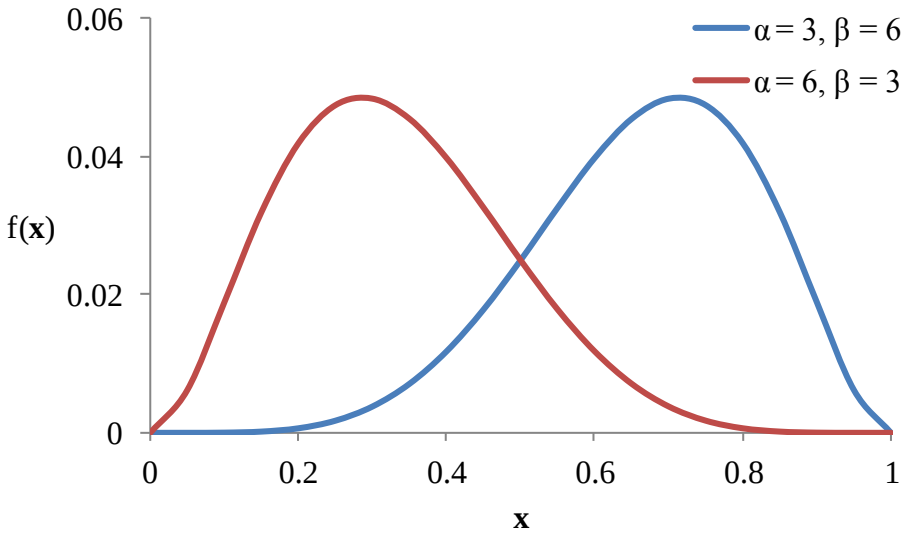

Figure 3.5. Examples to Beta distribution $\alpha = 6$, $\beta = 3$ and $\alpha = 3$, $\beta = 6$.

3.2. Monte Carlo Sampling Method

Uncertainty is modeled through a finite number of independent scenarios which are formed by random samples taken from the probability distributions of the uncertain parameters; i.e., through MCS. Large error bounds and variance can be observed in crude Monte Carlo methods. In order to reduce the variance in the Monte Carlo estimates some variance-reduction techniques are developed as in some other sampling techniques in stochastic modeling (James, 1985). Some of the variance-reduction techniques are Importance Sampling, Latin Hypercube Sampling (LHS; McKay *et al.*, 1979; Iman and Shortencarier, 1984; Iman and Helton, 1988), Hammersley Sequence Sampling (HSS) (Kalagnanam and Diwekar, 1997), Halton Sequence, Sobol Sequence, etc. Classical statistical methods can be used on MCS results. As the number of Monte Carlo (nMC) trials increases, smoother distributions are obtained. In this thesis work the value of nMC

trials are estimated via trial and error or by choosing the approximate value beyond which the changes in both the mean and standard deviation become steady. LHS and HSS improve the computational efficiency of sampling (Diwekar, 2008) compared to the Importance Monte Carlo sampling even at lower nMC trials. However, since the emphasis of this thesis is not on the sampling methods, only crude Monte Carlo sampling is used in the sequential and simultaneous approaches of optimization under uncertainty.

3.3. Sequential and Simultaneous Optimizations under Uncertainty via CVaR

In this thesis, uncertainties in process model inputs are propagated to output distributions through MCS of the uncertainties via generating samples from the normal distributions. The MCS is performed via two approaches; the sequential and simultaneous methods. In the sequential method, the MCS provides the distribution of the process model outputs and the CVaR of the results are then computed as off-line. Whereas, in the simultaneous approach, both the process model equations are augmented for all nMCS scenarios and the CVaR-related equations are optimized at once.

A generic deterministic optimization formulation for process design, synthesis, or operation under certainty may be given as follows:

$$\begin{aligned} \underset{\boldsymbol{d},\boldsymbol{u},\boldsymbol{x}}{opt} \quad & J(\boldsymbol{d},\boldsymbol{u},\boldsymbol{x},\boldsymbol{p}) \\ s.t. \quad & \boldsymbol{h}(\boldsymbol{d},\boldsymbol{u},\boldsymbol{x},\boldsymbol{p}) = \boldsymbol{0} \\ & \boldsymbol{g}(\boldsymbol{d},\boldsymbol{u},\boldsymbol{x},\boldsymbol{p}) \leq \boldsymbol{0} \end{aligned} \tag{3.10}$$

where $\boldsymbol{d}$ is the vector of design variables (reactor volume, number of stages, heat exchanger area, ...), $\boldsymbol{u}$ is the vector of free (manipulated, control) variables (reflux ratio, reaction temperature, flowrate, ...), $\boldsymbol{x}$ is the vector of state variables (intermediate stream temperatures, compositions, ...) whose values can be determined exactly from the equality constraint once the values of $\boldsymbol{d}$ and $\boldsymbol{u}$ are fixed (assuming that the cardinality of $\boldsymbol{x}$ and $\boldsymbol{h}$ are equal for fixed $\boldsymbol{d}$ and $\boldsymbol{u}$), $\boldsymbol{p}$ is the vector of fixed parameters (component properties, external feed properties, ...), $\boldsymbol{h}$ is the vector of equality constraints, mostly due to mass and energy balances or hard production constraints), $\boldsymbol{g}$ is the vector of inequaity constraints

that represents capacity/production limits, product purity limits, safety limits, etc., and J is the scalar objective function to be minimized (cost, total energy consumption, waste, ...) or maximized (profit, conversion, selectivity, purity, ...). The extra degrees of freedom necessary for optimization is due to unknown (free) values of the $\boldsymbol{d}$ and $\boldsymbol{u}$ vectors (or some components of these vectors). The bounds on these free variables ($\boldsymbol{d}$, $\boldsymbol{u}$) can be written as side constraints such as $\boldsymbol{d}_{\mathrm{LOWER}} \leq \boldsymbol{d} \leq \boldsymbol{d}_{\mathrm{UPPER}}$ and $\boldsymbol{u}_{\mathrm{LOWER}} \leq \boldsymbol{u} \leq \boldsymbol{u}_{\mathrm{UPPER}}$, or can be included in the set of inequality constraints, $\boldsymbol{g}$. For realistic Chemical Engineering applications the optimization model is highly nonlinear due to nonlinearity of the phase-equilibrium and thermophysical models, and thus the problem is an NLP problem. If some of the $\boldsymbol{d}$, $\boldsymbol{u}$, $\boldsymbol{x}$ variables are binary/integer then the problem becomes an MINLP problem.

In real life situations, there may be uncertainties associated with some or all of the model parameters, $\boldsymbol{p}$. The uncertainty may also be present in some of the design, $\boldsymbol{d}$, variables, however, in such a case, these uncertain design variables are not considered as decision variables of the optimization problem in Equation 3.10. In either of such cases, the optimal objective, J^*, and decision variables, $\boldsymbol{d}^*$, $\boldsymbol{u}^*$, $\boldsymbol{x}^*$ are not unique since their values depend on a particular realization of the uncertain parameter(s), $\boldsymbol{p}$. Therefore, in such cases, the probability distribution properties, such as the expected value, skewness, VaR^+, VaR^-, CVaR^+, CVaR^-, of the optimal objective, J^*, and decision variables, $\boldsymbol{d}^*$, $\boldsymbol{u}^*$, $\boldsymbol{x}^*$ are of interest. The post-optimal analysis of output uncertainties associated with J^*, $\boldsymbol{d}^*$, $\boldsymbol{u}^*$, $\boldsymbol{x}^*$ may be performed simply via discretization of the input uncertainty space of parameters, $\boldsymbol{p}$, using MCS. Under such a MCS scheme, the problem in Equation 3.10 may be solved either sequentially or simultaneously. Figure 3.6 depicts such MCS schemes.

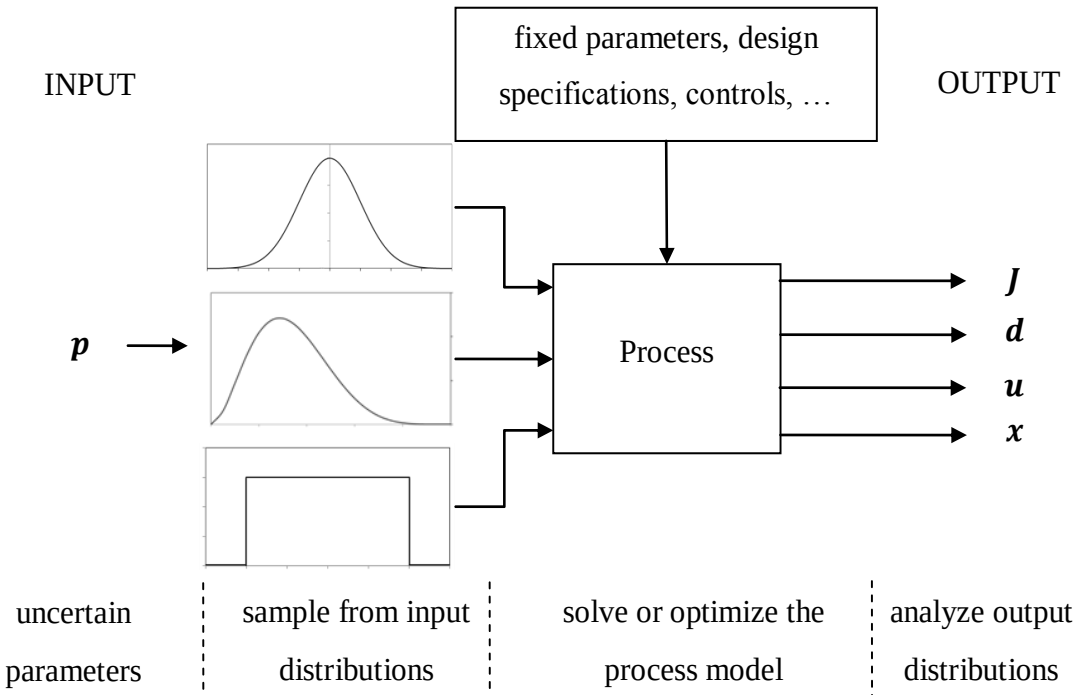

Figure 3.6. MCS of a process.

In the sequential approach, at the ith MCS step (iMCS), the uncertain parameter(s), $\boldsymbol{p}$, are sampled by drawing random number(s) from proper/assumed distribution(s) and the deterministic optimization problem in Equation 3.10, corresponding to this particular realization(s) of the uncertain parameter value(s), are solved to obtain the corresponding optimal objective $J_i^*(\boldsymbol{d}_i^*, \boldsymbol{u}_i^*, \boldsymbol{x}_i^*, \boldsymbol{p}_i)$ subject to $\boldsymbol{h}_i(\boldsymbol{d}_i^*, \boldsymbol{u}_i^*, \boldsymbol{x}_i^*, \boldsymbol{p}_i) = \boldsymbol{0}_i$ and $\boldsymbol{g}_i(\boldsymbol{d}_i^*, \boldsymbol{u}_i^*, \boldsymbol{x}_i^*, \boldsymbol{p}_i) \leq \boldsymbol{0}_i$. This procedure is repeated at each MCS step; i=1, ..., nMCS. nMCS is the maximum number of MCS steps just enough to obtain steady statistical properties from the accumulated J_i^* (or, $\boldsymbol{d}_i^*$, $\boldsymbol{u}_i^*$, $\boldsymbol{x}_i^*$) values. The expected value of the optimal objectives, $E[J_i^*]$, VaR$^{\pm}$ and CVaR$^{\pm}$ values of the optimal objectives, and other statistical parameters such as standard deviation, skewness, kurtosis, ..., can then be computed as off-line. Figure 3.7 gives the flowchart of the sequential approach. Particularly, for the evaluation of VaR$^{\pm}$ and CVaR$^{\pm}$ values of the distribution of optimal J^* values, Equations 2.8 and 2.9 (as quantiles), or Equations 2.28 and 2.29 (from Uryasev's LP optimization formulation) can be used where $f(\boldsymbol{x}, \boldsymbol{y})$ is the set of accumulated optimal objective values, J_i^*. It must be noted that, under such a sequential approach as depicted in Figure 3.7, optimization of the expected value of the objective, $E[J_i]^*$, is not possible. If $E[J_i]^*$ is desired, there must be an outer loop in Figure 3.7. The outer-loop decision variables must be presented as fixed values to the inner loop. The convergence of such an

interlocked-loops scheme may not be guaranteed. Therefore, in this thesis work, the sequential approach is used only to accumulate J_i^* (or, $\boldsymbol{d}_i^*$, $\boldsymbol{u}_i^*$, $\boldsymbol{x}_i^*$) values for the post-analysis (i.e., to compute $E[J_i^*]$, VaR$^{\pm}$ and CVaR$^{\pm}$) of the probability distributions of these accumulated optimal solutions. On the other hand, the simultaneous approach, as will be described below, directly yields the optimal value of the expected objective $E[J_i]^*$, VaR$^{\pm}$ and CVaR$^{\pm}$.

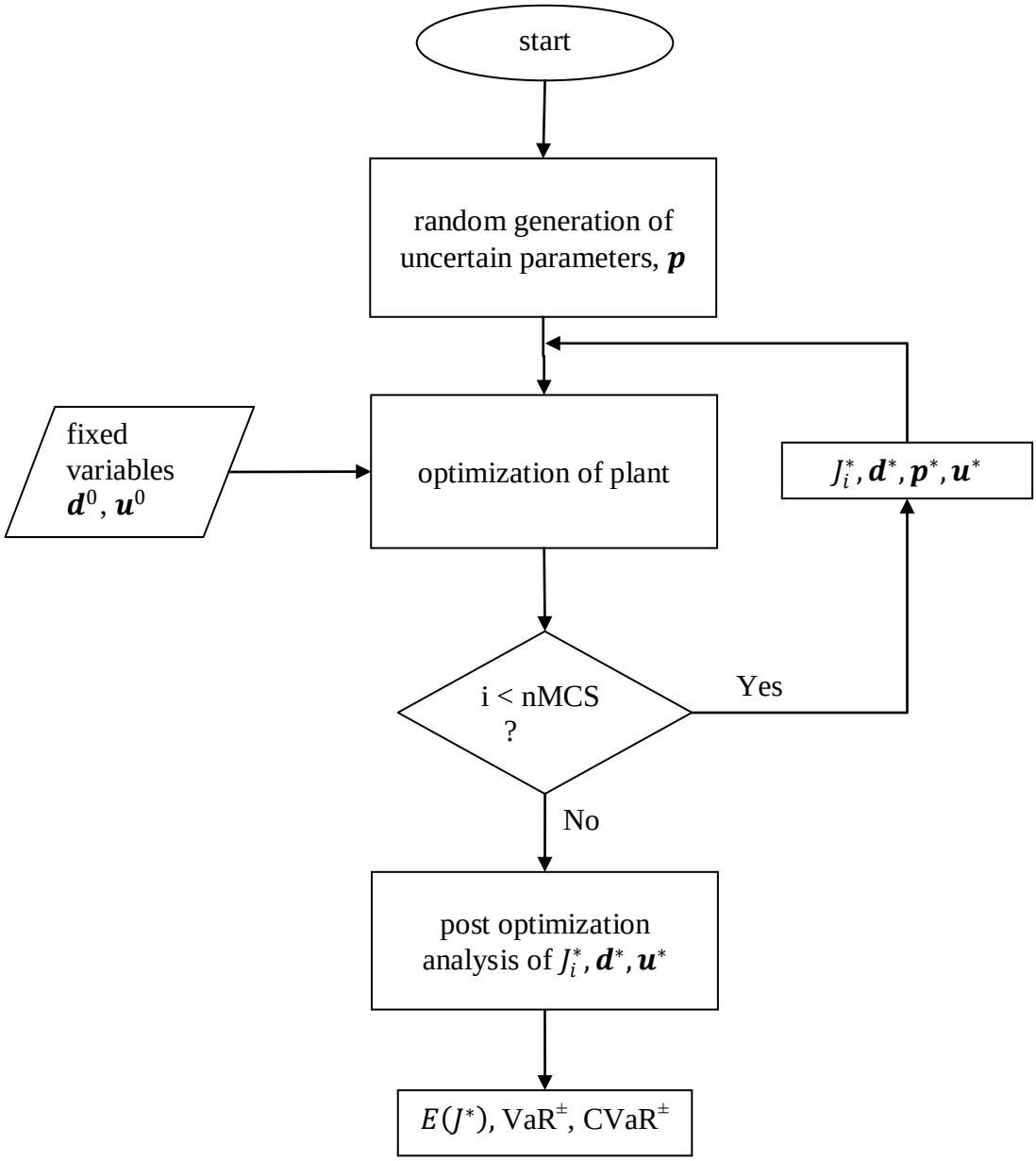

Figure 3.7. Sequential approach.

If there is uncertainty associated with some or all of the model parameters, $\boldsymbol{p}$, then the problem becomes an optimization problem under uncertainty. It should be noted that the uncertainty may also be in some of the design, $\boldsymbol{d}$, variables, and in such a case those design variables are not considered as decision variables of the optimization problem as mentioned before. In such a case, the objective J and the optimal values of other decision variables ($\boldsymbol{d}^*$, $\boldsymbol{u}^*$, $\boldsymbol{x}^*$) are not unique since their values depend on a particular realization of the uncertain parameter(s). Therefore, in such cases, usually the expected value (mean) of J is of concern.

A generic stochastic optimization formulation for process design, synthesis, or operation under uncertainty may thus be given as follows:

$$\begin{aligned} \underset{\boldsymbol{d},\boldsymbol{u},\boldsymbol{x}}{opt} \quad & E\{J(\boldsymbol{d},\boldsymbol{u},\boldsymbol{x},\boldsymbol{p})\} \\ s.t. \quad & \boldsymbol{h}(\boldsymbol{d},\boldsymbol{u},\boldsymbol{x},\boldsymbol{p}) = \boldsymbol{0} \\ & \boldsymbol{g}(\boldsymbol{d},\boldsymbol{u},\boldsymbol{x},\boldsymbol{p}) \leq \boldsymbol{0} \end{aligned} \tag{3.11}$$

It must be noted that in such a representation, the equality and inequality constraints are assumed (forced) to be satisfied exactly for each particular realization of the uncertainty in $\boldsymbol{p}$ values. As is the case in Chemical Engineering, the equality constraints are mostly due to mass/energy balances, and thus, their violation cannot be considered as possible. Therefore, in this thesis work, the probabilistic constraints (chance constraints) are not considered. In other words, the probabilities of violating the mass and energy balances are zero; they must be satisfied exactly at all circumstances. However, chance constraint formulation of the inequalities may be possible, and in such cases it can be represented as

$$P\{\boldsymbol{g}(\boldsymbol{d},\boldsymbol{u},\boldsymbol{x},\boldsymbol{p}) \leq \boldsymbol{0}\} \leq \alpha \tag{3.12}$$

where P represents the cumulative distribution functional (e.g., the expected value, variance, …), α is the confidence level, $\boldsymbol{g}$ specifies inequality constraints associated with $\boldsymbol{d}$ (vector of design variables), $\boldsymbol{u}$ (vector of control variables), $\boldsymbol{x}$ (vector of state variables) and $\boldsymbol{p}$ (vector of fixed parameters).

The generic process optimization formulation under uncertainty described by problem in Equation 3.11 may be solved simply via discretization of the uncertainty space using MCS. Under such a MCS scheme, the problem in Equation 3.11 may be solved via the simultaneous approach.

In the simultaneous approach, the uncertain parameter(s), $\boldsymbol{p}$, are sampled at the beginning, nMCS times, by drawing nMCS random numbers from proper/assumed distribution(s) and the deterministic optimization problem in Equation 3.10, is augmented correspondingly to these nMCS realizations of the uncertain parameter values by replicating each equality and inequality constraint nMCS times as described below:

$$\begin{aligned} \underset{\boldsymbol{d}_i, \boldsymbol{u}_i, \boldsymbol{x}_i}{opt} \quad & E[J_i(\boldsymbol{d}_i, \boldsymbol{u}_i, \boldsymbol{x}_i, \boldsymbol{p}_i)] = \textstyle\sum_{i=1}^{i=nMCS} \frac{J_i(\boldsymbol{d}_i, \boldsymbol{u}_i, \boldsymbol{x}_i, \boldsymbol{p}_i)}{nMCS} \\ s.t. \quad & \boldsymbol{h}_i(\boldsymbol{d}_i, \boldsymbol{u}_i, \boldsymbol{x}_i, \boldsymbol{p}_i) = \boldsymbol{0}_i \quad i = 1, \dots, nMCS \\ & \boldsymbol{g}_i(\boldsymbol{d}_i, \boldsymbol{u}_i, \boldsymbol{x}_i, \boldsymbol{p}_i) \leq \boldsymbol{0}_i \quad i = 1, \dots, nMCS \end{aligned} \tag{3.13}$$

Therefore, under the simultaneous scheme, the large optimization problem in Equation 3.13 is the nMCS times augmented form of Equation 3.11 (nMCS times the number of decision variables, equalities, inequalities), the solution of which yields directly the expected value of the objective $E[J_i(\boldsymbol{d}_i, \boldsymbol{u}_i, \boldsymbol{x}_i, \boldsymbol{p}_i)]^*$. It should be noted that although the problem in Equation 3.13 is a large NLP problem if there is nonlinearity, it becomes LP if the objective and constraints are all linear. Figure 3.8 gives the flowchart of the simultaneous approach. The VaR$^{\pm}$ and CVaR$^{\pm}$ values corresponding to the probability distribution of the optimal objectives, J_i^*, can be computed either as as off-line (as post-optimization analysis), or simultaneously. Particularly, for the simultaneous evaluation of VaR$^{\pm}$ and CVaR$^{\pm}$'s Equations 2.28 and 2.29 (Uryasev optimization of LPs) can be used where $f(\boldsymbol{x}, \boldsymbol{y})$ is the set of accumulated optimal objective values, J_i^*.

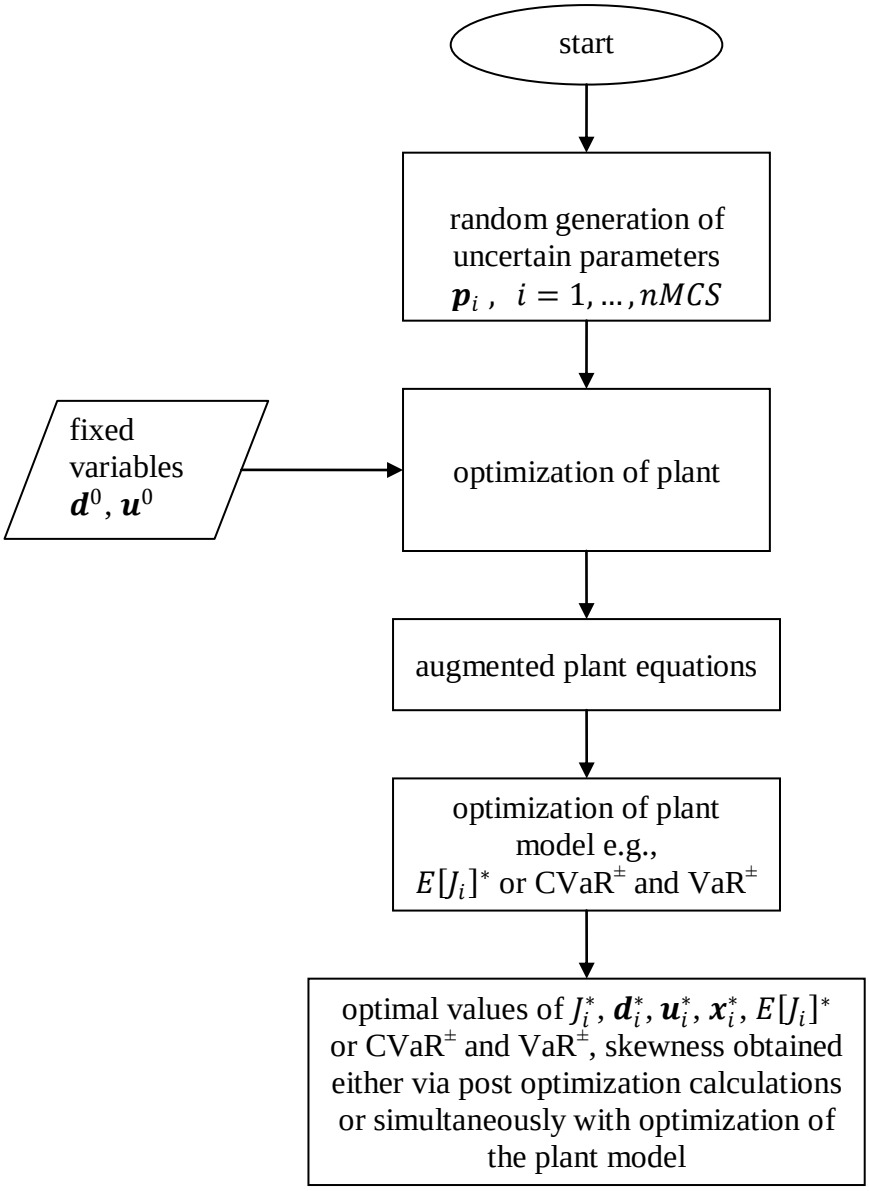

Figure 3.8. Simultaneous approach.

The optimization of the expected value of the objective function, $E[J_i]^*$, does not take into account the skewness and tail probabilities (and thus the risk) associated with the distribution of the objective, J_i^*. Depending on the nature of the problem, several different scenarios may occur in the probability distribution of J_i while optimizing just for the expected value. These hypothetical scenarios are depicted below in Figure 3.9.

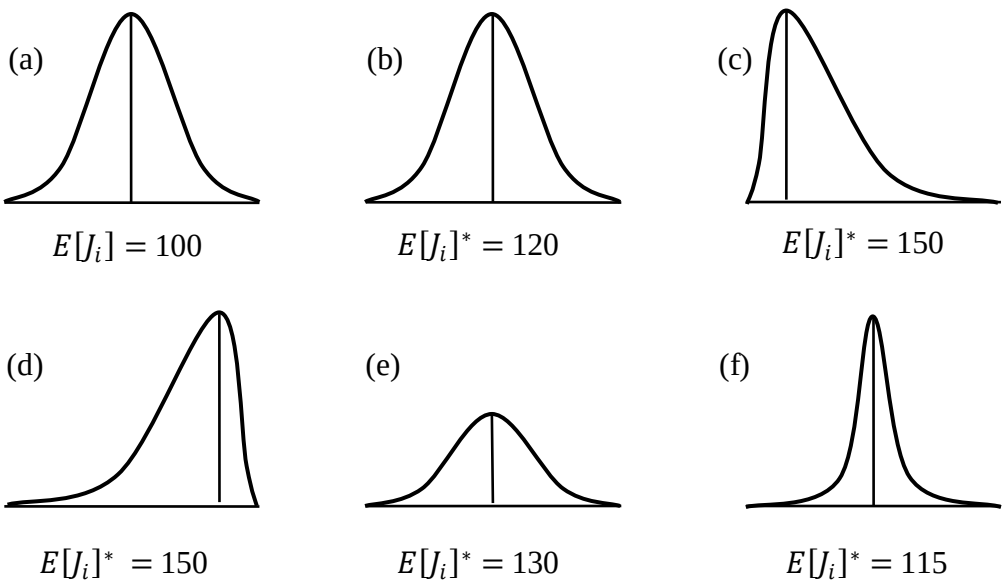

Figure 3.9. Hypothetical scenarios for the expected value of objective, $E[J_i]$, with/without optimization.

In Figure 3.9-a, it is assumed that there is no optimization, and the MCS are performed on a particular plant model using nominal values of decision variables ($\boldsymbol{d^o}$, $\boldsymbol{u^o}$) that satisfy the constraints $\boldsymbol{h}$ and $\boldsymbol{g}$ (owing to the presence of the state vector $\boldsymbol{x}$). It is also assumed that under such a case, the resulting probability distribution has zero skewness (symmetric around the mean with $E[J_i] = 100$). The solution of the problem in Equation 3.13 via, for example, the simultaneous approach may yield probability distributions as depicted by Figure 3.9-b through Figure 3.9-f for different plants. Also, assume that the objective is a profit function to be maximized.

In Figure 3.9-b, the solution of Equation 3.13, for a different plant, does not alter the shape (skewness and kurtosis) of the distribution but as expected increases the mean profit from 100 to 120 units. This outcome is desirable; however, as will be opened below, there

may be more desirable outcomes when not only the expected profit but the risks associated with the profit distribution are also considered.

In Figure 3.9-c, the solution of Equation 3.13, for a different plant, alters both the shape (skewness) and location of the mean profit. The distribution has positive skewness and thus the probability of realizing profit values greater than 150 is much greater than realizing profit values less than 150. This means that the risk of having a profit less than 150 is much less than the reward of having a profit greater than 150. Clearly, when computed off-line (post optimization), the $CVaR^{+}$ value will be much greater than the value of $CVaR^{-}$ for the same confidence level. The hypothetical outcome in Figure 3.9-c is highly desirable since, upon optimization, the company increases the expected profit and increases the chances of realizing even better profits (decreases the chances of getting lower profits).

In Figure 3.9-d, the solution of Equation 3.13, for a different plant, again alters both the shape (skewness) and location of the mean profit, compared to Figure 3.9-a. The distribution has negative skewness and thus the probability of realizing profit values lower than 150 is much greater than realizing profit values greater than 150. This means that the risk of having a profit less than 150 is much higher than the reward of having a profit greater than 150. Clearly, when computed off-line (post optimization), the difference between $CVaR^{-}$ value and optimal value of mean will be much greater than the difference between optimal value of mean and value of $CVaR^{+}$ for the same confidence level. The hypothetical outcome in Figure 3.9-d is not desirable since, upon optimization, the company increases the expected profit (compared to Figure 3.9-a) however increases the chances of realizing worse profits (increases the chances of getting lower profits).

In Figure 3.9-e, the solution of Equation 3.13, for a different plant, alters both the shape and location of the mean profit, compared to Figure 3.9-a, but the skewness is again close to zero (symmetric distribution). The distribution has no skewness however, compared to Figure 3.9-a, the fat tails of the profit distribution increases the probabilities of realizing profit values lower and higher than 130 units. This means that the risk of having a profit much less than 130 and the reward of having a profit much greater than 130 are equally probable. Clearly, when computed off-line (post optimization), the deviations

of the $CVaR^{+}$ and $CVaR^{-}$ values from the mean will be the same, for the same confidence level. The hypothetical outcome in Figure 3.9-e is not desirable either, since, upon optimization, the company increases the expected profit (compared to Figure 3.9-a) as well as increases the chances of realizing better profits at the expense of (perhaps more importantly) increasing the chances of realizing lower profits.

In Figure 3.9-f, the solution of Equation 3.13, for a different plant, again alters both the shape and location of the mean profit. Compared to Figure 3.9-a, and similar to Figure 3.9-e, the skewness is again close to zero (symmetric distribution). The distribution has no skewness however, compared to Figure 3.9-a, the short tails of the profit distribution decreases the probabilities of realizing profit values much lower and much higher than 115 units. This means that the risk of having a profit much less than 115 and the reward of having a profit much greater than 115 are equally probable. Clearly, when computed off-line (post optimization), the deviations of $CVaR^{+}$ and $CVaR^{-}$ values from the optimal value of the mean will be the same but lower than those for Figure 3.9-e, for the same confidence level. The hypothetical outcome in Figure 3.9-f is also desirable (as was the case in Figure 3.9-c) since, upon optimization, the company increases the expected profit (compared to Figure 3.9-a) and at the same time decreases the chances of realizing low profits. The situation in Figure 3.9-f is not as desirable as Figure 3.9-c since, in Figure 3.9-f, the chances of realizing high profits is much lower than that of Figure 3.9-c. However, compared to Figure 3.9-e, the situation in Figure 3.9-f is much more desirable since, in Figure 3.9-f, the narrower distribution increases the confidence in the expected profit. Compared to Figure 3.9-e, where the expected profit is 130 units, the expected profit of 115 units in Figure 3.9-f is lower, however, the risks of realizing expected profit of, for instance, 90 units is much higher in Figure 3.9-e as compared to Figure 3.9-f where company is more sure about its expected profit.

It is the object of this thesis work to obtain distribution of optimal objectives similar to Figure 3.9-c or Figure 3.9-f for, for example, profit type functions, and Figure 3.9-d or Figure 3.9-f for, for example, cost type functions by using / incorporating $CVaR^{+}$ and $CVaR^{-}$ risk measures. In other words, this thesis work aims at the re-shaping / control of distribution of optimal objective in order to favorably adjust the “tail risk” and/or “tail reward”, or certainty of the mean via inclusion of the $CVaR^{-}$ and $CVaR^{+}$ related functions

in the reformulation of problem in Equation 3.13. There are several possibilities of incorporating CVaR^{+} or CVaR^{-} into optimization problems of type Equation 3.13, and these will be elaborated on one by one below.

3.3.1. CVaR^{-} as the Objective Function

The most natural adaptation of portfolio optimization with CVaR^{-} objective to process optimization under uncertainty may be described with problem in Equation 3.14 given below, where the objective is to minimize the loss (left) side tail risk characterized by CVaR^{-}.

$$
\begin{aligned}
\min_{\boldsymbol{d},\boldsymbol{u}_i,\boldsymbol{x}_i,\eta,z_i} \quad & F_{(1-\alpha)} = \eta - \frac{1}{N(1-\alpha)}\sum_{i=1}^{N} z_i \\
s.t. \quad & \left.\begin{array}{c} z_i \geq \eta - J_i(\boldsymbol{d},\boldsymbol{x}_i,\boldsymbol{u}_i,\boldsymbol{p}_i) \\ z_i \geq 0 \end{array}\right\} \begin{array}{c} CVaR\ Constraints\ (linear) \\ i = 1,\dots,N \end{array} \\
& \left.\begin{array}{c} \boldsymbol{h}_i(\boldsymbol{d},\boldsymbol{x}_i,\boldsymbol{u}_i,\boldsymbol{p}_i) = \boldsymbol{0}_i \\ \boldsymbol{g}_i(\boldsymbol{d},\boldsymbol{x}_i,\boldsymbol{u}_i,\boldsymbol{p}_i) \leq \boldsymbol{0}_i \\ \boldsymbol{d}^{lb} \leq \boldsymbol{d} \leq \boldsymbol{d}^{ub} \\ \boldsymbol{u}_i^{lb} \leq \boldsymbol{u}_i \leq \boldsymbol{u}_i^{ub} \\ \boldsymbol{x}_i^{lb} \leq \boldsymbol{x}_i \leq \boldsymbol{x}_i^{ub} \end{array}\right\} \begin{array}{c} Plant\ Constraints \\ (linear\ or\ nonlinear) \\ i = 1,\dots,N \end{array}
\end{aligned}
\tag{3.14}
$$

where, $\boldsymbol{d}$ is vector of design variables, $\boldsymbol{p}$ is vector of uncertain parameters, $\boldsymbol{u}$ is vector of manipulated/control (free) variables, $\boldsymbol{x}$ is vector of state variables, $\boldsymbol{z}$ is N×1 vector of auxiliary variables, J is plant objective function (cost, profit, …), N is number of scenarios (nMCS samples, $N =$ nMCS), η^* is VaR of the distribution, ($\eta^* = VaR^{-}$), F^* is CVaR of the distribution, ($F^*_{(1-\alpha)} = CVaR^{-}$), α is confidence percentile (cl) (usually taken as 0.95), i is scenario index, ($i = 1,\dots,N$), lb is lower bound, ub is upper bound.

It should be noted that, in Equation 3.14, the design vector $\boldsymbol{d}$ does not have a sub-index, i, which, otherwise, would have denoted the dependence of the design vector on the ith realization of the uncertain parameter vector $\boldsymbol{p}$. The unindexed $\boldsymbol{d}$ signifies that the design should have an optimal value common for all realizations of the parameter vector. In other words, at the end of the optimization, the single optimal design vector, $\boldsymbol{d}^*$, should enable feasible operation of the plant for all possible values of the uncertain parameter

vector, $\boldsymbol{p}_i$, for $i = 1$, ..., nMCS. This is required to be so since the design decisions taken/implemented at the design stage (e.g., reactor volume, number of distillation trays, ...) cannot be altered in the operation stage as different realizations of the uncertain parameters are experienced. Such, operation-stage adjustments against random parameter realizations are handled via manipulated/control variable vector, $\boldsymbol{u}_i$, which has the sub-index, i. The equality, $\boldsymbol{h}_i$, and inequality, $\boldsymbol{g}_i$, constraints have sub-indexes since the plant mass and energy balances should be satisfied at all realizations of the uncertainty in $\boldsymbol{p}_i$, and their feasibility at the optimal solution are due to the presence of manipulated/control variable vector, $\boldsymbol{u}_i$, and the state variable vector, $\boldsymbol{x}_i$, both of which have the sub-index, i.

Under the simultaneous scheme, one-time solution of the large optimization problem in Equation 3.14 yields the optimal values of the design, control, and state vectors as well as the risk measures VaR^{-} and CVaR^{-}. The corresponding values of the plant objective values, J_i, though not included in Equation 3.14, can be evaluated afterwards, and thus the expected value of the plant objective, $E[J_i]$, can be computed offline. It should be noted that, the optimal values of CVaR^{-} and VaR^{-} are implicitly calculated from the set of plant objective values, J_i, corresponding to each realization of uncertainty in the parameter vector since the objective function of Equation 3.14 is the Uryasev's (Rockafellar and Uryasev, 2000) linear optimization representation of CVaR^{-} and VaR^{-}.

In general, the large-scale (due to augmented plant model for each random sample) problem in Equation 3.14 is an NLP problem. However, since the CVaR^{-} related part of the equations (objective function and first two vectors of constraints) are linear, if the plant model is also linear, then Equation 3.14 is an LP problem, and if some of the decision variables are binary or integer, problem in Equation 3.14 is an MILP problem. Therefore, if the problem in Equation 3.14 is completely linear, its solution is relatively straightforward even for large MCS samples.

It should be noted that problem in Equation 3.14 is a maximization problem since the loss-/left-side tail risk of the probability distribution of the plant objective values is minimized in terms of the risk measure CVaR^{-}. The problem should not be converted to minimization form since it is unbounded in that direction (due to unboundedness of the vector of auxiliary variables, $\boldsymbol{z}$, as mentioned in the previous chapter). Anyhow, an attempt

to minimize the objective of problem in Equation 3.14 corresponds to maximization of the loss-/left-side tail risk of the probability distribution of the plant objective values, which is meaningless.

Figure 3.10 depicts the conceived role of problem in Equation 3.14 in reshaping the probability distribution of the plant objective values, J_i. Before the application of Equation 3.14, the expected value of profit is 100 units, and, at α confidence level, the expected value of the tail profit, CVaR^{-}, is 20 units; very roughly indicating that even though the mean profit is 100 units, there is a certain chance that it may be expected to be as low as 20 units. On the other hand, after the application of Equation 3.14, although the expected value of profit is 90 units, at α confidence level, the expected value of the tail profit, CVaR^{-}, is 40 units; very roughly indicating that, upon optimization, even though the mean profit decreases from 100 to 90 units, the tail risk also decreases from 20 units to a better value of 40 units. One of the purposes of this hypothetical figure is to point out that, upon optimization of problem in Equation 3.14 to decrease the left-tail risk in terms of CVaR^{-}, there is no guarantee that the expected profit will be the same or better. Actually, Figure 3.10 depicts the trade-off between the mean profit and tail risk of the profit, which may be unavoidable in real-life applications. Finally, it should be noted that the above interpretations are still valid if the objective is not profit (positive quantity) but loss (negative quantity).

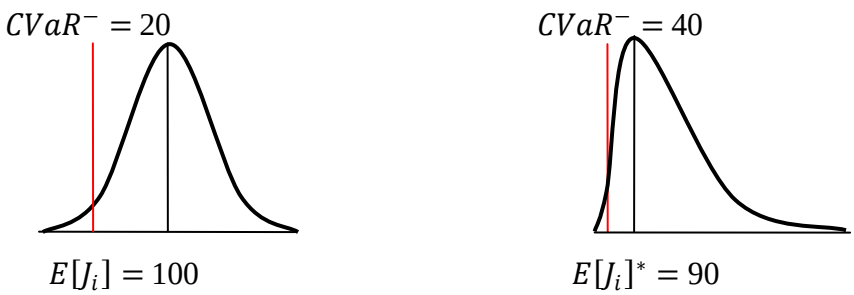

(a) before optimization (b) after optimization

Figure 3.10. Hypothetical scenarios for the CVaR^{-} objective.

3.3.2. CVaR$^+$ as the Objective Function

Optimization with CVaR$^+$ objective in process optimization under uncertainty may be described with problem in Equation 3.15 below, where the objective is to minimize the right-side tail risk of cost (positive quantity) distribution characterized by CVaR$^+$.

$$
\begin{aligned}
\min_{\boldsymbol{d},\boldsymbol{u}_i,\boldsymbol{x}_i,\gamma,z_i} \quad & F_\alpha = \gamma + \frac{1}{N(1-\alpha)}\sum_{i=1}^{N} z_i \\
s.t. \quad & \left.\begin{array}{c} z_i \geq J_i(\boldsymbol{d},\boldsymbol{x}_i,\boldsymbol{u}_i,\boldsymbol{p}_i) - \gamma \\ z_i \geq 0 \end{array}\right\} \begin{array}{c} CVaR\ Constraints\ (linear) \\ i = 1,\dots,N \end{array} \\
& \left.\begin{array}{c} \boldsymbol{h}_i(\boldsymbol{d},\boldsymbol{x}_i,\boldsymbol{u}_i,\boldsymbol{p}_i) = \boldsymbol{0}_i \\ \boldsymbol{g}_i(\boldsymbol{d},\boldsymbol{x}_i,\boldsymbol{u}_i,\boldsymbol{p}_i) \leq \boldsymbol{0}_i \\ \boldsymbol{d}^{lb} \leq \boldsymbol{d} \leq \boldsymbol{d}^{ub} \\ \boldsymbol{u}_i^{lb} \leq \boldsymbol{u}_i \leq \boldsymbol{u}_i^{ub} \\ \boldsymbol{x}_i^{lb} \leq \boldsymbol{x}_i \leq \boldsymbol{x}_i^{ub} \end{array}\right\} \begin{array}{c} Plant\ Constraints \\ (linear\ or\ nonlinear) \\ i = 1,\dots,N \end{array}
\end{aligned}
\tag{3.15}
$$

where, γ^* is VaR of the distribution, ($\gamma^* = VaR^+$), F^* is CVaR of the distribution, ($F_\alpha^* = CVaR^+$).

Under the simultaneous scheme, one-time solution of the large optimization problem in Equation 3.15 yields the optimal values of the design, control, and state vectors as well as the risk measures VaR$^+$ and CVaR$^+$. It should be noted that, the optimal values of CVaR$^+$ and VaR$^+$ are implicitly calculated from the set of plant objective values, J_i, corresponding to each realization of uncertainty in the parameter vector since the objective function of problem in Equation 3.15 is the Uryasev's (Rockafellar and Uryasev, 2000) linear optimization representation of CVaR$^+$ and VaR$^+$. It should be noted that problem in Equation 3.15 is a minimization problem since the reward-/right-side tail risk of the probability distribution of the plant objective values is minimized in terms of the risk measure CVaR$^+$. The problem should not be converted to maximization form since it is unbounded in that direction (due to unboundedness of the vector of auxiliary variables, $\boldsymbol{z}$, as mentioned in the previous chapter). Anyhow, an attempt to maximize the objective of problem in Equation 3.15, for example, when J is a cost, corresponds to maximization of the cost-/right-side tail risk of the probability distribution of the plant objective values, which is meaningless.

Figure 3.11 depicts the conceived role of problem in Equation 3.15 in reshaping the probability distribution of the plant objective (cost) values, J_i. Before the application of Equation 3.15, the expected value of cost is 100 units, and, at α confidence level, the expected value of the right-tail cost (risk), CVaR^+, is 150 units; very roughly indicating that even though the mean cost is 100 units, there is a certain chance that it may be expected to be as high as 150 units. On the other hand, after the application of problem in Equation 3.15, although the expected value of cost is 110 units, at α confidence level, the expected value of the tail cost (risk), CVaR^+, is 135 units; very roughly indicating that, upon optimization, even though the mean cost increases from 100 to 110 units, the tail risk decreases from 150 units to a better value of 135 units. One of the purposes of this hypothetical figure is to point out that there is no guarantee that the expected cost will be the same or lower upon optimization of problem in Equation 3.15 to decrease the right-tail risk in terms of CVaR^+, Actually, Figure 3.11 depicts the trade-off between the mean cost and tail risk of the cost, which may be unavoidable in real-life applications. Finally, it should be noted that the above interpretations are still valid if the objective is not cost (positive quantity) but a loss (negative quantity).

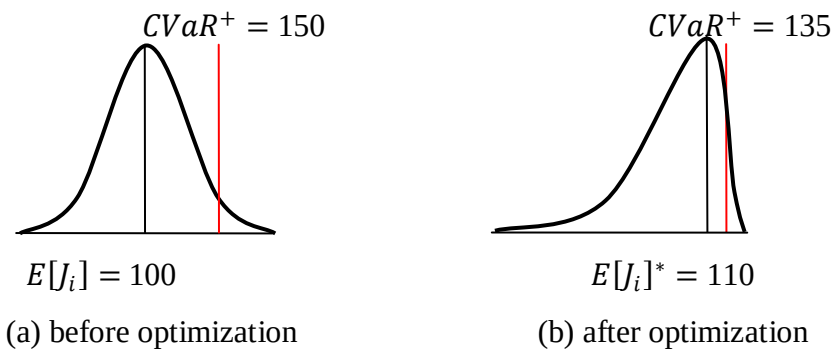

Figure 3.11. Hypothetical scenarios for the CVaR^+ objective.

3.3.3. $[\text{CVaR}^+ - \text{CVaR}^-]$ as the Objective Function

Optimization with the term ($\text{CVaR}^+ - \text{CVaR}^-$) as the objective in process optimization under uncertainty may be described with problem in Equation 3.16 below, where the aim is to minimize both the right- and left-tail risks of, for instance, the profit distribution characterized by the difference between CVaR^+ and CVaR^-.

$$\max_{\boldsymbol{d},\boldsymbol{u}_i,\boldsymbol{x}_i,\gamma,\eta,z_i^-,z_i^+} \quad \left(\gamma + \frac{1}{N(1-\alpha)}\sum_{i=1}^{N} z_i^+\right) - \left(\eta - \frac{1}{N(1-\alpha)}\sum_{i=1}^{N} z_i^-\right)$$

$$s.t. \quad \left.\begin{array}{l} z_i^- \geq \eta - J_i(\boldsymbol{d},\boldsymbol{x}_i,\boldsymbol{u}_i,\boldsymbol{p}_i) \\ z_i^+ \geq J_i(\boldsymbol{d},\boldsymbol{x}_i,\boldsymbol{u}_i,\boldsymbol{p}_i) - \gamma \\ z_i^- \geq 0 \\ z_i^+ \geq 0 \end{array}\right\} \begin{array}{c} CVaR\ Constraints\ (linear) \\ i = 1,\dots,N \end{array} \tag{3.16}$$

$$\left.\begin{array}{c} \boldsymbol{h}_i(\boldsymbol{d},\boldsymbol{x}_i,\boldsymbol{u}_i,\boldsymbol{p}_i) = \boldsymbol{0}_i \\ \boldsymbol{g}_i(\boldsymbol{d},\boldsymbol{x}_i,\boldsymbol{u}_i,\boldsymbol{p}_i) \leq \boldsymbol{0}_i \\ \boldsymbol{d}^{lb} \leq \boldsymbol{d} \leq \boldsymbol{d}^{ub} \\ \boldsymbol{u}_i^{lb} \leq \boldsymbol{u}_i \leq \boldsymbol{u}_i^{ub} \\ \boldsymbol{x}_i^{lb} \leq \boldsymbol{x}_i \leq \boldsymbol{x}_i^{ub} \end{array}\right\} \begin{array}{c} Plant\ Constraints \\ (linear\ or\ nonlinear) \\ i = 1,\dots,N \end{array}$$

where, γ^* is VaR of the distribution, ($\gamma^* = VaR^+$), η^* is VaR of the distribution, ($\eta^* = VaR^-$).

Under the simultaneous scheme, one-time solution of the large optimization problem in Equation 3.16 yields the optimal values of the design, control, and state vectors as well as the risk measures VaR^-, VaR^+, CVaR^-, and CVaR^+. It should be noted that, the optimal values of $\text{CVaR}^\pm$ and $\text{VaR}^\pm$ are implicitly calculated from the set of plant objective values, J_i, corresponding to each realization of uncertainty in the parameter vector since the objective function of Equation 3.16 is the Uryasev's (Rockafellar and Uryasev, 2000) linear optimization representation of $\text{CVaR}^\pm$ and $\text{VaR}^\pm$. It should be noted that problem in Equation 3.16 is a minimization problem and is bounded. Since the first bracketed term in the objective is the linear CVaR^+ function and the second bracketed term is the linear CVaR^- function, their difference is also linear and the mimimization of the "$-\text{CVaR}^-$" term corresponds to maximization of "$+\text{CVaR}^-$" function, which is bounded as explained in the previous chapter.

The problem in Equation 3.16 aims at compressing the left and right tails toward the mean of the probability distribution. Thus, as a result, the uncertainty about the mean of the distribution is minimized in terms of the difference between the CVaR^+ and CVaR^-. The problem should not be converted to maximization form, or the difference between CVaR^- and CVaR^+ ($\text{CVaR}^- - \text{CVaR}^+$) should not be minimized, since then both bracketed terms of the objective become unbounded (due to unboundedness of the vector of auxiliary

variables, $\boldsymbol{z}^{+}$ and $\boldsymbol{z}^{-}$, as mentioned in the previous chapter). In any case, an attempt to maximize the objective of problem in Equation 3.16 corresponds to maximization of the uncertainty about the mean of the distribution, which is generally meaningless.

Figure 3.12 depicts the conceived role of the formulaton in Equation 3.16 in reshaping the probability distribution of the plant objective (profit) values, J_i. Before the application of problem in Equation 3.16, the expected value of profit is 100 units, and, at α confidence level, the expected value of the left-tail risk, CVaR^{-}, is 20 units and right-tail reward, CVaR^{+}, is 180 units (the difference between CVaR^{+} and CVaR^{-} is 200 units); indicating that there is significant uncertainty about the expected profit. On the other hand, after the application of problem in Equation 3.16, although the expected value of profit is 90 units, at α confidence level, the expected value of the left-tail risk, CVaR^{-}, is 70 units and the right-tail reward, CVaR^{+}, is 110 units (the difference between CVaR^{+} and CVaR^{-} is 40 units); indicating that now, upon optimization, even though the mean profit decreases by 10 units, the "two-tails risk" (the difference between CVaR^{+} and CVaR^{-}) decreases from 160 units to a much better value of 40 units, which increases the confidence (certainty) about the expected profit of the plant. Finally, it should be noted that the above interpretations are still valid if the objective is not profit (positive quantity) but loss (negative quantity). It must be reminded here that if different α confidence levels are used for the left (α^{-}) and right (α^{+}) sides, at least in theory, it is possible to adjust also the skewness of the mean-compressed tails of the probability distribution of plant's profit.

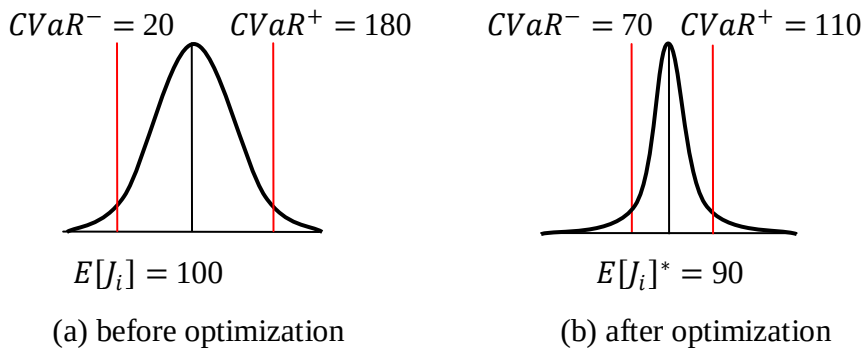

(a) before optimization (b) after optimization

Figure 3.12. Hypothetical scenarios for the ($\mathrm{CVaR}^{+} - \mathrm{CVaR}^{-}$) objective.

3.3.4. [$E[J]$ + CVaR^{-}] as the Objective Function

Multiobjective optimization with weighted plant profit (or cost) objective and CVaR^{-} objective for process optimization under uncertainty may be described with problem in Equation 3.17 below, where the aim is to maximize the expected value of the profit and at the same time minimize the left tail risk of the profit in terms of CVaR^{-}.

$$
\begin{aligned}
\max_{\boldsymbol{d},\boldsymbol{u}_i,\boldsymbol{x}_i,\eta,z_i} \quad & \lambda\left[\frac{1}{N}\sum_{i=1}^{N} J_i(\boldsymbol{d},\boldsymbol{x}_i,\boldsymbol{u}_i,\boldsymbol{p}_i)\right] + (1-\lambda)\left[\eta - \frac{1}{N(1-\alpha)}\sum_{i=1}^{N} z_i\right] \\
s.t. \quad & \left.\begin{array}{c} z_i \geq \eta - J_i(\boldsymbol{d},\boldsymbol{x}_i,\boldsymbol{u}_i,\boldsymbol{p}_i) \\ z_i \geq 0 \end{array}\right\} \begin{array}{c} CVaR\ Constraints\ (linear) \\ i = 1,\dots,N \end{array} \\
& \left.\begin{array}{c} \boldsymbol{h}_i(\boldsymbol{d},\boldsymbol{x}_i,\boldsymbol{u}_i,\boldsymbol{p}_i) = \boldsymbol{0}_i \\ \boldsymbol{g}_i(\boldsymbol{d},\boldsymbol{x}_i,\boldsymbol{u}_i,\boldsymbol{p}_i) \leq \boldsymbol{0}_i \\ \boldsymbol{d}^{lb} \leq \boldsymbol{d} \leq \boldsymbol{d}^{ub} \\ \boldsymbol{u}_i^{lb} \leq \boldsymbol{u}_i \leq \boldsymbol{u}_i^{ub} \\ \boldsymbol{x}_i^{lb} \leq \boldsymbol{x}_i \leq \boldsymbol{x}_i^{ub} \end{array}\right\} \begin{array}{c} Plant\ Constraints \\ (linear\ or\ nonlinear) \\ i = 1,\dots,N \end{array}
\end{aligned}
\tag{3.17}
$$

The first bracket of the objective function is the expected profit, $E[J_i]$, and the second one is the CVaR^{-} function. It must be noted that only at the optimal solution the value of the second bracket is CVaR^{-} and η^* is VaR^{-}. If the plant profit function J is linear then the objective function of problem in Equation 3.17 is linear (convex), and if the plant constraints $\boldsymbol{h}$, and $\boldsymbol{g}$ are also linear, then the entire problem in Equation 3.17 is an LP problem. However, if the plant objective, J, is nonlinear (nonconvex) then the problem in Equation 3.17 should be solved via a global optimizer, since a local extremum may prevent the CVaR^{-} term in the second bracket to be pushed till its limit, yielding meanless η^* value which cannot be taken as VaR^{-}. Also, it must be noticed that in maximization direction, the CVaR^{-} function inside the second bracket is bounded and has a finite value. The constant λ is weighing parameter such that $0 \leq \lambda < 1$. The upper bound of λ cannot be set to unity since then the CVaR^{-} term drops from the objective function and the CVaR^{-} related constraints alone have no meaning (vector of auxiliary variables, $\boldsymbol{z}$, has no upper bound), and thus the value of η cannot be taken as VaR^{-} of the distribution. When $\lambda = 0$, then the problem in Equation 3.17 becomes identical to the problem in Equation 3.14 (minimization of the left-tail risk by maximizing Uryasev's linear formulation). If the plant objective is not profit but cost, then the same formulation is valid after multiplying only the first

bracket by minus one, so that it reads as maximization of negative cost which is identical to minimization of cost.

Figure 3.13 depicts the conceived role of problem in Equation 3.17 in reshaping the probability distribution of the plant objective values, J_i. Compared to Figure 3.10 for which the only objective was the minimization of the left-tail risk, the multiobjective problem in Equation 3.17 increases the mean profit as well as decreasing the left-tail risk. It should be noted that the above interpretations are still valid if the objective is not profit (positive quantity) but loss (negative quantity).

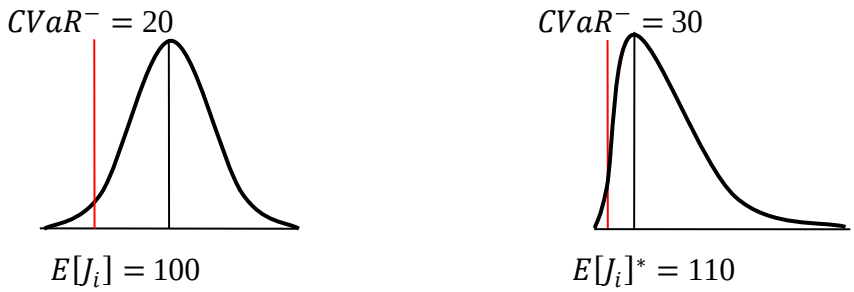

(a) before optimization (b) after optimization

Figure 3.13. Hypothetical scenarios for the ($E[J]$ + CVaR^{-}) objective.

3.3.5. [$E[J]$ + CVaR^{+}] as the Objective Function

Multiobjective optimization with weighted plant cost (positive quantity) objective and CVaR^{+} objective for process optimization under uncertainty may be described with problem in Equation 3.18 below, where the aim is to minimize the expected value of the cost and at the same time minimize the right-tail risk of the cost (probability of excess cost) in terms of CVaR^{+}.

$$
\begin{aligned}
\min_{\boldsymbol{d},\boldsymbol{u}_i,\boldsymbol{x}_i,\gamma,z_i} \quad & \lambda\left[\frac{1}{N}\sum_{i=1}^{N} J_i(\boldsymbol{d},\boldsymbol{x}_i,\boldsymbol{u}_i,\boldsymbol{p}_i)\right] + (1-\lambda)\left[\gamma + \frac{1}{N(1-\alpha)}\sum_{i=1}^{N} z_i\right] \\
s.t. \quad & \left.\begin{aligned} z_i &\geq J_i(\boldsymbol{d},\boldsymbol{x}_i,\boldsymbol{u}_i,\boldsymbol{p}_i) - \gamma \\ z_i &\geq 0 \end{aligned}\right\} \begin{aligned} &CVaR\ Constraints\ (linear) \\ &i = 1,\dots,N \end{aligned} \\
& \left.\begin{aligned} \boldsymbol{h}_i(\boldsymbol{d},\boldsymbol{x}_i,\boldsymbol{u}_i,\boldsymbol{p}_i) &= \boldsymbol{0}_i \\ \boldsymbol{g}_i(\boldsymbol{d},\boldsymbol{x}_i,\boldsymbol{u}_i,\boldsymbol{p}_i) &\leq \boldsymbol{0}_i \\ \boldsymbol{d}^{lb} \leq \boldsymbol{d} &\leq \boldsymbol{d}^{ub} \\ \boldsymbol{u}_i^{lb} \leq \boldsymbol{u}_i &\leq \boldsymbol{u}_i^{ub} \\ \boldsymbol{x}_i^{lb} \leq \boldsymbol{x}_i &\leq \boldsymbol{x}_i^{ub} \end{aligned}\right\} \begin{aligned} &Plant\ Constraints \\ &(linear\ or\ nonlinear) \\ &i = 1,\dots,N \end{aligned}
\end{aligned}
\tag{3.18}
$$

The first bracket of the objective function is the expected cost, $E[J_i]$, and the second one is the CVaR$^+$ function. It must be noted that only at the optimal solution the value of the second bracket is CVaR$^+$ and γ^* is VaR$^+$. If the plant cost function J is linear then the objective function of problem in Equation 3.18 is linear (convex), and if the plant constraints $\boldsymbol{h}$, and $\boldsymbol{g}$ are also linear, then the entire problem in Equation 3.18 is an LP problem. However, if the plant objective, J, is nonlinear (nonconvex) then the problem in Equation 3.18 should be solved via a global optimizer, since a local extremum may prevent the CVaR$^+$ term in the second bracket to be pushed till its limit, yielding meanless γ^* value which cannot be taken as VaR$^+$. Also, it must be noticed that in minimization direction, the CVaR$^+$ function inside the second bracket is bounded and has a finite value. The constant λ is weighing parameter such that $0 \leq \lambda < 1$. The upper bound of λ cannot be set to unity since then the CVaR$^+$ term drops from the objective function and the CVaR$^+$ related constraints alone have no meaning (vector of auxiliary variables, $\boldsymbol{z}$, has no upper bound), and thus the value of γ cannot be taken as VaR$^+$ of the distribution. When $\lambda = 0$, then the problem in Equation 3.18 becomes identical to the problem in Equation 3.15 (minimization of the left-tail risk by maximizing Uryasev's linear formulation). If the plant objective is not cost but profit, then the same formulation is valid after multiplying only the first bracket by minus one, so that it reads as minimization of negative profit which is identical to maximization of profit.

Figure 3.14 depicts the conceived role of problem in Equation 3.18 in reshaping the probability distribution of the plant objective values, J_i. Compared to Figure 3.11 for which the only objective was the minimization of the left-tail risk, the multiobjective problem in Equation 3.18 decreases the mean cost as well as decreasing the right-tail risk.

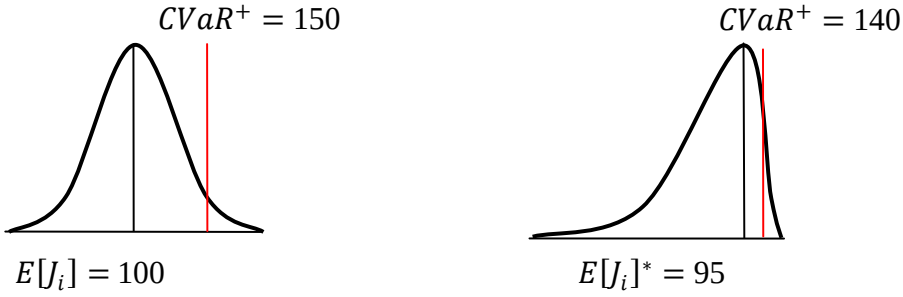

(a) before optimization (b) after optimization

Figure 3.14. Hypothetical scenarios for the ($E[J]$ + CVaR^{+}) objective.

3.3.6. [$E[J]$ + (CVaR^{+} – CVaR^{-})] as the Objective Function

Multiobjective optimization with weighted plant cost (positive quantity) objective and the (CVaR^{+} – CVaR^{-}) objective for process optimization under uncertainty may be described with problem in Equation 3.19 below, where the aim is to minimize the expected value of the cost and at the same time increase the confidence in the mean by minimizing the difference between the right- and let-tail risks in terms of CVaR^{+} and CVaR^{-}.

$$
\begin{aligned}
\min_{\boldsymbol{d},\boldsymbol{u}_i,\boldsymbol{x}_i,\gamma,\eta,z_i^-,z_i^+} \quad & \lambda\left[\frac{1}{N}\sum_{i=1}^{N} J_i(\boldsymbol{d},\boldsymbol{x}_i,\boldsymbol{u}_i,\boldsymbol{p}_i)\right] \\
& +(1-\lambda)\left[\left(\gamma+\frac{1}{N(1-\alpha)}\sum_{i=1}^{N} z_i^+\right)-\left(\eta-\frac{1}{N(1-\alpha)}\sum_{i=1}^{N} z_i^-\right)\right] \\
s.t. \quad & \left.\begin{aligned} & z_i^- \geq \eta - J_i(\boldsymbol{d},\boldsymbol{x}_i,\boldsymbol{u}_i,\boldsymbol{p}_i) \\ & z_i^+ \geq J_i(\boldsymbol{d},\boldsymbol{x}_i,\boldsymbol{u}_i,\boldsymbol{p}_i) - \gamma \\ & z_i^- \geq 0 \\ & z_i^+ \geq 0 \end{aligned}\right\} \begin{array}{c} CVaR\ Constraints\ (linear) \\ i = 1,\dots,N \end{array} \\
& \left.\begin{aligned} & \boldsymbol{h}_i(\boldsymbol{d},\boldsymbol{x}_i,\boldsymbol{u}_i,\boldsymbol{p}_i) = \boldsymbol{0}_i \\ & \boldsymbol{g}_i(\boldsymbol{d},\boldsymbol{x}_i,\boldsymbol{u}_i,\boldsymbol{p}_i) \leq \boldsymbol{0}_i \\ & \boldsymbol{d}^{lb} \leq \boldsymbol{d} \leq \boldsymbol{d}^{ub} \\ & \boldsymbol{u}_i^{lb} \leq \boldsymbol{u}_i \leq \boldsymbol{u}_i^{ub} \\ & \boldsymbol{x}_i^{lb} \leq \boldsymbol{x}_i \leq \boldsymbol{x}_i^{ub} \end{aligned}\right\} \begin{array}{c} Plant\ Constraints \\ (linear\ or\ nonlinear) \\ i = 1,\dots,N \end{array}
\end{aligned}
\tag{3.19}
$$

where, γ^{*} is VaR of the distribution, ($\gamma^{*} = VaR^{+}$), η^{*} is VaR of the distribution, ($\eta^{*} = VaR^{-}$).

Under the simultaneous scheme, one-time solution of the large optimization problem in Equation 3.19 yields the optimal values of the design, control and state vectors as well as the risk measures VaR^{-}, VaR^{+}, CVaR^{-}, and CVaR^{+}. It should be noted that, the optimal values of $\mathrm{CVaR}^{\pm}$ and $\mathrm{VaR}^{\pm}$ are implicitly calculated from the set of plant objective values, J_i, corresponding to each realization of uncertainty in the parameter vector since the second bracketed term in the objective function of problem in Equation 3.19 is the Uryasev's (Rockafellar and Uryasev, 2000) linear optimization representation of $\mathrm{CVaR}^{\pm}$ and $\mathrm{VaR}^{\pm}$. It should be noted that problem in Equation 3.19 is a minimization problem and is bounded. Since the second bracketed term in the objective is the linear CVaR^{+} function and the third bracketed term is the linear CVaR^{-} function, their difference is also linear and the minimization of the "$-\mathrm{CVaR}^{-}$" term corresponds to maximization of "$+\mathrm{CVaR}^{-}$" function, which is bounded as explained in the previous chapter. However, if the plant objective, J, is nonlinear (nonconvex) then the problem in Equation 3.19 should be solved via a global optimizer, since a local extremum may prevent the $\mathrm{CVaR}^{\pm}$ terms in the second bracket to be pushed till their limits, yielding meanless γ^* and η^* values that cannot be taken as $\mathrm{VaR}^{\pm}$ values. If the plant objective is not cost but profit, then the same formulation is valid after multiplying only the first bracket by minus one, so that it reads as minimization of negative profit which is identical to maximization of profit.

The problem in Equation 3.19 aims at minimizing the expected cost as well as compressing the left and right tails toward the mean of the probability distribution. Thus, as a result, the uncertainty about the optimized mean of the cost distribution is minimized in terms of the difference between the CVaR^{+} and CVaR^{-}. The problem should not be converted to maximization form, or the difference between CVaR^{-} and CVaR^{+} ($\mathrm{CVaR}^{-} - \mathrm{CVaR}^{+}$) should not be minimized, since then both of the last two bracketed terms of the objective become unbounded (due to unboundedness of the vector of auxiliary variables, $\boldsymbol{z}^{+}$ and $\boldsymbol{z}^{-}$, as mentioned in the previous chapter).

Figure 3.15 depicts the conceived role of problem in Equation 3.19 in reshaping the probability distribution of the plant cost values, J_i. Compared to Figure 3.12 for which the only objective was the minimization of the difference between the right- and left-tail risks, the multiobjective problem in Equation 3.19 decreases the mean cost as well as increases its certainty by compressing the tails towards the optimum expected cost value.

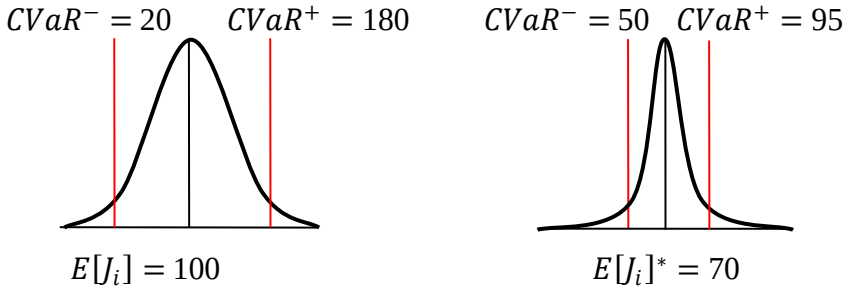

(a) before optimization (b) after optimization

Figure 3.15. Hypothetical scenarios for the [$E[J]$ + (CVaR$^+$ – CVaR$^-$)] objective.

3.3.7. $E[J]$ as the Objective Function and CVaR$^-$ as Constraint

Process optimization under uncertainty where the objective is the maximization of the expected profit with CVaR$^-$ as constraint may be described by Equation 3.20 given below, where the loss (left) side tail risk is imposed as an inequality constraint via CVaR$^-$.

$$
\begin{aligned}
\max_{\boldsymbol{d},\boldsymbol{u}_i,\boldsymbol{x}_i,\eta,z_i} \quad & E[J_i] = \frac{1}{N}\sum_{i=1}^{N} J_i(\boldsymbol{d},\boldsymbol{x}_i,\boldsymbol{u}_i,\boldsymbol{p}_i) \\
s.t. \quad & \left.\eta - \frac{1}{N(1-\alpha)}\sum_{i=1}^{N} z_i \geq C_{limit}^{-}\right\} \quad CVaR^- \ Limit \ Constraint \\
& \left.\begin{array}{c} z_i \geq \eta - J_i(\boldsymbol{d},\boldsymbol{x}_i,\boldsymbol{u}_i,\boldsymbol{p}_i) \\ z_i \geq 0 \end{array}\right\} \begin{array}{c} CVaR \ Constraints \ (linear) \\ i = 1,\dots,N \end{array} \\
& \left.\begin{array}{c} \boldsymbol{h}_i(\boldsymbol{d},\boldsymbol{x}_i,\boldsymbol{u}_i,\boldsymbol{p}_i) = \boldsymbol{0}_i \\ \boldsymbol{g}_i(\boldsymbol{d},\boldsymbol{x}_i,\boldsymbol{u}_i,\boldsymbol{p}_i) \leq \boldsymbol{0}_i \\ \boldsymbol{d}^{lb} \leq \boldsymbol{d} \leq \boldsymbol{d}^{ub} \\ \boldsymbol{u}_i^{lb} \leq \boldsymbol{u}_i \leq \boldsymbol{u}_i^{ub} \\ \boldsymbol{x}_i^{lb} \leq \boldsymbol{x}_i \leq \boldsymbol{x}_i^{ub} \end{array}\right\} \begin{array}{c} Plant \ Constraints \\ (linear \ or \ nonlinear) \\ i = 1,\dots,N \end{array}
\end{aligned}
\tag{3.20}
$$

The user-defined limit value of CVaR$^-$, C_{limit}^{-}, is used to restrict the left-tail risk of the profit distribution to be less than the desired value. Notice that the left-tail risk minimization corresponds to placing the target CVaR$^-$ value to a higher value (towards the right hand side) via the use of CVaR$^-$ constraint. However, it is very important to note that, at the optimal solution, the left-hand side of the risk constraint is indeed the true CVaR$^-$ if and only if the constraint is active at the solution; otherwise, the left-hand side of the risk constraint has no meaning (vector of auxiliary variables, $\boldsymbol{z}$, has no upper bound).

Figure 3.16 depicts the conceived role of problem in Equation 3.20 in reshaping the probability distribution of the plant objective values, J_i. Before the application of problem in Equation 3.20, the expected value of profit is 100 units, and, at α confidence level, the expected value of the tail profit, CVaR$^-$, is 20 units; very roughly indicating that even though the mean profit is 100 units, there is a certain chance that it may be expected to be as low as 20 units. On the other hand, after the application of problem in Equation 3.20, although the expected value of profit is 80 units, at α confidence level, the expected value of the tail profit, CVaR$^-$, is at its user-defined value of C^-_{limit}= 50 units; very roughly indicating that, upon optimization, even though the mean profit decreases from 100 to 80 units, the tail risk also decreases from 20 units to a better value of 50 units. It must be noted that there is no guarantee that any arbitrary desired limit value, C^-_{limit}, set by the user allows feasible solution to problem in Equation 3.20. Thus, depending on the problem characteristics, C^-_{limit} must be adjusted in an ad-hoc way.

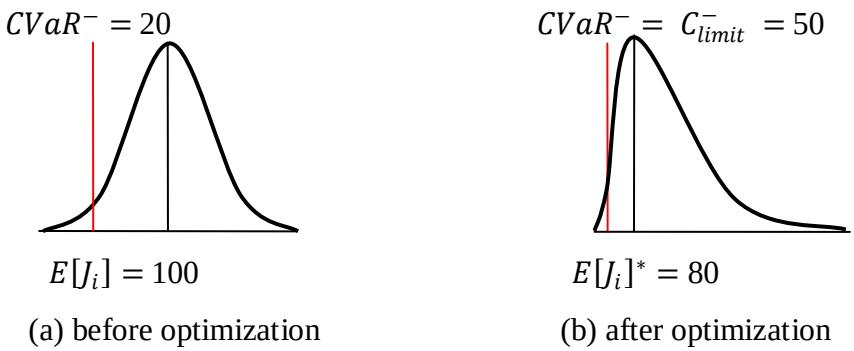

(a) before optimization (b) after optimization

Figure 3.16. Hypothetical scenarios for $E[J]$ as objective and CVaR– as constraint.

3.3.8. $E[J]$ as the Objective Function and CVaR$^+$ as Constraint

Process optimization under uncertainty where the objective is the minimization of the expected cost (positive value) with CVaR$^+$ as constraint may be described by Equation 3.21 given below, where the excess cost (right) side tail risk is imposed as an inequality constraint via CVaR$^+$.

$$
\begin{aligned}
\min_{\boldsymbol{d},\boldsymbol{u}_i,\boldsymbol{x}_i,\gamma,z_i} \quad & E[J_i] = \frac{1}{N}\sum_{i=1}^{N} J_i(\boldsymbol{d},\boldsymbol{x}_i,\boldsymbol{u}_i,\boldsymbol{p}_i) \\
s.t. \quad & \left.\gamma + \frac{1}{N(1-\alpha)}\sum_{i=1}^{N} z_i \le C_{limit}^{+}\right\} \quad CVaR^{+}\ Limit\ Constraint \\
& \left.\begin{aligned} z_i \ge J_i(\boldsymbol{d},\boldsymbol{x}_i,\boldsymbol{u}_i,\boldsymbol{p}_i) - \gamma \\ z_i \ge 0 \end{aligned}\right\} \begin{aligned} & CVaR\ Constraints\ (linear) \\ & i = 1,\dots,N \end{aligned} \\
& \left.\begin{aligned} \boldsymbol{h}_i(\boldsymbol{d},\boldsymbol{x}_i,\boldsymbol{u}_i,\boldsymbol{p}_i) &= \boldsymbol{0}_i \\ \boldsymbol{g}_i(\boldsymbol{d},\boldsymbol{x}_i,\boldsymbol{u}_i,\boldsymbol{p}_i) &\le \boldsymbol{0}_i \\ \boldsymbol{d}^{lb} \le \boldsymbol{d} &\le \boldsymbol{d}^{ub} \\ \boldsymbol{u}_i^{lb} \le \boldsymbol{u}_i &\le \boldsymbol{u}_i^{ub} \\ \boldsymbol{x}_i^{lb} \le \boldsymbol{x}_i &\le \boldsymbol{x}_i^{ub} \end{aligned}\right\} \begin{aligned} & Plant\ Constraints \\ & (linear\ or\ nonlinear) \\ & i = 1,\dots,N \end{aligned}
\end{aligned}
\tag{3.21}
$$

The user-defined limit vaue of CVaR^{+}, C_{limit}^{+}, is used to restrict the right-tail risk of the cost distribution to be less than the desired value. Notice that the right-tail risk minimization corresponds to placing the target CVaR^{+} value to a lower value (towards the left hand side) via the use of CVaR^{+} constraint. However, it is very important to note that, at the optimal solution, the left-hand side of the risk constraint is indeed the true CVaR^{+} if and only if the constraint is active at the solution; otherwise, the left-hand side of the risk constraint has no meaning (vector of auxiliary variables, $\boldsymbol{z}$, has no upper bound).

Figure 3.17 depicts the conceived role of problem in Equation 3.21 in reshaping the probability distribution of the plant objective values, J_i. Before the application of Equation 3.21, the expected value of cost is 100 units, and, at α confidence level, the expected value of the right-tail cost, CVaR^{+}, is 150 units; very roughly indicating that even though the mean cost is 100 units, there is a certain chance that it may be expected to be as high as 150 units. On the other hand, after the application of in Equation 3.21, the expected value of cost is 95 units, at α confidence level, the expected value of the tail cost, CVaR^{+}, is at its user-defined value of C_{limit}^{+}= 145 units; very roughly indicating that, upon optimization, even though the mean cost decreases from 100 to 95 units, the tail risk also decreases from 150 units to a better value of 145 units. It must be noted that there is no guarantee that any arbitrary desired limit value, C_{limit}^{+}, set by the user allows feasible solution to problem in Equation 3.21. Thus, depending on the problem characteristics, C_{limit}^{+} must be adjusted in an ad-hoc way.

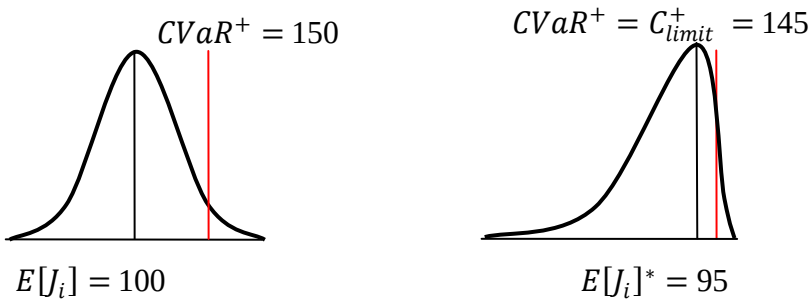

(a) before optimization (b) after optimization

Figure 3.17. Hypothetical scenarios for $E[J]$ as objective and CVaR^{+} as constraint.

3.3.9. $E[J]$ as the Objective Function and (CVaR^{+} – CVaR^{-}) as Constraint

Process optimization under uncertainty where the objective is the maximization of the expected profit with the gap between CVaR^{+} and CVaR^{-} as constraint may be described with Equation 3.22 given below, where the uncertainty (risk) limit around the mean profit is imposed as an inequality constraint formed by (CVaR^{+} – CVaR^{-}).

$$
\begin{aligned}
\max_{\boldsymbol{d},\boldsymbol{u}_i,\boldsymbol{x}_i,\gamma,\eta,z_i^-,z_i^+} \quad & E[J_i] = \frac{1}{N}\sum_{i=1}^{N} J_i(\boldsymbol{d},\boldsymbol{x}_i,\boldsymbol{u}_i,\boldsymbol{p}_i) \\
s.t. \quad & \left(\gamma + \frac{1}{N(1-\alpha)}\sum_{i=1}^{N} z_i^+\right) - \left(\eta - \frac{1}{N(1-\alpha)}\sum_{i=1}^{N} z_i^-\right) \le \Delta C_{limit}^{+/-} \\
& \left.\begin{aligned} z_i^- &\ge \eta - J_i(\boldsymbol{d},\boldsymbol{x}_i,\boldsymbol{u}_i,\boldsymbol{p}_i) \\ z_i^+ &\ge J_i(\boldsymbol{d},\boldsymbol{x}_i,\boldsymbol{u}_i,\boldsymbol{p}_i) - \gamma \\ z_i^- &\ge 0 \\ z_i^+ &\ge 0 \end{aligned}\right\} \begin{array}{c} CVaR\ Constraints\ (linear) \\ i = 1,\dots,N \end{array} \\
& \left.\begin{aligned} \boldsymbol{h}_i(\boldsymbol{d},\boldsymbol{x}_i,\boldsymbol{u}_i,\boldsymbol{p}_i) &= \boldsymbol{0}_i \\ \boldsymbol{g}_i(\boldsymbol{d},\boldsymbol{x}_i,\boldsymbol{u}_i,\boldsymbol{p}_i) &\le \boldsymbol{0}_i \\ \boldsymbol{d}^{lb} \le \boldsymbol{d} &\le \boldsymbol{d}^{ub} \\ \boldsymbol{u}_i^{lb} \le \boldsymbol{u}_i &\le \boldsymbol{u}_i^{ub} \\ \boldsymbol{x}_i^{lb} \le \boldsymbol{x}_i &\le \boldsymbol{x}_i^{ub} \end{aligned}\right\} \begin{array}{c} Plant\ Constraints \\ (linear\ or\ nonlinear) \\ i = 1,\dots,N \end{array}
\end{aligned}
\tag{3.22}
$$

The user-defined limit value of (CVaR^{+} – CVaR^{-}), $\Delta C_{limit}^{+/-}$, is used to compress the right- and left-tail risk of the profit distribution towards the mean of the distribution. Notice that this corresponds to placing the target CVaR^{-} value to a higher value (towards the right hand side) and the target CVaR^{+} value to a lower value (towards the left hand side) via the use of (CVaR^{+} – CVaR^{-}) gap constraint. However, it is very important to note

that, at the optimal solution, the left-hand side of this risk-gap constraint is indeed the true gap between ($\mathrm{CVaR}^{+} - \mathrm{CVaR}^{-}$) if and only if the constraint is active at the solution; otherwise, the left-hand side of the risk-gap constraint has no meaning (vector of auxiliary variables, $\boldsymbol{z}^{+}$ and $\mathbf{z}^{-}$, has no upper bound).

Figure 3.18 depicts the conceived role of problem in Equation 3.22 in reshaping the probability distribution of the plant objective values, J_i. Before the application of Equation 3.22, the expected value of profit is 100 units, and, at α confidence level, the expected value of the left-tail risk, CVaR^{-}, is 20 units and right-tail reward, CVaR^{+}, is 180 units (the difference between CVaR^{+} and CVaR^{-} is 200 units); indicating that there is significant uncertainty about the expected profit. On the other hand, after the application of Equation 3.22, the expected value of profit is 110 units, at α confidence level, the expected value of the left-tail risk, CVaR^{-}, is 80 units and right-tail reward, CVaR^{+}, is 135 units (the difference between CVaR^{+} and CVaR^{-}, $\Delta C_{limit}^{+/-}$, is 55 units); indicating that now, upon optimization, both the mean profit increases by 10 units, and the "two-tails risk" (the difference between CVaR^{+} and CVaR^{-}) decreases from 200 units to a much better value of 55 units, which increases the confidence about the expected profit of the plant. It must be reminded again that if different α confidence levels are used for the left (α^{-}) and right (α^{+}) sides, at least in theory, it is possible to adjust also the skewness of the mean-compressed tails of the probability distribution of plant's profit. It must be noted that there is no guarantee that any arbitrary desired limit value, $\Delta C_{limit}^{+/-}$, set by the user allows feasible solution to the problem in Equation 3.22. Thus, depending on the problem characteristics, $\Delta C_{limit}^{+/-}$ must be adjusted in an ad-hoc way.

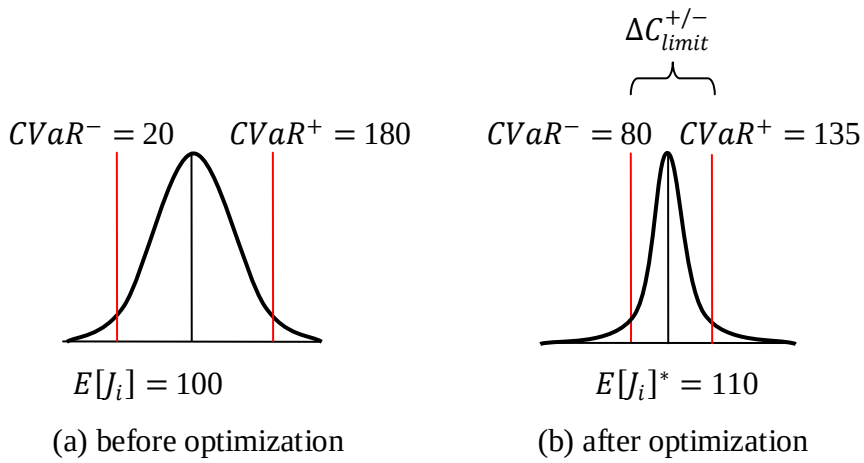

(a) before optimization (b) after optimization

Figure 3.18. Hypothetical scenarios for $E[J]$ as objective and ($\mathrm{CVaR}^{+} - \mathrm{CVaR}^{-}$) as constraint.

3.3.10. The Use of Rachev Ratio

As discussed in the previous chapter, the Rachev Ratio, $RR = CVaR^{+}/CVaR^{-}$, was proposed by Biglova *et al.* (2004) as "the ratio of expected surplus and expected shortfall" and, in finance applications, the RR is maximized to obtain a portfolio return distribution with positive skewness. In engineering applications under uncertainty, the minimization of the RR may be used to compress the probability distribution around the mean which makes the mean more certain, in other words, less risky. In the previous chapter, the LP form of the RR for minimization purpose had been developed. That LP form can be combined with the plant model. Similar to minimization of [$\mathrm{CVaR}^{+} - \mathrm{CVaR}^{-}$], the RR approach does basically the same job of compressing the probability distribution around the mean to make the mean more certain (less risky). However, the previous approach: minimization of [$\mathrm{CVaR}^{+} - \mathrm{CVaR}^{-}$], is much simpler and should be the choice. Nevertheless, for the sake of completeness, process optimization under uncertainty, with the RR as the objective, is given here by Equation 3.23 below, where the aim is to minimize both the right- and left-tail risks of, for instance, the profit distribution by the linearized ratio of CVaR^{+} to CVaR^{-}.

$$
\begin{aligned}
\min_{\boldsymbol{d},\boldsymbol{u}_i,\boldsymbol{x}_i,\boldsymbol{y}} \quad & \boldsymbol{c}_{1\times(2N+3)}\, \boldsymbol{y}_{(2N+3)\times 1} \\
s.t. \quad & \left.\begin{array}{c} \boldsymbol{A}_{(2N+1)\times(2N+3)}\, \boldsymbol{y}_{(2N+3)\times 1} \le \boldsymbol{B}_{(2N+1)\times 1} \\ \boldsymbol{d}_{1\times(2N+3)}\, \boldsymbol{y}_{(2N+3)\times 1} = \boldsymbol{1} \\ \boldsymbol{y}_{(2N+3)\times 1} \ge \boldsymbol{0} \end{array}\right\} \begin{array}{c} Linearized\ RR\ Constraints \\ (linear) \\ i = 1, \dots, N \end{array} \\
& \left.\begin{array}{c} \boldsymbol{h}_i(\boldsymbol{d}, \boldsymbol{x}_i, \boldsymbol{u}_i, \boldsymbol{p}_i) = \boldsymbol{0}_i \\ \boldsymbol{g}_i(\boldsymbol{d}, \boldsymbol{x}_i, \boldsymbol{u}_i, \boldsymbol{p}_i) \le \boldsymbol{0}_i \\ \boldsymbol{d}^{lb} \le \boldsymbol{d} \le \boldsymbol{d}^{ub} \\ \boldsymbol{u}_i^{lb} \le \boldsymbol{u}_i \le \boldsymbol{u}_i^{ub} \\ \boldsymbol{x}_i^{lb} \le \boldsymbol{x}_i \le \boldsymbol{x}_i^{ub} \end{array}\right\} \begin{array}{c} Plant\ Constraints \\ (linear\ or\ nonlinear) \\ i = 1, \dots, N \end{array}
\end{aligned}
\tag{3.23}
$$

where, as given in the previous chapter,

$$\boldsymbol{y}_{(2N+3)\times 1} = [\mathrm{z}_1^+\mathrm{t} \quad \mathrm{z}_2^+\mathrm{t} \quad \dots \quad \mathrm{z}_N^+\mathrm{t} \quad \mathrm{z}_1^-\mathrm{t} \quad \mathrm{z}_2^-\mathrm{t} \quad \dots \quad \mathrm{z}_N^-\mathrm{t} \quad \gamma\mathrm{t} \quad \eta\mathrm{t} \quad \mathrm{t}]' \tag{3.24}$$

$$\boldsymbol{c}_{1\times(2N+3)} = [(k \quad k \quad \dots \quad k)_{1\times N} \quad (0 \quad 0 \quad \dots \quad 0)_{1\times N} \quad 1 \quad 0 \quad 0] \tag{3.25}$$

$$\boldsymbol{d}_{1\times(2N+3)} = [(0 \quad 0 \quad \dots \quad 0)_{1\times N} \quad (-k \quad -k \quad \dots \quad -k)_{1\times N} \quad 0 \quad 1 \quad 0] \tag{3.26}$$

$$\mathbf{A} = \begin{bmatrix} (\ -\mathbf{I}\ )_{2N\times 2N} & \begin{pmatrix} -\mathbf{1} \\ \mathbf{0} \end{pmatrix}_{2N\times 1} & \begin{pmatrix} \mathbf{0} \\ \mathbf{1} \end{pmatrix}_{2N\times 1} & \begin{pmatrix} \mathbf{J} \\ -\mathbf{J} \end{pmatrix}_{2N\times 1} \\ 0 \dots & 0 & 0 & -1 \end{bmatrix}_{(2N+1)\times(2N+3)} \tag{3.27}$$

$$\mathbf{B} = [\mathbf{0}]_{(2N+1)\times 1} \tag{3.28}$$

In the next chapter, some of the process design under uncertainty problems, given here by Equation 3.13 through Equation 3.23, will be numerically illustrated using examples from Chemical Engineering literature.

4. CASE STUDIES

In this chapter, the problems defined and the formulations developed in Chapters 2 and 3 are illustratively applied to two examples of Chemical Engineering plant models that appear in the literature.

For the Benzoic Acid Plant (BAP) example, the Net Present Worth (NPW) of the plant is maximized. For this purpose, since the plant model equations cannot be written explicitly as equality/inequality constraints, the post-analyses of VaR and CVaR via percentile computations (Equations 2.8 and 2.9) are performed after Monte Carlo Simulation (MCS) of the plant.

The Alkylation Plant (AP) example, with seven nonlinear equality constraints and profit objective, is used as the basic Non-Linear Programming (NLP) example for both the sequential and simultaneous methods of computing VaR/CVaR which are depicted in Figures 3.9 and 3.10.

4.1. The Benzoic Acid Plant (BAP)

The plant model for “Recovery of Benzoic Acid from an Aqueous Stream”, as shown in Figure 4.1, is a system which produces 20% benzoic acid–benzene solution and is composed of “n” number of settlers (extractors), an evaporator, and three heat exchangers. Initially, a benzoic acid/water solution is fed to the system. Feed rate is specified as 10,000 kg/h. Mass fraction of benzoic acid to water amount in feed is 0.2%. The benzene phase and the aqueous phase are separated from each other in settlers. In the aqueous phase at the exit of the settler, benzene to water flow rate ratio is 0.0007. The benzene phase is then sent to the evaporator to manufacture the desired product composition with the desired yield. Year based production time for the product of benzoic acid solution is set as 8,400 h/y. Some stream temperatures are indicated in Figure 4.1.

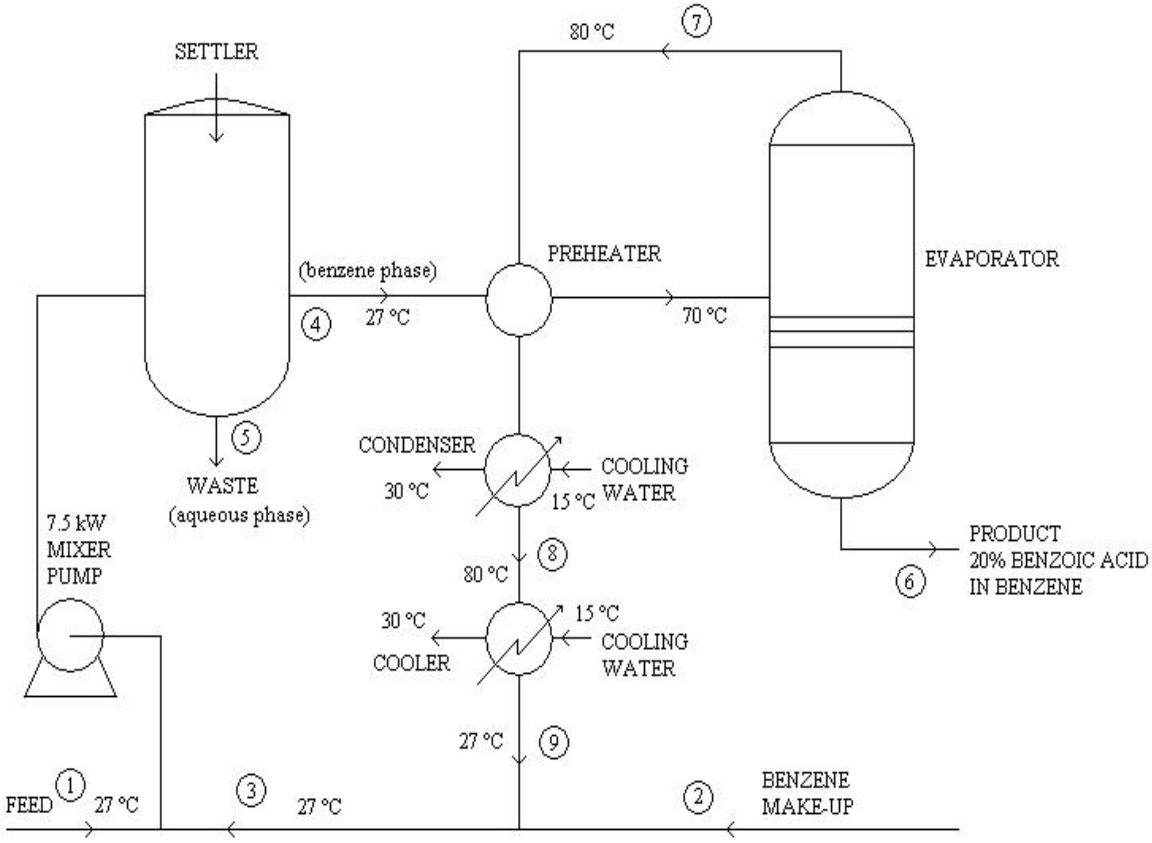

Figure 4.1. The flowsheet of the benzoic acid plant.

It is desired to maximize the Net Present Worth (NPW, \$/y) of the plant for one year of operation. For this purpose, first the mass and energy balances of the BAP are formed. Then, the operating and fixed costs of plant are computed in order to calculate NPW (\$/y); J_{NPW}. The raw material cost (p_1 \$/kg) and product price (p_2 \$/kg) are chosen as the vector of uncertain input parameters ($\boldsymbol{p}$, defined in Chapter 3), the values of which are assigned at each Monte Carlo Sampling (MCS), and benzene flow rate (u kg/h) is chosen as the manipulated (control) variable (scalar). The scalar design variable, d, is the number of settler stages and the vector of state variables, $\boldsymbol{x}$, consists of the intermediate stream flow rates. The confidence level in computing VaR/CVaR is taken as 95%, unless otherwise is specified. All the model equations related to the BAP example are given in Appendix A. Some selected MATLAB codes related to this model exist in Appendix B.

Initially, the approximate values for the optimum benzene flow rate, approach temperature, T_{apr}, which is the difference between the inlet stream to the evaporator and the outlet stream from the evaporator (stream 7 in Figure 4.1), and number of settler stages

are estimated. Then, they are taken constant at these presumed optimum values for the VaR/CVaR-related algorithms in order to provide consistency in calculations. For this purpose, holding the raw material cost and product price constant respectively at 0.25 $/kg and 1.0 $/kg, approximate values for the optimum benzene flow rate, T_{apr}, and number of settler stages, which give maximum NPW, are estimated separately.

Figure 4.2 shows the change in NPW with benzene flow rate ranging from 2,000 to 15,000 kg/h at raw material cost of 0.25 $/kg, product price of 1.0 $/kg, number of settler stages of 4, and T_{apr} of 10°C. It can be seen from Figure 4.2 that, the optimum value for the benzene flow rate, represented by the dashed line, is about 4,000 kg/h.

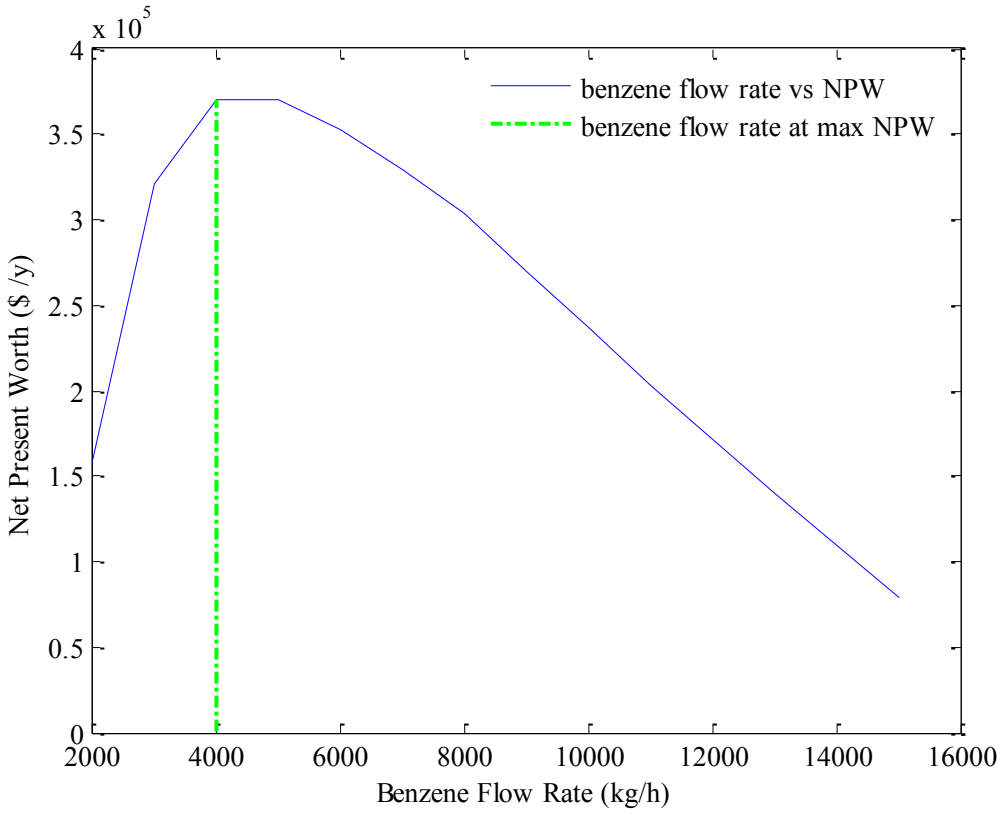

Figure 4.2. Change in the NPW with benzene flow rate.

Figure 4.3 shows the change in NPW with number of settler stages ranging from 1 to 10, at raw material cost of 0.25 $/kg, product price of 1.0 $/kg, benzene flow rate of 4,000 kg/h, and T_{apr} of 10°C. It can be seen from Figure 4.3 that the optimum value for the number of settler (extractor) stages, represented by the dashed line, is 4.

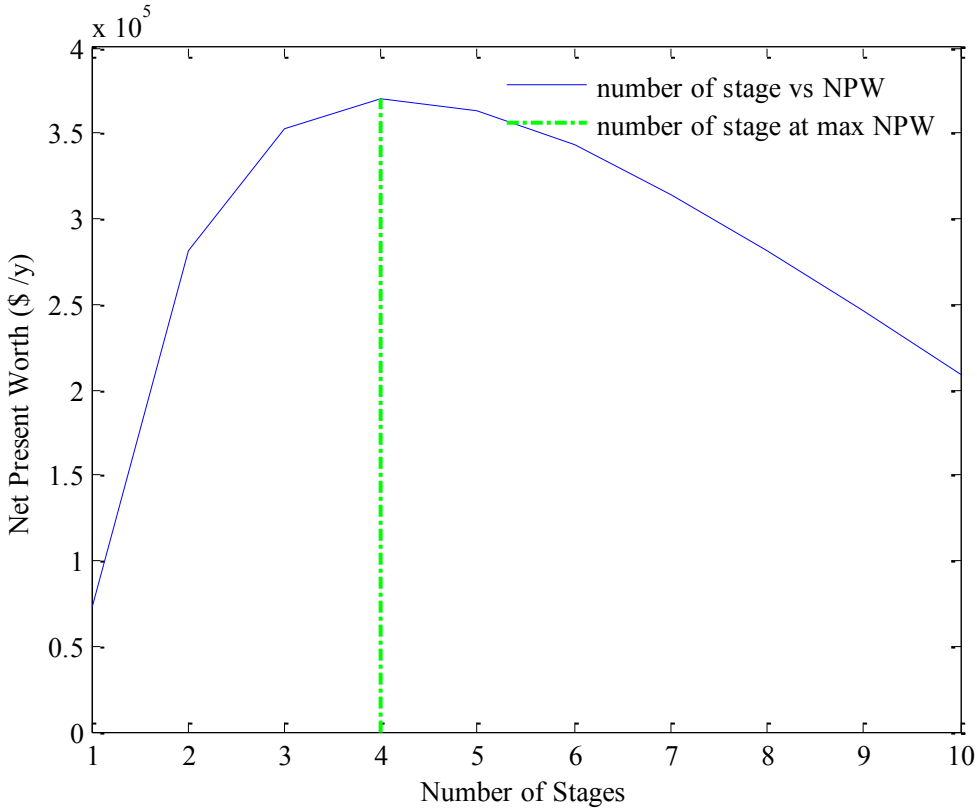

Figure 4.3. Change in the NPW with number of settler stages.

Figure 4.4 shows the change in NPW with T_{apr} ranging from 1 to 20 °C, at raw material cost of 0.25 $/kg, product price of 1.0 $/kg, benzene flow rate of 4,000 kg/h, and number of settler stages of 4. It can be seen from Figure 4.4 that the optimum value for the T_{apr} , represented by the dashed line, is about 8.9 °C. The previous computations related to estimation of optimum number of settler stages and benzene flow rate were repeated with T_{apr} of 8.9 °C and both of them gave almost the same previous optimal results. Hence, for consistency in further computations, T_{apr} is taken to be 8.9 °C, the number of stages is taken to be 4, and the benzene flow rate is taken as 4,000 kg/h.

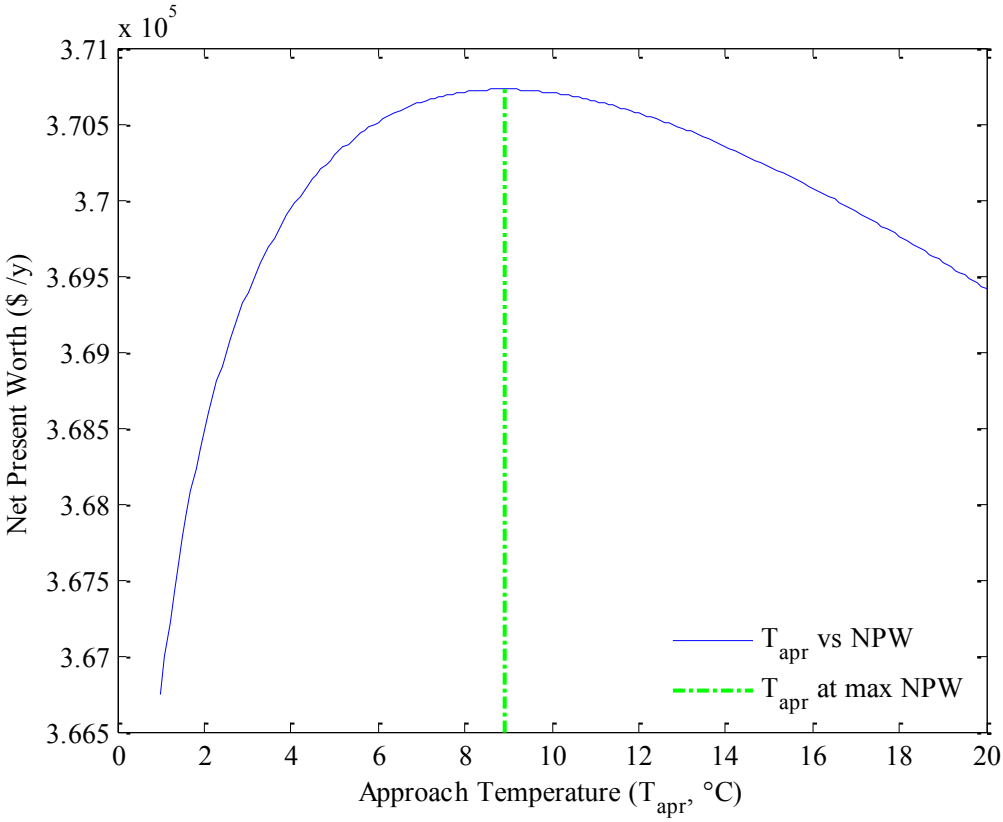

Figure 4.4. Change in the NPW with T_{apr}.

Next, the approximate minimum number of Monte Carlo Simulations (nMCS) necessary and sufficient to obtain a converged probability distribution of the the model output (NPW) is estimated. Instead of using the sampling methods presented in Section 3, which generate better randomness at low number of generation, the crude MCS technique is applied. An appropriate value for nMCS can be obtained by taking an approximate point where the mean value and standard deviation of NPW both reach stability with respect to nMCS. Therefore, with random p_1 and p_2 values (raw material cost and product price) genarated from the normal distributions ($\mu_1 = 0.25$ \$/kg, $\sigma_1 = 0.03$ and $\mu_2 = 0.95$ \$/kg, $\sigma_2 = 0.10$), the semilogarithmic graphs for mean value and standard deviation of NPW vs nMCS are formed as shown in Figure 4.5 and 4.6. From these figures, it can be observed that the stability is attained beyond about 10,000 nMCS.

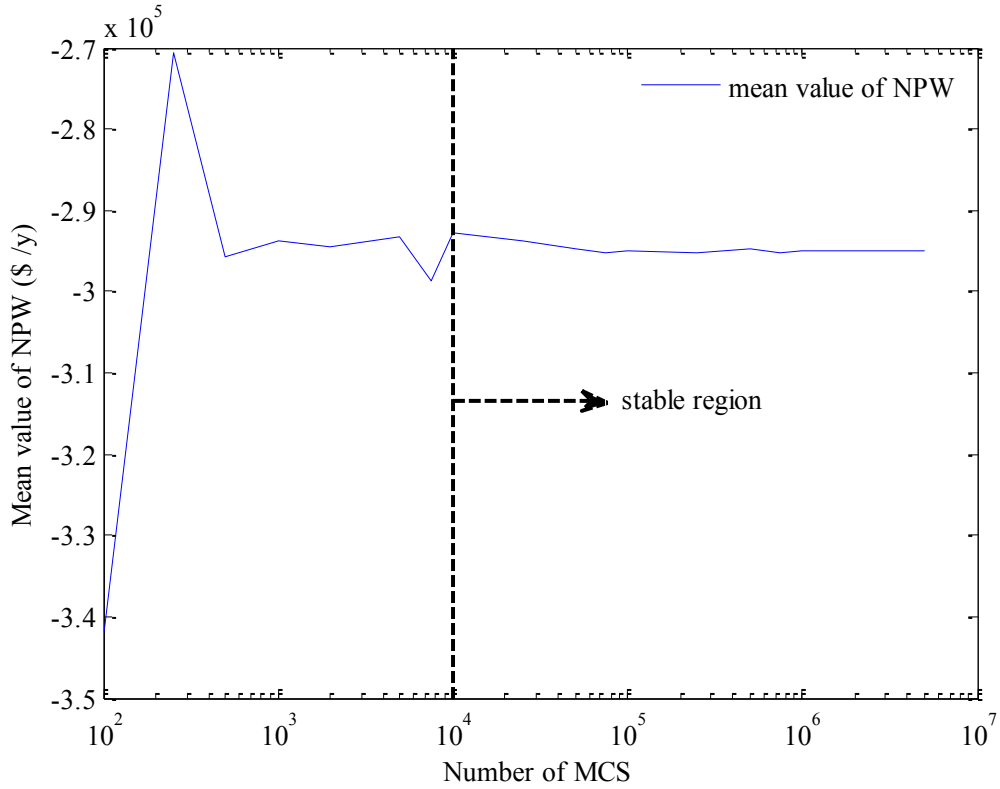

Figure 4.5. the change in the mean value of NPW ($/y) with nMCS.

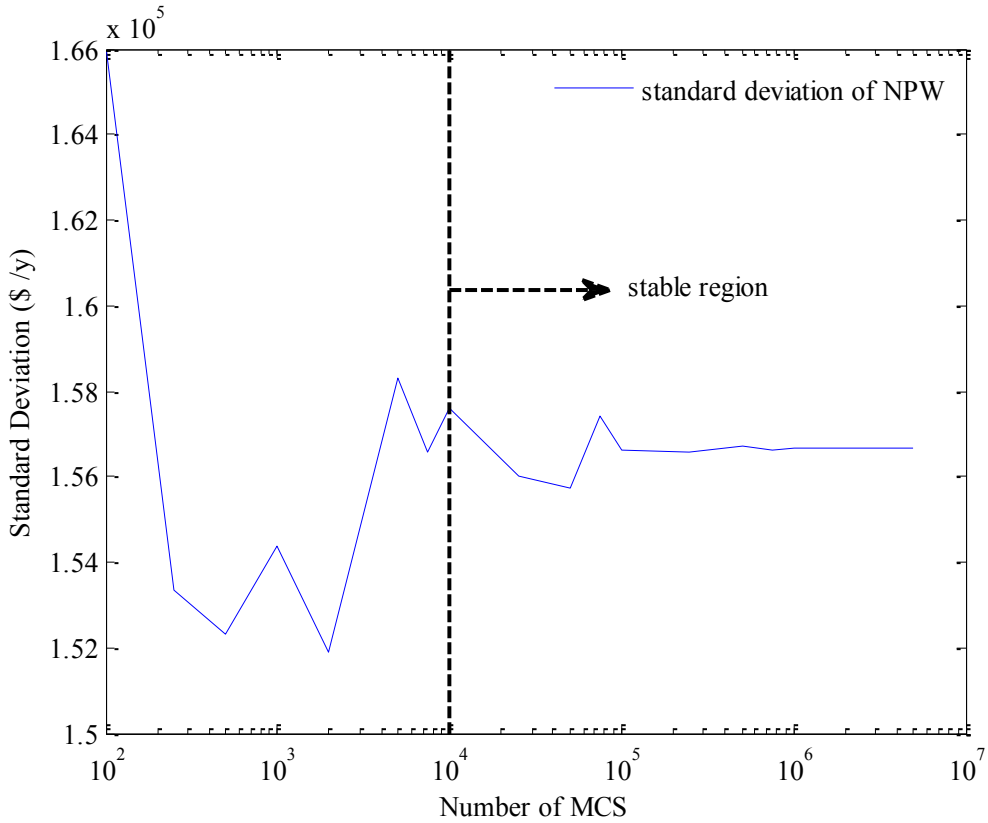

Figure 4.6. The change in the standard deviation of NPW ($/y) with nMCS.

4.1.1. VaR and CVaR Computations after MCS without Optimization

The BAP example was chosen to demonstrate the post-analyses of VaR and CVaR with MCS of the model for uncertain parameters. It can be seen from the equations in Appendix A that the BAP model has equality constraints (mass/energy balances) that cannot be written explicitly as $\boldsymbol{h}(d, \boldsymbol{x}, u, \boldsymbol{p}) = \boldsymbol{0}$, and therefore, the computation of J_{NPW} from the BAP model as a black box is more adequate.

The post-analyses of VaR$^{\pm}$ and CVaR$^{\pm}$ for the BAP model can be performed as follows. First, the uncertain parameters, $\boldsymbol{p}$, (raw material cost and product price), are generated randomly. Then, the BAP model (Appendix A) is solved at each MC trial and the outcomes of NPW values are accumulated in J_{NPW} (note that the J_{NPW} values are not the optimized values). Lastly, the expected (mean) value of NPW ($E(J_{NPW})$), VaR$^{\pm}$, and CVaR$^{\pm}$ are computed from the accumulated J_{NPW} values as off-line. This MCS methodology of the BAP model is depicted in Figure 4.7.

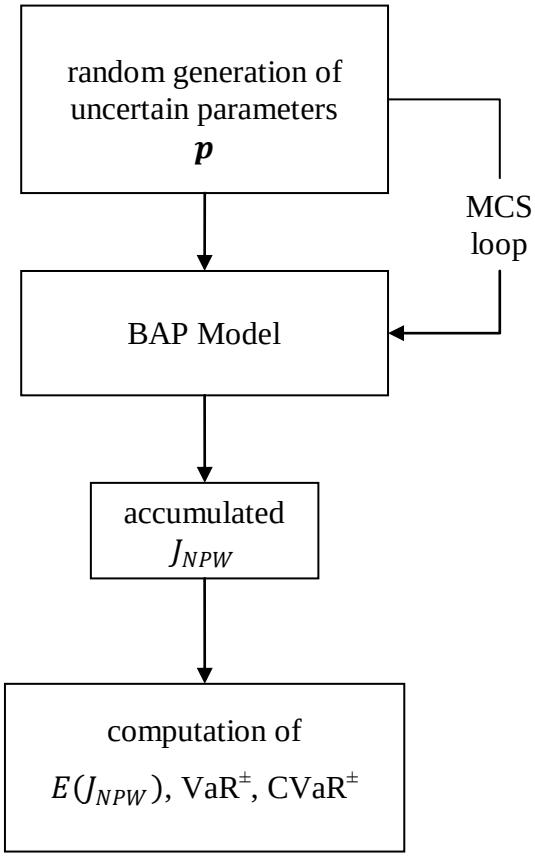

Figure 4.7. The post-analyses of VaR$^{\pm}$ and CVaR$^{\pm}$ for the BAP model via MCS.

The frequency plot of the NPW (J_{NPW}) values, at 10,000 MCS and the confidence level of 95%, is given in Figure 4.8 and some statistical results including parametric (PVaR$^{\pm}$, PCVaR$^{\pm}$, computed with Equation 2.24 and 2.25) and historical (VaR$^{\pm}$, CVaR$^{\pm}$, computed with the percentile form given by Equations 2.8 and 2.9 in Chapter 2) values for VaR and CVaR, the mean (μ) value, standard deviation (σ), skewness, kurtosis of the NPW, the difference of the mean (μ) from CVaR^{+} (DIFP) and CVaR^{-} (DIFM), the ratio of DIFP/DIFM, and the Rachev Ratio (RR = absolute value of CVaR^{+} / absolute value of CVaR^{-}) related to Figure 4.8 are given in Table 4.1. The calculations are based on four settler stages (n = 4), benzene flow rate of 4,000 kg/h, and T_{apr} of 8.9°C. Random values for the uncertain parameters of raw material cost (p_1) and product price (p_2) are drawn from normal distributions ($\mu_1 = 0.25$, $\sigma_1 = 0.03$ and $\mu_2 = 0.95$, $\sigma_2 = 0.10$, respectively).

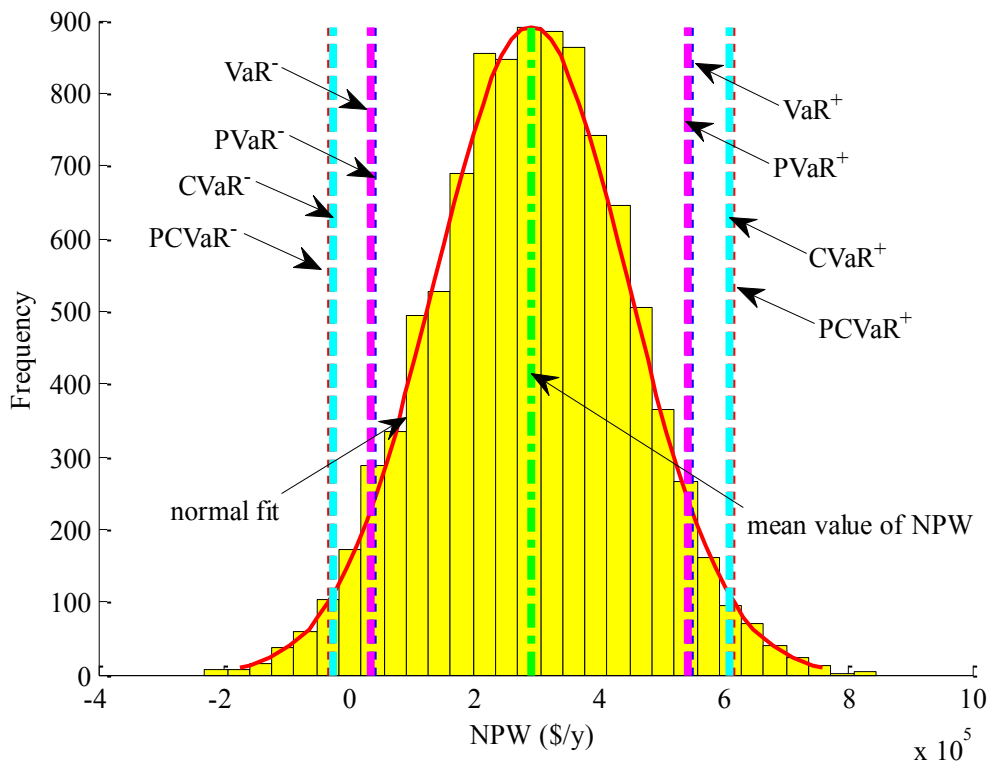

Figure 4.8. Parametric and historical VaR and CVaR values in frequency histogram of the NPW obtained via MCS.

Table 4.1. Statistical properties of the NPW distribution in Figure 4.8.

Mean Value (μ)	2.935×10^{5} \$/y
Standard Deviation (σ)	1.551×10^{5} \$/y
Skewness	-1.143×10^{-2}
Kurtosis	2.904
$PVaR^{+}$	5.486×10^{5} \$/y
$PVaR^{-}$	0.384×10^{5} \$/y
VaR^{+}	5.446×10^{5} \$/y
VaR^{-}	0.357×10^{5} \$/y
$PCVaR^{+}$	6.134×10^{5} \$/y
$PCVaR^{-}$	-0.264×10^{5} \$/y
$CVaR^{+}$	6.105×10^{5} \$/y
$CVaR^{-}$	-0.232×10^{5} \$/y
DIFP	3.171×10^{5} \$/y
DIFM	3.167×10^{5} \$/y
RR	26.31

When MCS are performed on the BAP model using the presumed nominal values of decision variables (benzene flow rate) i.e., when there is no optimization, the resulting probability distribution has negligibly negative skewness. This means that the distribution is slightly skewed to the left; increasing the probability of obtaining NPW values less than the mean value. The DIFP/DIFM ratio gives an idea about the proportion of the distances between $CVaR^{+}$ and mean value and between mean value and $CVaR^{-}$. If it is greater than one, the distance between $CVaR^{+}$ and mean value is higher than the distance between mean value and $CVaR^{-}$, i.e., the chance of obtaining a NPW value greater than the mean value is higher than obtaining a NPW value lower than the mean value. In this case, the ratio of DIFP/DIFM is close to one, which means that the chance of obtaining a NPW value greater than the mean value is almost equal to obtaining a lower NPW value than the mean value. Excess kurtosis (kurtosis–3) of −0.096 means that the distribution is platokurtic (i.e., peakedness is not prominent). Therefore, the probability of obtaining lower and higher NPW values than the mean value of NPW is high. Apart from these, the

histogram in Figure 4.8 well fits the normal curve thereby, parametric and historical $VaR^{\pm}$ and $CVaR^{\pm}$ values are close to each other as indicated also in Table 4.1.

The variations of $VaR^{\pm}$ and $CVaR^{\pm}$ with benzene flow rate, at 10,000 MCS and a confidence level of 95%, can be viewed in Figure 4.9. Benzene flow rate is changed from 1,000 to 25,000 kg/h with an interval of 100 kg/h, keeping the number of settlers, n, at 4 and the T_{apr} at 8.9 °C, as before. The curves in Figure 4.9 attain global maxima of VaR and CVaR at the benzene flow rates given in Table 4.2.

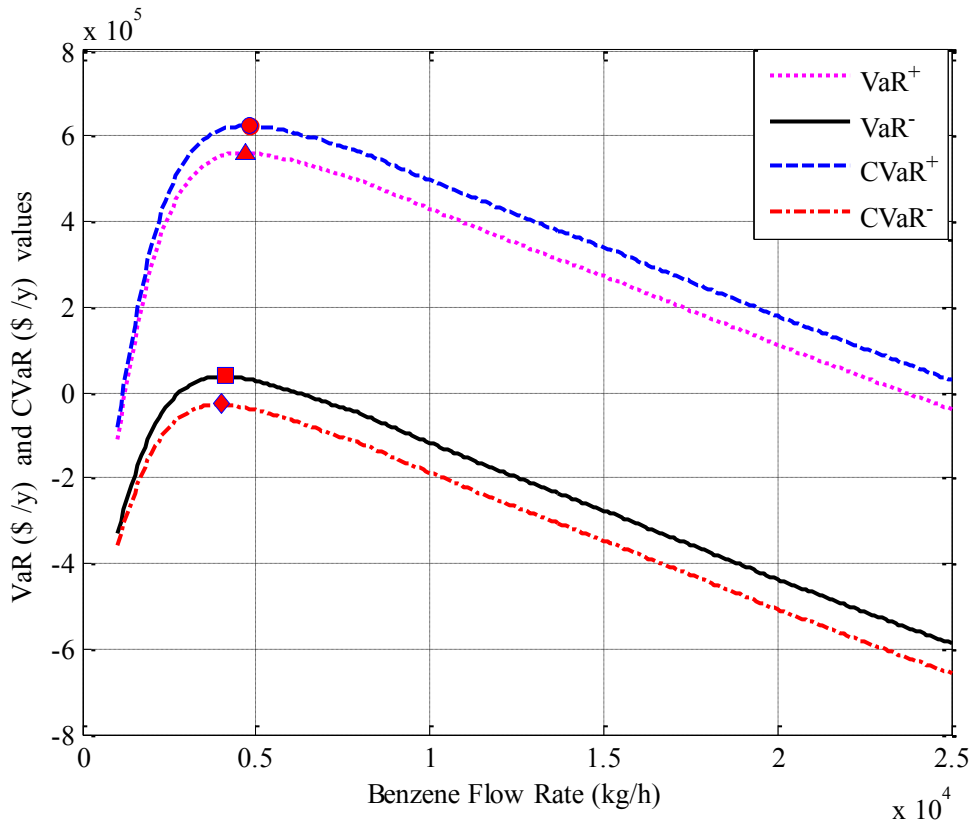

Figure 4.9. The benzene flow rate dependence of the VaR and CVaR values.

It can be seen from Figure 4.9 that, as the benzene flow rate increases, all risks ($VaR^{\pm}$ and $CVaR^{\pm}$) decrease with the same slope beyond a certain benzene flow rate, which is approximately equal to 0.5×10^4 kg/h. Showing the same trend means that for instance the difference between VaR^{+} (or $CVaR^{+}$) and VaR^{-} (or $CVaR^{-}$) at 1.0×10^4 kg/h of benzene flow rate is almost equal to the difference between VaR^{+} (or $CVaR^{+}$) and VaR^{-} (or $CVaR^{-}$) at 2.0×10^4 kg/h of benzene flow rate. In other words, beyond approximately

0.5×10^4 kg/h, as the benzene flow rate increases, the frequency distribution of NPW shifts to the left without altering the difference between right and left side risks (eg., $\text{CVaR}^+ - \text{CVaR}^-$) or the shape of the distribution. Therefore, with increasing benzene flow rate, the mean value of NPW also shifts to the left increasing the risk of having a lower NPW.

Nonlinearity is more pronounced for benzene flow rate lower than 0.5×10^4 kg/h. At benzene flow rates lower than approximately 0.25×10^4 kg/h, VaR^+ (or CVaR^+) and VaR^- (or CVaR^-) decrease and approach to each other indicating that the plant's response to uncertainties in the parameters p_1 and p_2 is to decrease the NPW values of the frequency distribution and increase the certainty of the mean value of NPW. The decrease in the NPW values is due to the frequency distribution of the NPW shifting to the left as the benzene flow rate decreases from about 0.4×10^4 kg/h to about 0.25×10^4 kg/h. The maximum values of $\text{VaR}^\pm$ and $\text{CVaR}^\pm$ lie at benzene flow rates between 4000 kg/h and 4800 kg/h, and the exact values are given in Table 4.2.

Table 4.2. Benzene flow rates at maximum VaR and CVaR.

	Maximum VaR and CVaR ($/y)	Benzene Flow Rate (kg/h)
VaR^+	5.5889×10^5	4700
VaR^-	0.3795×10^5	4100
CVaR^+	6.2357×10^5	4800
CVaR^-	-0.2797×10^5	4000

4.1.2. VaR and CVaR Computations after Optimization of NPW at each MCS

$\text{VaR}^\pm$ and $\text{CVaR}^\pm$ for BAP model are estimated via the formulations in Equations 2.8 and 2.9 in Chapter 2 after optimization (maximization) of the NPW. In this section, the values of $\text{VaR}^\pm$ and $\text{CVaR}^\pm$ are post-computed using the accumulated optimum NPW values obtained at every MCS. For this purpose, the uncertain parameters, raw material cost (p_1) and product price (p_2), are first sampled from their assumed normal distributions $\mu_1 = 0.25$, $\sigma_1 = 0.03$ and $\mu_2 = 0.95$, $\sigma_2 = 0.10$, respectively. At each such realization of the uncertain parameters, the BAP model was optimized via MATLAB's unconstrained optimizer "fminsearch" using the benzene flow rate as the only decision variable. The

optimum (maximum) value of the NPW objective function, J^*_{NPW}, is stored and the MCS continued. These optimal NPW values are accumulated in array J^*_{NPW}. Then, the expected (mean) value of NPW ($E(J^*_{NPW})$), VaR$^{\pm}$, and CVaR$^{\pm}$ are computed from the accumulated J^*_{NPW} values as off-line. Actually, this is the sequential approach explained in Chapter 3 (see Figure 3.7), except that the BAP model equations are not written explicitly as equality and inequality constraints, instead the model is computed as a black box. The flowchart for this sequential solution methodology of the BAP model is given in Figure 4.10.

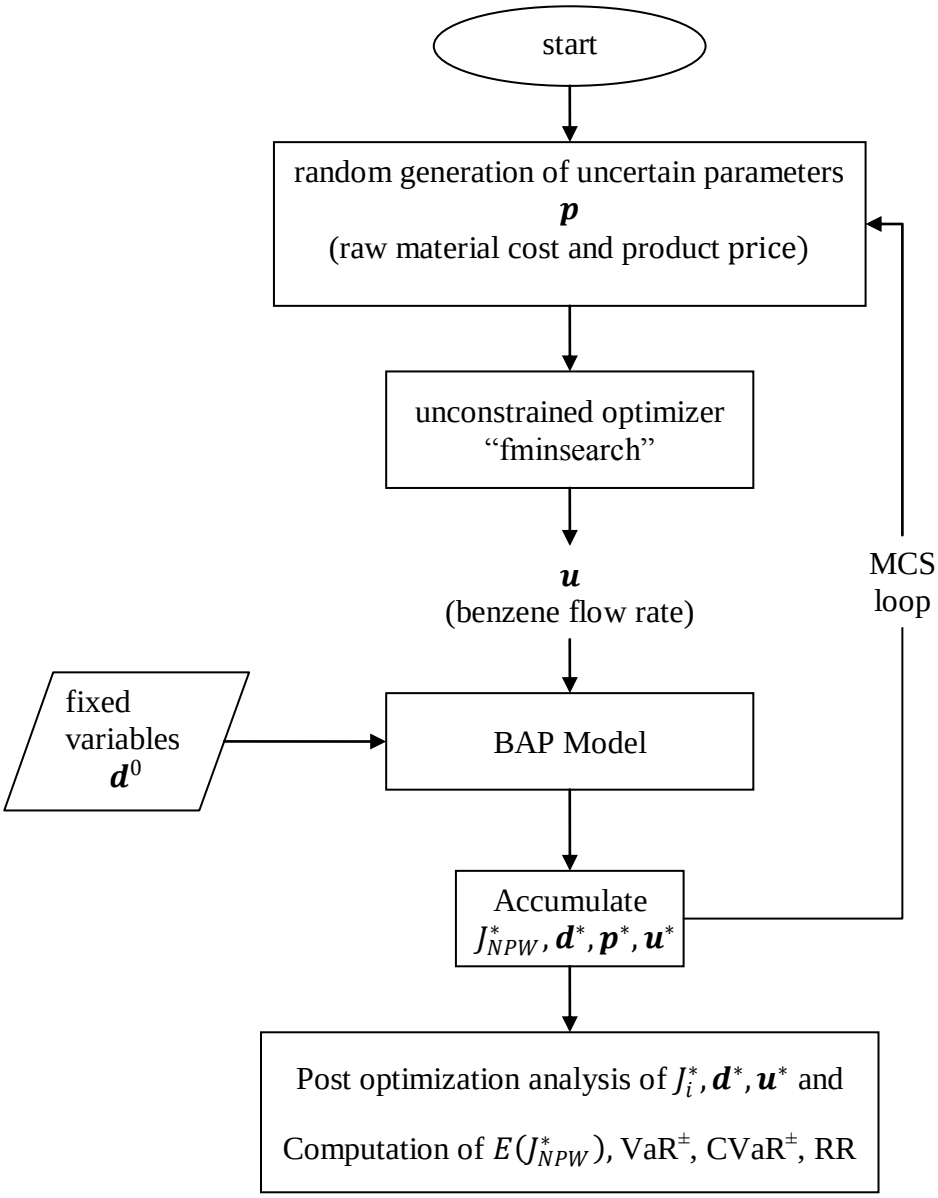

Figure 4.10. Flowchart of sequential VaR and CVaR computations for the BAP model with optimization of NPW at each MC simulation.

The distribution of the optimal NPW values (J^*_{NPW}) at 10,000 MCS is given in Figure 4.11 and some statistical results including parametric (PVaR$^{\pm}$, PCVaR$^{\pm}$, computed with Equation 2.24 and 2.25) and historical (VaR$^{\pm}$, CVaR$^{\pm}$, computed with the percentile form given by Equation 2.8 and 2.9 in Chapter 2) values at the confidence level of 95%, the mean (μ) value, standard deviation (σ), skewness, kurtosis of the NPW and the Rachev Ratio (RR) related to Figure 4.11 are given below in Table 4.3. The calculations are based on four settlers (n = 4) and T_{apr} of 8.9°C. Random values for the uncertain parameters of raw material cost (p_1) and product price (p_2) are drawn from normal distributions ($\mu_1 = 0.25$, $\sigma_1 = 0.03$ and $\mu_2 = 0.95$, $\sigma_2 = 0.10$, respectively). At the maximum frequency (i.e., at the mean value of NPW which is 2.963×10^5 \$/y), the mean value of the optimal decision variable (benzene flow rate) is 4989.6 kg/h showing an increase of approximately 1000 kg/h as compared to the previous non-optimized scenario in Section 4.1.1). Also, as compared to frequency distribution of the NWP for the non-optimized scenario (Figure 4.8), the optimization of NPW results in a small shift to the right in the distribution.

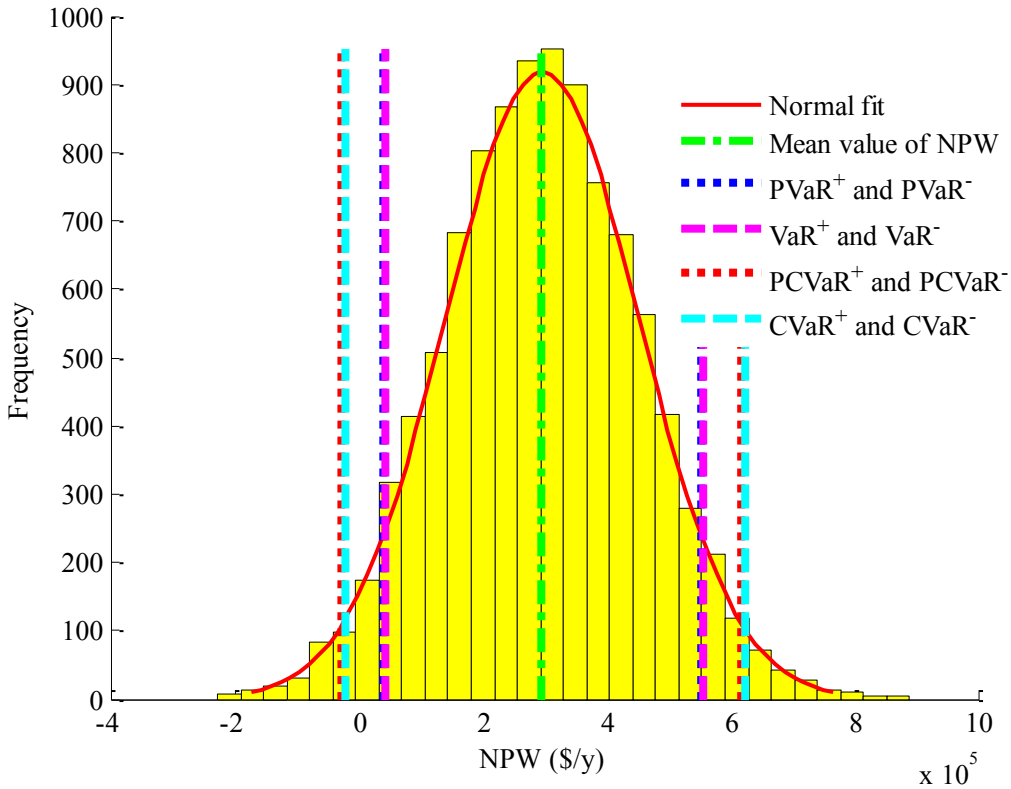

Figure 4.11. Parametric and historical VaR and CVaR values in frequency histogram of the optimized NPW values obtained at each MC simulation.

As compared to Figure 4.8, the mean value of the NPW increases from 2.935×10^5 \$/y to 2.963×10^5 \$/y (an increase of 2.8×10^3 \$/y which is about 1%), shifting the frequency distribution of the NPW to the right in Figure 4.11. The distribution of the optimal NPW values (J^*_{NPW}) in Figure 4.11, i.e., the distribution obtained via the optimization of the NPW values, shows that, as compared to Figure 4.8, Figure 4.11 has positive skewness and thus the probability of realizing NPW values greater than 2.963×10^5\$/y is greater than realizing NPW values less than 2.963×10^5\$/y. This means that the risk of having a NPW less than 2.963×10^5\$/y is lower than the reward of having a NPW greater than 2.963×10^5\$/y. Clearly, when computed off-line (post optimization), the absolute value of the $CVaR^+$ becomes greater than that of the $CVaR^-$ for the same confidence level. Figure 4.11 is desirable since, upon optimization, the company increases the mean NPW and increases the chances of realizing even better NPW (decreases the chances of getting lower NPW).

Table 4.3. Statistical properties of the NPW distribution in Figure 4.11.

Mean Value (μ)	2.963×10^5 \$/y
Standard Deviation (σ)	1.592×10^5 \$/y
Skewness	29.31×10^{-3}
Kurtosis	3.048
$PVaR^+$	5.582×10^5 \$/y
$PVaR^-$	0.344×10^5 \$/y
VaR^+	5.620×10^5 \$/y
VaR^-	0.356×10^5 \$/y
$PCVaR^+$	6.248×10^5 \$/y
$PCVaR^-$	-0.321×10^5 \$/y
$CVaR^+$	6.289×10^5 \$/y
$CVaR^-$	-0.317×10^5 \$/y
DIFP	3.326×10^5 \$/y
DIFM	3.280×10^5 \$/y
RR	19.86

On the other hand, as seen in Table 4.3, the frequency distribution is leptokurtic (i.e., having a positive excess kurtosis means that peakedness is prominent). Leptokurtic (peaked) distribution means that most of the possible NPW values are accumulated around the mean value. The difference between the parametric and historical $VaR^{\pm}$ and $CVaR^{\pm}$ values, is less than the case with no optimization in Table 4.1. The optimization (maximization) of NPW results in a higher mean value compared to the case without making any optimization. Furthermore, for optimization of NPW the difference between $CVaR^{+}$ value and optimal value of mean is greater than the difference between optimal value of mean and value of $CVaR^{-}$ for the same confidence level. This proves that, upon optimization, the company increases the mean NPW and increases the chances of realizing even better NPW (decreases the chances of getting lower NPW). The RR decreases from the non-optimized value of 26.31 (Table 4.1) to 19.86 since the increase in $CVaR^{-}$ upon optimization overwhelms the increase in $CVaR^{+}$.

4.1.3. Optimization of CVaR and Rachev Ratio with the Sequential Scheme

The optimal value of the benzene flow rate that optimizes $CVaR^{+}$ or $CVaR^{-}$ (or the Rachev Ratio, RR) can be found with the sequential scheme described in Chapter 3 / Section 3.3. In this section, the percentile forms of $VaR^{\pm}$ and $CVaR^{\pm}$ (or the RR) given in Chapter 2 / Equations 2.8 and 2.9 are used. In optimizing $CVaR^{\pm}$, the corresponding $VaR^{\pm}$ values are obtained indirectly; e.g., $VaR^{\pm}$ values are not optimized directly; the objective function is either $CVaR^{+}$, $CVaR^{-}$, or RR. At each optimization iteration of the unconstrained optimizer (when the optimizer calls the objective function subroutine) the uncertain parameters, $\boldsymbol{p}$, are generated randomly nMCS times, and at each generation, the BAP model was solved (within the optimizer's objective function subroutine) and the corresponding NPW values are accumulated in J_{NPW}. After nMCS of such computations, the $CVaR^{\pm}$ and $VaR^{\pm}$ (and thus the RR) are computed (within the optimizer's objective function subroutine) via their percentile representations given in Chapter 2 / Equations 2.8 and 2.9. Depending on the purpose of optimization, only the value of $CVaR^{+}$, $CVaR^{-}$, or RR was returned back to optimizer as the value of the objective function. It should be noted that, in the objective function of the optimizer, after nMCS, the expected (mean) value of NPW ($E(J_{NPW})$) may also be computed from the accumulated J_{NPW}. The flowchart for this sequential scheme of the BAP model is given in Figure 4.12.

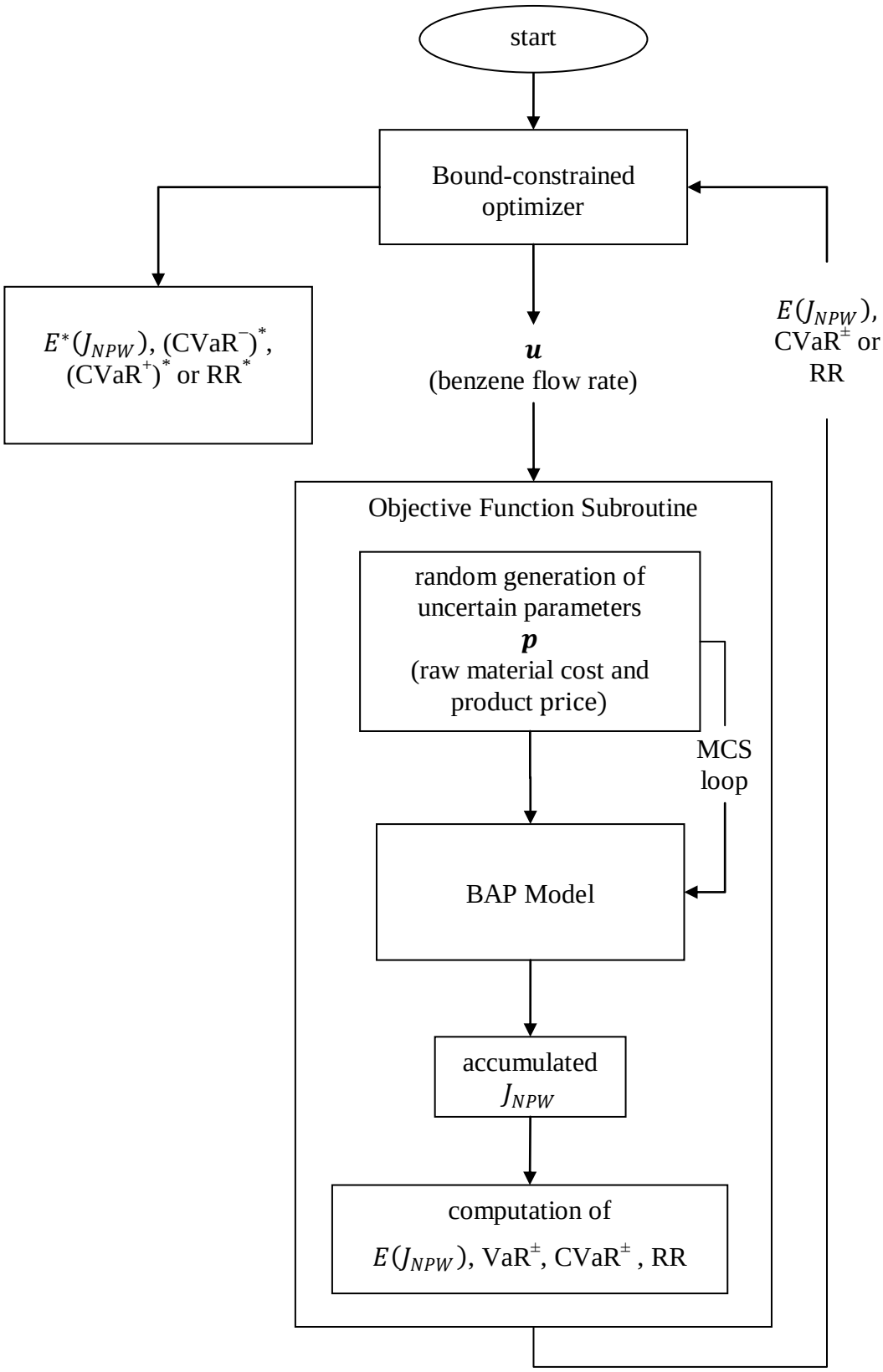

Figure 4.12. Flowchart for the optimization of CVaR or Rachev Ratio with the sequential scheme.

In order to check the effects of entirely positive or mixed (positive and negative) outcomes, the NPW values are adjusted to be either all positive values around the mean or both positive and negative values around the mean. The MATLAB's "patternsearch" function which is a mesh adaptive generalized pattern-search algorithm having the potential of finding the global solution to bound constrained problems is used to optimize $CVaR^{+}$, $CVaR^{-}$, and RR. Since the BAP model does not yield real-valued numbers when the benzene flowrate (decision variable) is less than 10 kg/h, the decision variable was bounded between 10 kg/h and 10,000 kg/h (see Figure 4.9).

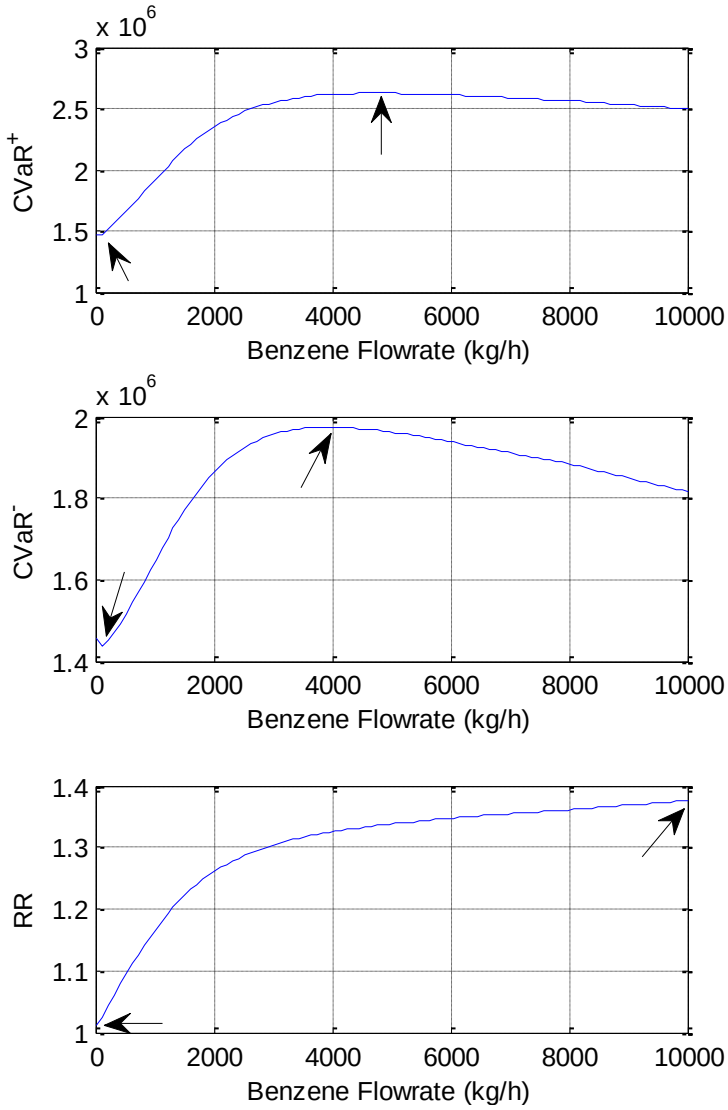

Figure 4.13. Dependence of $CVaR^{\pm}$ and Rachev Ratio on benzene flowrate for the positive valued NPW distribution.

Figure 4.13 shows the dependencies of the three objective functions ($CVaR^{\pm}$ and RR) on the decision variable (benzene flowrate) as well as their minimum and maximum locations via arrows for the case when the NPW values are adjusted to be positive only.

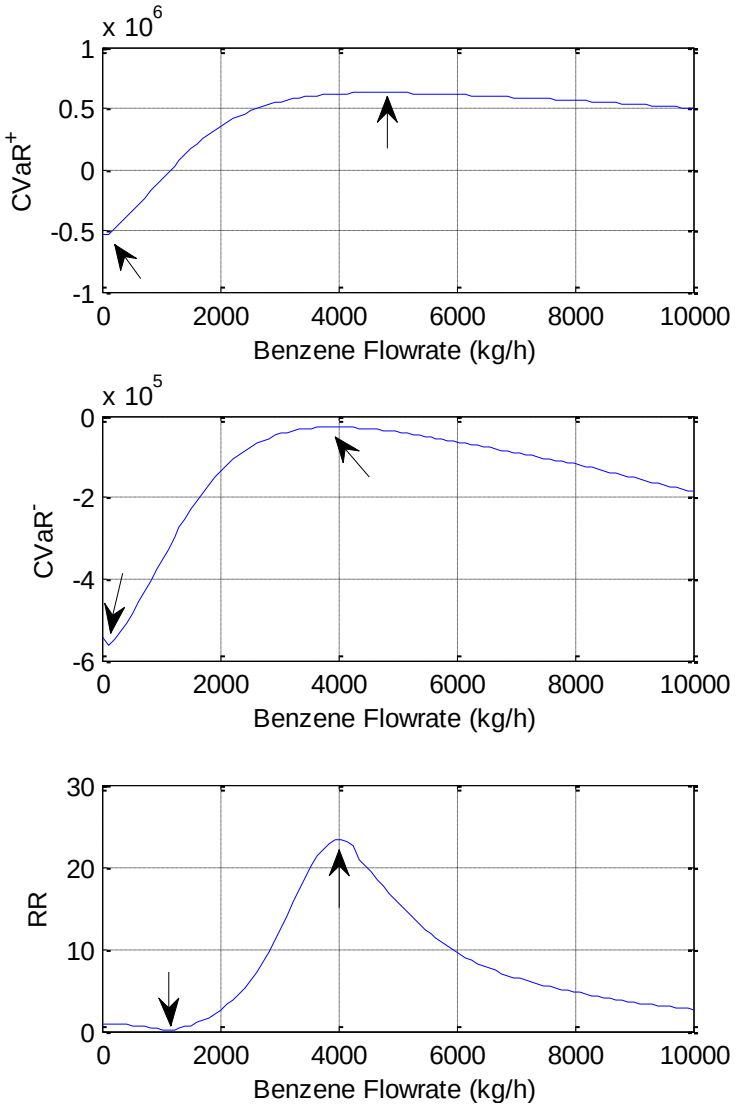

Figure 4.14. Dependence of $CVaR^{\pm}$ and Rachev Ratio on benzene flowrate for the positive and negative valued NPW distribution.

Figure 4.14 shows the dependencies of the three objective functions ($CVaR^{\pm}$ and RR) on the decision variable (benzene flowrate) as well as their minimum and maximum locations via arrows for the case when the NPW values are distributed around zero as positive and negative.

Some sample results for all positive and mixed (positive and negative) NPW outcomes are given in Figures 4.15 and 4.16.

At the optimal solution of the algorithm depicted in Figure 4.12, the NPW histograms in Figures 4.15 and 4.16 are obtained at 10,000 nMCS and at a confidence level of 95%. The calculations are based on four settlers (n = 4) and T_{apr} of 8.9°C. Random values for the uncertain parameters of raw material cost (p_1) and product price (p_2) are drawn from normal distributions ($\mu_1 = 0.25$, $\sigma_1 = 0.03$ and $\mu_2 = 0.95$, $\sigma_2 = 0.10$, respectively). Maximization and minimization of $CVaR^+$, $CVaR^-$, and RR are performed. Results consisting of the optimal values of $CVaR^\pm$, and the corresponding values of $VaR^\pm$, mean (μ), standard deviation (σ), skewness and kurtosis values for the optimal NPW distribution, the difference of the mean (μ) from $CVaR^+$ (DIFP) and $CVaR^-$ (DIFM), the ratio of DIFP/DIFM and the Rachev Ratio (RR) related to Figures 4.15 and 4.16 are listed respectively in Table 4.4 for the positive-valued NPW outcomes, and in Table 4.5 for the mixed-valued NPW outcomes.

As it is observed from Figure 4.15, the $VaR^\pm$, $CVaR^\pm$ and mean value of NPW of the positive-valued NPW distributions obtained with the sequential scheme are compressed around 1.45×10^6 \$/y upon minimization of $CVaR^+$, minimization of $CVaR^-$, minimization of RR, and expand to values around 2.3×10^6 \$/y upon the maximization of $CVaR^+$, maximization of $CVaR^-$ and maximization of RR. Figure 4.15 shows that the problem for the minimization of RR attains the lowest range of interval (the difference between $CVaR^+$ and $CVaR^-$ is the least) among the other optimization problems shown in the figure. Since RR is the ratio of $CVaR^+$ to $CVaR^-$, minimizing RR minimizes $CVaR^+$ and maximizes $CVaR^-$, narrowing the interval between $CVaR^+$ and $CVaR^-$ for the positive-valued NPW distribution. A narrow interval (lower $CVaR^+ - CVaR^-$) means that the certainty of the mean value of NPW is increased by compressing the tails towards the expected NPW value.

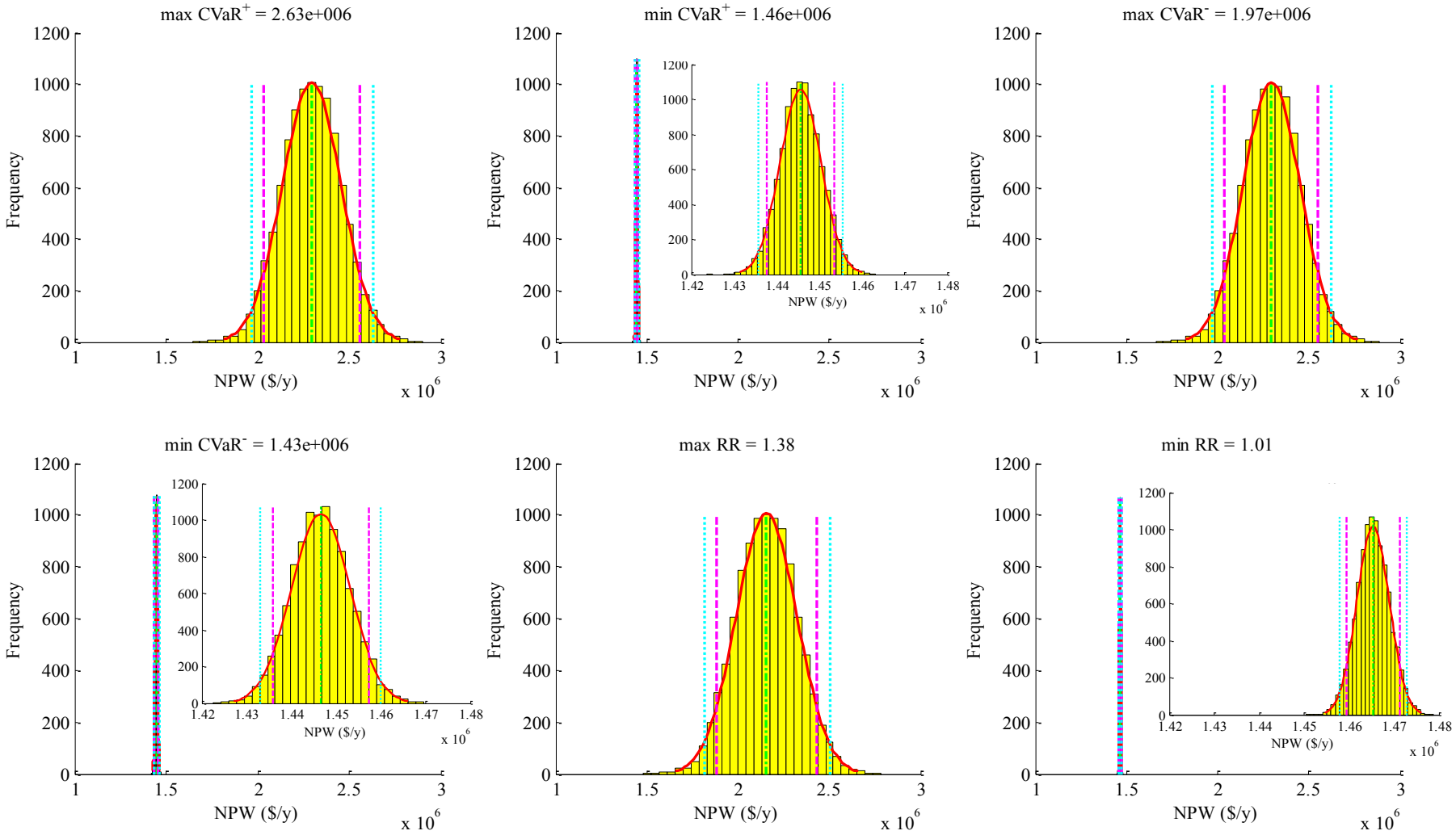

Figure 4.15. Some results for optimization of CVaR and Rachev Ratio of the positive-valued NPW distribution obtained with the sequential scheme.

Table 4.4 indicates that the optimization problems for the maximization of $CVaR^+$ and $CVaR^-$, maximization of $CVaR^-$ and minimization and maximization of RR have negative skewness which means that the NPW distribution is skewed to the left, i.e., left tail is longer and the distribution is concentrated on the left side increasing the risk of obtaining lower NPW values. Therefore, the chance of attaining a NPW value greater than the mean value of NPW distribution is lower when skewness is negative. However, for the minimization of $CVaR^-$ skewness is positive which means that the NPW distribution is skewed to the right, i.e., right tail is longer and the distribution is concentrated on the right side increasing the chance of obtaining higher NPW values. When kurtosis values are observed, it can be seen that all the frequency distributions are leptokurtic (i.e., having positive excess kurtosis meaning that peakedness is prominent). Minimization of RR can be achieved by decreasing $CVaR^+$ and increasing $CVaR^-$. In another aspect, decreasing $CVaR^+$, increasing $CVaR^-$ or doing both all bring about a decrease in the difference of $CVaR^+$ and $CVaR^-$ together with an increase in the certainty of the mean value of NPW. Additionally, Table 4.4 shows that DIFP/DIFM ratio takes a value less than one when $CVaR^-$, $CVaR^+$, and RR are minimized, i.e., having a NPW above the mean value of NPW is less probable than having a NPW below the mean value of NPW for the given optimization problems. For a positive-valued NPW distribution, the interval of ($CVaR^+ - CVaR^-$) with a high RR value is higher than the interval of ($CVaR^+ - CVaR^-$) with a low RR value. Among all the six optimization problems, RR takes the highest value of 1.38 at the optimization problem for the maximization of RR. Therefore, the maximization of RR gives a mean value with a low certainty (or high difference of $CVaR^+ - CVaR^-$). As opposed, RR takes the lowest value of 1.01 on minimization of RR which gives a mean value with a high certainty (or low difference of $CVaR^+ - CVaR^-$).

Table 4.4. Results for optimization of $CVaR^{\pm}$ and RR with all positive NPW values of the BAP.

	max $CVaR^{+}$	min $CVaR^{+}$	max $CVaR^{-}$	min $CVaR^{-}$	max RR	min RR
Benzene Flow Rate (kg/h)	4755.3	40.763	3980.9	72.785	10000	10
Mean Value (μ)	2.30E+06	1.45E+06	2.30E+06	1.45E+06	2.16E+06	1.47E+06
Standard Deviation (σ)	1.61E+05	4.80E+03	1.57E+05	6.52E+03	1.67E+05	3.61E+03
Skewness	-0.00508	-0.00023	-0.00507	0.00039	-0.00509	-0.00331
Kurtosis	3.07	3.08	3.07	3.07	3.07	3.08
VaR^{+}	2.56E+06	1.45E+06	2.55E+06	1.46E+06	2.43E+06	1.47E+06
VaR^{-}	2.03E+06	1.44E+06	2.04E+06	1.44E+06	1.88E+06	1.46E+06
$CVaR^{+}$	2.63E+06	1.46E+06	2.62E+06	1.46E+06	2.50E+06	1.47E+06
$CVaR^{-}$	1.96E+06	1.44E+06	1.97E+06	1.43E+06	1.81E+06	1.46E+06
DIFP	3.34E+05	9.89E+03	3.25E+05	1.34E+04	3.46E+05	7.47E+03
DIFM	3.31E+05	9.95E+03	3.22E+05	1.35E+04	3.43E+05	7.53E+03
Rachev Ratio	1.339	1.014	1.328	1.019	1.380	1.010

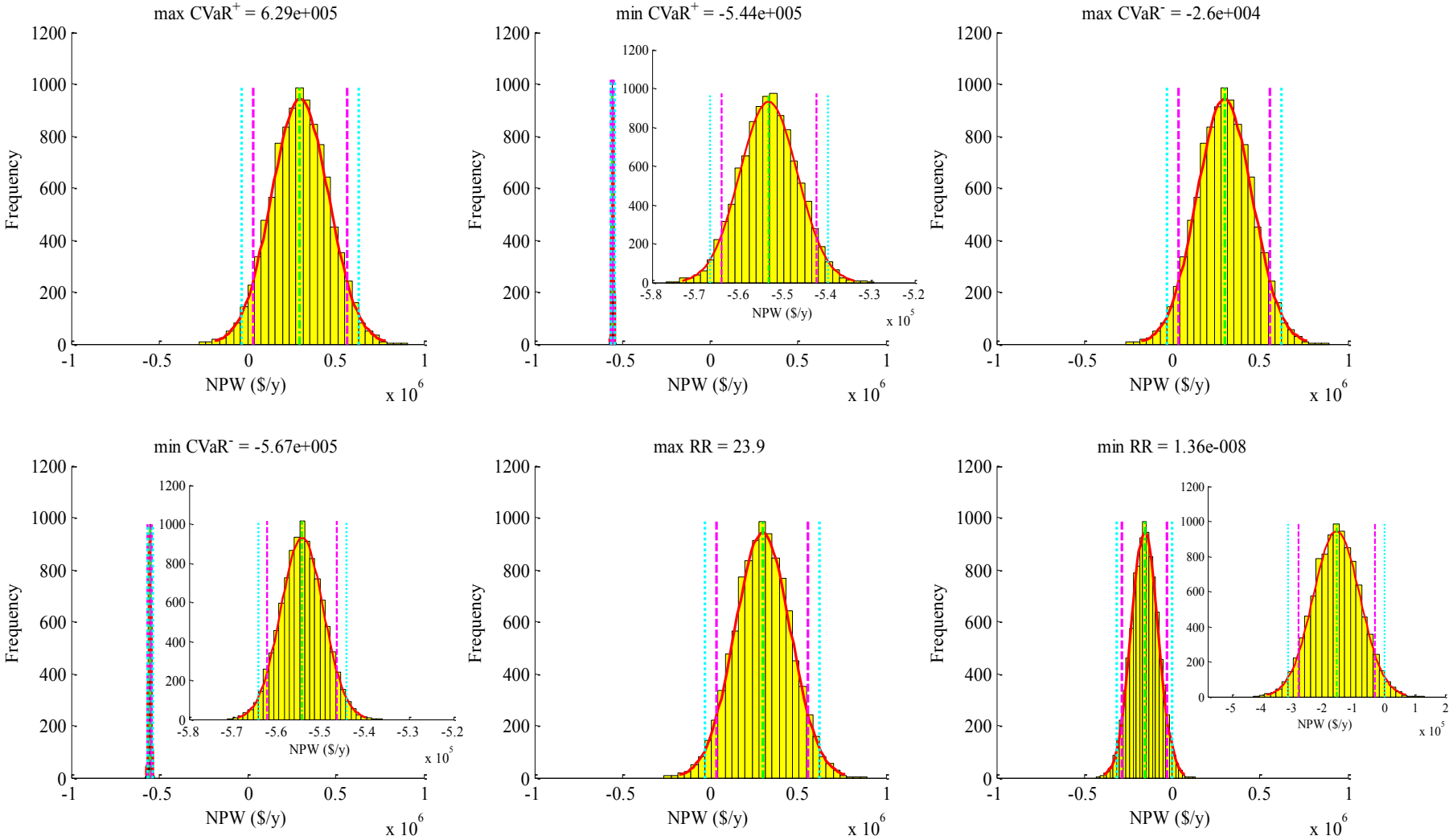

Figure 4.16. Some results for optimization of CVaR and Rachev Ratio of the positive and negative valued NPW distribution obtained with the sequential scheme.

As it is observed from Figure 4.16, the $VaR^{\pm}$, $CVaR^{\pm}$ and mean value of NPW of the mixed-valued NPW distribution obtained with the sequential scheme are compressed around -5.5×10^5 \$/y upon minimization of $CVaR^{+}$, minimization of $CVaR^{-}$, and expand to values between -5.0×10^5 and 1.0×10^6 \$/y of NPW upon maximization of $CVaR^{+}$, maximization of $CVaR^{-}$, minimization and maximization of RR. Figure 4.16 shows that the problem for the minimization of $CVaR^{-}$ attains the lowest range of interval for the difference of $CVaR^{-}$ from $CVaR^{+}$ among the other optimization problems shown in the figure.

Table 4.5 shows that, except maximization of $CVaR^{+}$, all the other applied optimization problems result in negative skewness. Accordingly, for the maximization of $CVaR^{+}$ which has positive skewness, the NPW distribution is skewed to the right, i.e., right tail is slightly longer and the distribution is concentrated on the right side increasing the chance of obtaining higher NPW values. Therefore, the chance of attaining a NPW value greater than the mean value of NPW distribution is higher when skewness is positive. In Table 4.5 it can also be seen that accordingly $CVaR^{-}$ and RR values also become maximum and minimum when they are maximized and minimized, respectively. When kurtosis values are observed, it can be seen that all the probability distributions obtained are platokurtic (i.e., have negative excess kurtosis meaning that peakedness is not prominent). Additionally, Table 4.5 shows that DIFP/DIFM ratio is greater than one for maximization of $CVaR^{+}$, which means that having a NPW above the mean value of NPW is more probable than having a NPW below the mean value of NPW.

Table 4.5. Results for optimization of $CVaR^{\pm}$ / RR with positive and negative NPW values of the BAP.

	max $CVaR^{+}$	max $CVaR^{-}$	min $CVaR^{+}$	min $CVaR^{-}$	max RR	min RR
Benzene Flow Rate (kg/h)	4754.9	40.914	3982.1	72.995	4025.4	1160.9
Mean Value (μ)	2.99E+05	-5.54E+05	2.99E+05	-5.53E+05	2.99E+05	-1.56E+05
Standard Deviation (σ)	1.62E+05	4.84E+03	1.57E+05	6.57E+03	1.58E+05	7.66E+04
Skewness	-0.02498	0.011519	-0.02498	-0.00533	-0.02498	-0.02487
Kurtosis	2.9398	2.9651	2.9398	2.9392	2.9398	2.938
VaR^{+}	5.65E+05	-5.46E+05	5.57E+05	-5.43E+05	5.59E+05	-3.04E+04
VaR^{-}	3.28E+04	-5.62E+05	4.00E+04	-5.64E+05	4.01E+04	-2.82E+05
$CVaR^{+}$	6.29E+05	-5.44E+05	6.20E+05	-5.40E+05	6.21E+05	4.27E-03
$CVaR^{-}$	-3.50E+04	-5.64E+05	-2.60E+04	-5.67E+05	-2.60E+04	-3.14E+05
DIFP	3.30E+05	9.95E+03	3.21E+05	1.34E+04	3.22E+05	1.56E+05
DIFM	3.34E+05	9.91E+03	3.25E+05	1.35E+04	3.25E+05	1.58E+05
Rachev Ratio	17.96	0.96	23.84	0.95	23.87	1.36E-08

4.1.4. Optimization of Linear Combinations of CVaR$^{\pm}$, RR and Expected NPW

In this section, VaR$^{\pm}$ and CVaR$^{\pm}$ for the BAP model are computed via optimizations of the linear combinations of CVaR$^{\pm}$, RR, and expected (mean) value of NPW. The three linear combinations considered are "CVaR^{+} and CVaR^{-}", "mean value of J_{NPW} and (CVaR^{+} − CVaR^{-})", and "mean value of J_{NPW} and RR", which are referred as C_1, C_2, C_3, and C_4 in Equations 4.1, 4.2, 4.3, and 4.4, respectively. The flowchart for the optimization problems is identical to the one shown in Figure 4.12 except the objective function.

Eleven values between 0 and 1 are assigned to coefficient λ (the weighting parameter for the objectives) and the optimization problems in Equation 4.1, 4.2, 4.3, and 4.4 are solved for each λ value according to Figure 4.12. The linear combination of C_1 in Equation 4.1 is the objective function of a minimization problem which aims at the maximization of CVaR^{-} and minimization of CVaR^{+} simultaneously for each λ value. Similarly, the linear combination of C_2 in Equation 4.2 is the objective function of a minimization problem which aims at the maximization of mean value of J_{NPW} and the difference between CVaR^{+} and CVaR^{-} simultaneously for each λ value. The linear combination of C_3 in Equation 4.3 is the objective function of a minimization problem which aims at the maximization of mean value of J_{NPW}, and maximization of CVaR^{-} simultaneously for each λ value. Finally, the linear combination of C_4 in Equation 4.4 is the objective function of a minimization problem which aims at the maximization of mean value of J_{NPW}, and minimization of RR simultaneously for each λ value. The motivation behind the use of such linear combinations had been introduced and illustrated with hypothetical scenarios in Chapter 3 (see e.g., Sections 3.3.3, 3.3.4, and 3.3.6).

$$C_1: min\ \{\lambda\ CVaR^{+} - (1-\lambda)\ CVaR^{-}\} \tag{4.1}$$

$$C_2: min\ \{\lambda\ (-\ E[J_{NPW}]) + (1-\lambda)\ (CVaR^{+} - CVaR^{-})\} \tag{4.2}$$

$$C_3: min\{\lambda\ (-\ E[J_{NPW}]) + (1-\lambda)\ (-CVaR^{-})\} \tag{4.3}$$

$$C_4: min\{\lambda\ (-\ E[J_{NPW}]) + (1-\lambda)\ RR\} \tag{4.4}$$

The NPW (or J_{NPW}) values are again adjusted to be composed of either positive and negative values together or all positive values. Some example frequency distribution results obtained from the minimizations of these four objective functions including both positive and negative NPW values are given below. Likewise, in the figures following the NPW distribution graphs, the changes in some of the statistical properties with λ are graphically demonstrated for the minimization problems in Equations 4.1, 4.2, 4.3 and 4.4, respectively.

The linear combination of C_1 in Equation 4.1 is used as the objective function of a minimization problem (i.e., minimization of CVaR^+ and maximization of CVaR^- simultaneously) which is performed at 10,000 MCS and at a confidence level of 95% for each λ value. The NPW histogram obtained from this optimization problem is shown in Figure 4.18. The calculations are based on four settlers (n = 4) and T_{apr} of 8.9 °C. Random values for the uncertain parameters of raw material cost (p_1) and product price (p_2) are drawn from normal distributions ($\mu_1 = 0.25$, $\sigma_1 = 0.03$ and $\mu_2 = 0.95$, $\sigma_2 = 0.10$, respectively).

Figure 4.17 shows the dependencies of the four objective functions (Equation 4.1 to 4.4) on the decision variable (benzene flowrate) as well as on the value of the weighting parameter λ when the NPW values are distributed around zero as positive and negative. The lower and upper bounds of the benzene flowrate were taken as 10 kg/h and 10,000 kg/h, respectively.

In Figure 4.17a, there are local minima within 25 – 40 kg/h benzene flowrate range for weighting parameter values between $0.6 \leq \lambda \leq 1.0$, and within 4000 – 2750 kg/h range for $0.0 \leq \lambda \leq 0.3$. For $\lambda = 0.4$ and $\lambda = 0.5$ there are no local minima; the left bound (10 kg/h) is the minimum for these two values. In Figure 4.17b, there are local minima within 1600 – 4350 kg/h benzene flowrate range for $0.4 \leq \lambda \leq 1.0$. For $0.0 \leq \lambda \leq 0.3$ there are no local minima; the left bound (10 kg/h) is the minimum. In Figure 4.17c, there are local minima within 4000 – 4350 kg/h range for $0.0 \leq \lambda \leq 1.0$. In Figure 4.17d, there are local minima within 1150 – 4350 kg/h range for $0.0 \leq \lambda \leq 1.0$.

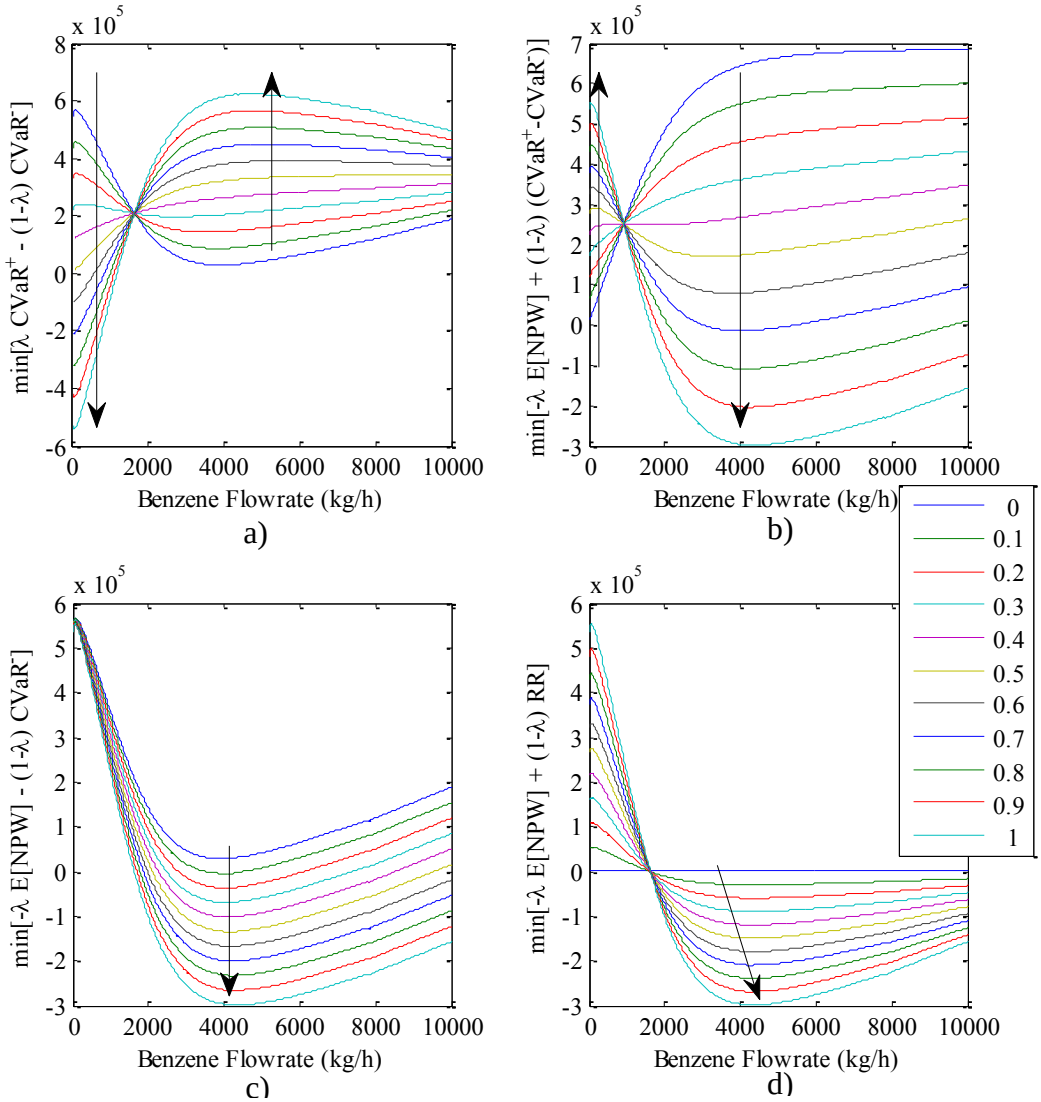

Figure 4.17. Dependencies of the objective functions on the decision variable and λ when the NPW values are distributed around zero (arrows show the direction of increasing λ).

In Figure 4.17a, objective function curves for different λ values intersect at benzene flowrate of about 1650 kg/h, where the objective function (Equation 4.1) takes a unique value of about 2.0×10^5 \$/y, irrespective of the λ values. The same occurs in Figure 4.17b and Figure 4.17c at benzene flowrates of about 950 kg/h and 1650 kg/h, respectively. In Figures 4.17a, 4.17b, and 4.17c, at these singular benzene flowrates (intersections of objective function values of different λ values), the BAP objective functions (Equations 4.1, 4.2, and 4.4) are not sensitive to λ values. In Figure 4.17d, when λ is zero, the objective function (Equation 4.4) becomes simply the minimization of the RR which does not change noticeably with benzene flowrate.

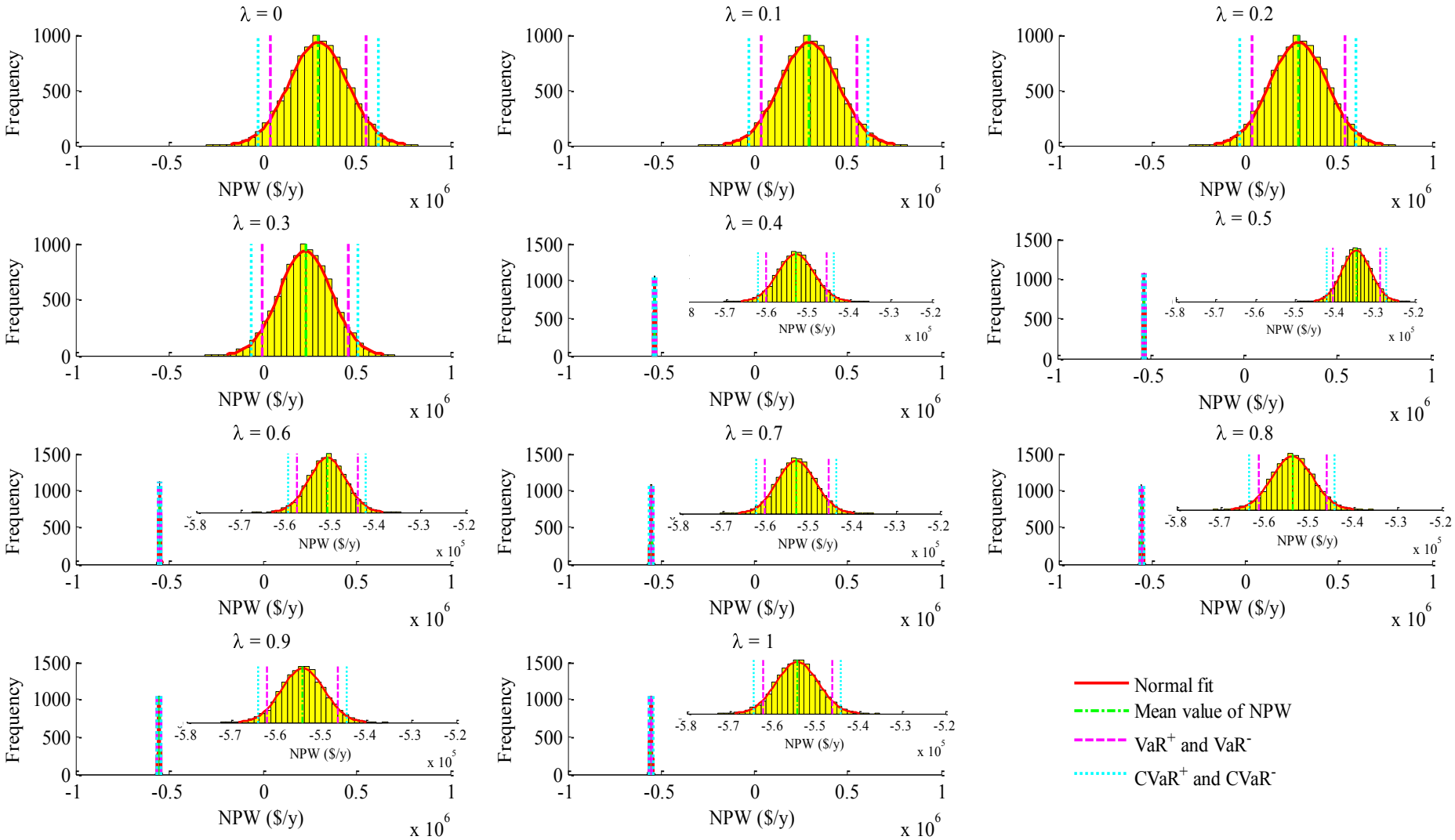

Figure 4.18. NPW distributions obtained with the objective min [λ CVaR^{+} − (1−λ) CVaR^{-}].

Figure 4.19a shows that VaR^+, VaR^-, $CVaR^+$, $CVaR^-$, and mean value of J_{NPW} have a sharp decrease when the weighting parameter is between $0.3 \leq \lambda \leq 0.4$. In Figure 4.17a it is also seen that the behavior of the curves change at the intersection point which refers to the benzene flowrate (decision variable) of 1650 kg/h. As the weight on $CVaR^+$ in the objective function (i.e., minimization of $CVaR^+$) increases and thus the weight on $CVaR^-$ in the objective function (i.e., maximization of $CVaR^-$) decreases, the $VaR^\pm$, $CVaR^\pm$, and the mean value of J_{NPW} decrease down to negative values, shifting the distribution to the left, and for $\lambda \geq 0.6$, they remain approximately constant. The mean value of J_{NPW} is lower than that of the case without optimization for $\lambda > 0.1$. $\lambda = 0$, refers to the maximization of only $CVaR^+$ and the mean value of J_{NPW} is higher compared to the case without optimization. Also the difference between $CVaR^+$ and $CVaR^-$ decreases as λ, weight for the minimization of $CVaR^+$ increases. These behaviors also comply with Figure 3.12 in Chapter 3. Similar to Figure 3.12, the mean value is lower (the NPW distribution shifts to the left), the difference between $CVaR^+$ and $CVaR^-$ is lower, and the deviation from the resulting mean value is also lower upon optimization of Equation 4.1 (the objective function) compared to the case without optimization. The NPW distribution obtained with optimization may be desirable because, although the mean NPW is lower, the NPW values mostly occur around the mean value, i.e., the mean of NPW is more certain (without optimization, the mean of NPW distribution is 2.94×10^5 \$/y and with optimization of $CVaR^+$ and $CVaR^-$, e.g., at $\lambda = 0.3$, the mean of NPW distribution is 2.27×10^5 \$/y). The mean NPW of 2.94×10^5 \$/y is higher but it has a lower probability. However, the NPW value of 2.27×10^5 \$/y is more probable. Figure 4.19b shows the changes in the skewness and kurtosis of the NPW distribution with λ. The skewness is negative for $\lambda < 0.4$. Therefore, for $\lambda < 0.4$, the distribution has left skewness, i.e., left tail is longer and the distribution is concentrated on the left side increasing the risk of obtaining lower NPW values. Additionally, Figure 4.19b and Figure 4.18 show that the resulting frequency distributions for $\lambda > 0.4$ are leptokurtic (i.e., they have positive excess kurtosis meaning that peakedness is prominent). This result reveals that when $\lambda > 0.4$, the resulting probability distribution clusters around the mean value indicating that the resulting mean value is more certain (or less risky). For $\lambda > 0.5$, with the same weight for $CVaR^+$ and $CVaR^-$, the problem directly turns into an optimization problem for the minimization of the difference between $CVaR^+$ and $CVaR^-$ which aims to attain a probability distribution with a more certain mean value. On the contrary, the frequency distributions for the $\lambda <$

0.4 region are platokurtic (i.e., they have negative excess kurtosis with a low, wide peak in the NPW distribution).

The change in the RR with λ is given in Figure 4.19c. The RR values have a sharp decrease from 22 to about 0.97 for about $\lambda < 0.4$, indicating that the absolute value (magnitude) of the ratio of $CVaR^+$ to $CVaR^-$ is large, which means positive NPW values (gain) are more probable than negative NPW values (loss) for $\lambda < 0.4$. The change in the optimal benzene flow rate with λ is given in Figure 4.19d. The optimal benzene flow rate shows a behavior similar to the RR.

In Figure 4.20, the NPW histograms were obtained with the objective function C_2 in Equation 4.2 which aims at the weighted maximization of the mean value of J_{NPW} and the difference between the $CVaR^+$ and $CVaR^-$. For each λ value, 10,000 MCS were performed at a confidence level of 95%. The calculations were based on four settlers (n = 4) and T_{apr} of 8.9 °C. Random values for the uncertain parameters of raw material cost (p_1) and product price (p_2) were drawn from normal distributions ($\mu_1 = 0.25$, $\sigma_1 = 0.03$ and $\mu_2 = 0.95$, $\sigma_2 = 0.10$, respectively).

The changes in some of the statistical properties of the NPW distribution with λ for the objective function in Equation 4.2 (i.e., minimization of the linear combination of mean value of J_{NPW} ($E[J_{NPW}]$) and the difference between $CVaR^+$ and $CVaR^-$) are graphically demonstrated in Figure 4.21. Figure 4.21a shows that VaR^+, VaR^-, $CVaR^+$, $CVaR^-$, mean value of J_{NPW} and standard deviation start to increase around $\lambda = 0.3$. In Figure 4.17b it is seen that the behavior of the curve changes at the intersection point of all λ values which refers to the benzene flowrate (decision variable) of 910 kg/h. It is observed from Figure 4.21a that, as the weight of $E[J_{NPW}]$ in the objective function (i.e., maximization of $E[J_{NPW}]$) increases and the weight of $[CVaR^+ - CVaR^-]$ (i.e., minimization of $CVaR^+$ and maximization of $CVaR^-$) decreases, the $VaR^{\pm}$, $CVaR^{\pm}$, and mean value of J_{NPW} increase significantly from large negative values to large positive values, and beyond $\lambda \geq 0.6$ they slightly increase. For $\lambda > 0.7$ the mean value of the probability distribution is higher than that of the case without optimization. When $\lambda = 0$, the problem becomes equivalent to the previous optimization problem with $\lambda = 0.5$ which was given by Equation 4.1. The mean

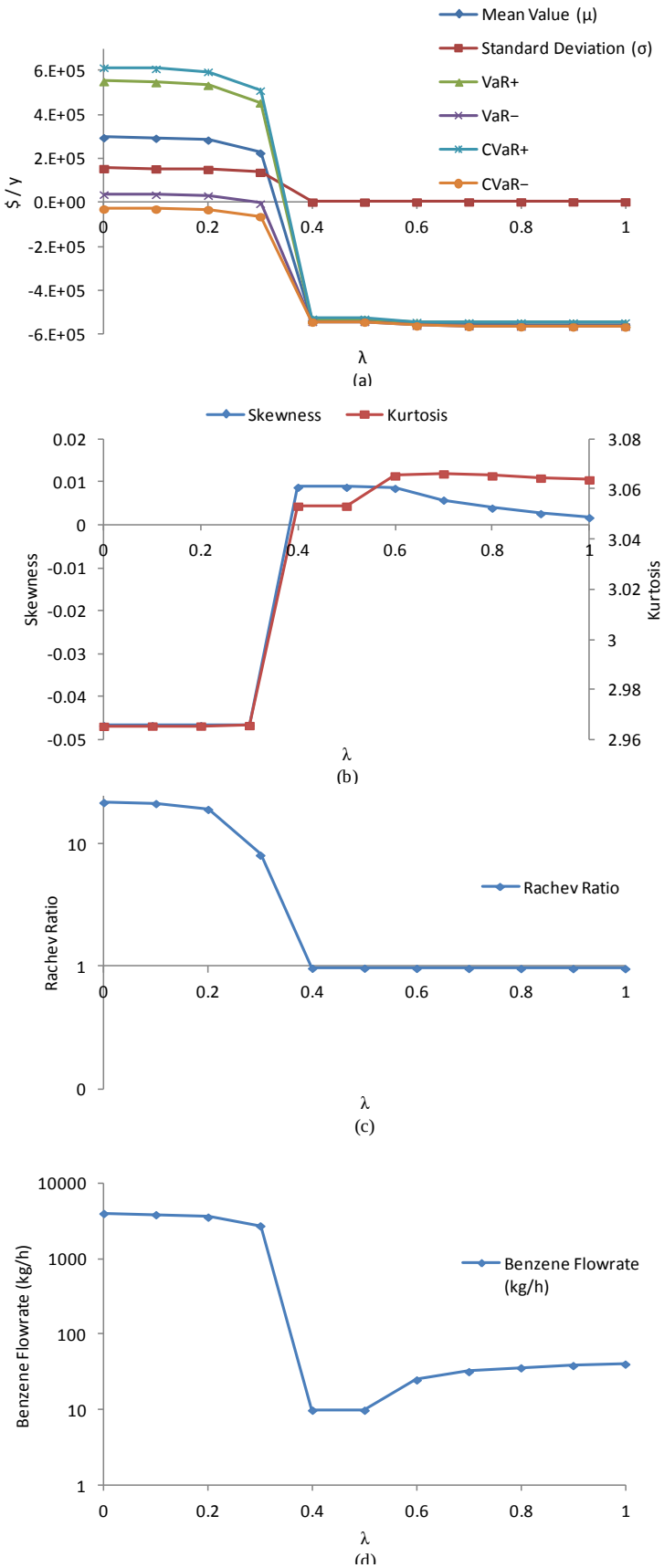

Figure 4.19. The change in some statistical properties of the NPW distribution with weighting parameter λ, for $\min[\lambda\ \mathrm{CVaR}^{+} - (1-\lambda)\ \mathrm{CVaR}^{-}]$.

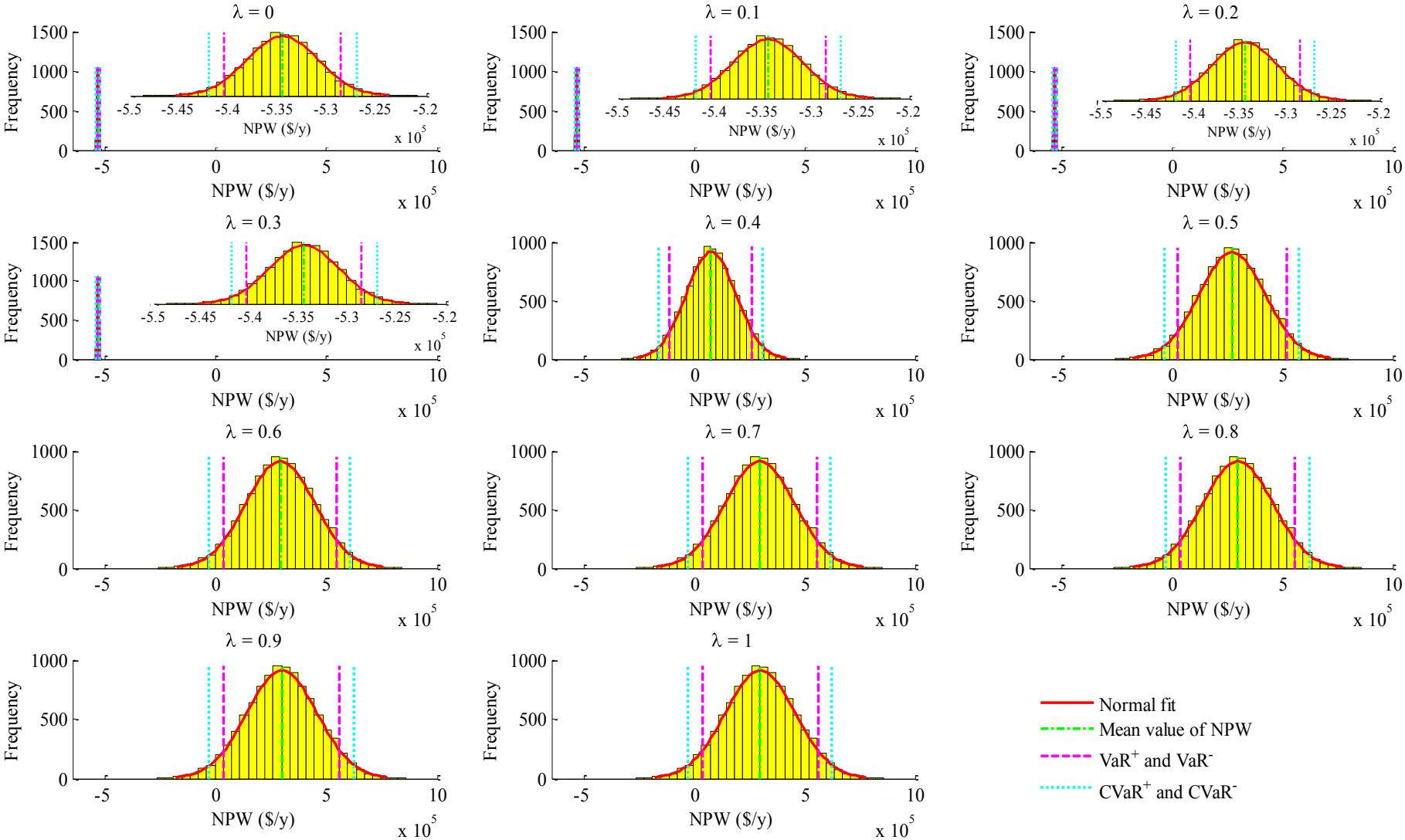

Figure 4.20. NPW distributions obtained with the objective min $[\lambda\,(-E[J_{NPW}]) + (1-\lambda)\,(\mathrm{CVaR}^{+} - \mathrm{CVaR}^{-})]$.

value of J_{NPW} is higher in this case compared to the case without optimization. It is seen in Figure 4.21a that the difference between CVaR^+ and CVaR^- increases as λ, weight for the minimization of $E[J_{NPW}]$ increases. These behaviors also comply with Figure 3.15 in Chapter 3. Similar to Figure 3.15 that was discussed in Chapter 3, the mean value is lower (the NPW distribution shifts to the right), the difference between CVaR^+ and CVaR^- is lower, and the deviation from the resulting mean value is lower upon the optimization of Equation 4.2 compared to the case without optimization. This means that the NPW distribution obtained with optimization may be desirable because, although the mean NPW is lower, the NPW values mostly occur around the mean value (i.e., the mean NPW is more certain). For the case without optimization, the mean NPW value is 2.94×10^5 \$/y and for the case where optimization of $E[J_{NPW}]$, CVaR^+ and CVaR^- is performed at $\lambda = 0.4$ the mean NPW value is 0.74×10^5 \$/y. The NPW of 0.74×10^5 \$/y is lower but it has a lower probability to occur as well. However, the lower NPW value of 0.74×10^5 \$/y is more probable. Therefore, its distribution may be considered as more desirable compared to the distribution obtained without optimization. Figure 4.21b shows the changes in the skewness and kurtosis of the NPW distribution with λ. The skewness is positive for $\lambda \leq 0.3$, and negative for $\lambda > 0.3$. Therefore, the NPW distributions for $\lambda > 0.3$ are skewed to the left, i.e., left tail is longer and the distribution is concentrated on the left side, increasing the risk of obtaining lower NPW values. Additionally, Figure 4.21b and Figure 4.20 show that the resulting frequency distributions for the optimization problem with the linear combination of $E[J_{NPW}]$ and $[\text{CVaR}^+ - \text{CVaR}^-]$ are leptokurtic (i.e., they have positive excess kurtosis meaning that peakedness is prominent) for $\lambda > 0.3$. Therefore, when $\lambda > 0.3$, the resulting probability distribution clusters around the mean value indicating that the resulting mean value is more certain (or less risky). On the contrary, the NPW distributions for $\lambda \leq 0.3$ are platokurtic (i.e.,they have negative kurtosis with a low, wide peak in the NPW distribution).

The change in the RR with the weighting coefficient, λ, is given in Figure 4.21c. When $\lambda \leq 0.3$, the RR takes a value which is stable at a value close to one (RR = 0.97), which means that the CVaR^+ and CVaR^- are close to each other and mass of the distribution is collected around the mean value of the NPW distribution. For $\lambda > 0.3$, a sharp increase is observed in RR until $\lambda = 0.7$ where RR becomes 20. For $\lambda > 0.3$, the absolute value (magnitude) of the ratio of CVaR^+ to CVaR^- is greater than one, which

means positive NPW values (gains) are more probable than negative NPW values (losses). The change in the optimal benzene flow rate with λ is given in Figure 4.21d. The optimal benzene flow rate increases for $\lambda > 0.3$.

In Figure 4.22, the NPW histograms were obtained with the objective function C_3 in Equation 4.3 which aims at the maximization of mean value of J_{NPW}, and maximization of CVaR$^-$ simultaneously. For each λ value, 10,000 MCS were performed at a confidence level of 95%. The calculations were based on four settlers (n = 4) and T_{apr} of 8.9 °C. Random values for the uncertain parameters of raw material cost (p_1) and product price (p_2) were drawn from normal distributions ($\mu_1 = 0.25$, $\sigma_1 = 0.03$ and $\mu_2 = 0.95$, $\sigma_2 = 0.10$, respectively).

The changes in some of the statistical properties of the NPW distribution with λ for the objective function in Equation 4.3 (i.e., maximization of the linear combination of mean value of J_{NPW} ($E[J_{NPW}]$) and CVaR$^-$) are demonstrated in Figure 4.23. Figure 4.23a shows that VaR$^+$ and CVaR$^+$ slightly increase whereas, VaR$^-$ and CVaR$^-$ slightly decrease as λ increases up to λ = 0.8. After that point, the VaR$^+$, CVaR$^+$, VaR$^-$ and CVaR$^-$ values all become stable. The mean value of the NPW distribution is higher compared to the case without optimization, for each λ value. It can be seen in Figure 4.23a that the difference between $E[J_{NPW}]$ and CVaR$^-$ increases as λ, weight for the maximization of $E[J_{NPW}]$ increases. These behaviors also comply with Figure 3.13 in Chapter 3. For the case without optimization, the mean of NPW is 2.94×10^5 \$/y and for the case where optimization of $E[J_{NPW}]$ and CVaR$^-$ is performed (eg. at $\lambda = 0.4$), the mean NPW value is 2.97×10^5 \$/y. The NPW of 2.94×10^5 \$/y has lower probability to occur. However, the J_{NPW}value of 2.97×10^5 \$/y, in the case for the optimization of $E[J_{NPW}]$ and CVaR$^-$, is more probable. The optimization maximizes the expected value of the J_{NPW} and, at the same time, minimizes the left tail risk of the J_{NPW} in terms of CVaR$^-$. Figure 4.23b indicates the changes in the skewness and kurtosis with λ. The skewness is positive within the entire range of λ values. Therefore, the NPW distribution is skewed to the right, i.e., right tail is longer and the distribution is concentrated on the right side, increasing the chance of obtaining higher NPW values. Additionally, Figure 4.23b and Figure 4.22 show that, for all

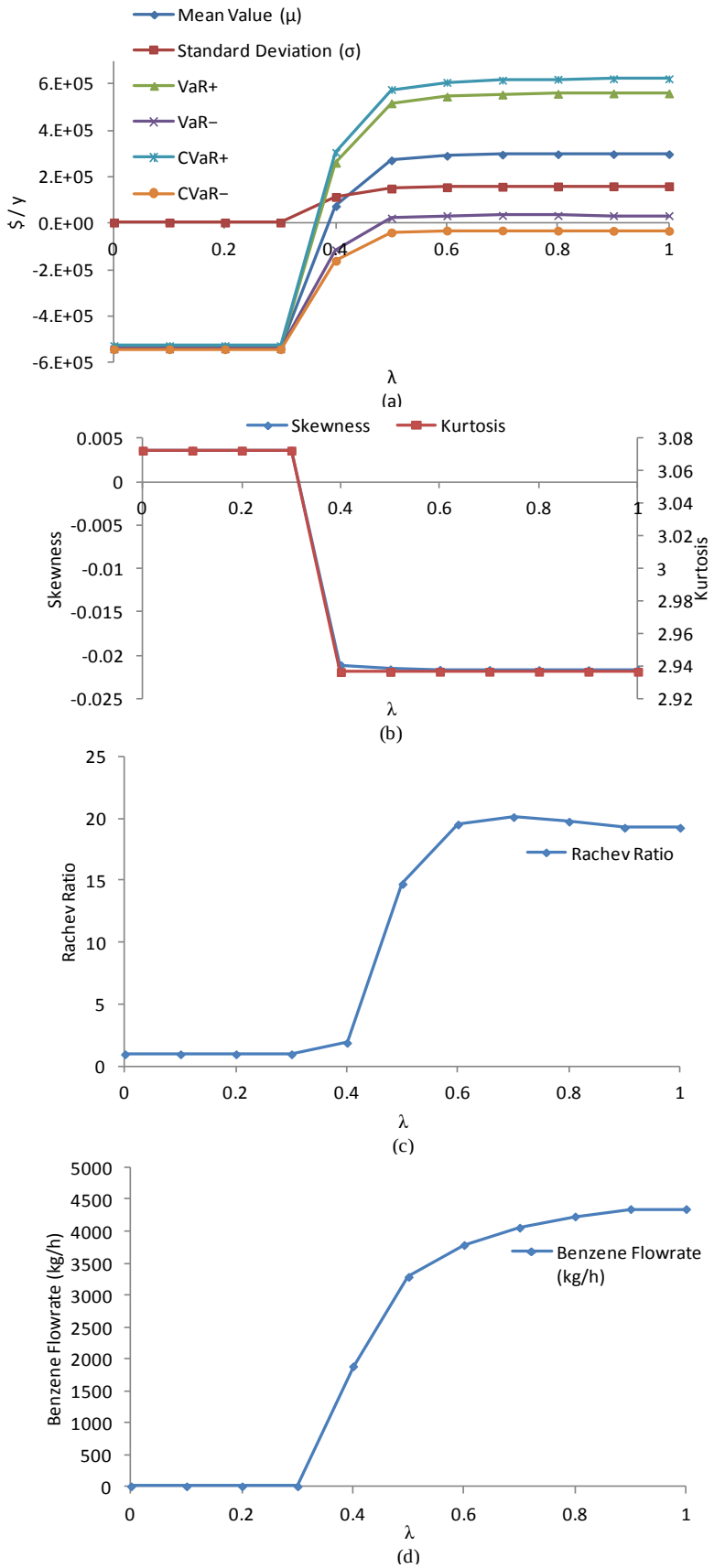

Figure 4.21. The change in some statistical properties of the NPW distribution with weighting parameter λ, for min $[\lambda\,(-E[J_{NPW}]) + (1-\lambda)\,(\mathrm{CVaR}^{+} - \mathrm{CVaR}^{-})]$.

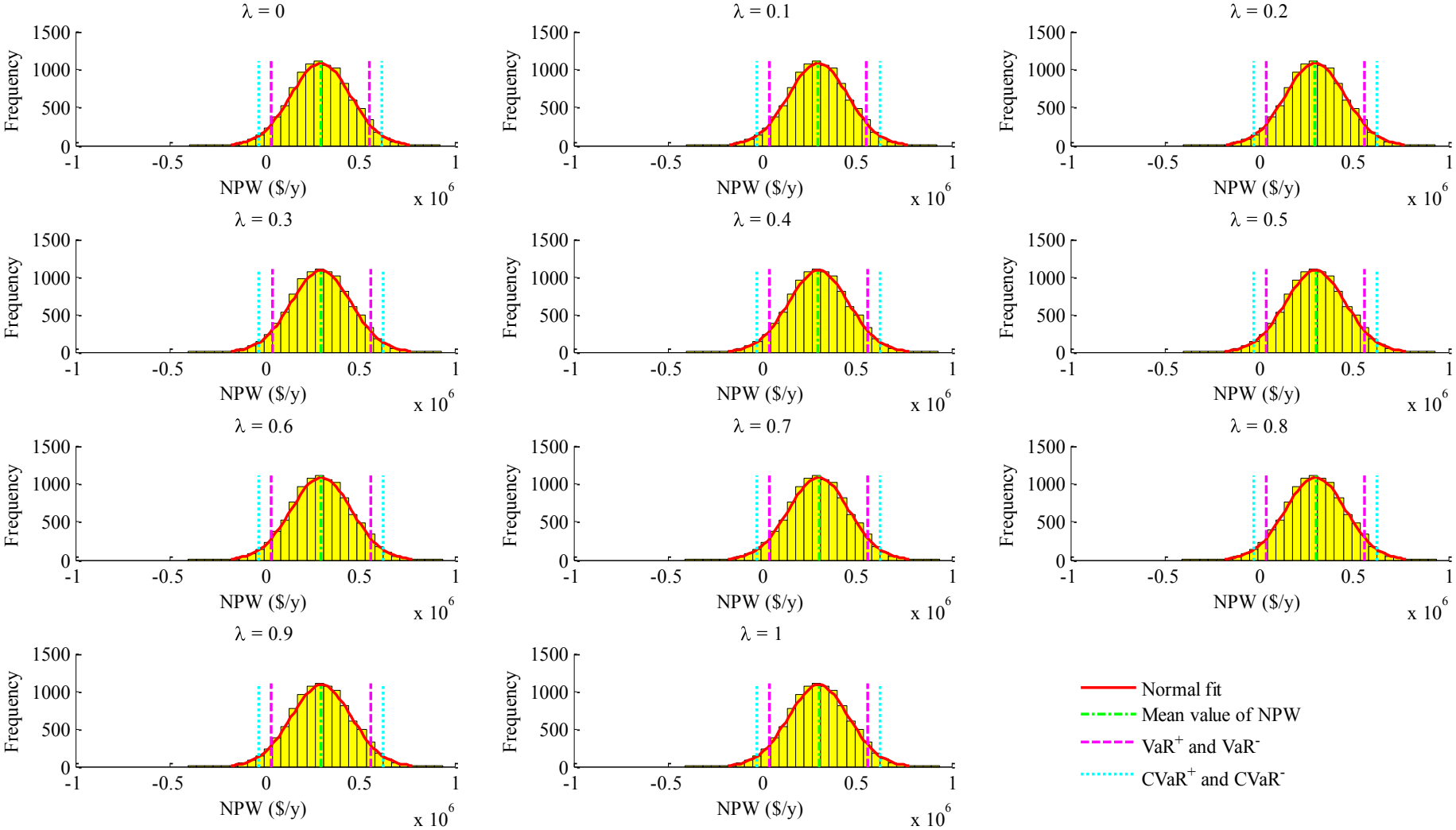

Figure 4.22. NPW distributions obtained with the objective min [λ ($-E[J_{NPW}]$) + (1−λ) (− CVaR⁻)].

λ values, the resulting distributions are leptokurtic (i.e., they have positive kurtosis with a peaked distribution).

The change in the RR with the weighting coefficient, λ, is given in Figure 4.23c. According to Equation 4.3, as λ decreases the optimization problem tends to maximize $CVaR^-$ and as λ increases the optimization problem tends to maximize $E[J_{NPW}]$. This brings about a rise in $E[J_{NPW}]$ and $CVaR^+$ and a fall in $CVaR^-$ value with an increase in λ. This causes RR (magnitude of the $CVaR^+$ / $CVaR^-$ ratio) to decrease. The absolute value (magnitude) of the ratio of $CVaR^+$ to $CVaR^-$ is greater than one, which means positive NPW values (gains) are more probable than negative NPW values (losses). According to Figure 4.23d, which shows the change in the optimal benzene flow rate with λ, as $E[J_{NPW}]$ increases the optimal benzene flow rate increases until $\lambda = 0.8$.

In Figure 4.24, the NPW histograms were obtained with the objective function C_4 in Equation 4.4 which aims at the maximization of mean value of J_{NPW}, and minimization of RR simultaneously. For each λ value, 10,000 MCS were performed at a confidence level of 95%. The calculations were based on four settlers (n = 4) and T_{apr} of 8.9 °C. Random values for the uncertain parameters of raw material cost (p_1) and product price (p_2) were drawn from normal distributions ($\mu_1 = 0.25$, $\sigma_1 = 0.03$ and $\mu_2 = 0.95$, $\sigma_2 = 0.10$, respectively).

The changes in some of the statistical properties of the NPW distribution with λ for the objective function in Equation 4.4 (i.e., minimization of the linear combination of mean value of J_{NPW} ($E[J_{NPW}]$) and Rachev Ratio (RR)) are demonstrated in Figure 4.25. Figure 4.25a shows that the VaR^+, VaR^-, $CVaR^+$, $CVaR^-$, mean value of J_{NPW}, and standard deviation do not change significantly with λ except for the case $\lambda = 0$ which corresponds to minimization of the RR only. The mean value of the NPW distribution is higher than that of the case without optimization, for each λ value. It can be seen in Figure 4.25a that the difference between $CVaR^+$ and $CVaR^-$ increases (rate of increase in RR decreases) as λ, the weight for the maximization of $E[J_{NPW}]$, increases. For the case without optimization, the mean of NPW distribution is 2.94×10^5 \$/y and for the case where optimization of $E[J_{NPW}]$ and RR is performed (eg. at $\lambda = 0.4$), the mean NPW value is 2.99×10^5 \$/y. The NPW of 2.94×10^5 \$/y has lower probability to occur. However, the

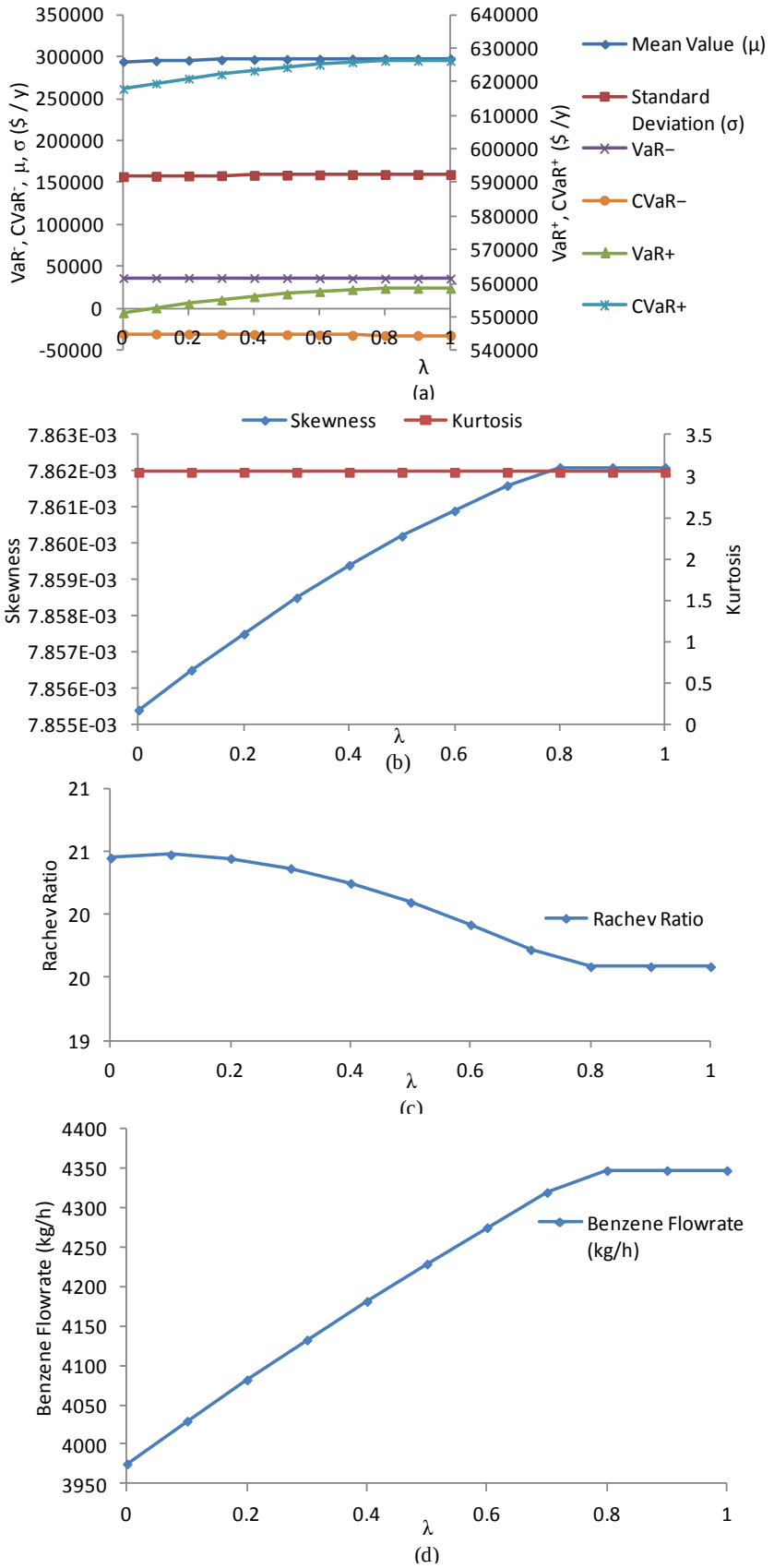

Figure 4.23. The change in some statistical properties of the NPW distribution with weighting parameter λ, for min [λ ($-E[J_{NPW}]$) + (1−λ) (−CVaR⁻)].

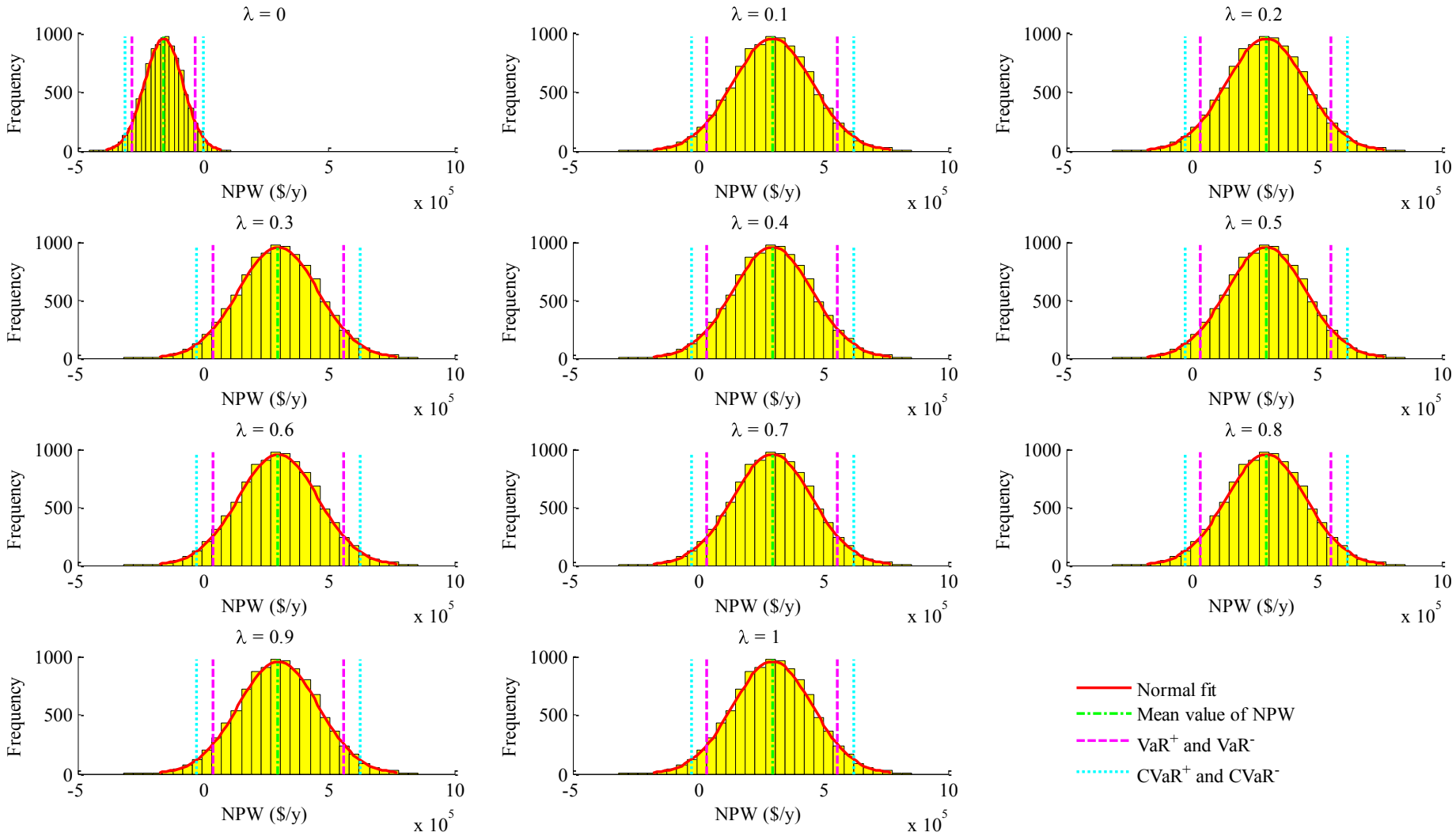

Figure 4.24. NPW distributions obtained with the objective min $[\lambda\,(-E[J_{NPW}]) + (1-\lambda)\ \mathrm{RR}]$.

J_{NPW}value of 2.99×10^5 \$/y, in the case for the optimization of $E[J_{NPW}]$ and RR, is more probable. The optimization maximizes the expected value of the J_{NPW} and, at the same time, minimizes the left tail risk and maximizes the right tail reward of the J_{NPW} in terms of CVaR$^-$ and CVaR$^+$. As Figure 4.25b shows, the changes in the skewness and kurtosis are not significant. The skewness is positive within the entire range of λ values. Therefore, the NPW distribution is skewed to the right, i.e., right tail is longer and the distribution is concentrated on the right side, increasing the chance of obtaining higher NPW values. Additionally, Figure 4.25b and Figure 4.24 show that, for all λ values, the resulting distributions are platokurtic (i.e., they have negative excess kurtosis meaning that peakedness is not prominent, they have a wide low peak). The change in the RR and optimal benzene flow rate with λ are given in Figure 4.25c and 4.25d, respectively. The RR value is stable at 23.4 for $\lambda \geq 0.01$, however when $\lambda = 0$, the RR takes a value which is close to zero. Additionally, according to Equation 4.4, as λ increases, the weight on maximization of $E[J_{NPW}]$ increases which indicates an increase in $E[J_{NPW}]$. The optimal benzene flow rate becomes 4346.7 kg/h for the weighting coefficients $\lambda \geq 0.01$, and it is estimated as 1162.8 kg/h when $\lambda = 0$. As λ increases benzene flow rate also increases.

Overall, the BAP exhibits a nonlinear behavior which is strongly dependent on the level of the benzene flow rate. This dependence on the benzene flowrate level is what determines both the BAP's sensitivity to uncertain inputs and the statistical properties of its NPW distribution. These observations demonstrate the importance of the task of selecting the nominal operating condition for a chemical plant at the plant-design stage, since both the plant's expected (mean) profitability as well as the risks and rewards (characterized in terms of left and right tail of the probability distribution of the profitability measure) associated with that design are strongly dependent upon the nominal operating point for the highly-nonlinear chemical plants. If the distributional (tail) properties of the profit measure of a chemical plant is not considered together with the mean value during the plant-design stage, it may be very difficult (costly), or even impossible, to tune them later in the operation stage.

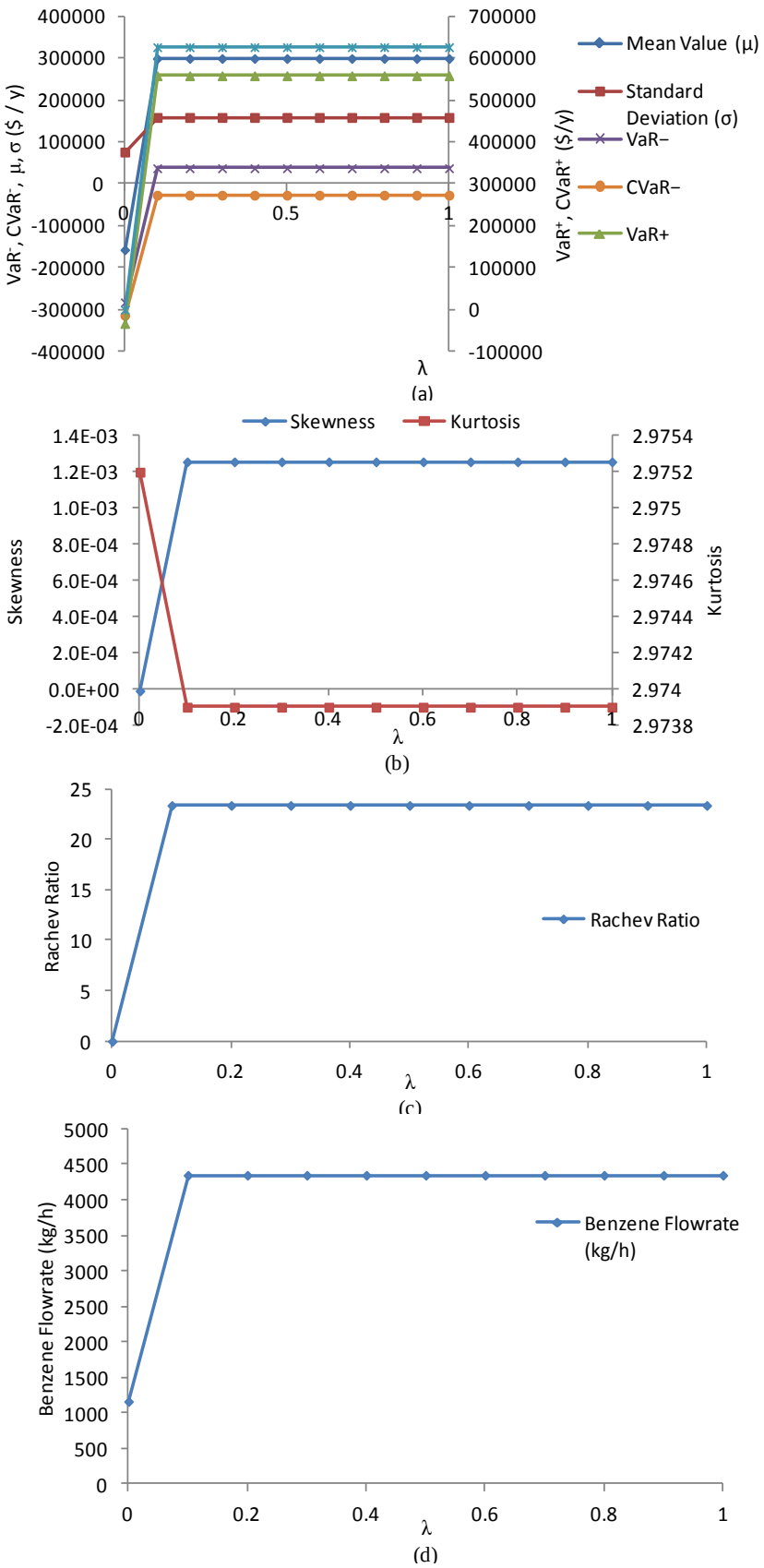

Figure 4.25. The change in some statistical properties of the NPW distribution with weighting parameter λ, for min [λ ($-E[J_{NPW}]$) + (1−λ) RR].

4.2. Alkylation Plant (AP)

The flowsheet of the Alkylation Plant (AP) example is shown in Figure 4.26. The problem had been considered for the first time by Sauer *et al*. (1964), and since then, it has been widely used as an example in many textbooks and journal articles related to process optimization (Grossmann, 1991). Some assumptions are proposed in the model itself to simplify the calculations. For example, the olefin feed is assumed to be pure butylene, isobutane input and recycle are taken as pure isobutane, fresh acid is assumed to be 98% by weight, and none of the spent acid is recycled. The objective is to maximize the profit ($/day) of the plant production.

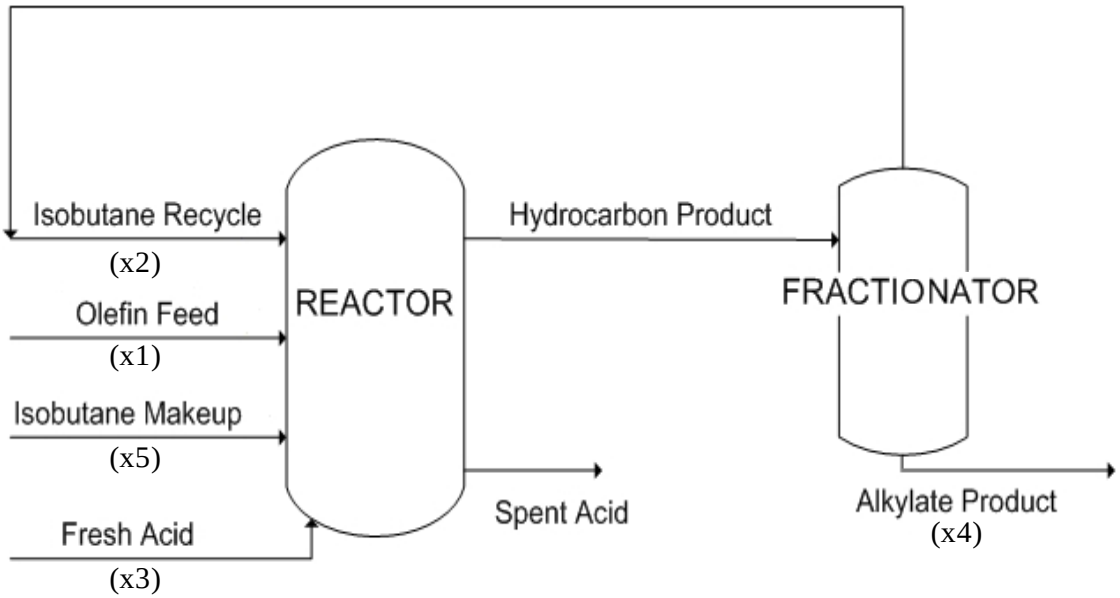

Figure 4.26. The flowsheet of the alkylation plant.

For the AP model, the objective function cost coefficients are considered as the uncertain parameters ($\boldsymbol{p}$). The decision variables are defined in a 10-component vector (x_i, where i = 1,2,…,10) which is defined as follows: x_1 is olefin feed (barrels per day), x_2 is isobutane recycle (barrels per day), x_3 is acid addition rate (1000s pounds per day), x_4 is alkylate yield (barrels per day), x_5 is isobutane input (barrels per day), x_6 is acid strength (wt %), x_7 is motor octane number of alkylate, x_8 is external isobutane-to-olefin ratio, x_9 is acid dilution factor, x_{10} is F-4 performance number of alkylate.

All decision variables defined for the AP are valid for all realizations of the uncertain cost coefficients (i.e., a unique set of optimal decision variables should satisfy the constraints under all possible realizations of the cost coefficients). All decision variables ($\boldsymbol{x}$) can simply be considered as the design variables ($\boldsymbol{d}$). Therefore, the manipulated / control variables vector ($\boldsymbol{u}$) can be omitted,

As opposed to BAP model, the AP model equations can be written explicitly as equality and inequality constraints. The mathematical formulation is given in terms of equality constraints ($\boldsymbol{h} = \boldsymbol{0}$) and variable bounds written as inequality constraints ($\boldsymbol{g} \leq \boldsymbol{0}$), together with the objective function which is the maximization of profit, Φ(\$/day):

$$
\begin{aligned}
\max_{\boldsymbol{x}} \quad & \Phi = c_1\, x_4 x_7 - c_2\, x_1 - c_3\, x_2 - c_4\, x_3 - c_5\, x_5 \\
s.t. \quad & -x_4 + x_1(1.12 + 0.13167\, x_8 - 0.0067\, {x_8}^2) = 0 \\
& -x_7 + 86.35 + 1.098\, {x_4}^2 + 0.325\, (x_6 - 89) = 0 \\
& -x_9 + 35.82 - 0.022 x_{10} = 0 \\
& -x_{10} + 3\, x_7 - 133 = 0 \\
& -x_8\, x_1 + x_2 + x_5 = 0 \\
& -x_5 + 1.22\, x_4 - x_1 = 0 \\
& -x_6(x_4\, x_9 + 1000\, x_3) + 98000\, x_3 = 0 \\
& x_j^L < x_j \\
& x_j < x_j^U \qquad \forall\, j \in \{1,2,..,10\}
\end{aligned}
\tag{4.5}
$$

The objective (profit) function, Φ (\$/day), is based on the following coefficients which are defined as uncertain parameters, $\boldsymbol{p}$: c_1 is alkylate product value, (\$ / octane-barrel), c_2 is olefin feed cost, (\$ / barrel), c_3 is isobutane recycle cost, (\$ / barrel), c_4 is acid addition cost, (\$ / barrel), c_5 is isobutane feed cost, (\$ / barrel).

The mean value and standard deviation of the uncertain coefficients are given in Table 4.6.

Table 4.6. Mean values and standard deviations for the objective function coefficients.

	Mean value (μ)	Standard deviation (σ)
c_1 ($ / octane-barrel)	0.075	0.001
c_2 ($ / barrel)	5	0.05
c_3 ($ / barrel)	0.05	0.001
c_4 ($ / barrel)	10	0.1
c_5 ($ / barrel)	3	0.05

The upper and lower limits of the decision variables, which may be treated as the inequality constraints, are given in Table 4.7 below.

Table 4.7. Bounds on the decision variables.

Decision Variable	x_j^L	x_j^U
x_1	1500	10000
x_2	5000	10000
x_3	50	500
x_4	500	10000
x_5	500	5000
x_6	50	500
x_7	50	500
x_8	1	50
x_9	1	20
x_{10}	50	500

4.2.1. Sequential Solution of the Alkylation Plant for CVaR$^{\pm}$ Computations

The optimization problem, with seven equality constraints and ten decision variables, has three degrees of freedom. The optimization problem is NLP and was solved with GAMS using CONOPT as the NLP solver. The MATLAB codes for this plant exist in Appendix B and GAMS codes are present in Appendix C.

In all the calculations, the uncertain parameters c_k's (where $k \in \{1, 2,\ldots,5\}$) are sampled randomly from normal distributions with mean (μ) and standard deviation (σ) values as given in Table 4.6. Then, the sufficient number of Monte Carlo Simulations (nMCS) is determined in order to obtain a stable probability distribution of the profit, Φ. For this purpose, the standard deviation and the mean values of the profit are plotted against the nMCS in Figure 4.27.

Repeated solutions of the AP model were performed for different number of samples of uncertain cost coefficients that were taken from normal distributions given in Table 4.6. The statistical properties of thus obtained distributions of objective function were computed off-line in MATLAB (sequentially, as depicted by Figure 3.7 of Chapter 3). Figure 4.27 shows that the mean profit and standard deviation against the nMCS reach stability at about 8,000 nMCS. Therefore, from now on, all computations are based on 8,000 nMCS. Historical $VaR^{\pm}$ and $CVaR^{\pm}$ at each nMCS are further given in the graph in Figure 4.27. It is interesting to note that especially $CVaR^{+}$ persists to be relatively unstable as compared to others. For the AP model, following Konno *et al.* (2011), a modified Rachev Ratio (RR) is defined as the ratio of the difference of the mean (μ) from $CVaR^{+}$ (DIFP = $CVaR^{+} - \mu$) and the difference of $CVaR^{-}$ from the mean (DIFM = $\mu - CVaR^{-}$); RR = DIFP/DIFM = $[CVaR^{+} - \mu]/[\mu - CVaR^{-}]$.

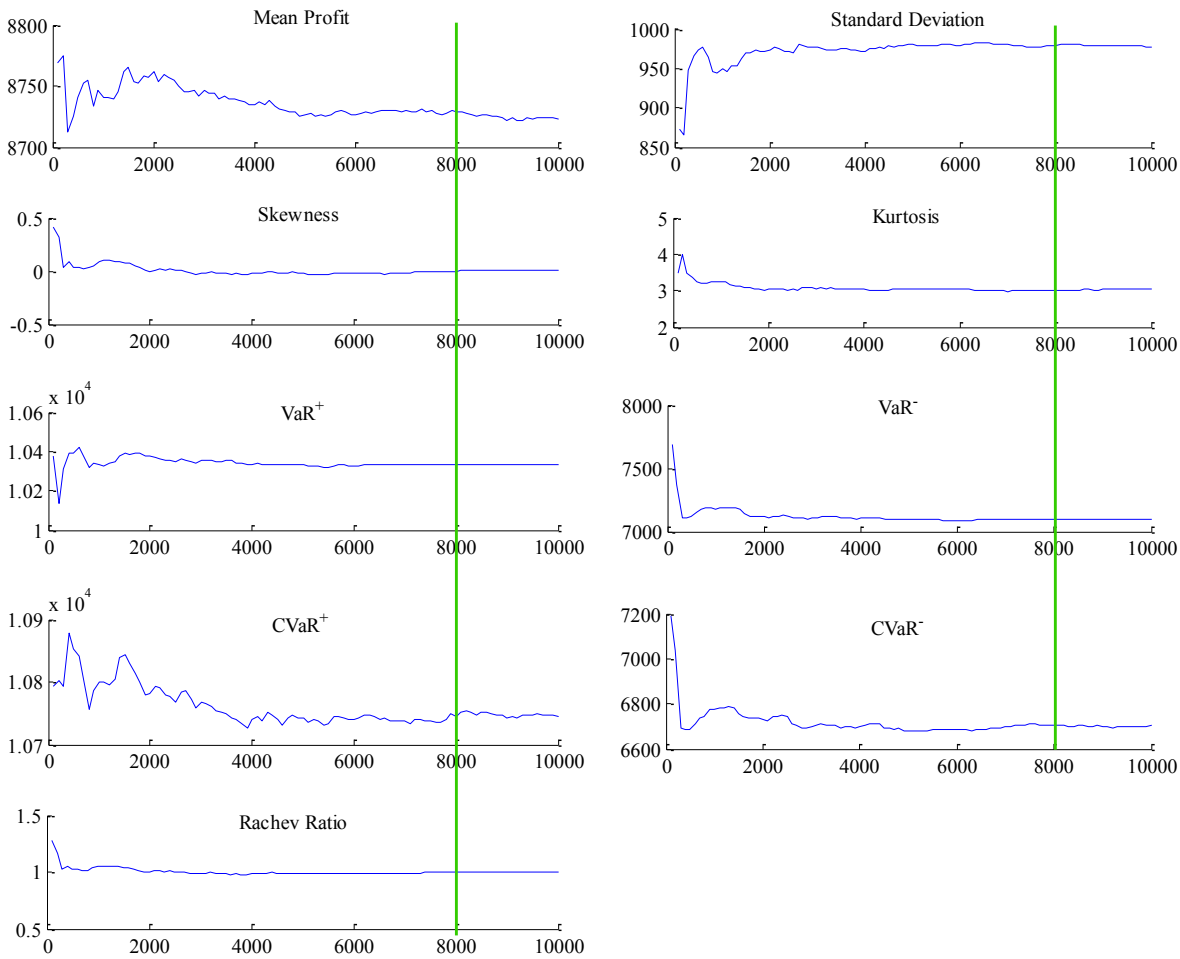

Figure 4.27. Changes in Mean Profit, Standard Deviation, Skewness, Kurtosis, $VaR^{\pm}$, $CVaR^{\pm}$ and Rachev Ratio with nMCS.

The frequency distribution plot of the optimal profits (Φ, \$/day) for 8,000 nMCS and at the confidence level of 95%, is given in Figure 4.28. Some statistical results including parametric ($PVaR^{\pm}$, $PCVaR^{\pm}$, computed with Equations 2.24 and 2.25) and historical ($VaR^{\pm}$, $CVaR^{\pm}$, computed with the percentile form given by Equations 2.8 and 2.9 in Chapter 2) values for VaR and CVaR, the mean (μ) value, standard deviation (σ), skewness, kurtosis of the cost, the difference of $CVaR^{+}$ and $CVaR^{-}$, the difference of the mean (μ) from $CVaR^{+}$ (DIFP) and $CVaR^{-}$ (DIFM), and the Rachev Ratio (RR) related to Figure 4.28 are given in Table 4.8. The optimal values for the decision variables for minimization of [$CVaR^{+} - CVaR^{-}$] using the sequential algorithm are presented in Table 4.9.

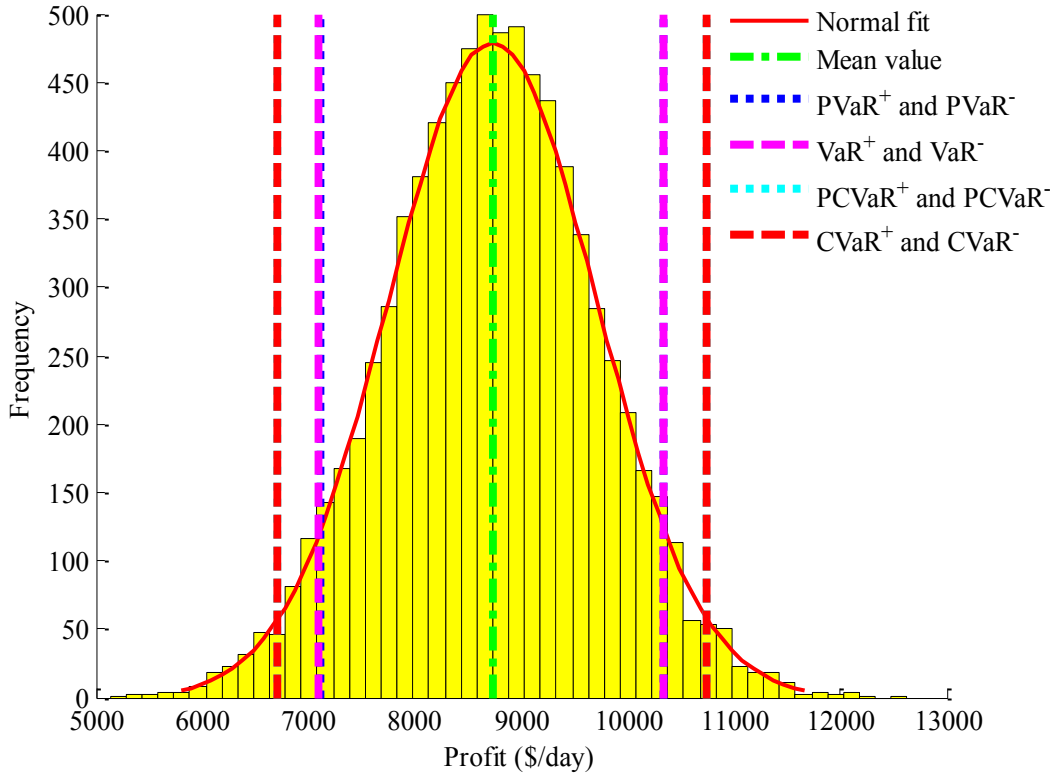

Figure 4.28. Frequency distribution of the optimal profits of the AP obtained using the sequential algorithm at 8,000 nMCS.

The resulting probability distribution has almost negligible negative skewness. This means that the distribution is very slightly skewed to the left; only faintly increasing the probability of obtaining profit values less than the mean value. The DIFP/DIFM ratio (RR) gives an idea about the proportion of the distances between $CVaR^{+}$ and mean value and between mean value and $CVaR^{-}$. If it is greater than one, the distance between $CVaR^{+}$ and mean value is higher than the distance between mean value and $CVaR^{-}$, i.e., the chance of obtaining a profit value greater than the mean profit is higher than obtaining a profit value lower than the mean profit. In this case, the RR is very close one, which means that the risk of obtaining a profit value lower than the mean profit is almost equal to taking a profit value higher than the mean profit.

Table 4.8. Statistical properties of the distribution of the optimal profits.

Mean Value (μ)	8729.3	$/day
Standard Deviation (σ)	978.71	$/day
Skewness	− 0.0029	
Kurtosis	3.0129	
$PVaR^{+}$	10339	$/day
$PVaR^{-}$	7119.4	$/day
VaR^{+}	10334	$/day
VaR^{-}	7098.3	$/day
$PCVaR^{+}$	10748	$/day
$PCVaR^{-}$	6710.4	$/day
$CVaR^{+}$	10744	$/day
$CVaR^{-}$	6705.2	$/day
$(CVaR^{+} - CVaR^{-})$	4039.3	$/day
DIFP	2015.2	$/day
DIFM	2024.1	$/day
RR	0.9956	

Table 4.9. Mean Values and Standard Deviations of the optimal values of decision variables ($\boldsymbol{x}$) for maximization of profit using the sequential algorithm at 8,000 nMCS.

Decision Variable	Mean Value	Standard Deviation
x_1	7363.2	constant
x_2	10000	constant
x_3	450	3.18
x_4	10000	constant
x_5	4836.8	constant
x_6	83.9	0.13
x_7	86.8	0.04
x_8	2.0	constant
x_9	7.6	0.03
x_{10}	127.2	0.13

4.2.2. Simultaneous Solution of the Alkylation Plant for CVaR$^{\pm}$ Computations

The flowchart for the simultaneous algorithm of optimization under uncertainty was given in Figure 3.8 of Chapter 3. Similarly, the flowchart for the simultaneous algorithm for the AP is given in Figure 4.29. In this algorithm, the uncertain parameters of cost coefficients ($\boldsymbol{p}$) are randomly generated. Then, the objective function, together with the augmented plant equations and CVaR equations as constraints, is optimized simultaneously.

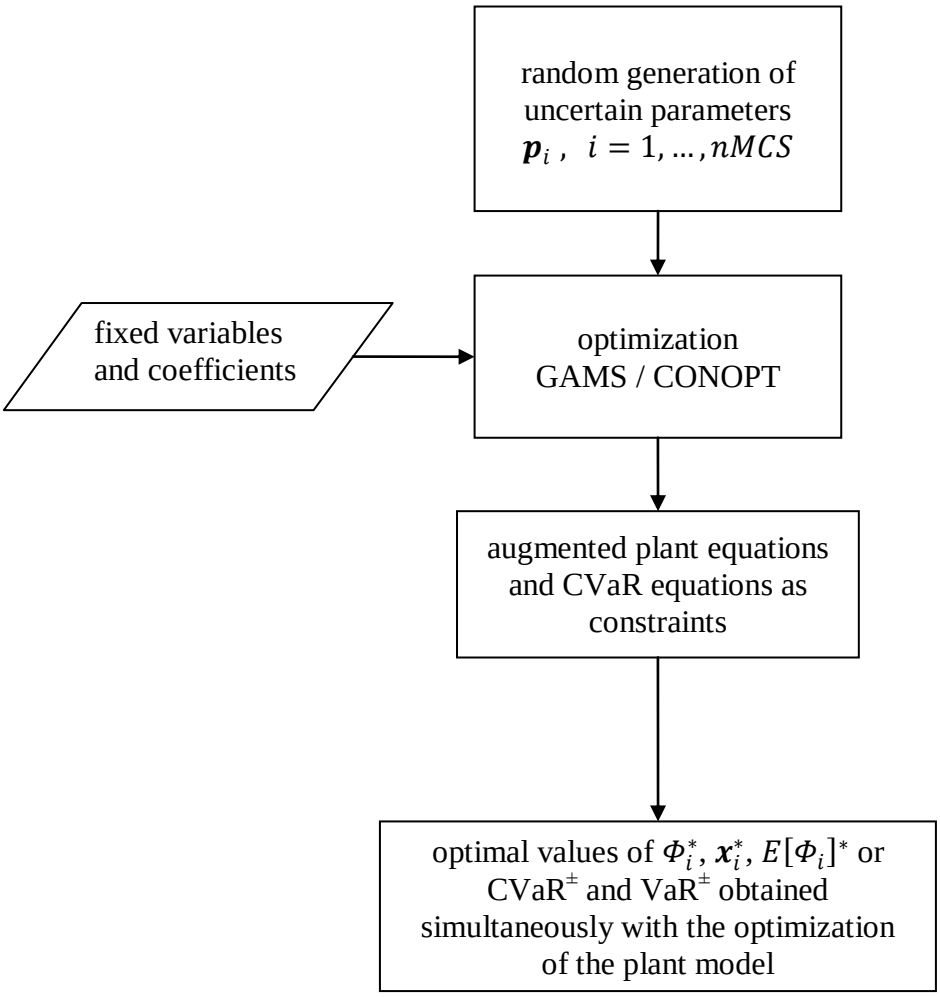

Figure 4.29. Flowchart for the simultaneous algorithm for the AP.

4.2.2.1. Objective Function: Minimization of [CVaR^{+} − CVaR^{-}]. The general formulation for the optimization of [CVaR^{+} − CVaR^{-}] under uncertainty given in Chapter 3 is restated in Equation 4.6 below.

$$\min_{\boldsymbol{d},\boldsymbol{u}_i,\boldsymbol{x}_i,\gamma,\eta,z_i^-,z_i^+} \quad \left(\gamma + \frac{1}{N(1-\alpha)}\sum_{i=1}^{N} z_i^+\right) - \left(\eta - \frac{1}{N(1-\alpha)}\sum_{i=1}^{N} z_i^-\right)$$

$$s.t. \quad \left.\begin{array}{l} z_i^- \geq \eta - J_i(\boldsymbol{d},\boldsymbol{x}_i,\boldsymbol{u}_i,\boldsymbol{p}_i) \\ z_i^+ \geq J_i(\boldsymbol{d},\boldsymbol{x}_i,\boldsymbol{u}_i,\boldsymbol{p}_i) - \gamma \\ z_i^- \geq 0 \\ z_i^+ \geq 0 \end{array}\right\} \begin{array}{c} CVaR\ Constraints\ (linear) \\ i = 1,\dots,N \end{array} \tag{4.6}$$

$$\left.\begin{array}{c} \boldsymbol{h}_i(\boldsymbol{d},\boldsymbol{x}_i,\boldsymbol{u}_i,\boldsymbol{p}_i) = \boldsymbol{0}_i \\ \boldsymbol{g}_i(\boldsymbol{d},\boldsymbol{x}_i,\boldsymbol{u}_i,\boldsymbol{p}_i) \leq \boldsymbol{0}_i \\ \boldsymbol{d}^{lb} \leq \boldsymbol{d} \leq \boldsymbol{d}^{ub} \\ \boldsymbol{u}_i^{lb} \leq \boldsymbol{u}_i \leq \boldsymbol{u}_i^{ub} \\ \boldsymbol{x}_i^{lb} \leq \boldsymbol{x}_i \leq \boldsymbol{x}_i^{ub} \end{array}\right\} \begin{array}{c} Plant\ Constraints \\ (linear\ or\ nonlinear) \\ i = 1,\dots,N \end{array}$$

Based on the general problem in Equation 4.6, the mathematical formulation for the minimization of [CVaR^{+} − CVaR^{-}] for the AP model is given by Equation 4.7.

$$\min_{\boldsymbol{x},\gamma,\eta,z_i^-,z_i^+} \quad \left(\gamma + \frac{1}{N(1-\alpha)}\sum_{i=1}^{N} z_i^+\right) - \left(\eta - \frac{1}{N(1-\alpha)}\sum_{i=1}^{N} z_i^-\right)$$

$$s.t. \quad \left.\begin{array}{l} z_i^- \geq \eta - \Phi_i(\boldsymbol{x},\boldsymbol{p}_i) \\ z_i^+ \geq \Phi_i(\boldsymbol{x},\boldsymbol{p}_i) - \gamma \\ z_i^- \geq 0 \\ z_i^+ \geq 0 \end{array}\right\} \begin{array}{c} CVaR\ Constraints\ (linear) \\ \forall\ i = 1,\dots,N \end{array}$$

$$\begin{aligned} -x_4 + x_1(1.12 + 0.13167\,x_8 - 0.0067\,{x_8}^2) &= 0 \\ -x_7 + 86.35 + 1.098\,{x_4}^2 + 0.325\,(x_6 - 89) &= 0 \\ -x_9 + 35.82 - 0.022\,x_{10} &= 0 \\ -x_{10} + 3\,x_7 - 133 &= 0 \\ -x_8\,x_1 + x_2 + x_5 &= 0 \\ -x_5 + 1.22\,x_4 - x_1 &= 0 \\ -x_6(x_4\,x_9 + 1000\,x_3) + 98000\,x_3 &= 0 \\ x_j^L < x_j & \\ x_j < x_j^U \quad \forall\, j \in \{1,2,..,10\} & \end{aligned} \tag{4.7}$$

where:

$$\Phi_i(\boldsymbol{x},\boldsymbol{p}_i) = +c_{1_i}\,x_4 x_7 - c_{2_i}\,x_1 - c_{3_i}\,x_2 - c_{4_i}\,x_3 - c_{5_i}\,x_5\ ;\ i = 1,\dots,nMCS$$

Upon feasible and optimal solution, VaR^+, VaR^-, $CVaR^+$, $CVaR^-$ are evaluated at the optimal values of γ, η, $\boldsymbol{z}^+$ and $\boldsymbol{z}^-$ as follows:

$$\begin{aligned} VaR^+ &= \gamma^* \\ VaR^- &= \eta^* \\ CVaR^+ &= \gamma^* + \frac{1}{N(1-\alpha)}\sum_{i=1}^{N}(z_i^+)^* \\ CVaR^- &= \eta^* - \frac{1}{N(1-\alpha)}\sum_{i=1}^{N}(z_i^-)^* \end{aligned} \tag{4.8}$$

All the decision variables, $\boldsymbol{x}$, are taken as valid for all realizations of uncertain variables, and the control ($\boldsymbol{u}$) and design variables ($\boldsymbol{d}$) in Equation 4.6 are omitted in the AP formulation. Among the plant equations, only the plant objective (profit, Φ_i) includes uncertain variables (p_i), therefore it involves the subscript *i* that shows the ith MC sampling. The equality ($\boldsymbol{h} = \boldsymbol{0}$) and inequality ($\boldsymbol{g} \leq \boldsymbol{0}$) constraints, for the plant model itself, depend only on the decision variables ($\boldsymbol{x}$). Since the plant constraints do not include uncertain variables ($\boldsymbol{p}$) they are independent of the MC samples. (i.e., *N* = *nMCS*, which is chosen as 8,000 for the AP), and therefore, do not take the subscript *i*. ($\boldsymbol{z}^+$) and ($\boldsymbol{z}^-$) vectors are taken as positive auxiliary variables, therefore they are not included in inequality constraints.

Since the decision variables are not related to MC samples, the number of decision variables is 2×N+12 (2×N is for the $\mathbf{z}^+$ and $\mathbf{z}^-$, 10 for decision variables $\boldsymbol{x}$, and 2 for γ and η). The number of equality constraints is 7 (plant's equality constraints). The number of inequality constraints is 2×N (2×N represents the inequalities coming from Uryasev's formulations, i.e., Equation 2.28 and 2.29). The number of variable bounds is 2×N+20 (2×N is for $\boldsymbol{z}^+ \geq \boldsymbol{0}$ and $\boldsymbol{z}^- \geq \boldsymbol{0}$, and 20 is for $\boldsymbol{x}^L \leq \boldsymbol{x} \leq \boldsymbol{x}^U$). Among the constraints only 4 of the 7 plant equality constraints are nonlinear, the rest of the constraints i.e., the remaining 3 equations and 2×N inequalities are all linear. The objective function is also linear in decision variables. For 8,000 nMCS, the simultaneous algorithm has 16,012 decision variables, 7 equality constraints, 16,000 inequality constraints, and 16,020 variable bounds.

For minimization of [$CVaR^+ - CVaR^-$] objective, the frequency plot of the profit ($\boldsymbol{\Phi}$) values, at 8,000 MCS and the confidence level of 95%, is given in Figure 4.30. Random

values for the uncertain parameters of cost coefficients ($\boldsymbol{p}$) are drawn from normal distributions using the mean values and standard deviations given in Table 4.6. Some statistical results including parametric ($PVaR^{\pm}$, $PCVaR^{\pm}$, computed with Equations 2.24 and 2.25) and historical ($VaR^{\pm}$, $CVaR^{\pm}$, computed with the percentile form given by Equations 2.8 and 2.9 in Chapter 2) values for VaR and CVaR, the mean (μ) value, standard deviation (σ), skewness, kurtosis of the profit distribution, the difference of the mean (μ) from $CVaR^{+}$ (DIFP) and $CVaR^{-}$ (DIFM), and the Rachev Ratio (RR) related to Figure 4.30 are given in Table 4.10. The optimal values for the decision variables for minimization of [$CVaR^{+} - CVaR^{-}$] using the simultaneous algorithm are presented in Table 4.11.

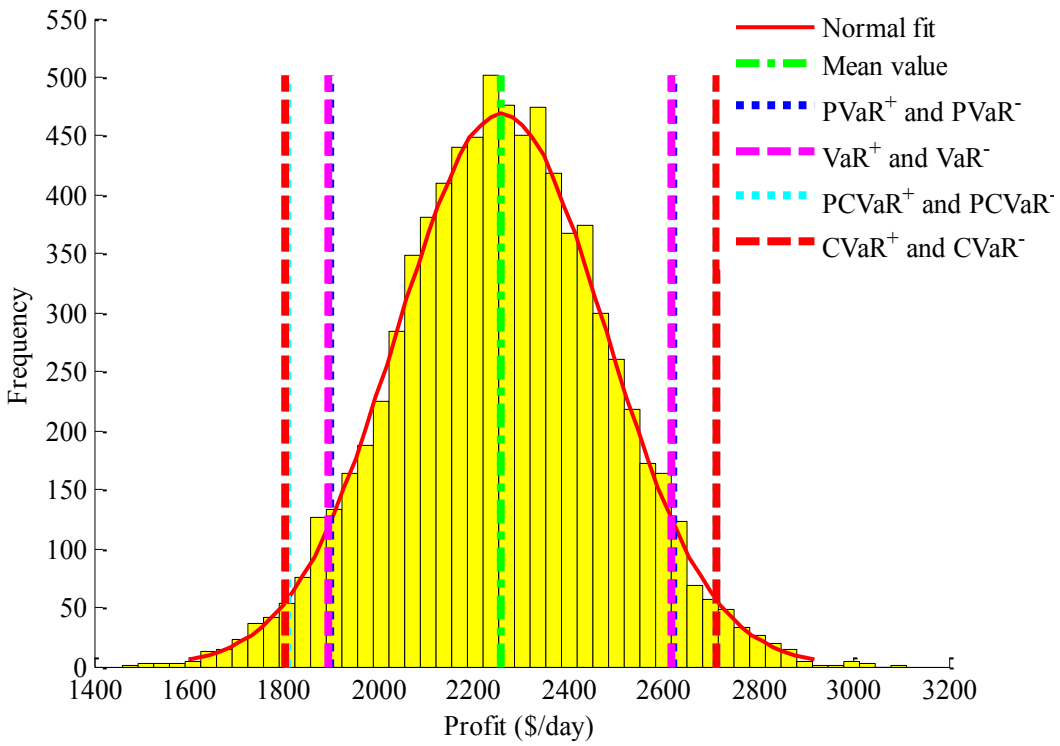

Figure 4.30. Frequency distribution of profit using simultaneous algorithm for minimization of [$CVaR^{+} - CVaR^{-}$].

The distribution of the profit values ($\boldsymbol{\Phi}$) in Figure 4.30, i.e., the distribution obtained via the minimization of [$CVaR^{+} - CVaR^{-}$] using simultaneous method, shows that, as compared to Figure 4.28 (sequential method, where the objective was the maximization of profit at each MCS), the mean value of the profit decreases from 8729.3 $/day to 2258.4

$/day (decreases by 74%), shifting the frequency distribution of the profit to the left in Figure 4.30. However, it also shows that when simultaneous method is followed (as in Figure 4.30) the difference of $CVaR^+$ and $CVaR^-$ becomes lower than the difference of $CVaR^+$ and $CVaR^-$ when sequential algorithm is implemented (as in Figure 4.28, where the objective was the maximization of profit at each MCS). Minimization of $[CVaR^+ - CVaR^-]$ shifts $CVaR^+$ to the left and $CVaR^-$ to the right as much as the constraints allow.

The difference between the parametric and historical $VaR^\pm$ and $CVaR^\pm$ values with simultaneous method (where the objective was the minimization of $[CVaR^+ - CVaR^-]$) is less than the case with sequential algorithm (where the objective was the maximization of profit at each MCS), since the minimization of $[CVaR^+ - CVaR^-]$ shifts the mean profit significantly to the left, as can be seen from comparison of Table 4.8 and Table 4.10. Furthermore, in the simultaneous method, the difference between $CVaR^+$ value and mean profit (DIFP = 452.3) is only slightly less than the difference between mean profit and value of $CVaR^-$ (DIFM = 455.1). On the other hand, in the sequential method (where the objective was the maximization of profit at each MCS) DIFP = 2015.2 and DIFM = 2024.1. This means that, with the minimization of $[CVaR^+ - CVaR^-]$ objective in the simultaneous method, the company significantly decreases the mean profit however increases the certainty of the mean profit. The decrease in RR from the value of 0.9956 in Table 4.8 (i.e., sequential method, where the objective was the maximization of profit at each MCS) to 0.9938 in Table 4.10 (i.e., simultaneous method, where the objective is the minimization of $[CVaR^+ - CVaR^-]$) shows that the decrease in $CVaR^-$ slightly overwhelms the increase in $CVaR^+$ while shifting the mean profit significantly to the left.

Table 4.10. Statistical properties of the profit distribution in Figure 4.30, as a result of minimization of [$CVaR^{+} - CVaR^{-}$].

Mean Value (μ)	2258.4	\$/day
Standard Deviation (σ)	219.98	\$/day
Skewness	-5.85×10^{-3}	
Kurtosis	2.9996	
$PVaR^{+}$	2620.2	\$/day
$PVaR^{-}$	1896.6	\$/day
VaR^{+}	2617.1	\$/day
VaR^{-}	1892.7	\$/day
$PCVaR^{+}$	2712.2	\$/day
$PCVaR^{-}$	1804.6	\$/day
$CVaR^{+}$	2710.7	\$/day
$CVaR^{-}$	1803.2	\$/day
($CVaR^{+} - CVaR^{-}$)	907.49	\$/day
DIFP	452.33	\$/day
DIFM	455.15	\$/day
RR	0.9938	

Optimal values of decision variables ($\boldsymbol{x}$) for minimization of [$CVaR^{+} - CVaR^{-}$] using the simultaneous algorithm are given in Table 4.11. A comparison with the sequential algorithm's decision variables (where the objective was the maximization of profit at each MCS) given in Table 4.8 shows that using simultaneous algorithm requires less olefin feed (x_1), acid addition (x_3), alkylate yield (x_4), acid strength (x_6) with higher external isobutane-to-olefin ratio (x_8) and acid dilution factor (x_9).

Table 4.11. Optimal values of decision variables ($\boldsymbol{x}$) for minimization of [CVaR^{+} − CVaR^{-}] using the simultaneous algorithm.

Decision Variable	x_i^*
x_1	1500.0
x_2	5000.0
x_3	50.0
x_4	2336.0
x_5	1349.9
x_6	66.8
x_7	83.1
x_8	4.2
x_9	10.0
x_{10}	116.3

<u>4.2.2.2. Objective Function: Minimization of CVaR^{+}.</u> Based on the general problem defined by Equation 3.15 of Chapter 3, the mathematical formulation for the minimization of CVaR^{+} for the AP model is given by Equation 4.9.

$$
\begin{aligned}
\min_{\boldsymbol{x},\gamma,z_i^+} \quad & \left(\gamma + \frac{1}{N(1-\alpha)}\sum_{i=1}^{N} z_i^+\right) \\
s.t. \quad & \left.\begin{aligned} z_i^+ &\geq \Phi_i(\boldsymbol{x},\boldsymbol{p}_i) - \gamma \\ z_i^+ &\geq 0 \end{aligned}\right\} \begin{aligned} &CVaR\ Constraints\ (linear) \\ &\forall\, i = 1,\dots,N \end{aligned} \\
& -x_4 + x_1(1.12 + 0.13167\, x_8 - 0.0067\, {x_8}^2) = 0 \\
& -x_7 + 86.35 + 1.098\, {x_4}^2 + 0.325\,(x_6 - 89) = 0 \\
& -x_9 + 35.82 - 0.022\, x_{10} = 0 \\
& -x_{10} + 3\, x_7 - 133 = 0 \\
& -x_8\, x_1 + x_2 + x_5 = 0 \\
& -x_5 + 1.22\, x_4 - x_1 = 0 \\
& -x_6(x_4\, x_9 + 1000\, x_3) + 98000\, x_3 = 0 \\
& x_j^L < x_j \\
& x_j < x_j^U \qquad \forall\, j \in \{1,2,..,10\}
\end{aligned}
\tag{4.9}
$$

where:

$$\Phi_i(\boldsymbol{x},\boldsymbol{p}_i) = +c_{1_i}\, x_4 x_7 - c_{2_i}\, x_1 - c_{3_i}\, x_2 - c_{4_i}\, x_3 - c_{5_i}\, x_5\ ;\ i = 1,\dots,nMCS$$

Upon feasible and optimal solution, VaR$^+$ and CVaR$^+$ are evaluated at the optimal values of γ and $\boldsymbol{z}^+$ as follows:

$$VaR^+ = \gamma^*$$
$$CVaR^+ = \gamma^* + \frac{1}{N(1-\alpha)}\sum_{i=1}^{N}(z_i^+)^* \tag{4.10}$$

As explained in Section 3.3.2 of Chapter 3, the problem in Equation 4.9 is a minimization problem since the profit (right-side) tail risk of the probability distribution of the plant objective is minimized in terms of the risk measure CVaR$^+$. The problem should not be converted to maximization form since it is unbounded in that direction. All the decision variables, $\boldsymbol{x}$, are taken as valid for all realizations of uncertain variables, and the control ($\boldsymbol{u}$) and design variables ($\boldsymbol{d}$) in Equation 4.6 are omitted in the AP formulation. The inequalities which belong to the left side of the resulting frequency distribution of profit and the left side related term in the objective function are also omitted from the model in Equation 4.9. Among the plant equations, only the plant objective (profit, Φ_i) includes uncertain variables (p_i), therefore it involves the subscript *i* that shows the ith MC sampling. The equality ($\boldsymbol{h} = \boldsymbol{0}$) and inequality ($\boldsymbol{g} \leq \boldsymbol{0}$) constraints, for the plant model itself, depend only on the decision variables ($\boldsymbol{x}$). Since the plant constraints do not include uncertain variables ($\boldsymbol{p}$) they are independent of the MC samples. (i.e., *N* = *nMCS*, which is chosen as 8,000 for the AP), and therefore, do not take the subscript *i*. ($\boldsymbol{z}^+$) vector is taken as positive auxiliary variable for the right side, therefore it is not included in inequality constraints.

Since the decision variables are not related to MC samples, the number of decision variables is N+11 (N is for the $\boldsymbol{z}^+$, 10 for decision variables $\boldsymbol{x}$, and 1 for γ). The number of equality constraints is 7 (plant's equality constraints). The number of inequality constraints is N (N represents the inequalities coming from Uryasev's formulations, i.e., Equation 2.28). The number of variable bounds is N+20 (N is for $\boldsymbol{z}^+ \geq \boldsymbol{0}$, and 20 is for $\boldsymbol{x}^L \leq \boldsymbol{x} \leq \boldsymbol{x}^U$). Among the constraints only 4 of the 7 plant equality constraints are nonlinear, the rest of the constraints i.e., the remaining 3 equations and N inequalities are all linear. The objective function is also linear in decision variables. For 8,000 nMCS, the simultaneous algorithm for the minimization of CVaR$^+$ has 8,011 decision variables, 7 equality constraints, 8,000 inequality constraints, and 8,020 variable bounds.

For minimization of $CVaR^+$ objective, the frequency plot of the profit ($\boldsymbol{\Phi}$) values, at 8,000 MCS and the confidence level of 95%, is given in Figure 4.31. Random values for the uncertain parameters of cost coefficients ($\boldsymbol{p}$) are drawn from normal distributions using the mean values and standard deviations given in Table 4.6. Some statistical results including parametric ($PVaR^{\pm}$, $PCVaR^{\pm}$, computed with Equations 2.24 and 2.25) and historical ($VaR^{\pm}$, $CVaR^{\pm}$, computed with the percentile form given by Equations 2.8 and 2.9 in Chapter 2) values for VaR and CVaR, the mean (μ) value, standard deviation (σ), skewness, kurtosis of the profit distribution, the difference of the mean (μ) from $CVaR^+$ (DIFP) and $CVaR^-$ (DIFM), the ratio of DIFP/DIFM, and the Rachev Ratio (RR) related to Figure 4.31 are given in Table 4.12. The optimal values for the decision variables for minimization of $CVaR^+$ using the simultaneous algorithm are presented in Table 4.13.

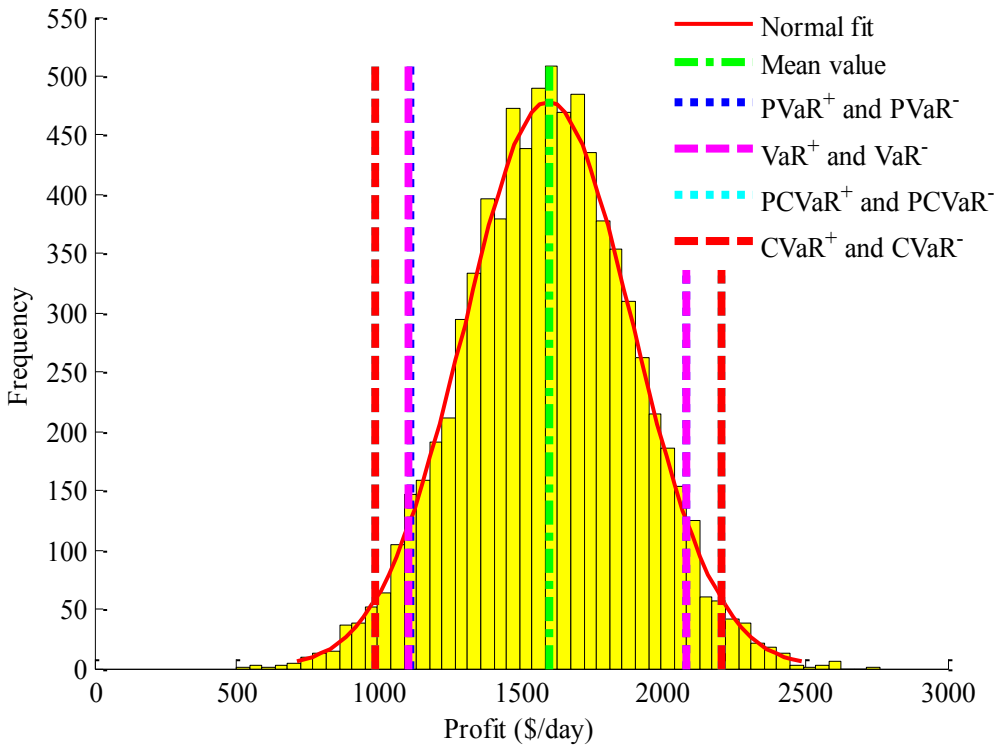

Figure 4.31. Frequency distribution of profit using simultaneous algorithm for minimization of $CVaR^+$.

The distribution of the profit values ($\boldsymbol{\Phi}$) in Figure 4.31, i.e., the distribution obtained via the minimization of $CVaR^+$ using simultaneous method, shows that, as compared to Figure 4.30 (where the objective was the minimization of $[CVaR^+ - CVaR^-]$), the mean

value of the profit decreases from 2258.4 \$/day to 1596.5 \$/day (decreases by 29%), shifting the frequency distribution of the profit to the left in Figure 4.31. When the objective is the minimization of [$CVaR^+ - CVaR^-$] (as in Figure 4.30), the difference of $CVaR^+$ and $CVaR^-$ is lower compared to the case when the objective is the minimization of $CVaR^+$ only (as in Figure 4.31). Minimization of $CVaR^+$ shifts both $CVaR^+$ and $CVaR^-$ to the left much more than the minimization of [$CVaR^+ - CVaR^-$]. When compared to the sequential method where the objective was the maximization of profit at each MCS, minimization of $CVaR^+$ using simultaneous method decreases profit from 8729.3 \$/day to 1596.5 \$/day (decreases by 82%). In the sequential method with maximization of profit (DIFP = 2015.2 \$/day, DIFM = 2024.1 \$/day), the standard deviation of the profit distribution was σ = 978.7 \$/day. In the simultaneous method with minimization of $CVaR^+$ (DIFP = 607.84 \$/day, DIFM = 612.41 \$/day), the standard deviation of the profit distribution becomes σ = 295.9 \$/day. This means that, with the minimization of $CVaR^+$, the company significantly decreases the mean profit however increases the certainty of the mean profit.

On minimization of $CVaR^+$ (Equation 4.9), the expected value of profit is 1596.5 \$/day, and, at $\alpha = 0.95$ confidence level, the expected value of the tail profit, $CVaR^+$, is 2204.3 \$/day; indicating that even though the mean profit is 1596.5 \$/day, there is a certain (5%) chance that it may be as high as 2204.3 \$/day. Although the mean value of profit for the minimization of [$CVaR^+ - CVaR^-$], is higher than the mean value of profit for the minimization of $CVaR^+$, the difference of ($CVaR^+$ – mean profit) (i.e., DIFP = 452.3) and (mean profit – $CVaR^-$) (i.e., DIFM = 455.1) for the minimization of [$CVaR^+ - CVaR^-$] are less than DIFP = 607.84 and DIFM = 612.41 for the minimization of $CVaR^+$. This shows that the minimization of [$CVaR^+ - CVaR^-$] indeed compresses the distribution around the mean. This means that, when the minimization of $CVaR^+$ is used as the objective, the company decreases the mean profit and the certainty of the mean profit compared to the minimization of [$CVaR^+ - CVaR^-$]. There is a decrease in RR from the value of 0.9938 in Table 4.10 (where the objective was the minimization of [$CVaR^+ - CVaR^-$]) to 0.9926 in Table 4.12 (where the objective is the minimization of $CVaR^+$), indicating a slightly more decrease of reward probability in the profit side than the decrease of risk probability in the loss side of the profit distribution.

Table 4.12. Statistical properties of the profit distribution in Figure 4.31, as a result of minimization of $CVaR^+$.

Mean Value (μ)	1596.5	\$/day
Standard Deviation (σ)	295.9	\$/day
Skewness	-8.58×10^{-3}	
Kurtosis	3.0063	
$PVaR^+$	2083.1	\$/day
$PVaR^-$	1109.8	\$/day
VaR^+	2080.2	\$/day
VaR^-	1101.5	\$/day
$PCVaR^+$	2206.8	\$/day
$PCVaR^-$	986.14	\$/day
$CVaR^+$	2204.3	\$/day
$CVaR^-$	984.05	\$/day
$(CVaR^+ - CVaR^-)$	1220.3	\$/day
DIFP	607.84	\$/day
DIFM	612.41	\$/day
RR	0.9926	

Optimal values of decision variables ($\boldsymbol{x}$) for minimization of $CVaR^+$ using the simultaneous algorithm are given in Table 4.13. A comparison with the decision variables for the minimization of $[CVaR^+ - CVaR^-]$ given in Table 4.11 shows that with the minimization of $CVaR^+$ objective, the plant requires higher olefin feed (x_1), alkylate yield (x_4), isobutane input (x_5), acid dilution factor (x_9) but lower acid strength (x_6), motor octane number of alkylate (x_7) and external isobutane-to-olefin ratio (x_8).

Table 4.13. Optimal values of decision variables ($\boldsymbol{x}$) for minimization of CVaR^{+} using the simultaneous algorithm.

Decision Variable	x_i^*
x_1	2309.0
x_2	5000
x_3	50
x_4	3344.6
x_5	1771.4
x_6	50
x_7	76.6
x_8	2.9
x_9	14.3
x_{10}	96.7

<u>4.2.2.3. Objective Function: Maximization of CVaR^{-}.</u> Based on the general problem defined by Equation 3.14 of Chapter 3, the mathematical formulation for the maximization of CVaR^{-} for the AP model is given by Equation 4.11.

$$
\begin{aligned}
\max_{\boldsymbol{x},\eta,z_i^-} \quad & \left(\eta - \frac{1}{N(1-\alpha)}\sum_{i=1}^{N} z_i^-\right) \\
s.t. \quad & \left.\begin{array}{l} z_i^- \geq \eta - \Phi_i(\boldsymbol{x},\boldsymbol{p}_i) \\ z_i^- \geq 0 \end{array}\right\} \; CVaR\ Constraints\ (linear) \quad \forall\, i = 1,\dots,N \\
& -x_4 + x_1(1.12 + 0.13167\, x_8 - 0.0067\, {x_8}^2) = 0 \\
& -x_7 + 86.35 + 1.098\, {x_4}^2 + 0.325\,(x_6 - 89) = 0 \\
& -x_9 + 35.82 - 0.022\, x_{10} = 0 \\
& -x_{10} + 3\, x_7 - 133 = 0 \\
& -x_8\, x_1 + x_2 + x_5 = 0 \\
& -x_5 + 1.22\, x_4 - x_1 = 0 \\
& -x_6(x_4\, x_9 + 1000\, x_3) + 98000\, x_3 = 0 \\
& x_j^L < x_j \\
& x_j < x_j^U \quad \forall\, j \in \{1,2,..,10\}
\end{aligned}
\tag{4.11}
$$

where:

$$\Phi_i(\boldsymbol{x},\boldsymbol{p}_i) = +c_{1_i}\, x_4 x_7 - c_{2_i}\, x_1 - c_{3_i}\, x_2 - c_{4_i}\, x_3 - c_{5_i}\, x_5 \;;\; i = 1,\dots,nMCS$$

Upon feasible and optimal solution, VaR^{-} and CVaR^{-} are evaluated at the optimal values of η and $\boldsymbol{z}^{-}$ as follows:

$$VaR^{-} = \eta^{*}$$
$$CVaR^{-} = \eta^{*} - \frac{1}{N(1-\alpha)}\sum_{i=1}^{N}(z_i^{-})^{*} \tag{4.12}$$

As explained in Section 3.3.1 of Chapter 3, the problem in Equation 4.11 is a maximization problem since the loss (left-side) tail risk of the probability distribution of the plant objective is minimized by maximizing the risk measure CVaR^{-}. The problem should not be converted to minimization form since it is unbounded in that direction. All the decision variables, $\boldsymbol{x}$, are taken as valid for all realizations of uncertain variables, and the control ($\boldsymbol{u}$) and design variables ($\boldsymbol{d}$) in Equation 4.6 are omitted in the AP formulation. The inequalities which belong to the right side of the resulting frequency distribution of profit and the right side related term in the objective function are also omitted from the model in Equation 4.11. Among the plant equations, only the plant objective (profit, Φ_i) includes uncertain variables (p_i), therefore it involves the subscript *i* that shows the ith MC sampling. The equality ($\boldsymbol{h} = \boldsymbol{0}$) and inequality ($\boldsymbol{g} \leq \boldsymbol{0}$) constraints, for the plant model itself, depend only on the decision variables ($\boldsymbol{x}$). Since the plant constraints do not include uncertain variables ($\boldsymbol{p}$) they are independent of the MC samples. (i.e., *N = nMCS*, which is chosen as 8,000 for the AP), and therefore, do not take the subscript *i*. ($\boldsymbol{z}^{-}$) vector is taken as positive auxiliary variable for the left side, therefore it is not included in inequality constraints.

Since the decision variables are not related to MC samples, the number of decision variables is N+11 (N is for the $\boldsymbol{z}^{-}$, 10 for decision variables $\boldsymbol{x}$, and 1 for η). The number of equality constraints is 7 (plant's equality constraints). The number of inequality constraints is N (N represents the inequalities coming from Uryasev's formulations, i.e., Equation 2.28). The number of variable bounds is N+20 (N is for $\boldsymbol{z}^{-} \geq \boldsymbol{0}$, and 20 is for $\boldsymbol{x}^{L} \leq \boldsymbol{x} \leq \boldsymbol{x}^{U}$). Among the constraints only 4 of the 7 plant equality constraints are nonlinear, the rest of the constraints i.e., the remaining 3 equations and N inequalities are all linear. The objective function is also linear in decision variables. For 8,000 nMCS, the simultaneous algorithm for the maximization of CVaR^{-} has 8,011 decision variables, 7 equality constraints, 8,000 inequality constraints, and 8,020 variable bounds.

For maximization of CVaR$^-$ objective, the frequency plot of the profit ($\boldsymbol{\Phi}$) values, at 8,000 MCS and the confidence level of 95%, is given in Figure 4.32. Random values for the uncertain parameters of cost coefficients ($\boldsymbol{p}$) are drawn from normal distributions using the mean values and standard deviations given in Table 4.6. Some statistical results including parametric (PVaR$^{\pm}$, PCVaR$^{\pm}$, computed with Equations 2.24 and 2.25) and historical (VaR$^{\pm}$, CVaR$^{\pm}$, computed with the percentile form given by Equations 2.8 and 2.9 in Chapter 2) values for VaR and CVaR, the mean (μ) value, standard deviation (σ), skewness, kurtosis of the profit distribution, the difference of the mean (μ) from CVaR$^+$ (DIFP) and CVaR$^-$ (DIFM), the ratio of DIFP/DIFM, and the Rachev Ratio (RR) related to Figure 4.32 are given in Table 4.14. The optimal values for the decision variables for maximization of CVaR$^-$ using the simultaneous algorithm are presented in Table 4.15.

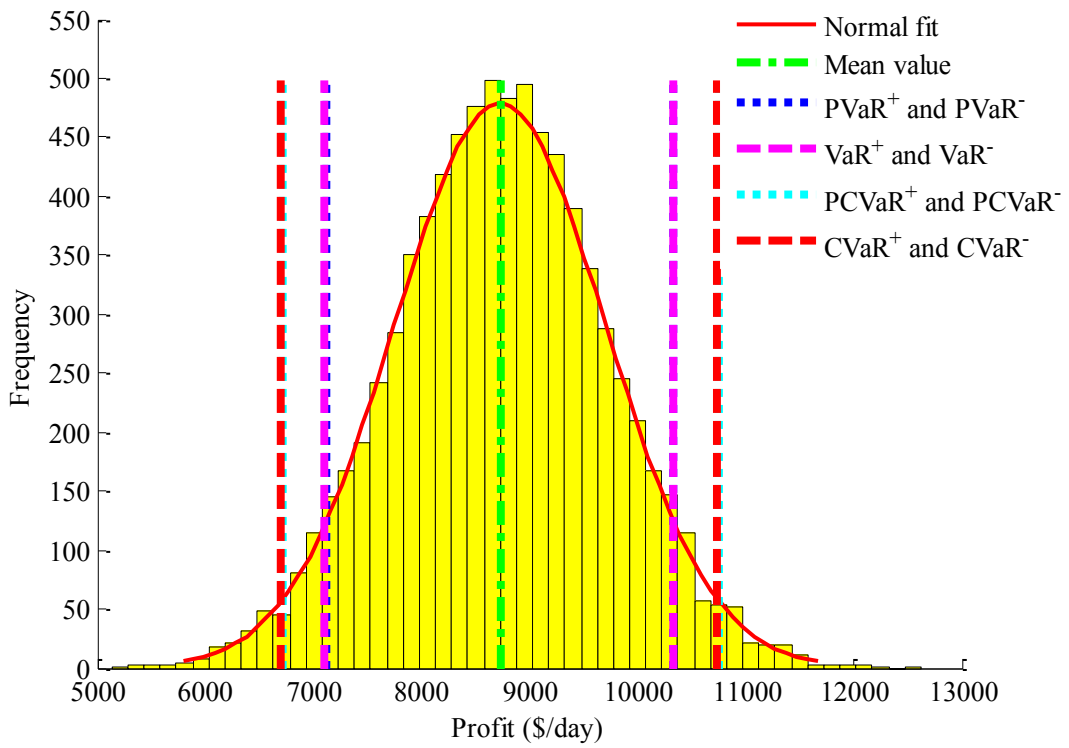

Figure 4.32. Frequency distribution of profit using simultaneous algorithm for maximization of CVaR$^-$.

The distribution of the profit values ($\boldsymbol{\Phi}$) in Figure 4.32, i.e., the distribution obtained via the maximization of CVaR$^-$ using simultaneous method, shows that, as compared to Figure 4.30 (where the objective was the minimization of [CVaR$^+$ − CVaR$^-$]), the mean value of the profit increases from 2258.4 $/day to 8728.3 $/day (increases by 286%),

shifting the frequency distribution of the profit to the right in Figure 4.32. When the objective is the minimization of [$CVaR^{+} - CVaR^{-}$] (as in Figure 4.30) the difference of $CVaR^{+}$ and $CVaR^{-}$ (907.49 \$/day) is lower than the difference of $CVaR^{+}$ and $CVaR^{-}$ (4036.70 \$/day) when the objective is the maximization of $CVaR^{-}$ (as in Figure 4.32). Maximization of $CVaR^{-}$ shifts both the $CVaR^{-}$ and $CVaR^{+}$ to the right much more than the minimization of [$CVaR^{+} - CVaR^{-}$]. When the sequential method where the objective was the maximization of profit at each MCS, and maximization of $CVaR^{-}$ using simultaneous method are compared, it is seen that they have almost the same results. For example, the mean profit for the sequential method was 8729.3 \$/day (maximized value) and mean profit for the simultaneous method with maximization of $CVaR^{-}$ objective is 8728.3 \$/day (decreases by 0.01%). This shows that the constraints of the AP that limit maximum possible $CVaR^{-}$ also limit the maximum possible expected profit.

On maximization of $CVaR^{-}$, the expected value of profit is 8728.3 \$/day, and, at $\alpha = 0.95$ confidence level, the expected value of the tail cost (risk), $CVaR^{-}$, is 6705 \$/day; indicating that even though the mean profit is 8728.3 \$/day, there is a certain (5%) chance that it may be as low as 6705 \$/day. The mean value of profit for the minimization of [$CVaR^{+} - CVaR^{-}$], is lower than the mean value of profit for the maximization of $CVaR^{-}$. The difference of ($CVaR^{+}$ – mean profit) (i.e., DIFP = 452.3) and (mean profit – $CVaR^{-}$) (i.e., DIFM = 455.1) for the minimization of [$CVaR^{+} - CVaR^{-}$] are less than DIFP = 2013.3 and DIFM = 2023.3 for the case of maximization of $CVaR^{-}$. When the objective for the simultaneous method is the maximization of $CVaR^{-}$, DIFP = 2013.3 and DIFM = 2023.3. This shows that the minimization of [$CVaR^{+} - CVaR^{-}$] indeed compresses the distribution around the mean. This means that, when the maximization of $CVaR^{-}$ is used as the objective, the company increases the mean profit however, it decreases the certainty of the mean profit compared to the case of minimization of [$CVaR^{+} - CVaR^{-}$]. The increase in RR from the value of 0.9938 in Table 4.10 (where the objective was the minimization of [$CVaR^{+} - CVaR^{-}$]) to 0.9951 in Table 4.14 (where the objective is the maximization of $CVaR^{-}$) shows that as compared to the minimization of [$CVaR^{+} - CVaR^{-}$], maximization of $CVaR^{-}$ results in an increase in $CVaR^{+}$ that overwhelms the increase in $CVaR^{-}$ while shifting the mean profit to the right.

Table 4.14. Statistical properties of the profit distribution in Figure 4.32, as a result of maximization of $CVaR^{-}$.

Mean Value (μ)	8728.3	\$/day
Standard Deviation (σ)	978.1	\$/day
Skewness	-3.87×10^{-3}	
Kurtosis	3.0127	
$PVaR^{+}$	10337	\$/day
$PVaR^{-}$	7119.5	\$/day
VaR^{+}	10332	\$/day
VaR^{-}	7098.1	\$/day
$PCVaR^{+}$	10746	\$/day
$PCVaR^{-}$	6710.8	\$/day
$CVaR^{+}$	10742	\$/day
$CVaR^{-}$	6705	\$/day
$(CVaR^{+} - CVaR^{-})$	4036.7	\$/day
DIFP	2013.3	\$/day
DIFM	2023.3	\$/day
RR	0.9951	

Optimal values of decision variables ($\boldsymbol{x}$) for maximization of $CVaR^{-}$ using the simultaneous algorithm are given in Table 4.15. A comparison with the decision variables for the minimization of $[CVaR^{+} - CVaR^{-}]$ given in Table 4.11 shows that with the maximization of $CVaR^{-}$ objective, the plant requires higher olefin feed (x_1), isobutene recycle (x_2), acid addition (x_3), alkylate yield (x_4), isobutane input (x_5), acid strength (x_6), motor octane number of alkylate (x_7), performance number of alkylate (x_{10}) but lower external isobutane-to-olefin ratio (x_8) and acid dilution factor (x_9). The same results for the change in decision variables can be deduced when Table 4.15 is compared with Table 4.13 (where the objective is the minimization of $CVaR^{+}$).

Table 4.15. Optimal values of decision variables ($\boldsymbol{x}$) for maximization of CVaR^{-} using the simultaneous algorithm.

Decision Variable	x_i^*
x_1	7363.2
x_2	10000
x_3	445.1
x_4	10000
x_5	4836.8
x_6	83.7
x_7	86.7
x_8	2.0
x_9	7.6
x_{10}	127.0

<u>4.2.2.4. Objective Function: Maximization of Expected Profit.</u> Based on the general formulation given by Equation 3.13 of Chapter 3, the mathematical formulation for the maximization of expected profit for the AP model is given by Equation 4.13.

$$\max_{\boldsymbol{x}} \quad \frac{1}{N}\sum_{i=1}^{N} \Phi_i(\boldsymbol{x}, \boldsymbol{p}_i)$$

$$\begin{aligned} s.t. \quad & -x_4 + x_1(1.12 + 0.13167\, x_8 - 0.0067\, {x_8}^2) = 0 \\ & -x_7 + 86.35 + 1.098\, {x_4}^2 + 0.325\,(x_6 - 89) = 0 \\ & -x_9 + 35.82 - 0.022\, x_{10} = 0 \\ & -x_{10} + 3\, x_7 - 133 = 0 \\ & -x_8\, x_1 + x_2 + x_5 = 0 \\ & -x_5 + 1.22\, x_4 - x_1 = 0 \\ & -x_6(x_4\, x_9 + 1000\, x_3) + 98000\, x_3 = 0 \\ & x_j^L < x_j \\ & x_j < x_j^U \qquad \forall\, j \in \{1,2,..,10\} \end{aligned} \tag{4.13}$$

where:

$$\Phi_i(\boldsymbol{x}, \boldsymbol{p}_i) = +c_{1_i}\, x_4 x_7 - c_{2_i}\, x_1 - c_{3_i}\, x_2 - c_{4_i}\, x_3 - c_{5_i}\, x_5 \; ; i = 1, \dots, nMCS$$

The problem in Equation 4.13 maximizes only the expected profit, $E[\boldsymbol{\Phi}]$ according to the probability distribution obtained from the AP, without considering any tail risk / tail reward in terms of $\text{VaR}^{\pm}$ and $\text{CVaR}^{\pm}$. All the decision variables, $\boldsymbol{x}$, are taken as valid for all realizations of uncertain variables, and the control ($\boldsymbol{u}$) and design variables ($\boldsymbol{d}$) are omitted in the formulation. Among the plant equations, only the plant objective (profit, Φ_i) includes uncertain variables ($\boldsymbol{p}$), therefore it involves the subscript *i* to show the outcome at the ith MC sampling (i.e., $i = 1, ..., N = nMCS$, which is chosen as 8,000 for the AP). The equality ($\boldsymbol{h} = \boldsymbol{0}$) constraints of the plant model depend only on the decision variables ($\boldsymbol{x}$). Since the plant constraints do not include uncertain variables ($\boldsymbol{p}$) they are independent of the MC samples, and therefore, do not take the subscript *i*.

Since the decision variables are not related to MC samples, the number of decision variables is 10 (for vector $\boldsymbol{x}$). The number of equality constraints is 7 (plant's equality constraints). There are not any inequality constraints in the problem for the maximization of expected profit. The number of variable bounds is 20 (for $\boldsymbol{x}^L \leq \boldsymbol{x} \leq \boldsymbol{x}^U$). Among the constraints only 4 of the 7 plant equality constraints are nonlinear, the rest of the 3 constraints are linear. The objective function is also linear in decision variables. The simultaneous algorithm for the maximization of $E[\boldsymbol{\Phi}]$ has 10 decision variables, 7 equality constraints and 20 variable bounds.

For maximization of $E[\boldsymbol{\Phi}]$ objective, the frequency plot of the profit ($\boldsymbol{\Phi}$) values, at 8,000 MCS and the confidence level of 95%, is given in Figure 4.33. Random values for the uncertain parameters of cost coefficients ($\boldsymbol{p}$) are drawn from normal distributions using the mean values and standard deviations given in Table 4.6. Some statistical results including parametric ($\text{PVaR}^{\pm}$, $\text{PCVaR}^{\pm}$, computed with Equations 2.24 and 2.25) and historical ($\text{VaR}^{\pm}$, $\text{CVaR}^{\pm}$, computed with the percentile form given by Equations 2.8 and 2.9 in Chapter 2) values for VaR and CVaR, the mean (μ) value, standard deviation (σ), skewness, kurtosis of the profit distribution, the difference of the mean (μ) from CVaR^{+} (DIFP) and CVaR^{-} (DIFM), the ratio of DIFP/DIFM, and the Rachev Ratio (RR) related to Figure 4.33 are given in Table 4.16. The optimal values for the decision variables for maximization of expected profit using the simultaneous algorithm are presented in Table 4.17.

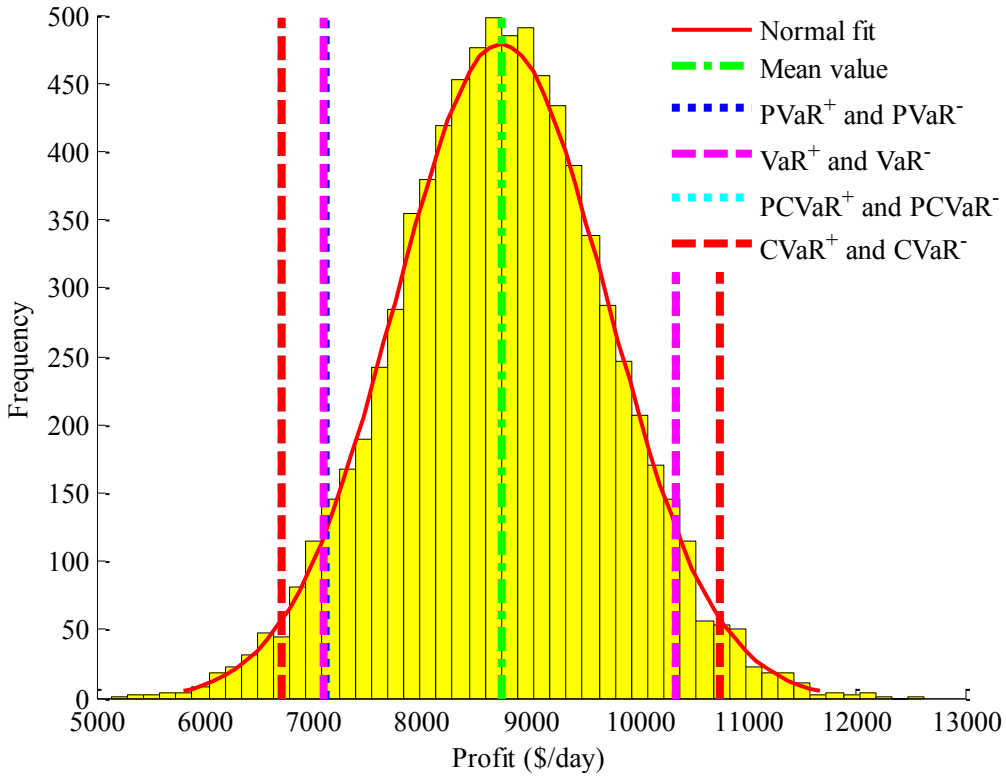

Figure 4.33. Frequency distribution of profit using simultaneous algorithm for maximization of the expected profit.

The distribution of the profit values ($\boldsymbol{\Phi}$) in Figure 4.33 (the distribution obtained via the maximization of expected profit using simultaneous method), shows that, as compared to Figure 4.30 (where the objective was the minimization of [$CVaR^{+} - CVaR^{-}$]), the mean value of the profit increases from 2258.4 $/day to 8729 $/day (increases by 286%), shifting the frequency distribution of the profit to the right in Figure 4.33. When the objective is the minimization of [$CVaR^{+} - CVaR^{-}$] (as in Figure 4.30) the difference of $CVaR^{+}$ and $CVaR^{-}$ (907.49 $/day) is lower than the difference of $CVaR^{+}$ and $CVaR^{-}$ (4039.30 $/day) when the objective is the maximization of expected profit (as in Figure 4.33). Maximization of expected profit shifts the $CVaR^{-}$ to the right much more than the minimization of [$CVaR^{+} - CVaR^{-}$]. When the sequential method where the objective was the maximization of profit at each MCS, and maximization of expected profit using simultaneous method are compared, it is seen that they have basically the same results. For example, the mean profit for the sequential method was 8729.3 $/day (maximized value) and mean profit for the simultaneous method with maximization of expected profit objective is 8729.0 $/day.

On maximization of the expected profit, the expected value of the tail cost (risk), $CVaR^{-}$, is 6704.4 \$/day; indicating that even though the mean profit is 8729 \$/day, there is a certain (5%) chance that it may be as low as 6704.4 \$/day. The difference of ($CVaR^{+}$ – mean profit) (i.e., DIFP = 452.3) and (mean profit – $CVaR^{-}$) (i.e., DIFM = 455.1) for the minimization of [$CVaR^{+} - CVaR^{-}$] are less than DIFP = 2014.7 and DIFM = 2024.6 for the case of maximization of expected profit. This shows that the minimization of [$CVaR^{+} - CVaR^{-}$] compresses the distribution around the mean, however, at the expense of a significant loss from the expected profit. This means that, when the maximization of expected profit is used as the objective, the company increases the mean profit however, it decreases the certainty of the mean profit compared to the case of minimization of [$CVaR^{+} - CVaR^{-}$]. The increase in RR from the value of 0.9938 in Table 4.10 (where the objective was the minimization of [$CVaR^{+} - CVaR^{-}$]) to 0.9951 in Table 4.16 (where the objective is the maximization of expected profit) shows that as compared to the minimization of [$CVaR^{+} - CVaR^{-}$], maximization of expected profit results in a subtle increase in $CVaR^{+}$ that overwhelms the increase in $CVaR^{-}$ while shifting the mean profit to the right.

As compared to Figure 4.31 (where the objective was the minimization of $CVaR^{+}$ that shifts the frequency distribution of the profit to the left), the mean value of the profit increases from 1596.5 \$/day to 8729 \$/day (increases by 448%) in Figure 4.33. When the objective is the minimization of $CVaR^{+}$, the difference of $CVaR^{+}$ and $CVaR^{-}$ (1220.3 \$/day) is also lower than the difference of $CVaR^{+}$ and $CVaR^{-}$ (4039.30 \$/day) when the objective is the maximization of expected profit (as in Figure 4.33). Although the minimization of $CVaR^{+}$ is expected to compress the right-tail of the profit distribution towards the mean assymmetrically, for the AP plant the minimization of $CVaR^{+}$ compresses the distribution's both the left and right tails towards a lower mean value, almost symmetrically. This means that, when the maximization of expected profit is used as the objective, the company increases the mean profit however, it decreases the certainty of the mean profit compared to the case of minimization of $CVaR^{+}$. RR for the minimization of $CVaR^{+}$ (0.9926) is lower than RR for the maximization of expected profit (0.9951). This shows that as compared to the maximization of expected profit, the minimization of $CVaR^{+}$ results in a subtle decrease in $CVaR^{+}$ that overwhelms the increase in $CVaR^{-}$ while shifting the $CVaR^{+}$ to the left.

Figure 4.32 (where the objective was the maximization of $CVaR^{-}$), is quite identical with Figure 4.33 (where the objective is the maximization of expected profit). When the objective is the maximization of $CVaR^{-}$ as in Figure 4.32) only $CVaR^{-}$ (6705 \$/day) is almost negligibly higher than $CVaR^{-}$ (6704.4 \$/day) when the objective is the maximization of expected profit (as in Figure 4.33). This observation indicates that both in maximization of $CVaR^{-}$ and in maximization of expected profit, the same constraints of the AP are limiting.

Table 4.16. Statistical Properties of the profit distribution in Figure 4.33, as a result of maximization of expected profit.

Mean Value (μ)	8729	\$/day
Standard Deviation (σ)	978.7	\$/day
Skewness	-3.82×10^{-3}	
Kurtosis	3.0128	
$PVaR^{+}$	10339	\$/day
$PVaR^{-}$	7119.1	\$/day
VaR^{+}	10334	\$/day
VaR^{-}	7098	\$/day
$PCVaR^{+}$	10748	\$/day
$PCVaR^{-}$	6710.2	\$/day
$CVaR^{+}$	10744	\$/day
$CVaR^{-}$	6704.4	\$/day
$(CVaR^{+} - CVaR^{-})$	4039.3	\$/day
DIFP	2014.7	\$/day
DIFM	2024.6	\$/day
RR	0.9951	

Optimal values of decision variables ($\boldsymbol{x}$) for maximization of expected profit using the simultaneous algorithm are given in Table 4.17. A comparison with the decision variables for the minimization of $[CVaR^{+} - CVaR^{-}]$ given in Table 4.11 shows that in

maximization of expected profit, the plant requires higher olefin feed (x_1), isobutene recycle (x_2), acid addition (x_3), alkylate yield (x_4), isobutane input (x_5), acid strength (x_6), motor octane number of alkylate (x_7), performance number of alkylate (x_{10}) but lower external isobutane-to-olefin ratio (x_8) and acid dilution factor (x_9). The same results for the change in decision variables can be deduced when Table 4.17 is compared with Table 4.15 (where the objective is the minimization of CVaR^+).

Table 4.17. Optimal values of decision variables ($\boldsymbol{x}$) for maximization of expected profit using the simultaneous algorithm.

Decision Variable	x_i^*
x_1	7363.2
x_2	10000
x_3	450.0
x_4	10000
x_5	4836.8
x_6	83.9
x_7	86.8
x_8	2.01
x_9	7.57
x_{10}	127.2

<u>4.2.2.5. Objective Function: Maximization of $[\lambda\, E[\Phi] - (1-\lambda)\,(\text{CVaR}^+ - \text{CVaR}^-)]$.</u> Based on the general problem defined by Equation 3.19 of Chapter 3, the mathematical formulation for the maximization of $[\lambda\, E[\boldsymbol{\Phi}] - (1-\lambda)\,(\text{CVaR}^+ - \text{CVaR}^-)]$ for the AP model is given by Equation 4.14.

The problem in Equation 4.14 maximizes the expected profit, $E[\boldsymbol{\Phi}]$ and CVaR^-, and minimizes CVaR^+ at different weighting parameters of λ ($0 \leq \lambda \leq 1$). All the decision variables, $\boldsymbol{x}$, are taken as valid for all realizations of uncertain variables, and the control ($\boldsymbol{u}$) and design variables ($\boldsymbol{d}$) in Equation 4.6 are omitted in the AP formulation. Among the plant equations, only the plant objective (profit, Φ_i) includes uncertain variables ($\boldsymbol{p}$),

therefore it involves the subscript *i* that shows the ith MC sampling. The equality ($\boldsymbol{h} = \mathbf{0}$) and inequality ($\boldsymbol{g} \leq \mathbf{0}$) constraints, for the plant model itself, depend only on the decision variables ($\boldsymbol{x}$). Since the plant constraints do not include uncertain variables ($\boldsymbol{p}$) they are independent of the MC samples. (i.e., *N* = *nMCS*, which is chosen as 8,000 for the AP), and therefore, do not take the subscript *i*. ($\boldsymbol{z}^{+}$) and ($\boldsymbol{z}^{-}$) vectors are taken as positive auxiliary variables, therefore they are not considered as inequality constraints.

$$
\begin{aligned}
\max_{\boldsymbol{x},\gamma,\eta,z_i^-,z_i^+} \quad & \lambda\left[\frac{1}{N}\sum_{i=1}^{N}\Phi_i(\boldsymbol{x},\boldsymbol{p}_i)\right] \\
& -(1-\lambda)\left[\left(\gamma+\frac{1}{N(1-\alpha)}\sum_{i=1}^{N}z_i^+\right)-\left(\eta-\frac{1}{N(1-\alpha)}\sum_{i=1}^{N}z_i^-\right)\right]
\end{aligned}
$$

$$
\begin{aligned}
s.t. \quad & \left.\begin{aligned} z_i^- &\geq \eta-\Phi_i(\boldsymbol{x},\boldsymbol{p}_i) \\ z_i^+ &\geq \Phi_i(\boldsymbol{x},\boldsymbol{p}_i)-\gamma \\ z_i^- &\geq 0 \\ z_i^+ &\geq 0 \end{aligned}\right\} \begin{array}{c} CVaR\ Constraints\ (linear) \\ \forall\, i=1,\dots,N \end{array} \\
& -x_4+x_1(1.12+0.13167\,x_8-0.0067\,{x_8}^2)=0 \\
& -x_7+86.35+1.098\,{x_4}^2+0.325\,(x_6-89)=0 \\
& -x_9+35.82-0.022\,x_{10}=0 \\
& -x_{10}+3\,x_7-133=0 \\
& -x_8\,x_1+x_2+x_5=0 \\
& -x_5+1.22\,x_4-x_1=0 \\
& -x_6(x_4\,x_9+1000\,x_3)+98000\,x_3=0 \\
& x_j^L < x_j \\
& x_j < x_j^U \qquad \forall\, j\in\{1,2,..,10\}
\end{aligned}
\tag{4.14}
$$

where:

$$\Phi_i(\boldsymbol{x},\boldsymbol{p}_i) = +c_{1_i}\,x_4x_7 - c_{2_i}\,x_1 - c_{3_i}\,x_2 - c_{4_i}\,x_3 - c_{5_i}\,x_5\ ;\ i=1,\dots,nMCS$$

Upon feasible and optimal solution, VaR^{+}, VaR^{-}, CVaR^{+}, CVaR^{-} are evaluated at the optimal values of γ, η, $\boldsymbol{z}^{+}$ and $\boldsymbol{z}^{-}$ as follows:

$$
\begin{aligned}
VaR^{+} &= \gamma^{*} \\
VaR^{-} &= \eta^{*} \\
CVaR^{+} &= \gamma^{*}+\frac{1}{N(1-\alpha)}\sum_{i=1}^{N}(z_i^+)^{*} \\
CVaR^{-} &= \eta^{*}-\frac{1}{N(1-\alpha)}\sum_{i=1}^{N}(z_i^-)^{*}
\end{aligned}
\tag{4.15}
$$

Since the decision variables are not related to MC samples, the number of decision variables is 2×N+12 (2×N is for the $\mathbf{z}^+$ and $\mathbf{z}^-$, 10 for decision variables $\boldsymbol{x}$, and 2 for γ and η). The number of equality constraints is 7 (plant's equality constraints). The number of inequality constraints is 2×N (2×N represents the inequalities coming from Uryasev's formulations, i.e., Equation 2.28 and 2.29). The number of variable bounds is 2×N+20 (2×N is for $\boldsymbol{z}^+ \geq \mathbf{0}$ and $\boldsymbol{z}^- \geq \mathbf{0}$, and 20 is for $\boldsymbol{x}^L \leq \boldsymbol{x} \leq \boldsymbol{x}^U$). Among the constraints only 4 of the 7 plant equality constraints are nonlinear, the rest of the constraints i.e., the remaining 3 equations and 2×N inequalities are all linear. The objective function is also linear in decision variables. For 8,000 nMCS, the simultaneous algorithm has 16,012 decision variables, 7 equality constraints, 16,000 inequality constraints, and 16,020 variable bounds.

For maximization of $[\lambda\, E[\boldsymbol{\Phi}] - (1-\lambda)\ (\mathrm{CVaR}^+ - \mathrm{CVaR}^-)]$ objective at 8,000 MCS, the frequency plots of the profit ($\boldsymbol{\Phi}$) values for different weights in the range $0 \leq \lambda \leq 1$ are given in Figure 4.34. Random values for the uncertain parameters of cost coefficients ($\boldsymbol{p}$) are drawn from normal distributions using the mean values and standard deviations given in Table 4.6. Some statistical results, at the confidence level of 95%, including historical values (computed with the percentile form given by Equations 2.8 and 2.9 in Chapter 2) for $\mathrm{VaR}^{\pm}$, $\mathrm{CVaR}^{\pm}$, the mean (μ) value, standard deviation (σ), skewness, kurtosis of the profit distribution, the difference of the mean (μ) from CVaR^+ (DIFP) and CVaR^- (DIFM), and the Rachev Ratio (RR) related to Figure 4.34 are given in Table 4.18. The optimal values for the decision variables for maximization of expected profit using the simultaneous algorithm are presented in Table 4.19.

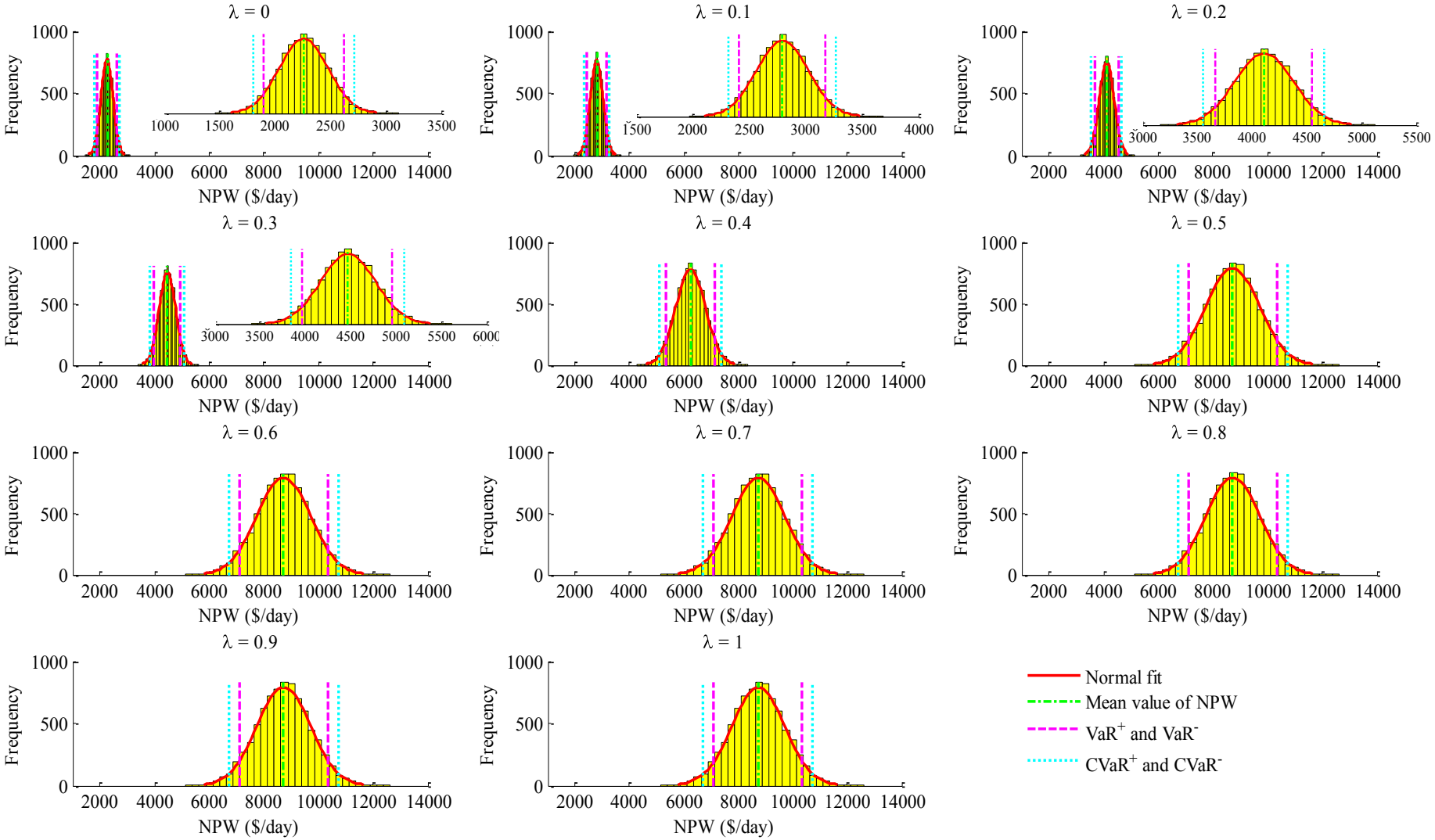

Figure 4.34. Frequency distributions of profit for maximization of $[\lambda\, E[\boldsymbol{\Phi}] - (1-\lambda)\,(\mathrm{CVaR}^{+} - \mathrm{CVaR}^{-})]$ at $0 \leq \lambda \leq 1$.

Table 4.18. Statistical Properties of the profit distributions in Figure 4.34, as a result of maximization of $[\lambda\, E[\boldsymbol{\Phi}] - (1-\lambda)\,(\mathrm{CVaR}^{+} - \mathrm{CVaR}^{-})]$ for different weights.

λ	Mean Value ($/day)	Standard Deviation	VaR^{+}	VaR^{-}	CVaR^{+}	CVaR^{-}	$(\mathrm{CVaR}^{+}-\mathrm{CVaR}^{-})$	DIFP	DIFM	RR
0	2258.4	220.0	2617.1	1892.7	2710.7	1803.2	907.49	452.33	455.15	0.99380
0.1	2795.4	229.8	3170.3	2412.5	3268.3	2320.1	948.24	472.94	475.30	0.99505
0.2	4111.2	267.7	4545.4	3665.4	4662.4	3557.3	1105.1	551.24	553.86	0.99527
0.3	4471.0	302.5	4962.8	3966.4	5093.9	3845.1	1248.8	622.91	625.85	0.99530
0.4	6248.0	544.5	7137.5	5341.9	7369.1	5121.9	2247.2	1121.1	1126.1	0.99558
0.5	8726.2	977.4	10330	7097.7	10738	6704.3	4033.8	2011.8	2021.9	0.99501
0.6	8727.8	977.9	10332	7098.0	10741	6704.9	4035.7	2012.8	2022.9	0.99503
0.7	8728.5	978.2	10333	7098.1	10742	6705.0	4037.0	2013.5	2023.5	0.99505
0.8	8728.8	978.4	10333	7098.2	10743	6704.9	4037.9	2014.0	2024.0	0.99507
0.9	8729.0	978.6	10334	7098.1	10743	6704.6	4038.7	2014.4	2024.3	0.99508
1	8729.0	978.7	10334	7098.0	10744	6704.4	4039.3	2014.7	2024.6	0.99509

When compared to Table 4.10 (results obtained via minimization of [CVaR^+ – CVaR^-]), the statistical results for the distribution of the profit values ($\boldsymbol{\Phi}$) in Table 4.18 (the distribution obtained via the maximization of [$\lambda\, E[\boldsymbol{\Phi}]$ – (1−λ) (CVaR^+ – CVaR^-)]), prove that, at $\lambda = 0$, the problem becomes identical with the minimization of [CVaR^+ – CVaR^-]. Similarly, the statistical results in Table 4.18 (results obtained via the maximization of [$\lambda\, E[\boldsymbol{\Phi}]$ – (1−λ) (CVaR^+ – CVaR^-)]), prove that, at $\lambda = 1$, the problem becomes identical with the maximization of $E[\boldsymbol{\Phi}]$, when compared to Table 4.16 (results obtained via the maximization of $E[\boldsymbol{\Phi}]$).

The results for skewness and kurtosis values are not given in Table 4.18 since, for 0 $\leq \lambda \leq$ 1, all the resulting frequency distributions for maximization of [$\lambda\, E[\boldsymbol{\Phi}]$ – (1−λ) (CVaR^+ – CVaR^-)] are skewed negligibly to the left and there is no excess kurtosis which means the distributions in Figure 4.34 are close to normal curve. Figure 4.34 shows that the frequency distribution of profit shifts to the right as λ increases. The increase in λ increases the weight of the expected profit ($E[\boldsymbol{\Phi}]$) and decreases the weight of the difference between CVaR^+ and CVaR^-, (CVaR^+ – CVaR^-), in the optimization problem for the maximization of [$\lambda\, E[\boldsymbol{\Phi}]$ – (1−λ) (CVaR^+ – CVaR^-)]. As λ decreases, the profit of the distribution decreases by shifting to the left but its certainty increases as a result of increasingly compressed distribution around the mean. In Figure 4.34, when the weight of $E[\boldsymbol{\Phi}]$ is higher than the weight of (CVaR^+ – CVaR^-), the frequency distribution of profit becomes almost constant. Consistently with the frequency distribution results in Figure 4.34, the changes in some statistical results given in Figure 4.35 show that, CVaR^+, CVaR^- and the mean profit increase with λ as $\lambda < 0.5$ and, beyond this value, they become stable. Change in RR with λ for maximization of [$\lambda\, E[\boldsymbol{\Phi}]$ – (1−λ) (CVaR^+ – CVaR^-)] is given Figure 4.36. For $\lambda = 0.4$, RR takes the highest value.

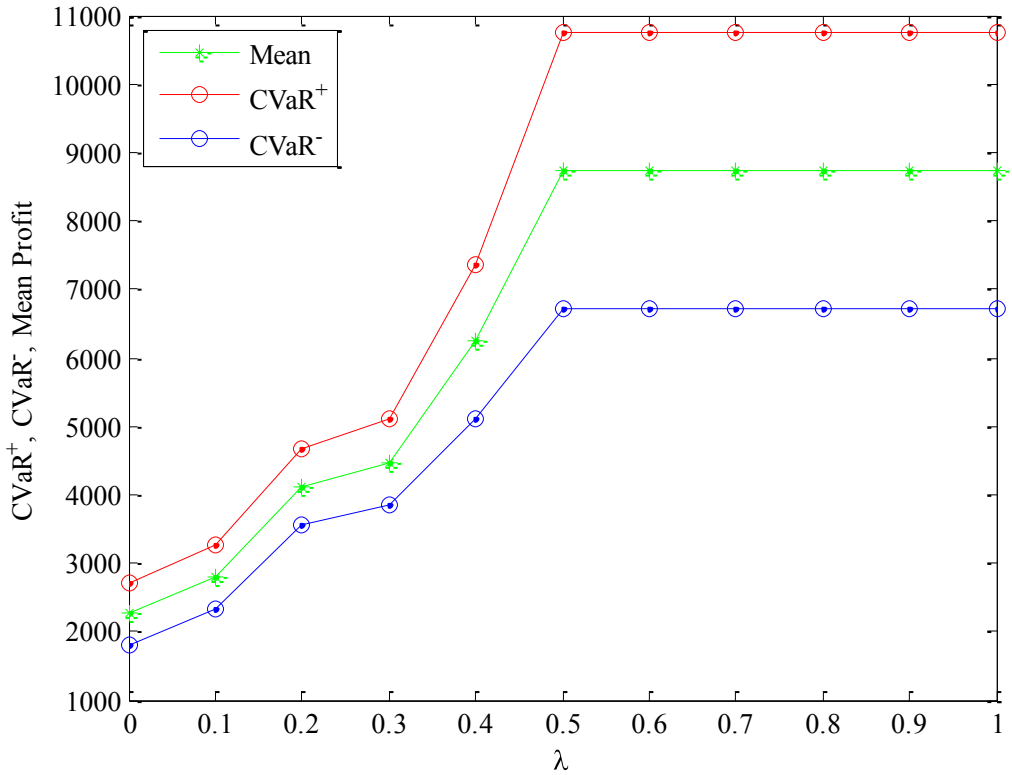

Figure 4.35. The change in $CVaR^+$, $CVaR^-$ and mean profit of the frequency distribution with weighting parameter λ, for max $[\lambda\, E[\boldsymbol{\Phi}] - (1-\lambda)\,(CVaR^+ - CVaR^-)]$.

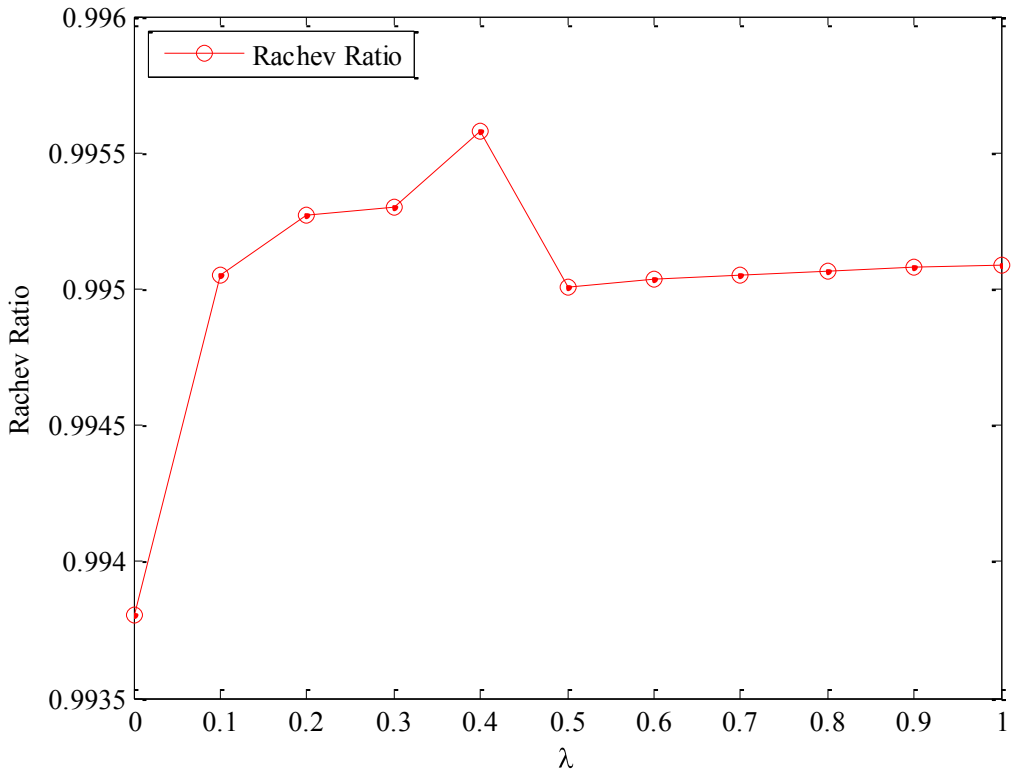

Figure 4.36. The change in RR of the profit distribution with weighting parameter λ, for max $[\lambda\, E[\boldsymbol{\Phi}] - (1-\lambda)\,(CVaR^+ - CVaR^-)]$.

Optimal values of decision variables ($\boldsymbol{x}$) for maximization of [$\lambda\, E[\boldsymbol{\Phi}]$ – (1−λ) (CVaR^{+} – CVaR^{-})] with $0 \leq \lambda \leq 1$ are given in Table 4.19. Table 4.19 shows that in maximization of [$\lambda\, E[\boldsymbol{\Phi}]$ – (1−λ) (CVaR^{+} – CVaR^{-})], as λ increases the plant requires higher acid addition (x_3), alkylate yield (x_4), isobutane input (x_5), but lower acid dilution factor (x_9). Also, as λ increases the profit distribution shifts to the right as it is seen in Figure 4.34, and therefore, as acid addition (x_3), alkylate yield (x_4), isobutane input (x_5) increase, the profit distribution shifts to the right. This also shows that profit decreases but certainty increases with lower acid addition (x_3), alkylate yield (x_4), and isobutane input (x_5).

Figure 4.37 show that acid strength (x_6), motor octane number of alkylate (x_7), performance number of alkylate (x_{10}) make a peak at $\lambda = 0.2$ and then at $\lambda > 0.2$ they show a sudden decrease followed by small increase ($\lambda \geq 0.5$) whereas, acid dilution factor (x_9) decreases to its lowest value at $\lambda = 0.2$ and then at $\lambda > 0.2$ it increases. Olefin feed (x_1) and external isobutane-to-olefin ratio (x_8) remain constant at $\lambda \geq 0.5$, isobutene recycle (x_2) remains constant at $\lambda > 0.1$, therefore they don't affect the objective function and risk properties when they are constant. The same results for the change in decision variables can be deduced when Table 4.17 is compared with Table 4.15 (where the objective is the minimization of CVaR^{+}).

Table 4.19. Optimal values of decision variables ($\boldsymbol{x}$) for maximization of [$\lambda\, E[\boldsymbol{\Phi}]$ – (1−λ) (CVaR^{+} – CVaR^{-})].

Decision Variable	$\lambda = 0$	$\lambda = 0.1$	$\lambda = 0.2$	$\lambda = 0.3$	$\lambda = 0.4$	$\lambda = 0.5$	$\lambda = 0.6$	$\lambda = 0.7$	$\lambda = 0.8$	$\lambda = 0.9$	$\lambda = 1$
x_1	1500.0	1500.0	1500.0	1736.6	3650.2	7363.2	7363.2	7363.2	7363.2	7363.2	7363.2
x_2	5000	5000	10000	10000	10000	10000	10000	10000	10000	10000	10000
x_3	50.00	76.94	89.54	108.66	227.99	439.87	443.27	445.68	447.48	448.87	449.99
x_4	2336.0	2336.0	2608.6	2964.7	5494.1	10000	10000	10000	10000	10000	10000
x_5	1349.9	1349.9	1682.5	1880.3	3052.7	4836.8	4836.8	4836.8	4836.8	4836.8	4836.8
x_6	66.78	80.95	88.03	87.71	84.81	83.45	83.60	83.70	83.77	83.83	83.88
x_7	83.09	87.70	92.28	91.66	88.43	86.60	86.65	86.68	86.71	86.73	86.74
x_8	4.23	4.23	7.78	6.84	3.57	2.01	2.01	2.01	2.01	2.01	2.01
x_9	10.00	6.93	3.88	4.29	6.45	7.66	7.63	7.61	7.59	7.58	7.57
x_{10}	116.30	130.10	143.85	142.00	132.29	126.82	126.96	127.06	127.13	127.19	127.23

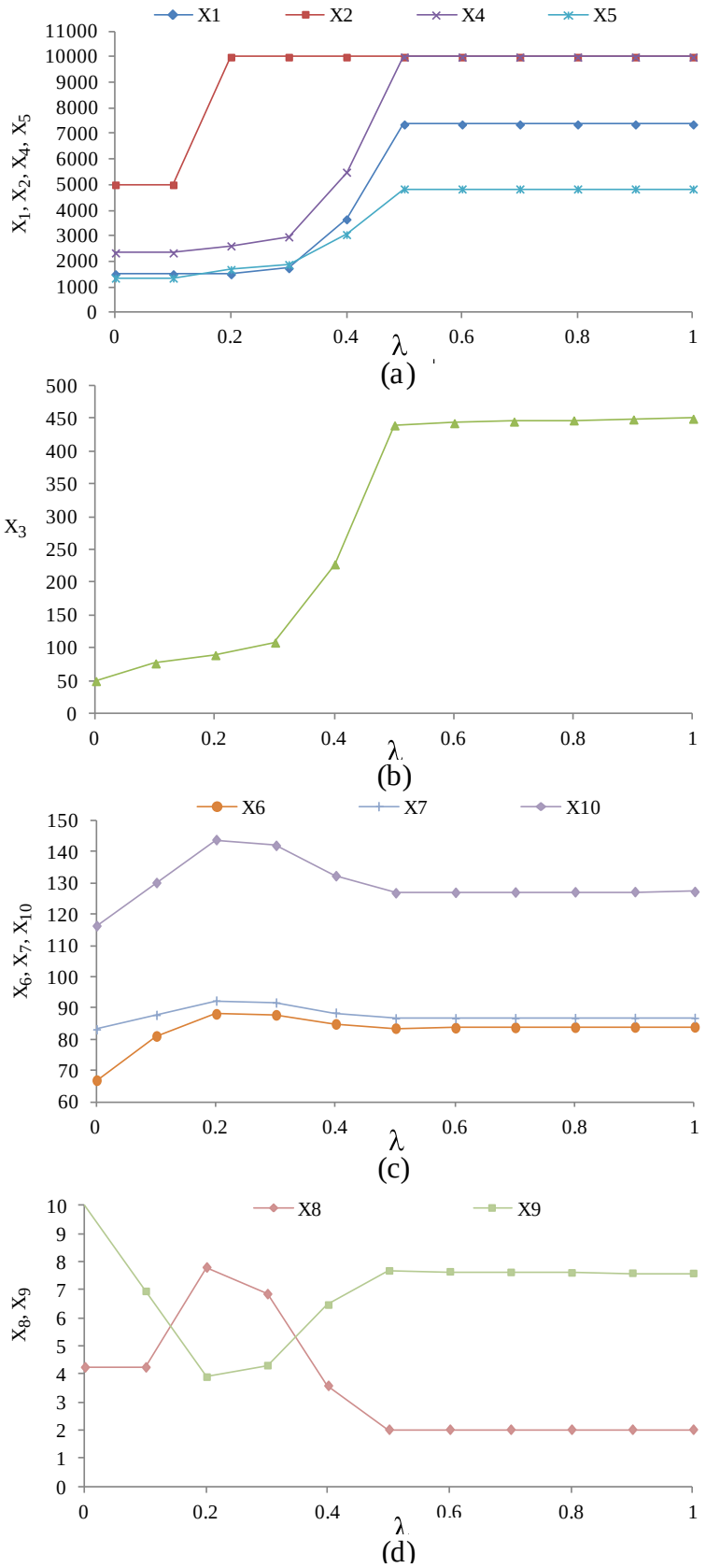

Figure 4.37. The change in values of decision variables ($\boldsymbol{x}$) for the profit distribution with weighting parameter λ, for max $[\lambda\, E[\boldsymbol{\Phi}] - (1-\lambda)\,(\mathrm{CVaR}^{+} - \mathrm{CVaR}^{-})]$.

4.2.2.6. Objective Function: Maximization of $E[\Phi]$ with Constraint of CVaR⁻. Based on the general problem defined by Equation 3.20 of Chapter 3, the mathematical formulation for the maximization of expected profit with CVaR⁻ as constraint for the AP model is given by Equation 4.16.

$$
\begin{aligned}
&\max_{\boldsymbol{x},\eta,z_i^-} && \tfrac{1}{N}\textstyle\sum_{i=1}^{N}\Phi_i(\boldsymbol{x},\boldsymbol{p}_i) \\
&s.t. && \left.\eta-\tfrac{1}{N(1-\alpha)}\textstyle\sum_{i=1}^{N}z_i\geq C_{limit}^-\right\} \quad CVaR^-\ Limit\ Constraint \\
& && \left.\begin{aligned} z_i^-&\geq\eta-\Phi_i(\boldsymbol{x},\boldsymbol{p}_i)\\ z_i^-&\geq 0\end{aligned}\right\} \begin{aligned}&CVaR\ Constraints\ (linear)\\ &\forall\, i=1,\dots,N\end{aligned} \\
& && -x_4+x_1(1.12+0.13167\,x_8-0.0067\,{x_8}^2)=0 \\
& && -x_7+86.35+1.098\,{x_4}^2+0.325\,(x_6-89)=0 \\
& && -x_9+35.82-0.022\,x_{10}=0 \\
& && -x_{10}+3\,x_7-133=0 \\
& && -x_8\,x_1+x_2+x_5=0 \\
& && -x_5+1.22\,x_4-x_1=0 \\
& && -x_6(x_4\,x_9+1000\,x_3)+98000\,x_3=0 \\
& && x_j^L<\ x_j \\
& && x_j<x_j^U \qquad \forall\, j\in\{1,2,..,10\}
\end{aligned}
\tag{4.16}
$$

where:

$$\Phi_i(\boldsymbol{x},\boldsymbol{p}_i)=+c_{1_i}\,x_4x_7-c_{2_i}\,x_1-c_{3_i}\,x_2-c_{4_i}\,x_3-c_{5_i}\,x_5\ ;\ i=1,\dots,nMCS$$

Upon feasible and optimal solution, VaR⁻ and CVaR⁻ are evaluated at the optimal values of η and $\boldsymbol{z}^-$ as follows:

$$
\begin{aligned}
VaR^-&=\eta^* \\
CVaR^-&=\eta^*-\tfrac{1}{N(1-\alpha)}\textstyle\sum_{i=1}^{N}(z_i^-)^*
\end{aligned}
\tag{4.17}
$$

In general, the optimal solution depends on the value of C_{limit}^-. However, for the particular model AP, the use of any C_{limit}^- value less than the value of CVaR⁻ obtained from section 4.2.2.4, as a result of solution of Equation 4.13 (maximization of expected profit only) leaves the CVaR constraints ($z_i^-\geq\eta-\Phi_i(\boldsymbol{x},\boldsymbol{p}_i)$) inactive at the termination of optimization, Therefore, $(\text{CVaR}^-)^*$ and $(\text{VaR}^-)^*$ values obtained from Equation 4.17 above leads to errenous results since they do not become equal to the actual CVaR⁻ and

VaR$^-$ values that can be obtained from percentile calculations based on Equation 2.8 and 2.9 as explained in Chapter 2. On the other hand, the use of any C^-_{limit} value greater than the (CVaR$^-$)* value obtained from section 4.2.2.4, as a result of solution of Equation 4.13 (maximization of expected profit only) makes the optimization problem infeasible. In other words, for the AP model, the maximized value of expected profit (Equation 4.13 in section 4.2.2.4), cannot be improved by forcing the distribution towards right side by imposing a higher C^-_{limit} value as constraint bound. Therefore, the solution of maximization of expected profit is actually a binding solution that gives CVaR$^-$ which is already at its rightmost limit. Thus, the solution of problem 4.13 (expected profit maximization) and 4.16 with C^-_{limit} 6704.4 \$/day (which is the CVaR$^-$ value obtained from solution of problem 4.13 of maximization of expected profit), are identical. The following figure and tables correspond to C^-_{limit} = 6705.0 \$/day and their comparison with Table 4.16, 4.17 and Figure 4.33 proves this within the uncertainty of MCS performed with 8000 samples. It should be noted that with 8000 MCS, $C^-_{limit} \geq$ 6705.01 \$/day makes the problem Equation 4.16 infeasible.

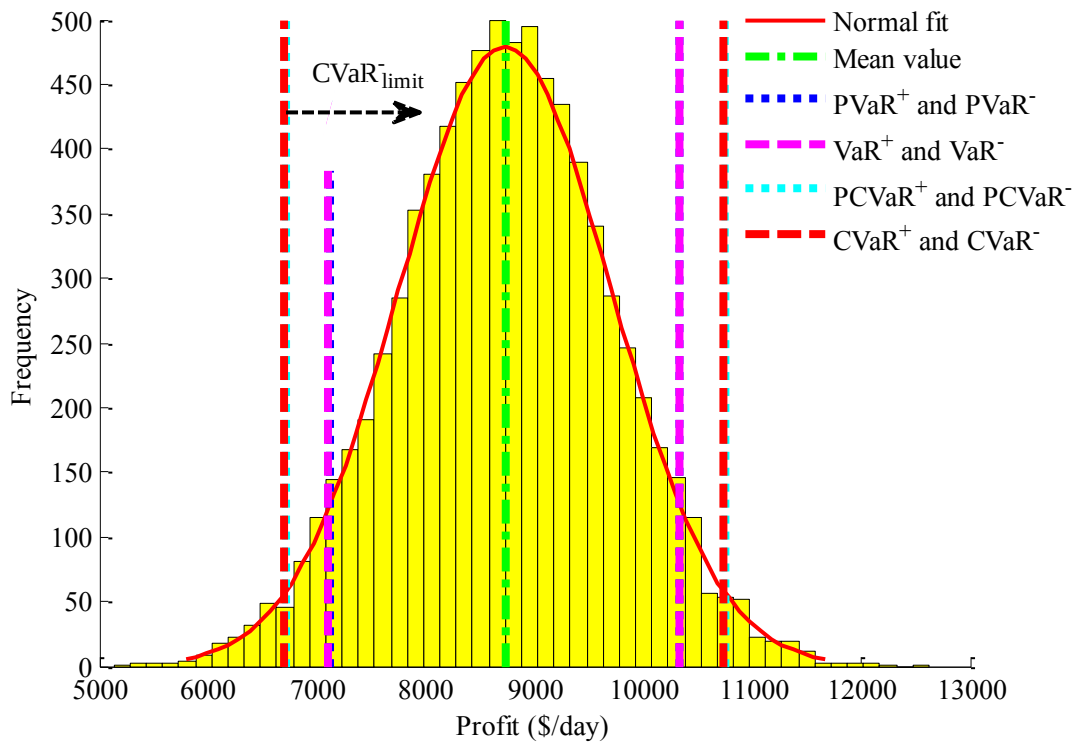

Figure 4.38. Frequency distribution of profit using simultaneous algorithm for maximization of expected profit with CVaR$^-$ as constraint.

Table 4.20. Statistical Properties of the profit distribution in Figure 4.38, as a result of maximization of expected profit with $CVaR^{-}$ as constraint.

Mean Value (μ)	8728.5	\$/day
Standard Deviation (σ)	978.2	\$/day
Skewness	-3.86×10^{-3}	
Kurtosis	3.0127	
$PVaR^{+}$	10337	\$/day
$PVaR^{-}$	7119.6	\$/day
VaR^{+}	10333	\$/day
VaR^{-}	7098.1	\$/day
$PCVaR^{+}$	10746	\$/day
$PCVaR^{-}$	6710.8	\$/day
$CVaR^{+}$	10742	\$/day
$CVaR^{-}$	6705	\$/day
$(CVaR^{+} - CVaR^{-})$	4037	\$/day
DIFP	2013.5	\$/day
DIFM	2023.5	\$/day
RR	0.99505	

<u>4.2.2.7. A CPU Time Comparison.</u> This section compares the CPU times of the simultaneous and sequential algorithms which had been discussed several times in earlier chapters of the thesis. Under the sequential approach, maximization of the expected value of the profit, $E[\Phi_i]^*$, is not possible, as mentioned in Chapter 3. If $E[\Phi_i]^*$ is desired, there must be an outer loop in the algorithm for the sequential approach in Section 4.2.1. The outer-loop decision variables must be presented as fixed values to the inner loop. The convergence of such an interlocked-loops scheme may not be guaranteed. Therefore, as compatible with the rest of this thesis work, the sequential approach in Section 4.2.1 is used only to accumulate the Φ_i^* values for the post-analysis (i.e., to compute $E[\Phi_i^*]$, $VaR^{\pm}$ and $CVaR^{\pm}$) of the probability distributions of these accumulated optimal solutions. The CPU time comparison was made between *i*) the sequential method for obtaining the

Table 4.21. Optimal values of decision variables ($\boldsymbol{x}$) for maximization of expected profit with CVaR^{-} as constraint using the simultaneous algorithm.

Decision Variable	x_i^*
x_1	7363.2
x_2	10000
x_3	445.7
x_4	10000
x_5	4836.8
x_6	83.7
x_7	86.7
x_8	2.0
x_9	7.6
x_{10}	127.1

maximum expected profit with post-computing the CVaR$^{\pm}$ / VaR$^{\pm}$ (Section 4.2.1) and *ii*) the simultaneous method with the objective of maximizing [$\lambda\, E[\Phi]$ – (1−λ) (CVaR^{+} – CVaR^{-})] (Section 4.2.2.5). The optimization problems *(i)* and *(ii)* are not identical to each other. The sequential one repeatedly solves the small-sized NLP (Equation 4.5) within the MC sampling loop nMCS times and then computes the CVaR$^{\pm}$ / VaR$^{\pm}$ of the resulting distribution of profit Φ. The simultaneous one first generates nMCS scenarios (cost coefficients of the profit function) and then solves the large-sized NLP (Equation 4.14) but only once to obtain the maximized values of the weighted objective function and the CVaR$^{\pm}$ / VaR$^{\pm}$ values of the resulting profit distribution. At first it may be thought that the latter large-sized NLP problem requires much more CPU time than the repeated solution of the small sized-NLP of the former problem. However, this section demonstrates that the simultaneous method require considerably less CPU time, especially as the nMCS increases.

For the sequential method (maximization of expected profit), since the decision variables are not related to MC samples, the number of decision variables is 10 (for vector x) for all nMCS. The number of equality constraints is 7 (plant's equality constraints). There are not any inequality constraints in the problem for the maximization of expected profit. Among the constraints only 4 of the 7 plant equality constraints are nonlinear, the rest of the constraints i.e., the remaining 3 equations are linear. The objective function is also linear in decision variables.

The number of decision variables for the simultaneous method (maximization of $[\lambda\, E[\Phi] - (1-\lambda)\,(\mathrm{CVaR}^{+} - \mathrm{CVaR}^{-})]$) is 2×N+12 (2×N is for the $\mathbf{z}^{+}$ and $\mathbf{z}^{-}$, 10 for decision variables $\boldsymbol{x}$, and 2 for γ and η). The number of equality constraints is 7 (plant's equality constraints). The number of inequality constraints is 2×N (2×N represents the inequalities coming from Uryasev's formulations, i.e., Equation 2.28 and 2.29). The number of variable bounds is 2×N+20 (2×N is for $\boldsymbol{z}^{+} \geq \mathbf{0}$ and $\boldsymbol{z}^{-} \geq \mathbf{0}$, and 20 is for $\boldsymbol{x}^{L} \leq \boldsymbol{x} \leq \boldsymbol{x}^{U}$). Among the constraints only 4 of the 7 plant equality constraints are nonlinear, the rest of the constraints i.e., the remaining 3 equations and 2×N inequalities are all linear. The objective function is also linear in decision variables. The number of equality and inequality constraints for the simultaneous method are given in Table 4.22 with respect to the corresponding nMCS.

The CPU times (as reported by the GAMS) for different nMCS values ranging from 250 to 10,000 are given in Table 4.22 and the results are summarized by Figure 4.39. As seen, although the simultaneous method involves higher number of equality/inequality constraints and variable bounds than the sequential method, the simultaneous method require considerably less CPU time, especially as the nMCS increases.

Table 4.22. CPU Times of the Sequential and Simultaneous Methods.

	Sequential Method	SimultaneousMethod		
nMCS	CPU Time (s)	CPU Time (s)	# of Decision Variables	# of Inequality Constraints
250	34.2	0.4	512	500
500	61.9	1.2	1012	1000
1000	123.4	2.8	2012	2000
2000	251.3	13.8	4012	4000
3000	367.7	24.0	6012	6000
4000	496.3	47.9	8012	8000
5000	621.2	83.4	10012	10000
6000	726.5	117.9	12012	12000
7000	839.8	162.2	14012	14000
8000	1015.3	216.8	16012	16000
9000	1109.6	282.9	18012	18000
10000	1277.8	376.2	20012	20000

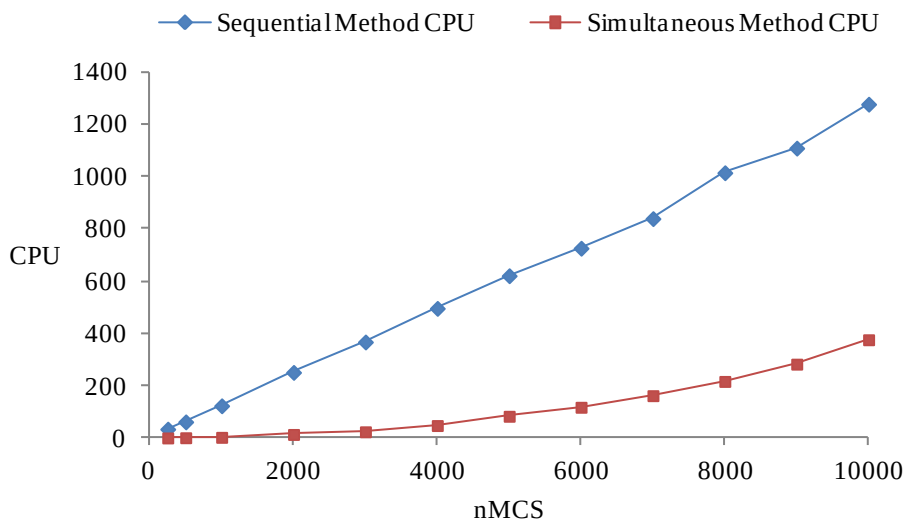

Figure 4.39. Change in CPU Times for the Sequential and Simultaneous Methods with nMCS.

5. CONCLUSIONS AND RECOMMENDATIONS

Risk management of uncertainty problems have drawn interest in both academic and industrial areas for decades. Some of the recent popular risk measures studied in this thesis are Conditional Value at Risk (CVaR), Value at Risk (VaR), and Rachev Ratio (RR). As defined previously in the Introduction, VaR is "the maximum loss you are likely to incur on your portfolio with a specified probability". It was mentioned in Chapter 2 that CVaR is a superior risk measure compared to VaR, because CVaR depicts the risks beyond VaR and it has a convex function with a global optimum but VaR may be non-convex. However, VaR has been a very popular measure of risk. Although CVaR, "the expected value beyond VaR", is superior than VaR, risk management programs based on VaR are still being widely used. CVaR (and/or VaR) can be defined for both risk (negative or $CVaR^{-}$) and reward (positive or $CVaR^{+}$) sides. Another risk measure RR, (i.e., positive value of the ratio, $CVaR^{+}/CVaR^{-}$), gives information about tail weight of frequency distribution. Intensive research has been conducted on RR recently.

This study aims to control / reshape the distribution of optimal design / synthesis problems under uncertainty via optimization of two chemical engineering examples, namely the Benzoic Acid Plant (BAP) and the Alkylation Plant (AP) involving various objective functions. For this purpose, Monte Carlo Simulation (MCS) was used as the sampling technique. MCS is a method which propagates the uncertainty in the inputs through outcomes by taking random samples from the probability distributions (e.g., normal distribution). The number of MCS (nMCS) for the BAP and the AP models was estimated by choosing the point at which both the mean and standard deviation versus nMCS became steady. For the BAP model the estimated nMCS was 10000 and for the AP model, the estimated nMCS was 8000. CVaR formulations were developed for the risk (negative or $CVaR^{-}$) and reward (positive or $CVaR^{+}$) sides mutually exclusively. The optimization formulations of $CVaR^{+}$ and $CVaR^{-}$ were given in Equation 2.28 and 2.29. Sequential and simultaneous methods were used for estimating some statistical results such as $VaR^{\pm}$, $CVaR^{\pm}$, expected value of profit/cost, standard deviation, skewness, kurtosis, difference between $CVaR^{+}$ and $CVaR^{-}$ and Rachev Ratio (RR). $VaR^{\pm}$ and $CVaR^{\pm}$ were estimated by means of both historica (Equation 2.8 and 2.9) and parametric methods

(Equation 2.24 and 2.25). Algorithms for the sequential and the simultaneous methods were given in Figure 3.7 and Figure 3.8, respectively. In all calculations, GAMS and/or MATLAB were used to solve the optimization models and/or to compute $CVaR^{\pm}$ / $VaR^{\pm}$ values. Results and conclusions of the applied procedures are summarized in the following section and possible future recommendations are included at the end of this chapter.

5.1. Conclusions for Benzoic Acid Plant Model

Plant for the recovery of benzoic acid is a combination of settlers, an evaporator and three heat exchangers. The benzoic acid plant (BAP) model aims to achieve benzoic acid concentration of 20 wt% in the product at optimum design under uncertainty for the current optimization problem, considering the maximization of net present worth of plant production in most of the cases. Method of Monte Carlo Simulations (MCS) was used to generate random values for uncertain variables of raw material cost and product price for each scenario. Where necessary, confidence limit was taken as 95%.

First of all, mass and energy balances were performed and objective function of net present worth to be utilized in most of the calculations was obtained in Appendix A. The BAP model equality constraints given in Appendix A cannot be written explicitly as $\boldsymbol{h}(\boldsymbol{d},\boldsymbol{x},\boldsymbol{u},\boldsymbol{p}) = \boldsymbol{0}$. Therefore, NPW ($J_{NPW}$) was calculated from the BAP model and then it was used for further calculations. For consistency in the subsequent calculations, holding the raw material cost and product price constant respectively at 0.25 \$/kg and 1.0 \$/kg, approximate values for the optimum benzene flow rate, T_{apr}, and number of settler stages, which give maximum net present worth (NPW), were determined separetely. The optimum benzene flow rate, number of settler stages and approach temperature that give the maximum NPW were estimated as 4000 kg/h, 4, and 8.9°C in Figure 4.2, 4.3, and 4.4, respectively. Net present worth increased up to benzene flow rate of 4000 kg/h and decreased almost linearly beyond benzene flow rate of about 5000 kg/h. At these optimum values, mean and standard deviation versus nMCS graphs are plotted, and from these graphs nMCS was chosen to be 10,000.

First, 10,000 random numbers were assigned to uncertain variables (raw material cost and product price) of the BAP model, i.e., MCS was performed, and the NPW

outcomes were accumulated in J_{NPW}. Then, the post-analyses of $VaR^{\pm}$ and $CVaR^{\pm}$ were conducted by computing the expected (mean) value of NPW ($E(J_{NPW})$), $VaR^{\pm}$, and $CVaR^{\pm}$ from the accumulated J_{NPW} as shown in Figure 4.7. In Figure 4.8, NPW histogram was plotted via historical and parametric methods at 10,000 MCS without making any optimization. Uncertain variables which were randomly generated from normal distributions were used in parametric and historical calculations. It can be observed from the Figure 4.8 that parametric and historical values for the risk measures $VaR^{\pm}$ and $CVaR^{\pm}$ were very close to each other, which indicates that the histogram well fits the normal curve. Standard deviation, $E(J_{NPW})$ and RR were found as 1.55×10^5 \$/y, 2.935×10^5 \$/y and 26.31, respectively. When there was no optimization, the resulting probability distribution had negligibly negative skewness, i.e., the distribution was slightly skewed to the left. Therefore, the probability of obtaining NPW values less than the mean value was higher than the probability of obtaining NPW values greater than the mean value. The resulting frequency distribution had negative excess kurtosis which showed that for this frequency distribution, peakedness was not prominent.

Variation of VaR and CVaR with benzene flow rate was also investigated at 10,000 MCS trials and at benzene flow rates from 0.1×10^4 kg/h to 2.5×10^4 kg/h in Figure 4.9. It can be seen in the figure that all the plotted lines in terms of risk measures ($CVaR^{+}$, $CVaR^{-}$, VaR^{+}, and VaR^{-}) took their maximum values between 4000 kg/h and 4800 kg/h, beyond that amount they showed a significant decrease. Additionally, the difference between VaR and CVaR for both right and left sides did not have a significant change after about 5000 kg/h of benzene flow rate, whereas up to that point the difference constantly increased. This means that as the benzene flow rate increased, the frequency distribution of NPW shifted to the left and the risk of taking a lower NPW increased without altering the difference between right and left side risks. Below benzene flowrate of 0.25×10^4 kg/h, as benzene flowrate decreased the frequency disrtibution shifted to the left and VaR^{+} (or $CVaR^{+}$) and VaR^{-} (or $CVaR^{-}$) values approach to each other indicating that the plant's response to uncertainties in the parameters p_1 and p_2 was to decrease the NPW values of the frequency distribution and to increase the certainty of the mean value of NPW.

$VaR^{\pm}$ and $CVaR^{\pm}$ for BAP model were estimated via the percentile equations (Equations 2.8 and 2.9) in Chapter 2 after maximization of the NPW. According to the

sequential optimization flowchart in Figure 4.10, NPW was maximized using MATLAB's unconstrained optimizer "fminsearch" at each MCS and resulting frequency histogram was given in Figure 4.11. After the optimization of NPW, $VaR^{\pm}$ and $CVaR^{\pm}$ were calculated from the optimum J^{*}_{NPW} values as off-line. Standard deviation was found as 1.59×10^{5} \$/y and $E(J_{NPW})$ was 2.963×10^{5} \$/y. This means that as compared to calculation of $VaR^{\pm}$ and $CVaR^{\pm}$ without optimization, maximization of J_{NPW} shifted the frequency distribution to the right increasing the expected (mean) value of J_{NPW}. The resulting frequency distribution had positive skewness and positive excess kurtosis. Positively skewed distribution has a probability of obtaining NPW values greater than the mean value higher than the probability of obtaining NPW values less than the mean value. Positive excess kurtosis means that most of the possible NPW values are accumulated around the mean value. These statistical results also prove that upon optimization, the company increases the mean NPW and increases the chances of realizing even better NPW (decreases the chances of getting lower NPW). The RR after maximization of NPW came out to be 19.86 which was lower than the result for the solution of the BAP model without optimization. This is because the decrease in $CVaR^{-}$ upon optimization overwhelmed the increase in $CVaR^{+}$.

Minimization and maximization of $CVaR^{+}$, $CVaR^{-}$, and RR were also investigated as presented in the subplots in Figure 4.15 and 4.16 for the positive-valued and mixed valued (both positive and negative) NPW. The results were tabulated in Table 4.4 and 4.5. The sequential optimization flowchart in Figure 4.12 was applied, 10,000 MCS trials were performed. Normal random values were assigned to the uncertain parameters (raw material cost, p_1 and product price, p_2). MATLAB's "fminbnd" function was used to solve these optimization problems. CVaR, VaR and RR values were calculated with historical method using the "percentile" function of MATLAB.

Some of the cases were theoretically unbounded in continuous distributions such as maximization of $CVaR^{+}$, minimization of $CVaR^{-}$, and maximization of RR. Maximization of $CVaR^{+}$ tends to reach the maximum number beyond VaR^{+} which is positive infinity in case of a continuous distribution and the maximum number in the series in case of discrete series. Minimization of $CVaR^{-}$ tends to reach the minimum number beyond VaR^{-} which is negative infinity in case of a continuous distribution and the minimum number in the series

in case of discrete series. Maximization of RR (where RR = $CVaR^+$ / $CVaR^-$) was unbounded because in this case $CVaR^+$ was tried to be maximized and $CVaR^-$ was tried to be minimized which tend to reach positive infinity over negative infinity resulting in an indefinite solution. Interval of the distribution gives information about the maximum and the minimum NPW that can most probably be achieved. The higher the RR, the wider the interval of the distribution was. Accordingly, the lower the RR, the more narrow the interval of distribution was.

Figure 4.15, which consisted of positive-valued NPW outcomes, showed that minimizations of $CVaR^+$, $CVaR^-$ or RR compress the tails of the fequency distribution curve of NPW towards the expected (mean) NPW (1.45×10^6 \$/y) and provide the possibility of being more confident about the mean value of the resulting distribution. Among the resulting frequency distributions, except the minimization of $CVaR^-$, all the remaining optimization problems related to this section had negative skewness. When skewness was negative, left tail was longer and the distribution was concentrated on the left side increasing the risk of obtaining lower NPW values. Minimization and maximization of $CVaR^+$, $CVaR^-$, or RR, all had positive excess kurtosis. RR took the highest value of 1.38 for the maximization of RR among all six optimization problems. Depending on the definition of RR (RR = $CVaR^+/CVaR^-$), the maximization of RR gave a mean value with a high difference of $CVaR^+ - CVaR^-$. Therefore, the resulting frequency distribution for maximization of RR had a low certainty. On the contrary, RR took the lowest value of 1.01 at the minimization of RR, which gave a mean value with a high certainty (or with a small difference of $CVaR^+ - CVaR^-$).

Figure 4.16, which consisted of mixed-valued NPW outcomes, also showed that minimizations of $CVaR^+$, $CVaR^-$ or RR compress the tails of the fequency distribution curve of NPW towards the expected (mean) NPW (-5.5×10^6 \$/y) and provide the possibility of being more confident about the mean value of the resulting distribution. Among the resulting frequency distributions, except the maximization of $CVaR^-$, all the remaining optimization problems related to this section had negative skewness. Therefore, for those which have negative skewness, left tail was longer and the distribution was concentrated on the left side increasing the risk of obtaining lower NPW values than the mean value. In this case, minimization and maximization of $CVaR^+$, $CVaR^-$, or RR, all had

negative excess kurtosis and peakedness was not prominent for the related frequency distribution. RR took the highest value of 23.9 again for the maximization of RR among all six optimization problems. Depending on the definition of RR (RR = $CVaR^{+}/CVaR^{-}$), the maximization of RR gave a mean value with a high difference of $CVaR^{+} - CVaR^{-}$. Therefore, the resulting frequency distribution for maximization of RR had a low certainty. On the contrary, RR took the lowest value of 1.36×10^{-8} at the minimization of RR, which gave a mean value with a high certainty (or with a small difference of $CVaR^{+} - CVaR^{-}$).

Linear combinations of $CVaR^{\pm}$, RR, and expected (mean) value of NPW were optimized according to the sequential optimization flowchart in Figure 4.12, and then $VaR^{\pm}$ and $CVaR^{\pm}$ for the BAP model were computed as off-line. The objective function in the sequential optimization flowchart in Figure 4.12 was replaced by the indicated linear combinations (Equations 4.1, 4.2, 4.3, and 4.4), sequentially. Eleven values between 0 and 1 were assigned to the weighting coefficient, λ in the linear combinations. 10,000 MCS trials were performed for each optimization problem. Normal random values were assigned to the uncertain parameters (raw material cost, p_1 and product price, p_2). MATLAB's "patternsearch" function was used to solve these optimization problems. VaR, CVaR and RR values were calculated with historical method using the "percentile" function of MATLAB. Results of frequency distributions obtained from the optimizations only for both positive and negative NPW values were given in Section 4.1.4.

Initially, the dependencies of the objective functions on the decision variable (benzene flowrate with the lower bound of 10 kg/h and the upper bound of 10,000 kg/h) were investigated (Figure 4.17). Until benzene flowrate was almost 1650 kg/h, minimization for the linear combination of $CVaR^{+}$ and $CVaR^{-}$ resulted in a decrease with the increase in the weight of $CVaR^{+}$ in the objective function. On the contrary, beyond 1650 kg/h, the result increased with the increase in the weight of $CVaR^{+}$ in the objective function. The same behavior was also valid for the linear combination of the expected value of NPW and the difference of $CVaR^{+}$ and $CVaR^{-}$. The behavior was reversed at almost 950 kg/h benzene flowrate. On the other side, until benzene flowrate was almost 1650 kg/h, the linear combination of the expected value of NPW and RR resulted in an increase with the increase in the weight of the expected value of NPW (or the decrease in the weight of RR) in the objective function. Beyond 1650 kg/h, the result decreased with

the increase in the weight of $CVaR^+$ in the objective function. At a benzene flowrate within the specified bounds, the result for the linear combination of the expected value of NPW and $CVaR^-$ decreased with the increase in the weight of the expected value of NPW.

Figures showing the NPW frequency distributions and the change in some statistical properties of the NPW distributions with the weighting coefficient for the linearized optimization problems were given successively. Results for the minimization of the linear combination of $CVaR^+$ and $CVaR^-$ showed that expected NPW values at $\lambda \geq 0.2$ (for $\lambda = 0.2$, $E[J_{NPW}] = 2.86\times10^5$ \$/y) were smaller than the expected NPW for the case without optimization (2.94×10^5 \$/y). The results also showed that when λ increases, i.e., when the weight of the minimization of $CVaR^+$ increases, the frequency distributions of NPW shifts to the left. In other words, as λ decreases, the weight of the maximization of $CVaR^-$ increases and the frequency distributions of NPW shifts to the right. As λ decreased, RR increased from 0.96 to 22. Benzene flowrate reached its lower boundary value when $\lambda = 0.4$ and $\lambda = 0.5$. Skewness and excess kurtosis were negative when $\lambda < 0.4$, then left tail was longer, increasing the risk of obtaining lower NPW values than the mean value and for this frequency distribution, peakedness was not prominent.

Results for the minimization of the linear combination of expected value of NPW and the difference of $CVaR^+$ and $CVaR^-$ showed that expected NPW values at $\lambda \leq 0.6$ (for $\lambda = 0.6$, $E[J_{NPW}] = 2.91\times10^5$ \$/y) were smaller than the expected NPW for the case without optimization (2.94×10^5 \$/y). The results also showed that when λ increases, i.e., when the weight of the minimization of $CVaR^+$ decreases (or when the weight of the maximization of NPW and the maximization of $CVaR^-$ increases), the frequency distributions of NPW shifts to the right. RR increased from 0.97 to 19. Benzene flowrate became equal to the lower boundary value for $\lambda < 0.3$. Skewness and excess kurtosis were negative when $\lambda \geq 0.4$, then left tail was longer, increasing the risk of obtaining lower NPW values than the mean value and for this frequency distribution, peakedness was not prominent.

Results for the minimization of the linear combination of expected value of NPW and $CVaR^-$ showed that expected NPW values were greater than the expected NPW for the case without optimization (2.94×10^5 \$/y). Expected NPW values increased until $\lambda \leq 0.8$

showing a slight shift to the right. Beyond $\lambda = 0.8$ the NPW distributions did not alter. The results also showed that when λ increases, i.e., when the weight of the maximization of $CVaR^{-}$ decreases (or when the weight of the maximization of NPW increases), the frequency distributions of NPW shifts to the right slightly. RR decreased from 20.5 to 19.6. Benzene flowrate increased from 3945 kg/h to 4346 kg/h until $\lambda = 0.8$. Skewness and excess kurtosis were positive for all λ values. Therefore, the right tail was longer, increasing the chance of obtaining lower NPW values than the mean value and for this frequency distribution, peakedness was prominent.

Results for the minimization of the linear combination of expected value of NPW and RR showed that when $\lambda = 0$, i.e., when the optimization problem became minimization of RR, the expected NPW value is -1.57×10^5 \$/y. Expected NPW values increased until $\lambda \leq 0.8$ showing a slight shift to the right which cannot be precisely seen from the Figure 4.25. Beyond $\lambda = 0.1$ the NPW distributions together with all their statistical values did not alter, the expected NPW values (2.99×10^5 \$/y) were greater than the expected NPW for the case without optimization (2.94×10^5 \$/y).

Overall, the BAP exhibits a nonlinear behavior which is strongly dependent on the level of the benzene flow rate. This dependence on the benzene flowrate level is what determines both the BAP's sensitivity to uncertain inputs and the statistical properties of its NPW distribution. These observations demonstrate the importance of the task of selecting the nominal operating condition for the BAP at the plant-design stage, since both the plant's expected (mean) profitability as well as the risks and rewards (characterized in terms of left and right tail of the probability distribution of the profitability measure) associated with that design are strongly dependent upon the nominal operating point of the nonlinear BAP.

5.2. Conclusions for Alkylation Plant Model

Plant for the alkylation process consists of a reactor and a fractionator system. The aklylation plant (AP) aims to maximize the profit (\$/day) from the plant production. The uncertain variables were considered as the objective function cost coefficients.

Uncertain parameters of objective function cost coefficients were sampled from normal distributions. For the AP model, following Konno *et al.* (2011), a modified Rachev Ratio (RR) is defined as the ratio of the difference of the mean (μ) from $CVaR^+$ (DIFP = $CVaR^+ - \mu$) and the difference of $CVaR^-$ from the mean (DIFM = $\mu - CVaR^-$); RR = DIFP/DIFM = $[CVaR^+ - \mu]/[\mu - CVaR^-]$. First, using the sequential method, the sufficient nMCS was determined as 8,000.

The simultaneous method was applied to the AP through various objective functions. First, minimization of $[CVaR^+ - CVaR^-]$ was used as the objective function where the constraints included both the $CVaR^+$ and $CVaR^-$ related terms. When compared to the sequential method, where the objective was the maximization of profit at each MCS, minimization of $[CVaR^+ - CVaR^-]$ using the simultaneous method decreased the mean value of the profit, the difference of $CVaR^+$ and $CVaR^-$ and the RR. This means that, minimization of $[CVaR^+ - CVaR^-]$ provided a more certain expected profit value at the expense of having a lower profit. In terms of the decision variables, using simultaneous algorithm with the objective function of minimization of $[CVaR^+ - CVaR^-]$ the AP required less olefin feed, acid addition, alkylate yield, acid strength but higher external isobutane-to-olefin ratio and acid dilution factor compared to the sequential algorithm with the objective function of maximization of expected profit.

The use of the minimization of $CVaR^+$ as the objective function under the simultaneous scheme, where the constraints included the $CVaR^+$ related terms besides the plant equations, decreased the mean value of the profit, the difference of $CVaR^+$ and $CVaR^-$ and the RR, compared to the sequential algorithm with the objective function of maximization of expected profit. Minimization of $CVaR^+$ provided a more certain expected profit at the expense of having a lower profit. On the other hand, when compared to minimization of $[CVaR^+ - CVaR^-]$, the minimization of $CVaR^+$ decreased the mean value of the profit and the RR, however resulted in a higher value for the difference of $CVaR^+$ and $CVaR^-$. This means that, minimization of $[CVaR^+ - CVaR^-]$ has the highest certainty with the lowest ($CVaR^+ - CVaR^-$) difference among the optimization problems implemented to the AP. Minimization of $CVaR^+$ had lower profit values than minimization of $[CVaR^+ - CVaR^-]$ and higher profit values than the sequential method with maximization of profit objective. The decrease in RR indicates a slightly more decrease of

reward probability in the right side than the decrease of risk probability in the left side of the profit distribution. In terms of the decision variables, minimization of $CVaR^{+}$ required higher olefin feed, alkylate yield, isobutane input, acid dilution factor but lower acid strength, motor octane number of alkylate and external isobutane-to-olefin ratio compared to minimization of $[CVaR^{+} - CVaR^{-}]$.

When maximization of $CVaR^{-}$ and the sequential method, where the objective was the maximization of profit, were compared, it was seen that they had similar results with only slight differences. This shows that the constraints of the AP that limit maximum possible $CVaR^{-}$ also limit the maximum possible expected profit. On the other hand, when compared to minimization of $[CVaR^{+} - CVaR^{-}]$, maximization of $CVaR^{-}$ increased the mean value of the profit and the RR, and showed a higher value for the difference of $CVaR^{+}$ and $CVaR^{-}$. This means that, minimization of $[CVaR^{+} - CVaR^{-}]$ still has the highest certainty with the lowest $(CVaR^{+} - CVaR^{-})$ difference as expected. Maximization of $CVaR^{-}$ had higher profit values and lower certainty of the mean profit than minimization of $[CVaR^{+} - CVaR^{-}]$. The increase in RR indicates a slightly more increase of reward probability in the right side than the increase of risk probability in the left side of the profit distribution. In terms of the decision variables, maximization of $CVaR^{-}$ required higher olefin feed, isobutene recycle, acid addition, alkylate yield, isobutane input, acid strength, motor octane number of alkylate, performance number of alkylate but lower external isobutane-to-olefin ratio and acid dilution factor compared to minimization of $[CVaR^{+} - CVaR^{-}]$.

Maximization of expected profit ($E[\boldsymbol{\Phi}]$) was used as the objective function where the constraints did not include the $CVaR^{+}$ and $CVaR^{-}$ related terms, but only the plant equations. When maximization of $E[\boldsymbol{\Phi}]$ using the simultaneous method and the sequential method, where the objective was the maximization of profit at each MCS were compared, it was seen that they had similar results with only slight differences. On the other hand, when compared to minimization of $[CVaR^{+} - CVaR^{-}]$, maximization of $E[\boldsymbol{\Phi}]$ increased the mean value of the profit and the RR, and yielded a higher value for the difference of $CVaR^{+}$ and $CVaR^{-}$. The minimization of $[CVaR^{+} - CVaR^{-}]$ remained as the one with the highest certainty and the lowest $(CVaR^{+} - CVaR^{-})$ difference among the optimization problems implemented. Maximization of $E[\boldsymbol{\Phi}]$ had higher profit values and lower certainty

of the mean profit than minimization of [CVaR^{+} − CVaR^{-}]. The increase in RR indicates a slightly more increase of reward probability in the right side than the increase of risk probability in the left side of the profit distribution. When compared to minimization of CVaR^{+}, maximization of $E[\boldsymbol{\Phi}]$ had a higher expected profit value and higher RR, and even a higher value for the difference of CVaR^{+} and CVaR^{-}. Maximization of CVaR^{-} had almost the same results with maximization of $E[\boldsymbol{\Phi}]$, except for the CVaR^{-} value which was slightly higher for the case of maximization of CVaR^{-} (6705 \$/day) compared to that for the maximization of $E[\boldsymbol{\Phi}]$ (6704.4 \$/day). This result indicated that the same constraints of the AP were limiting in both of the cases. In terms of the decision variables, the simultaneous algorithm with the objective function of maximization of $E[\boldsymbol{\Phi}]$ required higher olefin feed, isobutene recycle, acid addition, alkylate yield, isobutane input, acid strength, motor octane number of alkylate, performance number of alkylate but lower external isobutane-to-olefin ratio and acid dilution factor compared to minimization of [CVaR^{+} − CVaR^{-}].

Maximization of the linear combination of expected profit and (CVaR^{+} − CVaR^{-}) ($[\lambda\, E[\boldsymbol{\Phi}] - (1-\lambda)(CVaR^{+} - CVaR^{-})]$) was used as the objective function by assigning different values to λ ($0 \leq \lambda \leq 1$) where the constraints included both CVaR^{+} and CVaR^{-} related terms besides the plant equations. According to the results obtained, at $\lambda = 0$, the problem became identical with the minimization of [CVaR^{+} – CVaR^{-}] and at $\lambda = 1$, the problem became identical with the maximization of $E[\boldsymbol{\Phi}]$, as expected. With the increase in λ, the weight of the $E[\boldsymbol{\Phi}]$ increased dominating its effect on the objective function and the frequency distribution of profit shifted to the right. As λ decreased, the distribution shifted to the left, decreasing the mean profit but increasing the certainty of the mean of the distribution by compressing it around the mean value. When $\lambda \geq 5$, the frequency distribution of profit became almost constant. In terms of the decision variables, with increase in λ, maximization of $[\lambda\, E[\boldsymbol{\Phi}] - (1-\lambda)(CVaR^{+} - CVaR^{-})]$ required higher acid addition rate, alkylate yield, and isobutane input and lower acid dilution factor. As λ increased, the profit distribution shifted to the right. In other words, profit decreased but certainty increased with lower acid addition, alkylate yield, and isobutane input and higher acid dilution factor.

The maximization of expected profit ($E[\boldsymbol{\Phi}]$), where the constraints included the limiting value for CVaR^{-} (C_{limit}^{-}) and the CVaR^{-} related terms besides the plant equations, was performed. During the maximization of $E[\boldsymbol{\Phi}]$ with the C_{limit}^{-} constraint, the use of any C_{limit}^{-} value greater than the (CVaR^{-})* value obtained from section 4.2.2.4, as a result of solution of maximization of $E[\boldsymbol{\Phi}]$ made the optimization problem infeasible. This means that, for the AP model, the maximum value of $E[\boldsymbol{\Phi}]$ cannot be improved towards right side by imposing a higher C_{limit}^{-} value as constraint. Therefore, the solution of maximization of $E[\boldsymbol{\Phi}]$ without imposing limiting constraint was actually a binding solution that gave CVaR^{-} (6705 \$/day) which was already at its rightmost limit. It should be noted that with 8000 MCS, the use of $C_{limit}^{-} \geq 6705.01$ \$/day made the maximization of $E[\boldsymbol{\Phi}]$ problem infeasible.

Simultaneous method generates nMCS scenarios and solves the resulting large-sized augmented problem once. On the other hand, the sequential method is a small-sized problem which is solved repeatedly for nMCS times. In order to compare CPU times, GAMS models for the sequential and the simultaneous methods of AP model were run at different nMCS ranging from 250 to 10,000 and the CPU times were tabulated in Table 4.23 and graphically demonstrated in Figure 4.39. The larger-sized NLP problem (simultaneous method) may seem to require more CPU time than the repeated solution of the smaller-sized NLP problem (sequential method). However, it was seen that the sequential method took much higher CPU times compared to simultaneous method. The CPU times of the simultaneous approach rose exponentially with increasing nMCS, however those of the sequential approach showed almost linear dependence on nMCS.

5.3. General Conclusions

In this thesis, the possibility of controlling and (re)shaping the statistical probability distribution of optimal objective function values in optimization problems related to benzoic acid plant (BAP) and alkylation plant (AP) under uncertainty were investigated via imposing CVaR constraints. GAMS and/or MATLAB are used in solving the optimization models. Mass and energy balances and related tables for the plant models are present in Appendix A. Some selected MATLAB and GAMS codes are given in Appendix B and C, respectively.

First, the optimization formulations of CVaR (Conditional Value at Risk) via Uryasev's approach were developed in Chapter 2 for both the risk (left) and reward (right) sides of a probability distribution. Then, the mathematical formulations were developed for the optimal design under uncertainty via CVaR in Chapter 3. Uncertainties in the inputs were propagated through the MCS to the probability distributions of the process model outputs. $CVaR^{+}$ (for the reward/right side) and $CVaR^{-}$ (for the risk/left side) together with some other statistical results such as expected value, skewness/kurtosis, $CVaR^{+}$, $CVaR^{-}$, difference between $CVaR^{+}$ and $CVaR^{-}$, Rachev Ratio (RR), linearized RR, and some linear combinations of them were obtained via sequential and simultaneous methods. In the sequential approach, distribution of the optimal process output was generated first via MCS and then CVaR and the other statistical properties of this distribution were estimated. In the simultaneous approach, the process model equations for each and every realization of the input uncertainties were augmented and by solving these augmented equations together with the equations of the CVaR, the plant's frequency distribution of profit was obtained in a single stage.

BAP showed a nonlinear behavior and this behavior was strongly dependent on benzene flow rate. The effect of uncertainty in the inputs to the BAP and the statistical properties of its NPW distribution were affected by the change in benzene flow rate. Therefore, at the design stage, it is recommended to consider the tail properties and the mean value of the plant's profit distribution as to determine the nominal operating point for a highly-nonlinear chemical plant, since it may be impossible to adjust the tail properties and mean value of the distribution later in the operation stage.

Unlike BAP, the AP model had equality and inequality constraints which could explicitly be written in its mathematical formulation. The aim was to maximize the plant's profit. For this purpose, plant's profit was maximized using sequential method and the sufficient nMCS was determined as 8,000 from the results obtained by maximization of profit using the sequential method. Then, at 8,000 nMCS various other objective functions were optimized using simultaneous method and the results obtained were compared. The results prove that it is basically possible to reshape the profit distribution of the AP. The CPU time comparison, which was performed for the AP between the sequential (maximization of expected profit with post-computing the $CVaR^{\pm}$ / $VaR^{\pm}$) and the

simultaneous methods (maximization of $[\lambda\, E[\boldsymbol{\Phi}] - (1-\lambda)(CVaR^{+} - CVaR^{-})]$), showed that especially at high nMCS, the larger-sized NLP problem with the simultaneous method required less CPU time than the smaller-sized NLP problem with the sequential method.

All in all, this thesis work shows that when minimization of the difference between $CVaR^{+}$ and $CVaR^{-}$ or minimization of the RR is used as the objective, or when they are linearly combined with the expected profit or cost measures, it is possible to (re)shape the probability distribution of optimal objective function values as favorably as possible, i.e., the difference between $CVaR^{+}$ and $CVaR^{-}$ or the RR were both successfully utilized to compress the distribution of the optimal profit around its mean in order to increase certainty on the mean optimal profit, despite uncertainties in process inputs.

5.4. Recommendations for Future Work

Considering the methods worked and the results obtained in this study, the following suggestions are provided for future work. Related to the work done in this thesis, some additional results can be investigated by taking different confidence levels for the risk and the reward sides instead of taking the same confidence level for both of the two sides. On the other hand, random values for the uncertain variables are taken from normal distributions in this thesis work. Besides normal distributions, the random values can be taken from various distribution types such as uniform distribution, beta distribution, etc. In addition to applying the methods to different models, sampling methods of Conventional Uniform, Halton, and Sobol can also be compared in order to increase randomness at the minimum possible number of MC trials. Therefore, the effect of taking various distribution types for assigning random values to the uncertain variables, can be analyzed and compared. Different optimizers may also be tried and compared.

Since the methods used in this study are highly plant dependent due to the mass and energy balance equations (plant constraints dictate allowable $CVaR^{\pm}$ values), they can be applied to other plant models described by different class of optimization formulations such as MINLP, MILP, and pure LP based models to see the applicability and flexibility of the methods studied in this work on such different models. Although Uryasev's formulation for $CVaR^{\pm}$ is linear formulation, when it is combined with plant model the

resulting optimization model is generally nonlinear (NLP or MINLP) since most of the Chemical Engineering problems include nonlinear plant equations. When linear plant models are tried, the computation time elapsed for the simultaneous method will have a significant decrease especially for large scale computations.

APPENDIX A: BENZOIC ACID PLANT MODEL

Matlab codes for Benzoic Acid Plant (BAP) model include a plant function which takes vectors of p_1 (v_1, \$/kg) as raw material cost and p_1 (v_2, \$/kg) as product price and gives the value of Net Present Worth (NPW) as output at each Monte Carlo Simulation (MCS) trial.

Subscripts a,b,w refer to benzoic acid, benzene and water, respectively. Number of stages for settler, *n*, approach temperature, T_{apr}, which is the difference between the inlet stream to evaporator and the outlet stream from the evaporator (stream 7 in Figure 4.1), benzene flow rate, *benz*, Marshall & Swift Cost Index, *msd* and *msb*, are as follows: $n = 5$, $T_{apr} = 5$, $benz = 4000$ kg/h, $msd = 930.6$, $msb = 236$.

Overall heat-transfer coefficients for benzene-water evaporator, heat exchanger and condenser are taken as follows.

$$U_{ev} = 1950 \times 3600/1000 \text{ kJ/m}^2\text{K}$$
$$U_{exc} = 150 \times 3600/1000 \text{ kJ/m}^2\text{K}$$
$$U_{con} = 1200 \times 3600/1000 \text{ kJ/m}^2\text{K}$$

Table A.1. Specific heat capacity and density for benzoic acid benzene and water.

	a	b	w
C_p (kJ/molK)	2.14	1.84	4.19
ρ (kg/m^3)	1262	875	996

Average specific heat capacities and densities are given in Table A.1 above. Production time per year, distribution coefficient, feed rate, and mass fraction of benzoic acid to water amount in feed are as follows: $time = 8400$ h/y, $d = 4$, $F = 10000$ kg/h, $x_b = 0.002$.

Lang factor and discount factors (time value conversion factors, *frp*) are given as follows: $lang = 3.8$, $frp1 = 3.1611$, $frp2 = 3.3289$.

Enthalpy of vaporization of benzene, superheated steam, saturated steam-vapor, and saturated steam-liquid are given in Table A.2.

Table A.2. Enthalpy values

	H_{vap}	H_{steam}	H_v^{sat}	H_l^{sat}
Enthalpy (kJ/kg)	394	2963	2803	1049

Required temperature values for condenser outflow, stream 4 before preheater as seen in Figure 4.1, hot stream of cooling water, cold stream of cooling water, superheated steam, and saturated steam are stated in Table A.3.

Table A.3. Temperature values

	T_{out}	T_{pre}	T_h^w	T_c^w	T_{steam}	T^{sat}
Temperature (K)	353	300	303	288	567	517

Evaporator inlet stream temperature, T_{in}, temperature difference of outlet and inlet stream of cooling water, ΔT^w, and temperature difference of outlet (inlet to evaporator) and inlet stream (stream 4 in Figure 4.1) of preheater, T_{diff}, are found sequentially by

$$T_{in} = T_{out} - T_{apr}$$

$$\Delta T^w = T_h{}^w - T_c{}^w$$

$$T_{diff} = T_{in} - T_{pre}$$

Mass flow rates, w (kg/h), of components of 10 streams shown in Figure 4.1 are estimated from the following equalities,

$$w_{a_1} = F/(1 + 1/x_b)$$

$$w_{w_1} = F - w_{a_1}$$

$$w_{w_5} = w_{w_1}$$

$$w_{b_5} = 0.0007 \times w_{w_5}$$

$$e = benz \times d/\, w_{w_1}$$

$$x_5 = x_b \times (1 - e)/(1 - e^{(n+1)})$$

$$w_{a_5} = x_5 \times w_{w_5}$$

$$w_{a_4} = w_{a_1} - w_{a_5}$$
$$w_{b_4} = benz - w_{b_5}$$
$$w_{a_6} = w_{a_4}$$
$$w_{b_6} = w_{a_4} \times 4$$
$$w_{b_7} = w_{b_4} - w_{b_6}$$
$$w_{b_8} = w_{b_7}$$
$$w_{b_9} = w_{b_8}$$
$$w_{b_{10}} = w_{b_9}$$
$$w_{b_3} = benz$$
$$w_{b_2} = w_{b_5} + w_{b_6}$$

The mass flow rates of all streams are found by summation of individual components in each stream.

$$w = w_a + w_b + w_w$$

Volumetric flow rate (m^3/h) of feed stream to settler, *vol*, is estimated by

$$\rho_a{}' = (\rho_b benz + \rho_a w_{a_1} + \rho_w w_{w_1})/(benz + F)$$
$$vol = ((benz + F)/\rho_a{}') \times 15/60$$

Evaporator balances are as follows:

$$Q = H_{vap}\, w_{b_7} + (w_{a_4} C_{p_a} + w_{b_4} C_{p_b}) T_{apr}$$
$$Q_1 = (H_{steam} - H_v{}^{sat})/(H_{steam} - H_l{}^{sat}) \times Q$$
$$T_{lm}{}^1 = (T_{steam} - T^{sat})/log((T_{steam} - T_{out})/(T^{sat} - T_{out}))$$
$$Q_2 = (C_{p_a} w_{a_4} + C_{p_b} w_{b_4}) T_{apr}$$
$$T_{lm}{}^2 = T_{apr}\, /log((T^{sat} - T_{in})/(T^{sat} - T_{out}))$$
$$Q_3 = Q - Q_1 - Q_2$$
$$T_{lm}{}^3 = T^{sat} - T_{out}$$
$$\Delta T = (Q_1 T_{lm}{}^1 + Q_2 T_{lm}{}^2 + Q_3 T_{lm}{}^3)/Q$$

$$S_1 = Q/(H_{steam} - H_l^{sat})$$

The evaporator area, A_e, is obtained from

$$A_e = Q/U_{ev}/\Delta T$$

Condenser/Evaporator – Preheater calculations can be written as

$$Q_1' = (C_{p_a}\, w_{a_4} + C_{p_b}\, w_{b_4})T_{diff}$$
$$T_{lm}^{\ 4} = (T_{out} - T_{pre} - (T_{out} - T_{in}))/log((T_{out} - T_{pre})/(T_{out} - T_{in}))$$
$$b_1 = Q_1'/H_{vap}$$
$$A_{pc} = Q_1'/T_{lm}^{\ 4}/U_{con}$$

Benzene condenser calculations are as follows:

$$Q_2' = w_{b_7}H_{vap} - Q_1'$$
$$w_1 = Q_2'/(C_{p_w}\Delta T^w)$$
$$T = T_h^{\ w} - ((w_{b_7} - b_1)H_{vap}/\, w_1\, /C_{p_w})$$
$$T_{lm}^{\ 5} = (T - T_h^{\ w})/log((T_{out} - T_h^{\ w})/(T_{out} - T))$$
$$\Delta T_6 = ((80 - 15) - (80 - 30))/log((80 - 15)/(80 - 30))$$

The condenser area, A_c, is obtained from

$$A_c = Q_2'/U_{con}/T_{lm}^{\ 5}$$

Benzene cooler calculations are as follows:

$$T_{lm}^{\ 6} = ((T_{out} - T) - (T_{pre} - T_c^{\ w}))/log((T_{out} - T)/(T_{pre} - T_c^{\ w}))$$
$$Q_3' = w_{b_8}C_{p_b}(T_{out} - T_{pre})$$
$$A_{cool} = Q_3'/U_{exc}/T_{lm}^{\ 6}$$
$$w_2 = Q_3'/(\Delta T^w C_{p_w})$$

Overdesign factors are inserted by multiplying the resulting areas and settler volume with an overdesign factor of 1.1.

$A_e = 1.1\ A_e$
$A_c = 1.1\ A_c$
$A_{cool} = 1.1\ A_{cool}$
$vol = 1.1\ vol$
$A_{pc} = 1.1\ A_{pc}$

Equipment costs are estimated via the following equations. If the evaporator area, A_e, is less than 0.8 then the following equation is used to estimate evaporator cost, exc_1.

$$exc_1 = (msd/msb) \times 9200 \times (A_e/0.35)^{0.24}$$

If $0.8 < A_e < 3$ the following equation is used.

$$exc_1 = (msd/msb) \times 11200 \times (A_e/0.8)^{0.36}$$

If $3 < A_e < 6$, then

$$exc_1 = (msd/msb) \times 17900 \times (A_e/3)^{0.55}$$

If $6 < A_e < 13$, then

$$exc_1 = (msd/msb) \times 26300 \times (A_e/6)^{0.67}$$

If A_e is neither above, then

$$exc_1 = (msd/msb) \times 44560 \times (A_e/13)^{0.72}$$

If condenser area, A_c, is less than 27 then the following equation is used to estimate condenser cost, exc_2.

$$exc_2 = msd/msb \times 1350 \times (A_c/4.5)\text{^}0.48$$

If the condenser area, A_c, is not less than 27, then

$$exc_2 = (msd/msb) \times 5400 \times (A_c/63)^{0.58}$$

Cost for cooler, exc_3 , and partial condenser, exc_4, are estimated in the same way as condenser cost.

Pump cost is estimated by

$$pump = (n + 2) \times msd \times ((1300/236) + (550/260))$$

Total settler cost, set_1, is calculated by multiplying one stage settler cost, *set*, with number of settler stages, *n*.

$$set = (msd/msb) \times 240 \times (vol/1)^{0.66}$$
$$set_1 = set \times n$$

Total equipment cost is estimated,

$$equip = exc_1 + exc_2 + exc_3 + exc_4 + pump + set_1$$

Fixed capital investment, *FCI*, working capital, *WC*, and total capital investment, *TCI*, are estimated.

$$FCI = equip \times lang$$
$$WC = FCI \times 0.1$$
$$TCI = FCI \times 1.1$$
$$S_1 = S_1 \times 1.1$$
$$z = (w_{w_1} + w_{w_2}) \times 1.1$$

Cost of steam, water, benzene make up, electricity, labor, maintenance, supervision, depreciation, tax and insurance, overhead and from them operating cost are estimated.

$$steam = S_1 \times time \times 1.25/1000$$
$$water = z \times time \times 0.025/\rho_w$$
$$ben = v_1 \times time \times w_{b_2}$$
$$elect = 10 \times 1.1/1.341 \times time \times n \times 0.025$$
$$labor = 10 \times time$$
$$maint = 0.05 \times equip$$
$$sup = 0.15 \times labor$$
$$dep = FCI/7$$
$$taxin = 0.03 \times FCI$$
$$overh = 0.5 \times (labor + maint)$$
$$ocost = ben + steam + water + elect + labor + maint + sup + taxin + overh + dep$$

Then sales and annual cash flow are estimated.

$$sales = v_2 \times time \times w_6$$
$$cash_1 = (sales - ocost) \times 0.5 + dep$$
$$cash_2 = (sales - ocost) \times 0.5$$

At the end, net present worth is found by

$$npw = -TCI + cash1 \times frp1 + cash2 \times frp2 \times 0.2097 + WC \times 0.0352$$

APPENDIX B: SOME SELECTED MATLAB CODES

B.1. Source Code for Section 4.1.2 of Benzoic Acid Plant

(i) Main Code

```
clear all
close all
clc
format long

% Optimization of NPW

global v1 v2 ct

NRUN=10000;

v1=normrnd(0.25, 0.03, 1,NRUN);
v2=normrnd(0.95, 0.10, 1,NRUN);

for ct=1:NRUN
IG=1000;
[XB,fval,EXITFLAG] = fminsearch(@plant_randopt,IG);
if EXITFLAG == 1
   benz(:,ct)=XB;
   npw(ct)=-fval; % minus sign converts maximization to minimizatiion
else
   error('Error: No convergence in optimization')
end
end

[C, I]=max(npw);
benzene_flow=benz(1,I)

wts=1;
ts=npw;
T=1;
ci=0.95;
```

```
if T<1
   error('Error: Holding period must be positive')
end
T=fix(T)
[N M]=size(ts);
r=ts;
figure
plot(ts)

figure
[Np X]=hist(r,30);
hold on
histfit(r,30)
h = findobj(gca,'Type','patch');
set(h,'FaceColor','y','EdgeColor','black')
xlabel('NPW ($/y)'), ylabel('Frequency')

stdr=std(r)
meanr=mean(r)
skw = skewness(r)
kur = kurtosis(r)
InvErrFctVaR=sqrt(2)*erfinv(2*ci-1);
VaRparP = meanr + InvErrFctVaR*stdr
VaRparM = meanr - InvErrFctVaR*stdr
VaRhistP = prctile(r,ci*100)
VaRhistM = prctile(r,(1-ci)*100)
InvErrFctCVaR=(sqrt(2*pi)*exp((erfinv(2*ci-1))^2)*(1-ci))^-1;
CVaRparM = meanr - InvErrFctCVaR*stdr
CVaRparP = meanr + InvErrFctCVaR*stdr
CVaRM = mean( r ( find( r <= prctile(r,(1-ci)*100) ) ) )
CVaRP = mean( r ( find( r >= prctile(r,(ci)*100) ) ) )
RATIO = CVaRP/CVaRM

h1=plot ([meanr meanr],[0 max(Np)/1],'LineStyle','-.','color','green',
      'LineWidth',3)
h2=plot ([VaRparM VaRparM],[0 max(Np)/1],'LineStyle',':','color','b',
      'LineWidth',3)
h3=plot ([VaRhistM VaRhistM],[0 max(Np)/1],'LineStyle','--','color','m',
      'LineWidth',3)
h4=plot ([CVaRparM CVaRparM],[0 max(Np)/1],'LineStyle',':','color','r',
```

```
      'LineWidth',3)
h5=plot ([CVaRM CVaRM],[0 max(Np)/1],'LineStyle','--','color','c',
      'LineWidth',3)
z=legend('','Normal fit','Mean value of NPW','PVaR^+ and PVaR^-','VaR^+
      and VaR^-','PCVaR^+ and PCVaR^-','CVaR^+ and CVaR^-','Location',
      'NW')
plot([VaRparP VaRparP],[0 max(Np)/1],'LineStyle',':','Color','b',
      'LineWidth',3)
plot([VaRhistP VaRhistP],[0 max(Np)/1],'LineStyle','--','Color',
      'magenta','LineWidth',3)
plot([CVaRparP CVaRparP],[0 max(Np)/1],'LineStyle',':','Color','red',
      'LineWidth',3)
plot([CVaRP CVaRP],[0 max(Np)/1],'LineStyle','--','Color','cyan',
      'LineWidth',3)
```

(ii) Function Code

```
function npw=plant_randopt(x)

global v1 v2 ct
n=4;
tapr=8.9;
benz=x;

msd=930.6;
msb=236;
uev=1950*3600/1000;
uexc=150*3600/1000;
ucon=1200*3600/1000;
cpb=1.84;
cpa=2.14;
cpw=4.19;
denb=875;
dena=1262;
denw=996;
time=8400;
d=4;
f=10000;
xb=0.002;
hvap=394;
```

```
hsteam=2963;
hsatv=2803;
hsatl=1049;
tout=353;
tpre=300;
hotw=303;
coldw=288;
tsteam=567;
tsat=517;
lang=3.8;
frp1=3.1611;
frp2=3.3289;
tin=tout-tapr;
deltw=hotw-coldw;
tdiff=tin-tpre;

    wa=zeros(10,1);
    wb=zeros(10,1);
    ww=zeros(10,1);
    wa(1)=f/(1+1/xb);
    ww(1)=f-wa(1);
    ww(5)=ww(1);
    wb(5)=0.0007*ww(5);
    e=benz*d/ww(1);
    x5=xb*(1-e)/(1-e^(n+1));
    aden=(denb*benz+dena*wa(1)+denw*ww(1))/(benz+f);
    vol=(benz+f)/aden*15/60;
    wa(5)=x5*ww(5);
    wa(4)=wa(1)-wa(5);
    wb(4)=benz-wb(5);
    wa(6)=wa(4);
    wb(6)=wa(4)*4;
    wb(7)=wb(4)-wb(6);
    wb(8)=wb(7);
    wb(9)=wb(8);
    wb(10)=wb(9);
    wb(3)=benz;
    wb(2)=wb(5)+wb(6);
    w=wa+wb+ww;
```

```
    q=hvap*wb(7)+(wa(4)*cpa+wb(4)*cpb)*tapr;
    qq1=(hsteam-hsatv)/(hsteam-hsatl)*q;
    tlm1=(tsteam-tsat)/log((tsteam-tout)/(tsat-tout));
    qq2=(cpa*wa(4)+cpb*wb(4))*tapr;
    tlm2=tapr/log((tsat-tout+tapr)/(tsat-tout));
    qq3=q-qq1-qq2;
    tlm3=tsat-tout;
    delt=(qq1*tlm1+qq2*tlm2+qq3*tlm3)/q;
    s1=q/(hsteam-hsatl);
    ae=q/uev/delt;

    q1=(cpa*wa(4)+cpb*wb(4))*(tin-tpre);
    tlm4=(tout-tpre-tapr)/log((tout-tpre)/tapr);
    b1=q1/hvap;
    apc=q1/tlm4/ucon;

    q2=wb(7)*hvap-q1;
    w1=q2/(cpw*deltw);
    t=hotw-((wb(7)-b1)*hvap/w1/cpw);
    tlm5=(t-hotw)/log((tout-hotw)/(tout-t));
    delt6=15/log(65/50);
    ac=q2/ucon/tlm5;

    tlm6=((tout-t)-(tpre-coldw))/log((tout-t)/(tpre-coldw));
    q3=wb(8)*cpb*(tout-tpre);
    acool=q3/uexc/tlm6;
    w2=q3/(deltw*cpw);
%     w2=q/15;

    ae=1.1*ae;
    ac=1.1*ac;
    acool=1.1*acool;
    vol=1.1*vol;
    apc=apc*1.1;

    if ae<0.8
        exc1=msd/msb*9200*(ae/0.35)^0.24;
    elseif ae<3
        exc1=msd/msb*11200*(ae/0.8)^0.36;
    elseif ae<6
```

```
    exc1=msd/msb*17900*(ae/3)^0.55;
elseif ae<13
    exc1=msd/msb*26300*(ae/6)^0.67;
else
    exc1=msd/msb*44560*(ae/13)^0.72;
end
pump=(n+2)*msd*((1300/236)+(550/260));
if ac<27
    exc2=msd/msb*1350*(ac/4.5)^0.48;
else
    exc2=msd/msb*5400*(ac/63)^0.58;
end
if acool<27
    exc3=msd/msb*1350*(acool/4.5)^0.48;
else
    exc3=msd/msb*5400*(acool/63)^0.58;
end
if apc<27
    exc4=msd/msb*1350*(apc/4.5)^0.48;
else
    exc4=msd/msb*5400*(apc/63)^0.58;
end
set=msd/msb*240*(vol/1)^0.66;
set1=set*n;
equip=exc1+exc2+exc3+exc4+pump+set1;
fci=equip*lang;
wc=fci*0.1;
dep=fci/7;
tci=fci*1.1;

s1=s1*1.1;
z=(w1+w2)*1.1;
steam=s1*time*1.25/1000;
water=z*time*0.025/denw;
elect=10*1.1/1.341*time*n*0.025;
ben=v1(ct)*time*wb(2);
labor=10*time;
maint=0.05*equip;
sup=0.15*labor;
taxin=0.03*fci;
```

```
    overh=0.5*(labor+maint);
    ocost=ben+steam+water+elect+labor+maint+sup+taxin+overh+dep;
    sales=v2(ct)*time*w(6);
    cash1=(sales-ocost)*0.5+dep;
    cash2=(sales-ocost)*0.5;
    npw=-tci+cash1*frp1+cash2*frp2*0.2097+wc*0.0352;

    npw=-npw;
```

B.2. Source Code for Section 4.2.1 of Alkylation Plant

```
% Grossmann, I. E., 1991, "Chemical Engineering Optimization Models with
% GAMS", CACHE Design Case Study Series, Vol. 6.
% Biegler, L.T., Department of Chemical Engineering, "Alkylation Process
% Optimization"

clear all; close all; clc; format short g;
load ALKYLOUT0.TXT;
r=ALKYLOUT0(:,1);
nMCS=[100:100:8000]';
t=r;

ciP=0.95;
ciM=0.95;
[N M]=size(r);

figure('NumberTitle','on','Name',['Distribution VaR & CVaR']);
[Np X]=hist(r,50);
hold on
histfit(r,50)
h = findobj(gca,'Type','patch');
set(h,'FaceColor','y','EdgeColor','black')
xlabel('Profit ($/day)'), ylabel('Frequency')

stdr=std(r)
meanr=mean(r)
skewr=skewness(r)
kurtr=kurtosis(r)
InvErrFctVaRM=sqrt(2)*erfinv(2*ciM-1);
InvErrFctCVaRM=(sqrt(2*pi)*exp((erfinv(2*ciM-1))^2)*(1-ciM))^-1;
```

```
InvErrFctVaRP=sqrt(2)*erfinv(2*ciP-1);
InvErrFctCVaRP=(sqrt(2*pi)*exp((erfinv(2*ciP-1))^2)*(1-ciP))^-1;
VaRparP = meanr + InvErrFctVaRP*stdr
VaRparM = meanr - InvErrFctVaRM*stdr
CVaRparP = meanr + InvErrFctCVaRP*stdr
CVaRparM = meanr - InvErrFctCVaRM*stdr

disp(' ')
VaRhistP = prctile(r,ciP*100)
VaRhistM = prctile(r,(1-ciM)*100)
disp(' ')
CVaRhistP = mean( r ( find( r >= prctile(r,(ciP)*100) ) ) )
CVaRhistM = mean( r ( find( r <= prctile(r,(1-ciM)*100) ) ) )
disp(' ')
RachevRatio = (CVaRhistP - meanr)/(meanr - CVaRhistM)
disp(' ')

CVaRpmRAT = CVaRhistP/CVaRhistM
CVaRpmDIF = CVaRhistP-CVaRhistM

MeanDIFp = CVaRhistP - meanr
MeanDIFm = meanr - CVaRhistM
MeanDIFRAT = MeanDIFp/MeanDIFm

plot ([meanr meanr],[0 max(Np)/1],'LineStyle','-.','color','green',
      'LineWidth',3)
plot ([VaRparM VaRparM],[0 max(Np)/1],'LineStyle',':','color','b',
      'LineWidth',3)
plot ([VaRhistM VaRhistM],[0 max(Np)/1],'LineStyle','--','color','m',
      'LineWidth',3)
plot ([CVaRparM CVaRparM],[0 max(Np)/1],'LineStyle',':','color','c',
      'LineWidth',3)
plot ([CVaRhistM CVaRhistM],[0 max(Np)/1],'LineStyle','--','color','r',
      'LineWidth',3)
legend('','Normal fit','Mean value','PVaR^+ and PVaR^-','VaR^+ and VaR^-
','PCVaR^+ and PCVaR^-','CVaR^+ and CVaR^-','Location','NW')

plot([VaRparP VaRparP],[0 max(Np)/1],'LineStyle',':','Color','b',
      'LineWidth',3)
plot([VaRhistP VaRhistP],[0 max(Np)/1],'LineStyle','--','Color',
```

```
      'magenta','LineWidth',3)
plot([CVaRparP CVaRparP],[0 max(Np)/1],'LineStyle',':','Color','cyan',
      'LineWidth',3)
plot([CVaRhistP CVaRhistP],[0 max(Np)/1],'LineStyle','--','Color','red',
      'LineWidth',3)

for i=1:80
StandardDeviation(i,1)=std(t(1:nMCS(i,1),1));
MeanProfit(i,1)=mean(t(1:nMCS(i,1),1));
Skewness(i,1)=skewness(t(1:nMCS(i,1),1));
Kurtosis(i,1)=kurtosis(t(1:nMCS(i,1),1));
end

table2 = [MeanProfit StandardDeviation Skewness Kurtosis VaRP VaRM CVaRP
CVaRM RRatio]

figure
for i=1:9
subplot(5,2,i)
hold on
if i==1
    plot (nMCS,MeanProfit)
    title('Mean Profit')
    elseif i==2
    plot (nMCS,StandardDeviation)
    title('Standard Deviation')
    elseif i==3
        plot (nMCS,Skewness)
    title('Skewness')
    elseif i==4
        plot (nMCS,Kurtosis)
    title('Kurtosis')
    elseif i==5
        plot (nMCS,VaRP)
    title('VaR^+')
    elseif i==6
        plot (nMCS,VaRM)
    title('VaR^-')
    elseif i==7
        plot (nMCS,CVaRP)
```

```
    title('CVaR^+')
    elseif i==8
        plot (nMCS,CVaRM)
    title('CVaR^-')
else
    plot (nMCS,RRatio)
    title('Rachev Ratio')
end
end
hold off
```

B.3. Source Code for Section 4.2.2.1 of Alkylation Plant

```
% Grossmann, I. E., 1991, "Chemical Engineering Optimization Models with
% GAMS", CACHE Design Case Study Series, Vol. 6.
% Biegler, L.T., Department of Chemical Engineering, "Alkylation Process
% Optimization"

clear all; close all; clc; format short g;
load ALKYLOUT.TXT;
r=ALKYLOUT(:,1);
nMCS=[100:100:8000]';
t=r;

ciP=0.95;
ciM=0.95;
[N M]=size(r);

figure('NumberTitle','on','Name',['Distribution VaR & CVaR']);
[Np X]=hist(r,50);
hold on
histfit(r,50)
h = findobj(gca,'Type','patch');
set(h,'FaceColor','y','EdgeColor','black')
xlabel('Profit ($/day)'), ylabel('Frequency')

stdr=std(r)
meanr=mean(r)
skewr=skewness(r)
kurtr=kurtosis(r)
```

```
InvErrFctVaRM=sqrt(2)*erfinv(2*ciM-1);
InvErrFctCVaRM=(sqrt(2*pi)*exp((erfinv(2*ciM-1))^2)*(1-ciM))^-1;
InvErrFctVaRP=sqrt(2)*erfinv(2*ciP-1);
InvErrFctCVaRP=(sqrt(2*pi)*exp((erfinv(2*ciP-1))^2)*(1-ciP))^-1;
VaRparP = meanr + InvErrFctVaRP*stdr
VaRparM = meanr - InvErrFctVaRM*stdr
CVaRparP = meanr + InvErrFctCVaRP*stdr
CVaRparM = meanr - InvErrFctCVaRM*stdr

disp(' ')
VaRhistP = prctile(r,ciP*100)
VaRhistM = prctile(r,(1-ciM)*100)
disp(' ')
CVaRhistP = mean( r ( find( r >= prctile(r,(ciP)*100) ) ) )
CVaRhistM = mean( r ( find( r <= prctile(r,(1-ciM)*100) ) ) )
disp(' ')
RachevRatio = (CVaRhistP - meanr)/(meanr - CVaRhistM)
disp(' ')

CVaRpmRAT = CVaRhistP/CVaRhistM
CVaRpmDIF = CVaRhistP-CVaRhistM

MeanDIFp = CVaRhistP - meanr
MeanDIFm = meanr - CVaRhistM
MeanDIFRAT = MeanDIFp/MeanDIFm

plot ([meanr meanr],[0 max(Np)/1],'LineStyle','-.','color','green',
      'LineWidth',3)
plot ([VaRparM VaRparM],[0 max(Np)/1],'LineStyle',':','color','b',
      'LineWidth',3)
plot ([VaRhistM VaRhistM],[0 max(Np)/1],'LineStyle','--','color','m',
      'LineWidth',3)
plot ([CVaRparM CVaRparM],[0 max(Np)/1],'LineStyle',':','color','c',
      'LineWidth',3)
plot ([CVaRhistM CVaRhistM],[0 max(Np)/1],'LineStyle','--','color','r',
      'LineWidth',3)
legend('','Normal fit','Mean value','PVaR^+ and PVaR^-','VaR^+ and VaR^-
','PCVaR^+ and PCVaR^-','CVaR^+ and CVaR^-','Location','NW')

plot([VaRparP VaRparP],[0 max(Np)/1],'LineStyle',':','Color','b',
```

```
      'LineWidth',3)
plot([VaRhistP VaRhistP],[0 max(Np)/1],'LineStyle','--','Color',
      'magenta','LineWidth',3)
plot([CVaRparP CVaRparP],[0 max(Np)/1],'LineStyle',':','Color','cyan',
      'LineWidth',3)
plot([CVaRhistP CVaRhistP],[0 max(Np)/1],'LineStyle','--','Color','red',
      'LineWidth',3)

for i=1:80
StandardDeviation(i,1)=std(t(1:nMCS(i,1),1));
MeanProfit(i,1)=mean(t(1:nMCS(i,1),1));
Skewness(i,1)=skewness(t(1:nMCS(i,1),1));
Kurtosis(i,1)=kurtosis(t(1:nMCS(i,1),1));
end

table2 = [MeanProfit StandardDeviation Skewness Kurtosis VaRP VaRM CVaRP
CVaRM RRatio]

figure
for i=1:9
subplot(5,2,i)
hold on
if i==1
    plot (nMCS,MeanProfit)
    title('Mean Profit')
    elseif i==2
    plot (nMCS,StandardDeviation)
    title('Standard Deviation')
    elseif i==3
        plot (nMCS,Skewness)
    title('Skewness')
    elseif i==4
        plot (nMCS,Kurtosis)
    title('Kurtosis')
    elseif i==5
        plot (nMCS,VaRP)
    title('VaR^+')
    elseif i==6
        plot (nMCS,VaRM)
    title('VaR^-')
```

```
    elseif i==7
        plot (nMCS,CVaRP)
    title('CVaR^+')
    elseif i==8
        plot (nMCS,CVaRM)
    title('CVaR^-')
else
    plot (nMCS,RRatio)
    title('Rachev Ratio')
end
end
hold off
```

APPENDIX C: SOME SELECTED GAMS CODES

C.1. Source Code for Section 4.2.1 of Alkylation Plant

```
$ Grossmann, I. E., 1991, "Chemical Engineering Optimization Models with
$ GAMS", CACHE Design Case Study Series, Vol. 6.
$ Biegler, L.T., Department of Chemical Engineering, "Alkylation Process
$ Optimization"
$TITLE Alkylation Plant
$OFFSYMLIST OFFSYMXREF OFFUELLIST OFFUELXREF
OPTION DECIMALS=4, LIMROW=0, LIMCOL=0, SYSOUT=OFF, SOLPRINT=OFF;

scalar time0, time1, hour0, hour1, minute0, minute1, second0, second1;
scalar dtimeh,dtimem,dtimes;
time0 = jstart;
hour0  = ghour(time0); minute0 = gminute(time0);
second0 = gsecond(time0);

*x1 : Olefin feed (barrels per day)
*x2 : Isobutane recycle (barrels per day)
*x3 : Acid addition rate (1000s pounds per day)
*x4 : Alkylate yield (barrels per day)
*x5 : Isobutane input (barrels per day)
*x6 : Acid strength (wt %)
*x7 : Motor octane number of alkylate
*x8 : External isobutane-to-olefin ratio
*x9 : Acid dilution factor
*x10: F-4 performance number of alkylate

PARAMETER TOTAL_CPU;
TOTAL_CPU = 0;
SET K TRIAL COUNTER /1*8000/;
PARAMETER COEF1,COEF2,COEF3,COEF4,COEF5;
POSITIVE VARIABLES X1,X2,X3,X4,X5,X6,X7,X8,X9,X10;
VARIABLE OBJ;

EQUATIONS E1,E2,E3,E4,E5,E6,E7,E8;
E1   .. X4 =E= X1*(1.12+.13167*X8-0.0067*X8**2);
```

```
E2   .. X7 =E= 86.35+1.098*X8-0.038*X8**2+0.325*(X6-89.);
E3   .. X9 =E= 35.82-0.222*X10;
E4   .. X10 =E= 3*X7-133;
E5   .. X8*X1 =E= X2+X5;
E6   .. X5 =E= 1.22*X4-X1;
E7   .. X6*(X4*X9+1000*X3) =E= 98000*X3;
E8   .. OBJ =E= COEF1*X4*X7-COEF2*X1-COEF3*X2-COEF4*X3-COEF5*X5;

X1.LO  =  1500;
X1.UP  = 10000;
X2.LO  =  5000;
X2.UP  = 10000;
X3.LO  =    50;
X3.UP  =   500;
X4.LO  =   500;
X4.UP  = 10000;
X5.LO  =   500;
X5.UP  =  5000;
X6.LO  =    50;
X6.UP  =   500;
X7.LO  =    50;
X7.UP  =   500;
X8.LO  =     1;
X8.UP  =    50;
X9.LO  =     1;
X9.UP  =    20;
X10.LO =    50;
X10.UP =   500;

X1.L  =  1500;
X2.L  = 15000;
X3.L  =   100;
X4.L  =  3000;
X5.L  =  2000;
X6.L  =   100;
X7.L  =   100;
X8.L  =    10;
X9.L  =     5;
X10.L =   150;
```

```
Model ALKYLUA / ALL / ;
OPTION NLP = CONOPT;

FILE ALKYLOUT0/ALKYLOUT0.TXT/;

PARAMETER OBJF(K);
PARAMETER COEF1F(K),COEF2F(K),COEF3F(K),COEF4F(K),COEF5F(K);

LOOP (K,
      COEF1=NORMAL( 0.075, 0.001);
      COEF2=NORMAL( 5.000, 0.050);
      COEF3=NORMAL( 0.050, 0.001);
      COEF4=NORMAL(10.000, 0.100);
      COEF5=NORMAL( 3.000, 0.050);

SOLVE ALKYLUA USING NLP MAXIMIZING OBJ;
TOTAL_CPU = TOTAL_CPU + ALKYLUA.RESUSD;

OBJF(K) = OBJ.L;
COEF1F(K)=COEF1;
COEF2F(K)=COEF2;
COEF3F(K)=COEF3;
COEF4F(K)=COEF4;
COEF5F(K)=COEF5;

PUT ALKYLOUT0;
PUT OBJ.L:12:4, X1.L:14:4, X2.L:12:4, X3.L:12:4, X4.L:12:4, X5.L:12:4,
                X6.L:12:4, X7.L:12:4, X8.L:12:4, X9.L:12:4, X10.L:12:4/;
DISPLAY OBJ.L;
DISPLAY X1.L, X2.L, X3.L , X4.L, X5.L, X6.L, X7.L, X8.L, X9.L, X10.L;
DISPLAY TOTAL_CPU;
);
DISPLAY TOTAL_CPU;

*********************************************************************
Scalar alphap plus  probability level / 0.95 /;
Scalar alpham minus probability level / 0.95 /;
Variables cvarp     CVaRp of portfolio
          cvarm     CVaRm of portfolio
          varp      VaRp of portfolio
```

```
          varm      VaRm of portfolio
          zp(K)     plus dummy variables
          zm(K)     minus dummy variables
          objcvar ;
Positive Variable zp,zm;
Equations etcvarp(K) CVaRp related constraint
          etcvarm(K) CVaRm related constraint
          ecvarp     definition of CVaRp
          ecvarm     definition of CVaRm
          objeq ;

ecvarp     .. varp+(1/((1-alphap)*card(K)))*sum(K, zp(K)) =E= cvarp;
ecvarm     .. varm-(1/((1-alpham)*card(K)))*sum(K, zm(K)) =E= cvarm;
etcvarp(K) .. OBJF(K) - varp =L= zp(K);
etcvarm(K) .. varm - OBJF(K) =L= zm(K);

objeq .. cvarp - cvarm =E= objcvar;
*objeq .. SUM(K, OBJF(K))/card(K) =E= objcvar;

Model VARCVAR / etcvarp,etcvarm,ecvarp,ecvarm,objeq / ;
Solve VARCVAR using LP minimizing objcvar;

TOTAL_CPU = TOTAL_CPU + VARCVAR.RESUSD;
PARAMETER MeanProfit Mean Profit Value;
MeanProfit=SUM(K,OBJF(K))/card(K);
PARAMETER CVaRpmDIF CVaRp-CVaRm;
CVaRpmDIF=cvarp.L-cvarm.L;
PARAMETER MeanDIFp CVaRp-MeanProfit;
MeanDIFp=cvarp.L-MeanProfit;
PARAMETER MeanDIFm MeanProfit-CVaRm;
MeanDIFm=MeanProfit-cvarm.L;
PARAMETER RacRat Rachev Ratio;
RacRat=(cvarp.L-MeanProfit)/(MeanProfit-cvarm.L);
PARAMETER MeanIncome Mean Income;
MeanIncome=SUM(K,COEF1F(K))/card(K)*X4.L*X7.L;
PARAMETER MeanCost Mean Cost;
MeanCost=(-SUM(K,COEF2F(K))*X1.L-SUM(K,COEF3F(K))*X2.L
          -SUM(K,COEF4F(K))*X3.L-SUM(K,COEF5F(K))*X5.L)/card(K);
DISPLAY OBJF;
display zp.L, zm.L;
```

```
DISPLAY X1.L, X2.L, X3.L , X4.L, X5.L, X6.L, X7.L, X8.L, X9.L, X10.L;
display varp.L, varm.L;
display cvarp.L, cvarm.L;
display CVaRpmDIF,MeanDIFp,MeanDIFm,RacRat;
display MeanIncome,MeanCost,MeanProfit;
display objcvar.L;
DISPLAY TOTAL_CPU;
time1 = jnow;
hour1  = ghour(time1); minute1 = gminute(time1);
second1 = gsecond(time1);
display hour0, minute0, second0;
display hour1, minute1, second1;
dtimeh=hour1-hour0;
dtimem=minute1-minute0;
dtimes=second1-second0;
display dtimeh,dtimem,dtimes;
```

C.2. Source Code for Section 4.2.2.1 of Alkylation Plant

```
$ Grossmann, I. E., 1991, "Chemical Engineering Optimization Models with
$ GAMS", CACHE Design Case Study Series, Vol. 6.
$ Biegler, L.T., Department of Chemical Engineering, "Alkylation Process
$ Optimization"
$TITLE Alkylation Plant
$OFFSYMLIST OFFSYMXREF OFFUELLIST OFFUELXREF
OPTION DECIMALS=4, LIMROW=0, LIMCOL=0, SYSOUT=OFF, SOLPRINT=OFF;

scalar time0, time1, hour0, hour1, minute0, minute1, second0, second1;
scalar dtimeh,dtimem,dtimes;
time0 = jstart;
hour0  = ghour(time0); minute0 = gminute(time0);
second0 = gsecond(time0);
*x1 : Olefin feed (barrels per day)
*x2 : Isobutane recycle (barrels per day)
*x3 : Acid addition rate (1000s pounds per day)
*x4 : Alkylate yield (barrels per day)
*x5 : Isobutane input (barrels per day)
*x6 : Acid strength (wt %)
*x7 : Motor octane number of alkylate
*x8 : External isobutane-to-olefin ratio
```

```
*x9 : Acid dilution factor
*x10: F-4 performance number of alkylate
PARAMETER TOTAL_CPU;
TOTAL_CPU = 0;
Scalar alphap plus  probability level / 0.95 /;
Scalar alpham minus probability level / 0.95 /;
SET K TRIAL COUNTER /1*8000/;
PARAMETER Weight ObjFct Weighting Coefficient /0.5/;
*PARAMETER CVARLIMm / 6770/;
PARAMETER COEF1(K),COEF2(K),COEF3(K),COEF4(K),COEF5(K);
LOOP (K,
      COEF1(K)=NORMAL( 0.075, 0.001);
      COEF2(K)=NORMAL( 5.000, 0.050);
      COEF3(K)=NORMAL( 0.050, 0.001);
      COEF4(K)=NORMAL(10.000, 0.100);
      COEF5(K)=NORMAL( 3.000, 0.050); );
POSITIVE VARIABLES X1,X2,X3,X4,X5,X6,X7,X8,X9,X10,
                   zp(K), zm(K);
Variables objcvar, cvarp, varp, cvarm,varm, OBJ(K);
EQUATIONS E1,E2,E3,E4,E5,E6,E7,E8(K),
          etcvarp(K), ecvarp, etcvarm(K), ecvarm, objeq
*          ECVARLIMM
;
E1   .. X4 =E= X1*(1.12+.13167*X8-0.0067*X8**2);
E2   .. X7 =E= 86.35+1.098*X8-0.038*X8**2+0.325*(X6-89.);
E3   .. X9 =E= 35.82-0.222*X10;
E4   .. X10 =E= 3*X7-133;
E5   .. X8*X1 =E= X2+X5;
E6   .. X5 =E= 1.22*X4-X1;
E7   .. X6*(X4*X9+1000*X3) =E= 98000*X3;
E8(K)..  OBJ(K)  =E=  COEF1(K)*X4*X7-COEF2(K)*X1-COEF3(K)*X2-COEF4(K)*X3-
COEF5(K)*X5;
ecvarp     .. varp+(1/((1-alphap)*card(K)))*sum(K, zp(K)) =E= cvarp;
ecvarm     .. varm-(1/((1-alpham)*card(K)))*sum(K, zm(K)) =E= cvarm;
etcvarp(K) .. OBJ(K) - varp =L= zp(K);
etcvarm(K) .. varm - OBJ(K) =L= zm(K);
objeq .. -(cvarp - cvarm) =E= objcvar;
*objeq .. -cvarp =E= objcvar;
*objeq .. cvarm =E= objcvar;
*objeq .. SUM(K, OBJ(K))/card(K) =E= objcvar;
```

```
*objeq .. Weight*SUM(K,OBJ(K))/card(K) - (1-Weight)*(cvarp-cvarm) =E=
*          objcvar;
*objeq .. Weight*SUM(K,OBJ(K))/card(K) - (1-Weight)*cvarp =E= objcvar;
*objeq .. Weight*SUM(K,OBJ(K))/card(K) + (1-Weight)*cvarm =E= objcvar;
*ECVARLIMM .. cvarm =E= CVARLIMm;
X1.LO  =  1500;
X1.UP  = 10000;
X2.LO  =  5000;
X2.UP  = 10000;
X3.LO  =    50;
X3.UP  =   500;
X4.LO  =   500;
X4.UP  = 10000;
X5.LO  =   500;
X5.UP  =  5000;
X6.LO  =    50;
X6.UP  =   500;
X7.LO  =    50;
X7.UP  =   500;
X8.LO  =     1;
X8.UP  =    50;
X9.LO  =     1;
X9.UP  =    20;
X10.LO =    50;
X10.UP =   500;

X1.L  =  1500;
X2.L  = 15000;
X3.L  =   100;
X4.L  =  3000;
X5.L  =  2000;
X6.L  =   100;
X7.L  =   100;
X8.L  =    10;
X9.L  =     5;
X10.L =   150;
Model ALKYLUA / ALL / ;
OPTION NLP = CONOPT;
FILE ALKYLOUT/ALKYLOUT.TXT/;
Solve ALKYLUA using NLP maximizing objcvar;
```

```
TOTAL_CPU = TOTAL_CPU + ALKYLUA.RESUSD;
PARAMETER MeanProfit Mean Profit Value;
MeanProfit=SUM(K,OBJ.L(K))/card(K);
PARAMETER CVaRpmDIF CVaRp-CVaRm;
CVaRpmDIF=cvarp.L-cvarm.L;
PARAMETER MeanDIFp CVaRp-MeanProfit;
MeanDIFp=cvarp.L-MeanProfit;
PARAMETER MeanDIFm MeanProfit-CVaRm;
MeanDIFm=MeanProfit-cvarm.L;
PARAMETER RacRat Rachev Ratio;
RacRat=(cvarp.L-MeanProfit)/(MeanProfit-cvarm.L);
PARAMETER MeanIncome Mean Income;
MeanIncome=SUM(K,COEF1(K))/card(K)*X4.L*X7.L;
PARAMETER MeanCost Mean Cost;
MeanCost=(-SUM(K,COEF2(K))*X1.L-SUM(K,COEF3(K))*X2.L
          -SUM(K,COEF4(K))*X3.L-SUM(K,COEF5(K))*X5.L)/card(K);
DISPLAY OBJ.L;
display zp.L, zm.L;
DISPLAY X1.L, X2.L, X3.L , X4.L, X5.L, X6.L, X7.L, X8.L, X9.L, X10.L;
display varp.L, varm.L;
display cvarp.L, cvarm.L;
display CVaRpmDIF,MeanDIFp,MeanDIFm,RacRat;
display MeanIncome,MeanCost,MeanProfit;
display objcvar.L;
DISPLAY TOTAL_CPU;
time1 = jnow;
hour1  = ghour(time1); minute1 = gminute(time1);
second1 = gsecond(time1);
display hour0, minute0, second0;
display hour1, minute1, second1;
dtimeh=hour1-hour0;
dtimem=minute1-minute0;
dtimes=second1-second0;
display dtimeh,dtimem,dtimes;
PUT ALKYLOUT;
Loop (K,
*PUT OBJ.L(K):12:4/;
PUT OBJ.L(K):12:4, X1.L:14:4, X2.L:12:4, X3.L:12:4, X4.L:12:4, X5.L:12:4,
                 X6.L:12:4, X7.L:12:4, X8.L:12:4, X9.L:12:4, X10.L:12:4/;
);
```

REFERENCES

Aseeri A. and M. Bagajewicz, 2004, "New Measures and Procedures to Manage Financial Risk with Applications to the Planning of Gas Commercialization in Asia", *Computers and Chemical Engineering*, Vol. 28, pp. 2791–2821.

Acevedo, J. and E.N. Pistikopoulos, 1996, "A Parametric MINLP Algorithm for Process Synthesis Problems under Uncertainty", *Ind. Eng. Chem. Res.*, Vol. 35, No. 1, pp. 147−158.

Acevedo, J. and E.N. Pistikopoulos, 1998, "Stochastic Optimization Based Algorithms for Process Synthesis under Uncertainty", *Computers and Chemical Engineering*, Vol. 22, pp. 647–671.

Artzner, P., F. Delbaen, J. Eber and D. Heath, 1997, "Thinking Coherently", *Risk*, Vol. 10, pp. 68–71.

Artzner, P., F. Delbaen, J. Eber and D. Heath, 1999, "Coherent Measures of Risk", *Mathematical Finance*, Vol. 9, pp. 203–228.

Bagajewicz, M. J., 2005, "Integration of Process Systems Engineering and Business Decision Making Tools: Financial Risk Management and Other Emerging Procedures", M. A. Galán and E. M. del Valle (eds.), *Chemical Engineering Trends and Developments*, pp. 324, 337–347, John Wiley & Sons.

Barbaro, A. and M. Bagajewicz, 2003, *Financial Risk Management in Planning under Uncertainty*, Foundations of Computer-Aided Process Operations (FOCAPO 2003), Coral Springs, FL, USA.

Barbaro, A. and M. Bagajewicz, 2004, "Managing Financial Risk in Planning under Uncertainty", *AIChE Journal*, Vol. 50, No. 5, pp. 963–989.

Ballesca-Loyo, L., 1999, "Value at Risk and Technical Analysis", *Technical Analysis of Stocks & Commodities*, Vol. 17, pp. 351–354.

Biglova, A., S. Ortobelli, S. Rachev and S. Stoyanov, 2004, "Different Approaches to Risk Estimation in Portfolio Theory", *Journal of Portfolio Management*, Vol. 31, pp. 103–112.

Charnes, A. and W.W. Cooper, 1959, "Chance Constrained Programming", *Management Science*, Vol. 6, pp. 73–79.

Charnes, A. and W. W. Cooper, 1962, "Programming with Linear Fractional Functional", *Naval Research Logistics*, Quarterly 9, pp. 181–186.

DeVuyst, E. A. and P. V. Preckel, 2007, "Gaussian Cubature: A Practitioner's Guide", *Mathematical and Computer Modelling*, Vol. 45, pp. 787–794.

Diwekar, U., 2003, "A Novel Sampling Approach to Combinatorial Optimization under Uncertainty", *Computational Optimization and Applications*, Vol. 24, pp. 335–371.

Diwekar, U., 2008, "Optimization under Uncertainty", *Introduction to Applied Optimization*, 2nd ed., pp. 125–172, Springer.

Diwekar, U. and J. R. Kalagnanam, 1997, "Efficient Sampling Technique for Optimization under Uncertainty", *AIChE Journal*, Vol. 43, No. 2, pp. 440–447.

Diwekar, U. M. and E.S. Rubin, 1991, "Stochastic Modeling of Chemical Processes", *Computers and Chemical Engineering*, Vol. 15, p. 105.

Dowd, K., 2005, "Measuring Market Risk", 2nd ed., *Wiley Finance*, pp. 12–13, John Wiley & Sons.

Goyal, V. and M. G. Ierapetritou, 2007, "Stochastic MINLP Optimization Using Simplicial Approximation", *Computers and Chemical Engineering*, Vol. 31, pp. 1081–1082.

Grossmann, I. E., 1991, “Chemical Engineering Optimization Models with GAMS”, *CACHE Design Case Study Series*, Vol. 6.

Grossmann, I. E. and C. A. Floudas, 1987, “Active Constraint Strategy for Flexibility Analysis in Chemical Processes”, *Computers and Chemical Engineering*, Vol. 11, No. 6, pp. 675–693.

Guldimann, T., 2000, “The Story of Risk Metrics”, *Risk*, Vol. 13, No. 1, pp. 56–58.

Gupta, A. and C. Maranas, 2003, “Managing Demand Uncertainty in Supply Chain Planning”, *Computers and Chemical Engineering*, Vol. 27, pp. 1219–1227.

Halemane, K. P and I. E. Grossmann, 1983, “Optimal Process Design under Uncertainty”, *AIChE Journal*, Vol. 29, pp. 425–433.

Ierapetritou, M. G., J. Acevedo and E. N. Pistikopoulos, 1996, “An Optimization Approach for Process Engineering Problems under Uncertainty”, *Computers and Chemical Engineering*, Vol. 20, p. 703.

Iman, R. L. and J. C. Helton, 1988, “An Investigation of Uncertainty and Sensitivity Analysis Techniques for Computer Models”, *Risk Analysis*, Vol. 8, No. 1, p. 71.

Iman, R. L. and M. J. Shortencarier, 1984, A FORTRAN77 Program and User’s Guide for Generation of Latin Hypercube and Random Samples for Use with Computer Models, *NUREG/CR-3624, SAND83-2365*, Sandia National Laboratories, Albuquerque, N.M.

James, B. A. P., 1985, “Variance reduction techniques”, *Journal of the Operations Research Society*, Vol. 36, No. 6, p. 525.

Kalagnanam, J. R. and U. M. Diwekar, 1997, “An Efficient Sampling Technique for Offline Quality Control”, *Technometrics*, Vol. 39, pp. 308–319.

Keown, A. J., J. D. Martin, J. W. Petty and D. F. Scott, 2002, *Financial Management: Principles and Applications*, 9th ed., Prentice Hall, New Jersey.

Kim, K. J. and U. Diwekar, 2002, "Efficient Combinatorial Optimization under Uncertainty 1. Algorithmic Development", *Ind. Eng. Chem. Res.*, Vol. 41, pp. 1276–1284.

Kolman, J. *et al*., 1998, "Roundtable: The Limits of VaR", *Derivatives Strategy*.

Konno, H., K. Tanaka and R. Yamamoto, 2011, "Construction of a Portfolio with Shorter Downside Tail and Longer Upside Tail", *Computational Optimization and Applications*, Vol. 48, No. 2, pp. 199-212.

Krokhmal, P., Palmquist J. and S. Uryasev, 2001, "Portfolio Optimization with Conditional Value-at-Risk Objective and Constraints", *The Journal of Risk*, Vol. 4, No. 2.

Larsen, N., Mausser, H. and S. Uryasev, 2002, "Algorithms for Optimization of Value-At-Risk", *Research Report*, ISE Dept., University of Florida.

Mak, W.K., D.P. Morton and R.K. Wood, 1999, "Monte Carlo Bounding Techniques for Determining Solution Quality in Stochastic Programs", *Operational Research Letters*, Vol. 24, p. 47.

McCray, A.W., 1975, *Petroleum Evaluations and Economic Decisions*, Prentice Hall, New Jersey.

McKay M. D., R. J. Beckman and W. J. Conover, 1979, "A Comparison of Three Methods of Selecting Values of Input Variables in the Analysis of Output from a Computer Code", *Technometrics*, Vol. 21, No. 2, p. 239.

Miller, A. C. and T. R. Rice, 1983, "Discrete Approximations of Probability Distributions", *Management Science*, Vol. 29, pp. 352–362.

Nemhauser, G. L., A. H. G. Ronnooy Kan and M. J. Todd, 1989, *Optimization: Handbooks in operations research and management science*, Vol. 1. North-Holland Press, New York.

Nolan, J. P., 2011, *Stable Distributions - Models for Heavy Tailed Data*, pp. 3–24, in progress, Chapter 1 online at http://academic2.american.edu/~jpnolan, Birkhauser, Boston.

Paules, G. E. and C. A. Floudas, 1992, "Stochastic Programming in Process Synthesis: A Two-Stage Model with MINLP Recourse for Multiperiod Heat-Integrated Distillation Sequences", *Computers and Chemical Engineering*, Vol. 16, Issue 3, pp. 189–210.

Pflug, G., 2001, "Some Remarks on the Value-at-Risk and the Conditional Value-at-Risk", *Probabilistic Constrained Optimization: Methodology and Applications* (S. Uryasev ed.), Kluwer Academic Publishers.

Pintaric, Z. N. and Z. Kravanja, 2000, "The two-level strategy for MINLP synthesis of process flowsheets under uncertainty", *Computers & Chemical Engineering*, Vol. 24, Issue 2-7, pp. 195-201,

Pistikopoulos, E. N., 1995, "Uncertainty in Process Design and Operations", *Computers & Chemical Engineering*, Vol. 19, pp. 553–563.

Pistikopoulos, E. N. and M. G. Ierapetritou, 1995, "Novel approach for Optimal Process Design under Uncertainty", *Computers and Chemical Engineering*, Vol. 19, No. 10, pp. 1089–1110.

Pongsakdia, A., P. Rangsunvigit, K. Siemanond and M. J. Bagajewicz, 2006, "Financial risk management in the planning of refinery operations", *Int. J. Production Economics*, Vol. 103, pp. 64–86.

Powell, R. J. and D. E. Allen, 2009, “CVaR and Credit Risk Measurement”, *Working Paper 0905*, Finance and Economics & FEMARC Working Paper Series, Edith Cowan University.

Riggs, J. L., 1968, *Economic Decision Models for Engineers and Managers*, McGraw Hill, New York.

Rockafellar, R. T. and S. Uryasev, 2000, “Optimization of Conditional Value-at-Risk”, *The Journal of Risk*, Vol. 2, No. 3, pp. 21–41.

Rockafellar, R.T. and S. Uryasev, 2001, “Conditional Value-at-Risk for General Loss Distributions”, *Research Report 2001-5*, ISE Dept., University of Florida.

Rodera, H. and M. Bagajewicz, 2000, *Risk Assessment in Process Planning under Uncertainty*, AIChE Annual Meeting, Los Angeles.

Sauer, R. N., A. R. Coville and C. W. Burwick, 1964, "Computer Points Way to More Profits." *Hydrocarbon Process. Petrol Ref.*, Vol. 43, pp. 84-92.

Sharpe, W. F., 1966, "Mutual Fund Performance." *Journal of Business*, pp. 119-138.

Stoyanov, S. V., S. T. Rachev and F. J. Fabozzi, 2007, “Optimal Financial Portfolios”, *Applied Mathematical Finance*, Vol. 14, No. 5, pp. 401–436.

Stroud, A. H., 1971, *Approximate Calculation of Multiple Integrals*, Prentice-Hall, New Jersey.

Swaney, R. E. and I. E. Grossmann, 1985, “An Index for Operational Flexibility in Chemical Process Design”, *AIChE Journal*, Vol. 31, No 4, pp. 621–630.

Uryasev, S., 2000, “Conditional Value-at-Risk: Optimization Algorithms and Applications”, *Financial Engineering News*, Vol. 14, pp. 1–5.

Uryasev, S., 2010, “VaR vs CVaR in Risk Management and Optimization”, *CARISMA Conference*, pp. 4–7, online at http://www.ise.ufl.edu/uryasev/pubs.html.

Vajda, S., 1972, *Probabilistic Programming*, Academic Press, New York.

Verderame, P. M. and C. A. Floudas, 2010, “Operational Planning of Large-Scale Industrial Batch Plants under Demand Due Date and Amount Uncertainty: II. Conditional Value-at-Risk Framework”, *Ind. Eng. Chem. Res.*, Vol. 49, pp. 260–275.

Verderame, P. M. and C. A. Floudas, 2011, “Multisite Planning under Demand and Transportation Time Uncertainty: Robust Optimization and Conditional Value-at-Risk Frameworks”, *Ind. Eng. Chem. Res.*, Vol. 50, pp. 4959–4982.

Walck, C., 1996, “Hand-book on Statistical Distributions for Experimentalists”, *Internal Report*, University of Stockholm, p. 13.

Whitnack, C., A. Heller, M. T. Frow, S. Kerr and M. J. Bagajewicz, 2009, “Financial Risk Management in the Design of Products under Uncertainty”, *Computers and Chemical Engineering*, Vol. 20, pp. 1056–1066.